STUDY OF DIAMOND LIKE CARBON (DLC) FILMS GROWN BY SOME NOVEL TECHNIQUES

THESIS

Submitted in partial fulfilment

of the requirements for the degree of

DOCTOR OF PHILOSOPHY

By

DEBAJYOTI SARANGI

Under the supervision of

Dr. R. Bhattacharyya

Thin Film Technology Group, NPL, New Delhi

BIRLA INSTITUTE OF TECHNOLOGY AND SCIENCE
PILANI (RAJASTHAN) INDIA
1998

Dedicated to my Parents

Acknowledgements

To try to express my gratitude for my guide Dr. R. Bhattacharyya, Scientist-in-charge, Thin Film Technology Group, National Physical Laboratory, New Delhi, would be an exercise in futility. The aspect of learning while working on this thesis could not have been so pleasant without his rich wealth of personal experience and incisive insight into the specific area of study. I am beholden to Dr. Bhattacharyya for his continuous encouragement and patience in handling my queries and providing an ambient working environ.

For the intellectual nourishment and constructive criticism, not to mention the help and support, I am indebted to Dr. O.S. Panwar, Dr. P.N. Dixit, Dr. B.S. Verma, Dr. A. Basu, Dr. (Mrs.) M. Kar, Mr. S.S. Rajput, Dr. Senguttuvan, Thin Film Technology Group and Dr. C. Anandan and Dr. Shivaprasad, Surface Science Group.

I would be falling in my own eyes without according special thanks to Mr. Sushil Kumar, Mr. Rajnish Sharma, Dr. Tanay Seth and Mr. C. Mukherjee for their constant help in thesis preparation as well as friendly support during this academic endeavour.

For technical co-operation I must acknowledge the contributions of Mr. T.K. Chakraborty, Mr. T.K. Bhattacharyya, Mr. R.K. Sodhi, Mr. Jagdish Chand, Mr. Amar Singh, Mrs. Suman Bhardawaj, Mr. Ramrajjan who were always very co-operative.

I am indebted to Rajiv Chopra & Dr. B.P. Singh, NPL, for hardness measurement, to Prof. A.K. Pal, IACS, Calcutta, for providing stress measurement in the early stage, to Dr. B.R. Singh, CEERI, Pilani for allowing me to use optical microscope, to Dr. D. K. Avasthi & Mr. D. Kabiraj, to carry out ERDA analysis, to Dr. G.C. Dubey & Mrs. Meena Mishra, SSPL, Delhi to confirm stress values and Dr. B.B. Sharma & Mr. Raman, SSPL, Delhi for providing FTIR measurement, to Prof. V.D. Vankar and Dr. B.R. Mehta, IIT, Delhi for providing spectroscopic ellipsometry data and Dr. S. Bera for providing XPS and XAES data, to Prof. G.K. Mehta (Director), Mr. Ajith Kumar and Mr. Venkatramanan of Nuclear Science Centre, New Delhi made it possible for us to have a indigenously produced VHF generator. I am indebted to them for their kind gesture.

For putting up with my idiosyncrasies and the absurdity of timings imposed by the pressure of work I am deeply thankful to Mr. Tuhin Mandal, Mr. R.R. Ramanan who shared not only my room but also my moments of grief and joy in equal measure.

I would also like to thank my friends Ajay, Deepak Kumar, S. Bose, N. Saxena, M. Das, Manju, Nimal, Hari, Jaikumar, Kaustuv, Murthy, Biswajit, Sharma for the constant support in day to day work that I received from them.

Financial assistance from CSIR for research fellowship and from CSIR and DST for sponsoring me to present some portion of my thesis work at the International Conference of Metallurgical Coatings and Thin Films-97, USA are gratefully acknowledged. I am indebted to Director, NPL for providing me facilities to carry out this work.

I express my sincere thanks to Dr. B.K. Das, NPL and Prof. L.K. Maheswari, BITS, Pilani for organising useful course work during the first year of the thesis period.

For satisfying my urges for meaningful social interactions I am thankful to Dr. and Mrs. Chowdhury, Dr. A. Chowdhury, Mr. S. Chowdhury, Dr. P.K. Basu, Mrs. Ratna Basu, Dr. and Mrs. Lal Chandra, Dr. Sanjit Das, Dr. A.K. Sarkar, Mr.. Kulwant Singh Nagi and his family.

I am indebted, for constant support and encouragement, to my parents, sisters, brothers, cousins and relatives throughout the period of my stay at NPL, for completing the task I had undertaken.

The acknowledgement would be incomplete without acknowledging the warm company that my niece Munai and nephew Samrat provided to my thoughts.

Debajyoti Sarangi

(*Debajyoti Sarangi*)

BIRLA INSTITUTE OF TECHNOLOGY & SCIENCE
PILANI, RAJASTHAN

CERTIFICATE

This is to certify that the thesis entitled ***STUDY OF DIAMOND LIKE CARBON (DLC) FILMS GROWN BY SOME NOVEL TECHNIQUES*** and submitted by **Debajyoti Sarangi** I.D. No. **92PZYF013** for award of Ph.D. Degree of the Institute, embodies original work done by him under my supervision.

Signature in full of the Supervisor R. Bhattacharya

Name in capital block letters Dr. R. BHATTACHARYA

Date: 8.3.98 Designation Sc.F

वैज्ञानिक
SCIENTIST
राष्ट्रीय भौतिक प्रयोगशाला
National Physical Laboratory
डॉ० के० एस० कृष्णन मार्ग
Dr. K. S. Krishnan Road,
नई दिल्ली-110012
New Delhi-110012

Preface

The present thesis embodies a number of investigations that have been carried out by the researcher in pursuit of a process that is capable of producing low residual stress diamond like carbon (DLC) films which could be applied over large areas for many promising device applications of this material. For such applications one is not only looking for films which have inherently low loss thereby allowing such films to adhere to a large variety of substrate materials and also to be grown to a sufficient thickness, the films should also have low optical absorption in the visible and IR ranges of the electro-magnetic spectrum. This requires them to have low amount of bound and unbound hydrogen as also high value of sp^3 content giving them thereby the diamond like properties, which, in turn, make them suitable candidate for many electronic applications. It may be noted that the present investigations formed a part of a large effort which this particular group at NPL, New Delhi, was required to make in order to meet the requirements of a development contract given to them by a defence agency which was interested in producing these films for a large area AR application in IR. It was also required that processing facility for such films be also designed and developed. This has naturally allowed the researcher many opportunities to experiment with a range of DLC deposition techniques such that RF magnetron sputtering, RF bias sputtering coupled with plasma decomposition of hydrocarbon gases (a method which was found to have many superlative properties as reported by Zelez from RCA laboratory, USA in the year 1983), PECVD of various kinds, PECVD at high frequencies etc. The fact that none of these above technique could either be perfected, led the researcher to consider saddle field fast atom beam (FAB) deposition as a alternative technique. It is emphasised here that this particular technique has many attractive features of the RF discharge coupled which the simplicity of operation of a DC power supply.

What is most important, however, is that by this uncomplicated technique one is able to produce films, which could have properties, if the process of growth is properly optimised, such as low hydrogen incorporation and high sp^3 content.

Thus the genesis of the problem lied in the deep felt need to develop a suitable process to meet the requirements of a particular development contract. The insight developed during this process and the appreciation of the problem of containing the very high residual stresses in these films led the researcher to define the present research problem.

This is an example where the needs of development research defines the outlines of a research problem for a Ph.D. thesis. This has, therefore, been a very satisfying experience for the researcher to be involved in unfolding the intricacies of growth of a fascinating material and its device applications.

Contents

Chapter I

Introduction

Chapter II

Growth and Characterisation of Diamond Like Carbon Films

Chapter III

Growth of Diamond Like Carbon Films by Plasma Enhanced Chemical Vapour Deposition Techniques

Chapter IV

Saddle Field Fast Atom Beam Deposited DLC Films

Chapter V

Filtered Fast Atom Beam Deposition of DLC Films

Chapter VI

Conclusions and Future Scope

Chapter I

Introduction

In the following a review of the existing knowledge relating to the material aspects of diamond, diamond like carbon (DLC) and nanocomposites is presented. In writing this review the researcher has drawn heavily from various published literature and, therefore, no claims to the originality is made. This is followed by the definition of the problem to be tackled.

1.1 Diamond : The Wonder Material

Diamond is a wide bandgap (5.5 eV) and probably the hardest (~105 GPa) known semiconductor.[1] The hardness of diamond makes it very attractive as a protective window for a softer optical material. Diamond has a high breakdown voltage, 20-40 times that of silicon and high electron and hole mobilities.[2,3] This makes diamond a material of choice for use in a transistor application. The use of diamond in a semiconductor device will ensure a high frequency and high power capability as compared to GaAs and Si. Since diamond has an exceptionally high thermal conductivity, it is efficient in use as a heat spreader (heat sink). The low coefficient of friction (0.05) compared with lubricant metals and graphite, extend the tool life of diamond cutting tools by reducing the heat generation. Due to the negative electron affinity of diamond, it can be used as a cold cathode, which may be applied to high power, high frequency vacuum devices and flat panel displays.[4-7] The chemical inertness of diamond makes it suitable as a protective coating. The efficiency of solar cell may be increased using diamond coatings. As an example, at wavelength 0.6 nm, the reflection from a silicon detector or solar cell is about 30%, but when coated with a 1/4 wavelength thick diamond film reflectivity is reduced to 6.6%. Silicon solar cell efficiency, thus, can typically be increased by 40% while that of germanium cells can be improved by as much as 88% by diamond coatings. Diamond is the most transparent material (refractive index of diamond

is 2.41 to 2.44). It transmits wavelengths from below 100 nm to above 1000 μm. The operating region of diamond is large as compared to Si and GaAs as shown in **Fig. 1.1**. The comparison of electrical properties of diamond with Si and GaAs are tabulated in **Table 1.1**.

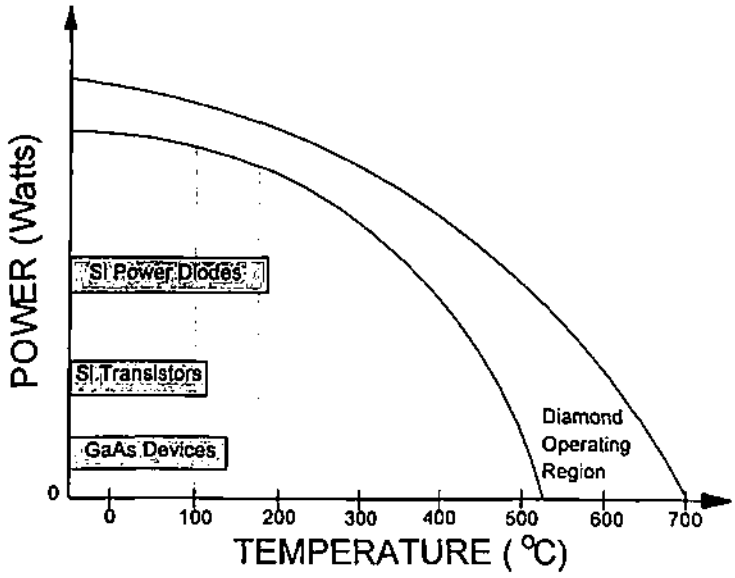

Fig 1.1 : Operating region of diamond in comparison to Si and GaAs[1]

Table 1.1 Comparison of semiconductor parameters between Si, GaAs, and Diamond[1]

Parameter	**Si**	**GaAs**	**Diamond**
Bandgap (eV)	1.11	1.43	5.45
Hole mobility (cm^2/volt sec)	1350	300	1800
Electron mobility (cm^2/volt sec)	480	8000	2000
Acceptor level (eV)	0.045(B)	O.035(Si)	0.35(B)
Donor level (eV)	0.045(P)	0.058(P)	0.1(P)
Resistivity (Ω cm)	10^5-10^2	10^8	10^{16}-10^{-2}
Breakdown field (volt/cm)	3×10^5	4×10^5	10^7
Saturation velocity (cm/sec)	1×10^7	1×10^7	2.7×10^7
Dielectric constant	11.7	15.8	5.6
Thermal conductivity(watt/cm K)	1.45	0.46	20.0
Work function (eV)	4.8	4.7	4.8

These interesting properties of diamond have, naturally, resulted in a tremendous amount of research work. **Table 1.2** shows some of the interesting applications of diamond films.

Table 1.2 Application of diamond films[1]

Application	Properties Required
Resonator diaphragms for tweeter loud speaker	High modulus of elasticity
Ultrahard tool coatings	High hardness
Sunglass lenses	High hardness, scratch resistance, optical transparency
Computer hard disk coatings	High hardness, low wear
Watch cases	High hardness, scratch resistance
Prosthetic coatings	High hardness, low wear
Optical coatings	High refractive index
Infrared laser window	Transparency to IR
Semiconductor device heat sinks	High thermal conductivity
Semiconductor devices	Large bandgap
Abrasive grain	High hardness

1.1.1 Deposition of Diamond Thin Films and its Limitations

The potential applications of diamond films have stimulated a great deal of research during the past few years on the synthesis of such films.[7-10] In general, the process of depositing diamond films can be classified as **A.** Chemical vapour deposition (CVD) process viz. hot filament CVD, electron assisted CVD, **B.** Plasma assisted chemical vapour deposition (PACVD) process viz. microwave assisted CVD, electron cyclotron resonance (ECR) plasma, PACVD using hollow cathode and **C.** Ion beam deposition process viz. ion beam sputtering, dual beam sputtering and laser ion beam technique.

The polycrystalline nature of diamond obtained through the different processes mentioned above, has certain inherent limitations.[11] For example **1.** It is difficult to grow large crystalline diamond at reasonable growth rates, **2.** It is difficult to achieve smooth diamond films because its polycrystalline nature results in a rough faced surface, **3.** It is difficult to coat diamond films over large areas with required thickness uniformity, **4.** High substrate temperature (>900°C) is required to grow such films and **5.** It is difficult to nucleate diamond on various substrates which would be necessary for most applications.

To overcome these difficulties for different applications, consistent scientific research efforts made possible yet another type of film which retains most of the properties of diamond and overcomes the above mentioned limitations to a large extent. These films are amorphous in nature and are called amorphous carbon or diamond like carbon (DLC) films.

1.2 Diamond Like Carbon (DLC)

Diamond like carbon (DLC) films constitute a new class of amorphous material having high hardness values and other important properties very close to diamond. Carbon exists in nature in different allotropic forms. It can form the stable trigonally (π) bonded crystal structure graphite, which is soft, optically opaque, electrically conducting and chemically active. Carbon can also form the metastable tetragonal bonded (σ) crystal structure diamond, which is the hardest material, transparent from far ultra violet to the far infrared, insulating and chemically inactive. Carbon, with the dilution of hydrogen, can also form polymer like structures. By controlling the amount of graphite, diamond and polymer phase a new type of material is described. If it is hard then it is termed as DLC or a-C:H (**Fig. 1.2**). In general to produce diamond a very high temperature is needed, but smoother DLC films can be grown on a variety of substrates over large areas, even at room temperature. This leads to a new area of interest for the scientists and technologists to use it for a variety of different applications.

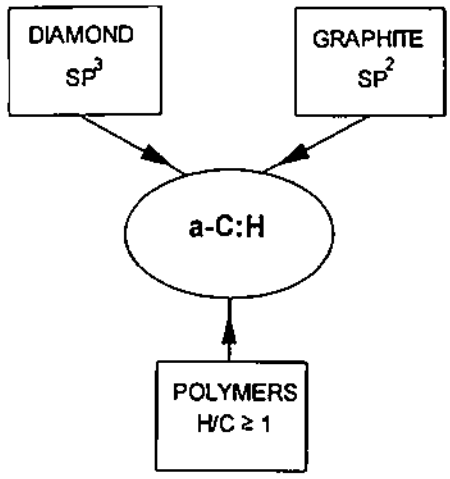

Fig 1.2 Limitations of a-C:H properties by the properties of diamond, graphite and hydrocarbon polymers[12]

1.2.1 Nomenclature

Aisenberg and Chabot[13] found that the films deposited from carbon ion beams were very hard, electrically insulating and wear resistant i.e. with properties very close to diamond. They used the term "*diamond like carbon*" to describe these films. These films were found to have mixed phases of diamond and graphite but no long range order i.e. they were amorphous in nature. So the term "*diamond like*" emphasises a set of properties akin to diamond and at the same time implies the absence of crystalline diamond order. By this definition, ***all diamond like carbon films are amorphous, but not all amorphous carbon are diamond like***.

A variety of nomenclature comes into the picture depending upon the preparation techniques and properties. Amorphous carbon (a-C) containing mostly graphite phase is prepared by pyrolysis, thermal evaporation and are very soft as compared to DLC. The various forms of DLC may be divided into two broad categories **1.** DLC films formed by carbon only are called amorphous carbon or amorphous diamond (i-C, ta-C) and **2.** DLC films containing a mixture of hydrogen and carbon are called hydrogenated amorphous carbon (a-C:H) or hydrogenated DLC. A

small fraction of metal (M) incorporation can also change the notation as M-C:H. Dilution of N_2 etc. can lead to another form a-C:H:N.

Figure 1.3 shows the atom number density vs. atom fraction of hydrogen expressed in gram atom/cm^3. This type of plot provides a convenient way of categorising the different classes of hydrocarbon and carbonaceous films.[14,15] Films with atom number density greater than 0.19 are designated as "*dense carbonaceous films*". Films containing significant amount of hydrogen are called "*dense hydrocarbon films*". The diamond like hydrocarbon (a-C:H) ranges from approximately 0.20 to 0.60 atom fraction hydrogen. The atom number density of a-C:H films increases with hydrogen content in contrast to the conventional hydrocarbons. The diamond like carbon (a-C) appears to be a different class of material, with little or no hydrogen and with atom number density from approximately 0.20 to 0.28 gram atom/cm^3. A comparison of the basic properties of several crystalline and amorphous carbon materials is listed in **Table 1.3.**[10]

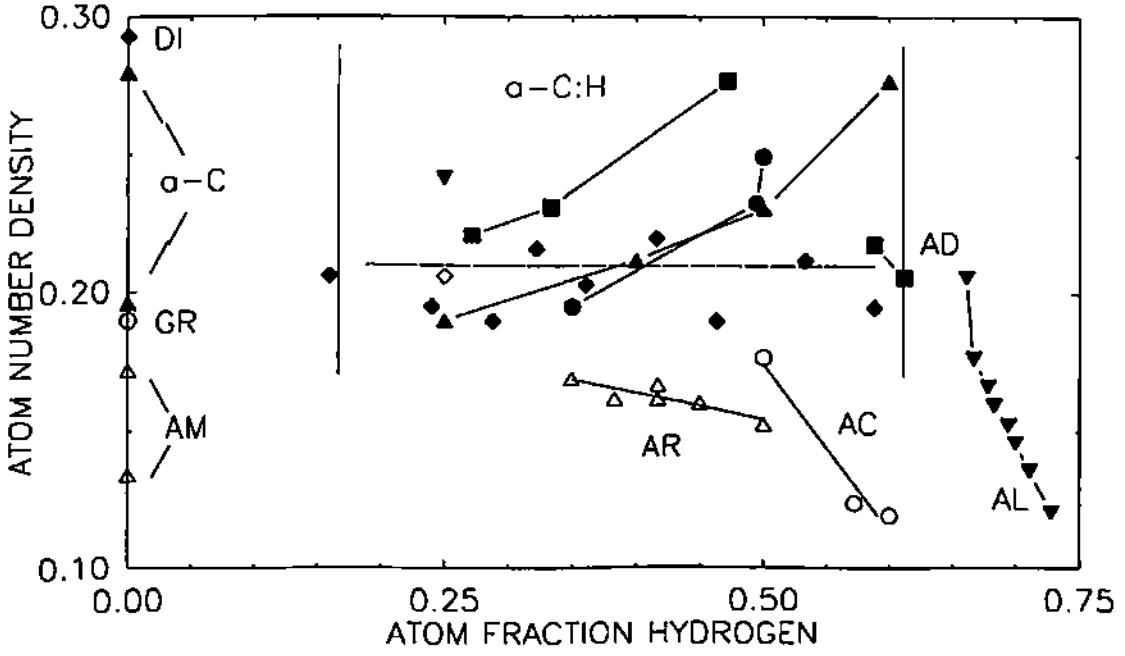

Fig. 1.3 Atom number density vs. atom fraction of hydrogen expressed in gram atom/cm^3. Symbols used are, AC - oligomers of acetylene, AD - adamantanes, AL - n-alkanes, AM - amorphous carbon, AR - polynuclear aromatics, DI - diamond and GR - graphite[15]

Table 1.3 Basic properties of several crystalline and amorphous carbon materials[10]

Material	Density (g/cm^3)	Optical bandgap (eV)	Hardness (GPa)	sp^3(%)	H(%)
Graphite	2.27	0.0	---	0	0
Glassy carbon	1.3-1.6	0.0	2-3	~0	~0
Evaporated C	1.9-2.0	0.4-0.7	2-5	<5	<5
Sputtered C	2.2-2.6	0.6-0.9	10	5-10	<5
i-C or a-C	2.9-3.4	2.5	100	>85	<5
Hard a-C:H	1.6-2.0	1.2-1.6	10-30	40-50	30-50
Soft a-C:H	0.9-1.2	1.6-4.0	<5	50-80	50-60
Polyethylene	0.9	6.0	0.01	100	66
Diamond	3.52	5.5	100	100	0

1.2.2 Hydrogenated Diamond Like Carbon (a-C:H)

Incorporation of hydrogen in DLC matrix makes the films diamond like hydrocarbon or hydrogenated diamond like carbon or hydrogenated amorphous carbon (a-C:H). Hydrogen in the DLC matrix, both in unbound and bound form, plays an important role in altering the film structure and properties. Of all types of DLC, a-C:H films are the easiest and probably cheapest to produce. Properties such as hardness, optical gap, hydrogen content, density etc. correlate in nearly the same manner for a variety of deposition techniques.

1.3 Deposition Techniques of DLC

The diamond like carbon films are formed when hydrocarbon radicals hit a substrate with impact energies from 50 to several hundred electron volts. The influence of impact energy on the type of film obtained is summarised in **Fig. 1.4.**[14] Holland and Ojha[16] first deposited hydrogenated diamond like carbon films from a hydrocarbon plasma. The properties of the DLC films depend on the type of technique used to grow the films and the process gas used.

DLC films have been prepared by a variety of methods,[11,14,17] including DC or RF plasma enhanced chemical vapour deposition (PECVD), sputtering, ion beam deposition, pulse laser deposition etc., using different carbon bearing, solid or gaseous source material. Different forms of the PECVD technique constitute the main methods for depositing hydrogenated DLC films. Among the PECVD methods, parallel plate RF reactor systems are the most common type employed, but microwave and electron cyclotron resonance (ECR) plasma reactors are also used occasionally.

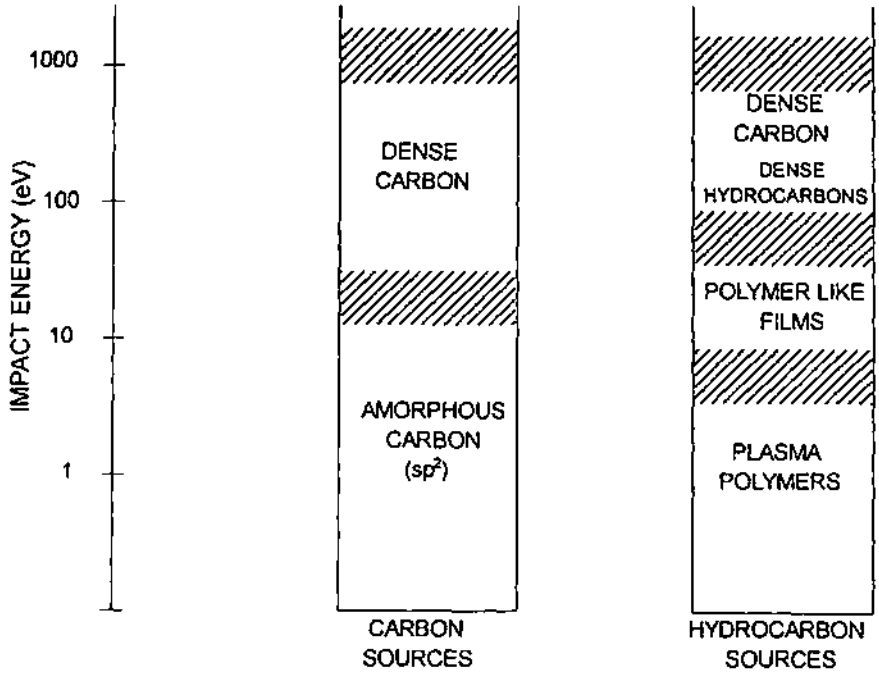

Fig. 1.4 Influence of impact energy on type of film produced[14]

Any hydrocarbon with sufficient vapour pressure can in principle be used as the source material for PECVD of DLC films. Among these are acetylene, benzene, butane, cyclohexane, ethane, ethylene, hexane, isopropane, methane, pentane, propane and propylene. Hydrogen has on occasion been added to these hydrocarbons; however, it appears that this addition is not required for the deposition of DLC films and does not significantly alter their properties.

Some of the techniques to deposit DLC films are shown in **Fig. 1.5(a)** and **1.5(b)** and also listed in **Table 1.4** with some of their specific advantages.

Table 1.4 Comparison of various deposition techniques for DLC deposition[11,14,17]

Process	**Type and quality of films produced**	**Advantages**	**Limitations**
Physical vapour deposition			
Ion beam sputtering	smooth, transparent a-C / a-C:H (with H_2 pressure) films	extremely good operational control	very low deposition rate, for small area
Dual sputtering beam	smooth, transparent a-C/a-C:H films	same as above	same as above
Laser-ion beam technique	a-C films	high deposition rate are possible	difficult to scale up to large area
Electron beam evaporation	a-C/a-C:H films in presence of hydrocarbon gas	wide variety depending upon substrate bias and precursors used	low dep. rate and process parameter dependent
Cathodic arc deposition	a-C films	transparent, good electronic quality	high internal stress, scaling difficult
Plasma assisted chemical vapour deposition			
RF & DC plasma assisted	smooth, transparent a-C:H films	high deposition rate on large area possible	large internal stress
Microwave and ECR plasma	transparent a-C:H films	high dep. rate	over heating at the resonance point
Cascaded arc plasma	smooth a-C:H films	high deposition rate on large area substrate, low contamination	large internal compressive stress

1.4 Deposition Mechanism

It has been discussed, in an earlier section, that the deposition of DLC films involves two basic methods, the ion beam related techniques and the glow discharge techniques. In both these cases of growing DLC films assistance from the gaseous plasma is obtained. But the two processes are different in the sense that in the ion beam related techniques films are deposited away from the plasma and in the glow discharges substrates are generally immersed in the plasma and the growing films are subjected to various interaction with energetic species in the plasma. The growth mechanism of DLC films may be different in these two cases.

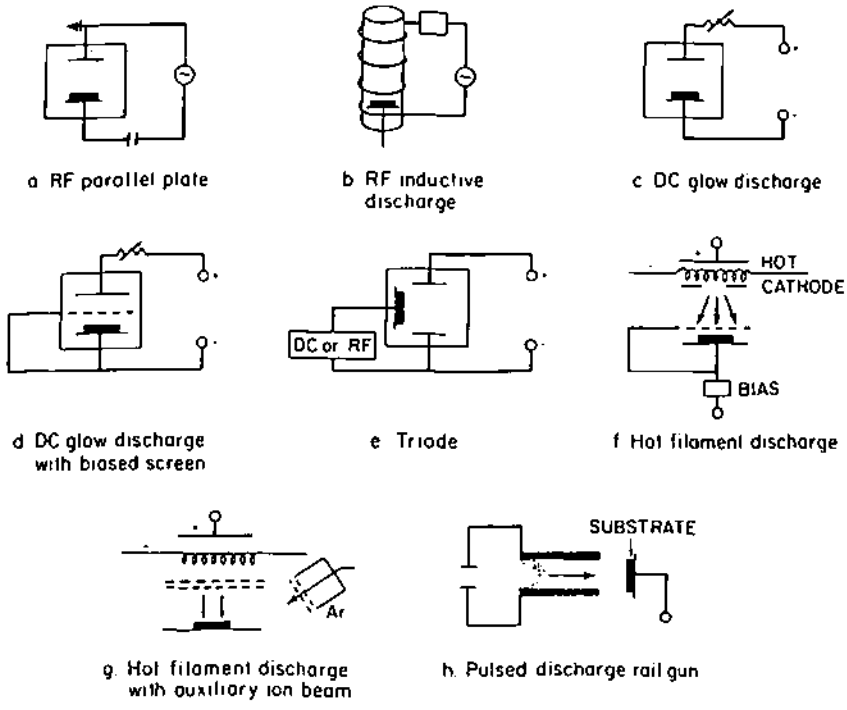

Fig. 1.5 (a) Process for growing DLC films from hydrocarbon gases[14]

To qualify amorphous carbon (a-C) or hydrogenated amorphous carbon (a-C:H) as good DLC material it should have properties like high sp^3 content, high hardness and density. Again any mechanism which is proposed to explain the growth of DLC films should explain the initial

nucleation, high sp^3 content, high hardness and high stress. Several such mechanisms have been proposed as explained below:

Kersten *et al.*[18] proposed that the incorporation of reactive particle into the growing film may be intermediated by an adsorbed layer (*adsorbed layer model*). The adsorption model is based on chemical reactions between the substrate and the film, and particles physisorbed form a weakly bound layer (monolayer). The decrease of deposition rate with temperature supports this model. But this growth mechanism can not explain by itself the low amount of hydrogen and the initial nucleation of sp^3 structure.

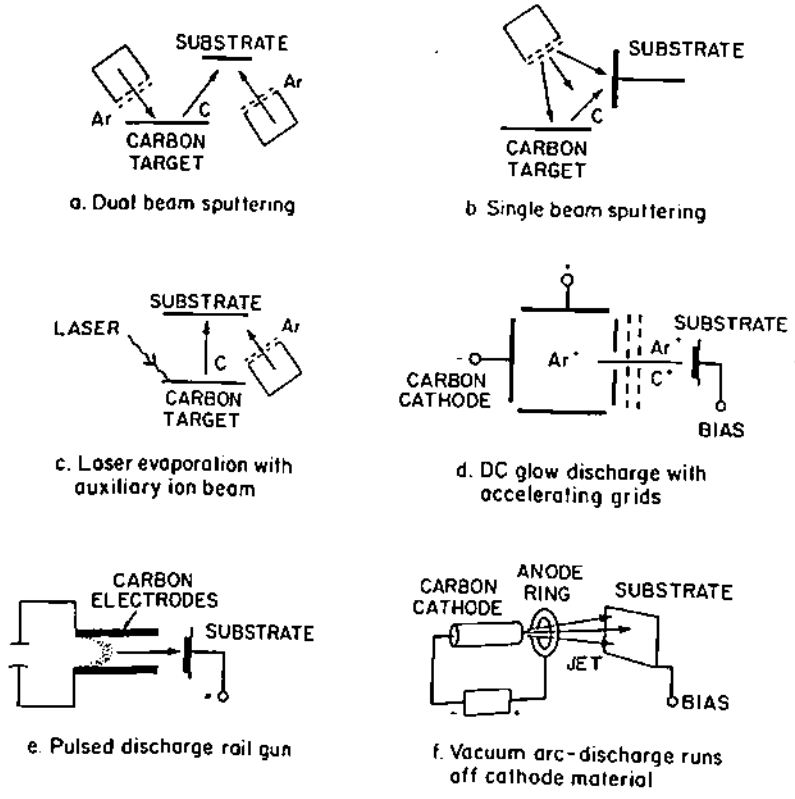

Fig 1.5 (b) Process for growing DLC films using solid carbon[14]

Spencer *et al.*[19] suggested the *"preferential sputtering"* mechanism to explain the growth of DLC films. Trigonally bonded (sp^2) structures sputter more easily than tetrahedrally bonded (sp^3) structures. The ion flux on the growing surface allows the film to grow and simultaneously sputters

the non-sp^3 structures. Both sputtering (etching) and deposition occur simultaneously. Since the C-H bond energy is less than C-C bond energy, low mass hydrogen sputters preferentially from the growing surface.

The energetic particles, involved in the growth of DLC films cause the atomic displacement and condensation of ion or atom, leading to a "*thermal agitation*" or "*thermal spikes*".[20] Transformation to sp^3 structure takes place during the life time of these spikes. A region of few nm in diameter is heated up to more than 10^3 K by particles of about 50 eV energy, and the spikes collapse within time intervals of the order of 10^{-11} sec. So the proposed transformation must take place extremely rapidly. Therefore, conventional phase transformation to a tetrahedral structure appears unlikely.

Another mechanism proposed to explain the formation of DLC films is that the very energetic and mobile surface species, in contact with the plasma or ion beams, are quenched by the underlying cold surface.[21,22] The metastable, constrained structure is "*frozen in*" by this process. The mechanism is supported by the fact that diamond like character is not obtained at high temperature. The elemental composition of the material "*frozen in*" is determined by competing kinetic processes at the surface and can be expected to be strongly dependent on the incident ion energy. In this view, the final sp^3/sp^2 ratio may be determined more by the energy of the rearrangement to form the solid than by the preferential sputtering of non sp^3 bonded structures or the presence of transient high pressure or temperature spikes. The presence of hydrogen during film condensation facilitates the formation of a network structure with an average co-ordination number close to that of a fully network terminator thus enhancing the rate of rearrangement of the network structure.

Experimental observations by Lifshitz *et al.*[23] are not satisfactorily explained by the concept of "*preferential sputtering*" and "*thermal spikes*" discussed above. They proposed that a shallow subsurface implantation process, called "*subplantation*", is involved in the formation of DLC films. The mechanism involved in the subplantation is the preferential displacement of sp^2 sites

leading to accumulation of sp^3 sites. This idea was based on estimates of the displacement threshold of graphite and diamond as 30 eV and 80 eV, respectively. But different researchers found that the displacement threshold for graphite is 35 eV[24] and for diamond is 37-47 eV[25] which are quite similar. This observation questioned the validity of the subplantation mechanism.

Robertson[26] proposed a similar deposition mechanism involving subplantation of incident ions. Incident ions of sufficient energy penetrate the solid, enter interstitial positions below the surface layer and increase the local density. Slower ions cannot penetrate the surface and just stick to the surface, forming sp^2 structure of low density. Faster ions penetrate further into the solid. However, only a certain energy, roughly the displacement threshold energy, is used to penetrate the surface. The rest of the energy is liberated as heat, in a thermal spike. The thermal spikes allow the local density to relax back towards that of sp^2 a-C. The subplantation process in effect compresses a-C into a denser but metastable phase.

In case of a-C:H films, ions, radicals and undissociated hydrocarbon gas molecules control the growth process. Temperature dependent growth rates confirm the contribution of neutrals in the growth process by an adsorbed layer. The neutrals are then fully incorporated into the film by *"ion-stitching"* being knocked into the film by an incident ion.[27]

In general, the incident ions cause two effects:**1.** Incident ions dehydrogenate the a-C:H by the preferential displacement of H atoms and **2.** Incident ions, via subplantation, compress the C-C skeleton into a denser phase at constant hydrogen content, raising the sp^3 fraction. The retained hydrogen is mobile during the thermal spike and will reform C-H bonds afterwards. This emphasises that while hydrogenation can raise the fraction of sp^3 sites, these would be only polymeric $(CH_2)_n$ groups, giving soft a-C:H. Only ion bombardment produces the quaternary C (unhydrogenated sp^3 C) needed to give hard a-C:H.

1.5 Properties of DLC

The properties of the DLC films largely depend upon the energy of the hydrocarbon ions striking the growing substrate.[14] With the increase of impact energy a-C:H evolves from transparent, hydrogen rich, polymerlike material to brittle, nearly opaque, conducting material resembling carbon glass. The most diamond like properties, for instance maximum hardness and density, are obtained at an intermediate energy range.

The atomic fraction of hydrogen (X_H) incorporated into the DLC matrix, in both bound and unbound form, controls the film properties. Bound hydrogen content in the film is mainly dependent upon the incident energy of the film forming radicals and it may also depend on the type of precursors and the preparation technique of the DLC films. The unbound hydrogen mainly depends upon the DLC growth techniques. The limit on X_H is influenced by the proportion of hydrogen in the source gas; a film with X_H>0.5 (H/C > 1) cannot be formed from benzene or acetylene (H/C =1).[10]

Thin DLC films (~1000A°) are fairly transparent in the visible region ($\propto \approx 10^3$-10^4 cm^{-1}). DLC films having thickness ~2000 A° are red brown in transmission, while thicker films are opaque. DLC films are quite transparent in the near infrared range with the exception of a strong absorption band near 3.4 μm due to C-H bond stretching. The optical bandgap (E_g) of the DLC films lies in the range of 0.8 to 2.5 eV. But E_g value as large as 3.0eV is also reported. As the hydrogen content increases, the E_g value increases to 2.5 eV and beyond, and the films appear transparent in the visible region. These films are, however, polymer like and soft. Optical bandgap is also found to decrease with the increase of deposition temperature.[28,29] It is reported recently that M/s Diamonex[30] have succeeded in preparing high visible transmission films of acceptable hardness in thickness of few microns.

DLC films are characterised by a large refractive index with relatively low dispersion. The refractive index varies from 1.8 to 2.3 in these films.[31,32] Hydrogen appears to lower the refractive

index. There have also been reports of good correlation between mass density and refractive index.[31]

The DLC films have mass densities in the range of 1.4 to 2.0 g/cm^3. Density is well correlated with the incident ion energy.[31] The highest density is obtained in harder films. Higher mass densities in the range of 2 to 3.4 g/cm^3 have been reported for films with lower H_2 content.[33,34] DLC films have hardness values of typically 9-30 GPa. Hardness of the DLC films is a strong function of growth conditions. The hardness is found to increase with the incident ion energy.[35] DLC films are very slippery and wear resistant even in dry sliding. The value of coefficient of friction (COF) is between 0.01 to 0.28 and is sensitive to humidity[36] and is reduced considerably in a very dry atmosphere or vacuum. Wear of DLC films is always much less than that of other very hard materials such as SiC, Si_3N_4 and TiN.

The adhesion of the films largely depends on the substrate and the method of preparation. Best adhesion is obtained on substrates that form carbides e.g. Si, Fe and Ti. Good adhesion has also been obtained on Ge and quartz.

The DLC films are usually found in a state of high compressive stress (4-7 GPa). The stress level increases with increasing hydrogen content.[37] Compressive stress arises when a growing film is bombarded by atoms or ions with energies of tens or hundreds of electron volts by a process of "*atomic peening*". The energetic ions cause atoms to be incorporated into spaces in the growing film which are smaller than the usual atomic volume and this leads to an expansion of the film outwards from the substrate. In the plane of the film, however, the film is not free to expand and the entrapped atoms cause macroscopic compressive stress.

The conditions of energetic bombardment which leads to the creation of high compressive stresses also favour the formation of dense thin films. Unfortunately, excessive compressive stress can cause adhesion failure and other undesirable effects. Reduction of compressive stress is, therefore, an important technological issue.

Studies of the temperature dependence of the electrical conductivity in the DLC films indicate that conduction is via *"thermally activated hopping"* of charge carriers between localised states. This localisation is presumed to occur on graphitic clusters. Usually conductivity of the order of 10^{-10} -10^{-12} $\Omega^{-1}cm^{-1}$ is observed in these films. Addition of dopants including B, P, N_2 and various metals increases the conductivity of DLC. However, this increase is usually accompanied by a decrease in optical gap. Thus it is not certain whether *n* or *p* type doping is actually achieved.

The electron spin resonance (ESR) spectra shows the presence of significant number of unpaired electrons. The value of spin density is in the order of 10^{18} cm^{-3} and is found to decrease with hydrogenation.[38]

DLC films are extremely resistant to chemical attack by both strong acids and strong bases. However, they are stable only to temperatures between 300°C and 400°C. Hydrogen evolves from DLC at higher temperature as the material converts to graphite in several steps.[39] After annealing to 600°C, almost all hydrogen is removed and DLC films become conducting, opaque, and much softer, similar to carbon glass.

1.6 Structure of DLC

To visualise fully the properties of DLC films it is very desirable to understand the detailed bonding and structure of DLC network. The detailed structure of the bonding network is still under study. Much attention has been given to the amount of tetrahedral and trigonal cross section i.e. the relative concentration of sp^3 and sp^2 hybridised carbon in these films. The sp^3/sp^2 ratio of DLC matrix depends on the growth techniques and conditions, hydrogen concentration and doping on the films etc. **Figure 1.6** shows the phase diagram showing composition of a-C:H, ta-C:H and ta-C (ta-tetrahedral). A variety of techniques have been used to estimate sp^3/sp^2 ratio,[39-42] including electron spin resonance (ESR), Raman spectroscopy, electron diffraction, optical spectroscopy, infrared spectroscopy (IR), X-ray photo electron spectroscopy (XPS), X-ray excited Auger electron spectroscopy (XAES), electron energy loss spectroscopy (EELS), nuclear magnetic resonance

(NMR) etc. In all cases, the measurements are sensitive to changes in films structure and properties.

Knowledge of sp^3/sp^2 ratio does not alone provide a full understanding of the microstructure of the DLC films. Information on homogeneity and to a lesser extent on structure has been obtained by transmission electron microscopy and diffraction analysis. The DLC films were found to be amorphous.[43] Sometimes crystalline phases in an amorphous matrix have been proposed, especially in films of lower hydrogen content.

For amorphous materials like a-Si:H, a-C:H, different structural models have been proposed, none of which has been generally accepted. The simplest model consistent with the observed H/C and sp^3/sp^2 bonding ratio would be a covalent network consisting of tetrahedrally and trigonally co-ordinated covalent atoms with some bonds being terminated by hydrogen.[46] McKenzie *et al.*[45] suggested a noncrystalline two phase structure consisting of polycyclic aromatic hydrocarbon regions interconnected by tetrahedral carbon. Smith[46] interpreted the optical constants in the frame work of an effective medium approximation, assuming a multiphase structure consisting of amorphous graphitic, diamond like and polymeric regions.

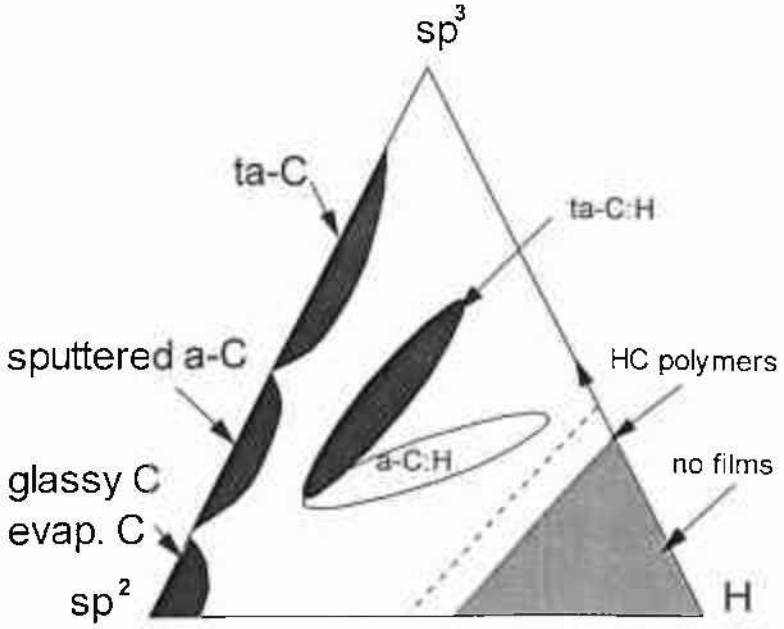

Fig. 1.6 Phase diagram showing composition of a-C:H, ta-C and ta-C:H[26]

The optical and electronic properties of DLC films are governed by their optical bandgap and electrical resistivity. Bredas *et al.*[47] proposed only a fused ring aromatic structure leading to optical bandgap lower than 2.0 eV. The electronic properties of DLC films are governed by the graphitic moieties. Robertson *et al.*[48-50] reviewed the electronic structure of DLC films. DLC films contain both sp^3 and sp^2 sites. The sp^3 sites form σ bonds while the sp^2 sites form both σ and π bonds. The strong σ bonds form the skeleton of the covalent network. The π bonds favour the segregation of sp^2 sites into graphitic cluster, embedded in a sp^3 bonded matrix. The π states lie closest to the Fermi level, so they control the electronic properties like the bandgap as shown in Fig. 1.7. Robertson and O'Reilly[49] showed that, the bandgap varies with cluster size as $E_g=6.0/M^{1/2}$ eV, where M is the number of six fold rings in the cluster. Using electronic structure calculations they also showed that as the overall hydrogen content decreases, these bonded clusters increase in size, giving rise to increased optical absorption and decreased bandgap. The lack of conductivity is explained by the fact that the clusters are sufficiently spatially isolated so that there is no π electron orbital overlap.

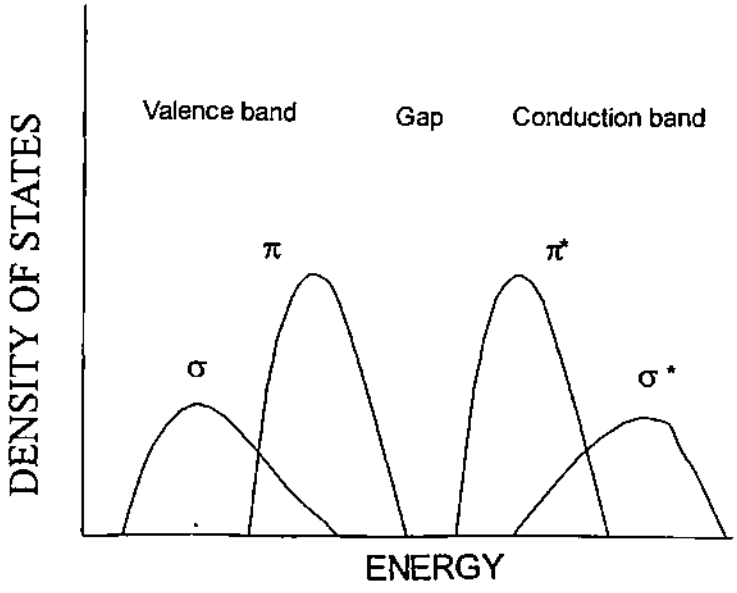

Fig. 1.7 Schematic electronic density of states (DOS) of DLC[26]

The connection between local co-ordination and macroscopic properties is made through the concept of random covalent networks (RCN). Two types of RCN treatments have been applied to DLC:

(i) The theory of optimally constrained networks described by Thrope,[51] which defines the minimal degree of network connectivity required to achieve macroscopic rigidity, and

(ii) A treatment of overconstrained networks in which the degree of overconstraint is connected to macroscopic elastic properties by a simple empirical relationship.[52]

The concept of an optimally constrained network is based on the fundamental statement that a network cannot be rigid unless the number of translational oscillations of nonzero frequency is equal to the number of degrees of freedom in the network, 3N-3, where N is the number of nodes in the network. In the absence of clustering, each atom is a node. A straightforward derivation shows that this condition is met when mean atomic co-ordination, N_{av} is exactly 2.4. For a random network consisting of carbon and hydrogen only, the overall degree of fourfold carbon co-ordination must vary with hydrogen content as

$$f_4 = (8X_H - 3)/5(1 - X_H)$$

The relationship defines the solid curve labelled RCN in the hydrocarbon "*phase diagram*" shown in **Fig. 1.8**. The degree to which overconstraint translates into hardness is determined by the amount of clustering in the network; N_{av} may be inflated by locally overconstrained clusters that cannot contribute to the macroscopic elastic properties. The graphitic clustering inferred from Raman and optical measurements can be accommodated by grouping all threefold co-ordinated carbon into larger multi atom nodes and renormalising to the newly reduced number of nodes. The curve for optical constraint with large graphitic clusters is given by

$$f_4 = 5X_H/8(1-X_H)$$

and is shown on the "*phase diagram*" as the dashed line labelled C-RCN. The modified form of the RCN model coincides well with the NMR measurements. This indicates that a-C:H consists of graphite clusters, which define most optical properties, locked in a slightly overconstrained network that defines its mechanical properties.

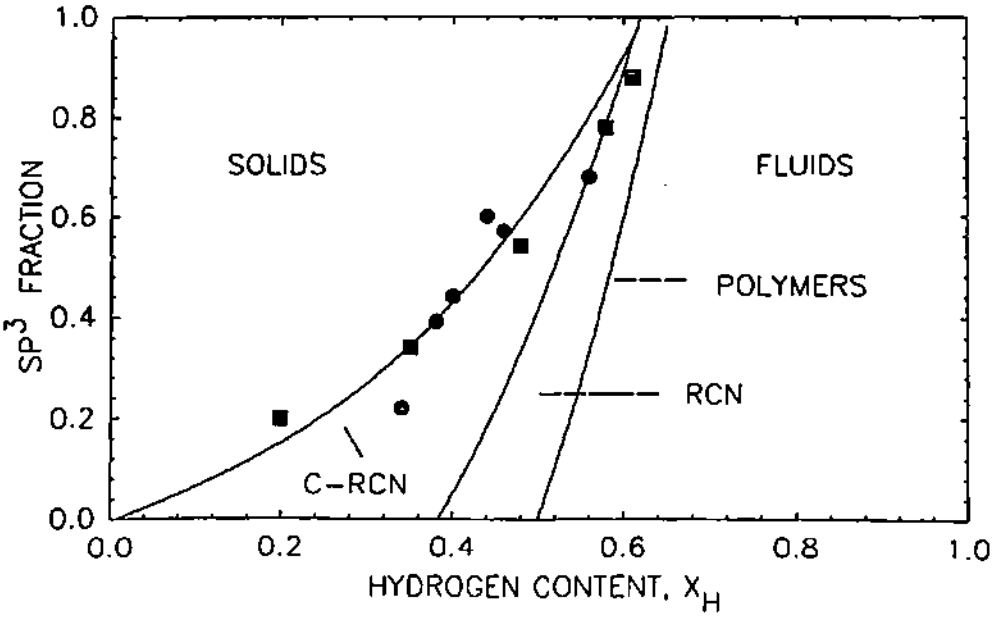

Fig. 1. 8 The hydrocarbon phase diagram. The solid curve (RCN) represents optimally constrained random covalent networks without clustering and the dashed curve (C-RCN) is for random network with large graphitic clustering[10]

Although formally rigid, optimally constrained networks cannot be macroscopically hard. It must be confirmed that the small degree of overconstraint is sufficient to account for the observed hardness of DLC. He and Thrope[52] treated an overconstrained RCN in a simulation in which bonds were randomly deleted from a diamond lattice and the resulting elastic properties calculated as a function of the average constraint in the remaining network. They found an empirical relationship between N_{av} and elastic modulus,

$$E = E_o[(N_{av}-2.4) / (N_o-2.4)]$$

where N_o=4 and E_o is the modulus of the original lattice. Because hardness is approximately linear with modulus, this can be used to estimate hardness, H, by replacing E_o with H_o for diamond.

Thus, it is seen that, the hard, rigid mechanical nature of the films must arise from the structure of the matrix that makes up the bulk of the film. Angus and Jansen[53] modelled the diamond like hydrocarbon films as a fully constrained non crystalline network (FCN model) using the constraint counting arguments of Phillips,[54] Thrope[51] and Dohler.[55] The predictions of sp^3/sp^2 ratio and the average co-ordination number are in general agreement within the available experimental observations, particularly at the upper end of the hydrogen composition range. The model, as originally derived, predicts a range of compositions, from 0.17 to 0.62 atom fraction hydrogen, over which a fully constrained network comprising sp^3 and sp^2 co-ordinated carbon atoms and hydrogen atoms can exist. The predicted stability range is in agreement with the observations.

Tamor has proposed a "*defective graphite model*" for the structure of the diamond like hydrocarbon.[56] In this model an initially perfect graphite crystal is modified by removing carbon atoms and saturating the resulting dangling bonds with hydrogen. Percolation theory is used to predict the upper and lower limits of hydrogen concentration. The defective graphite model predicts an existence range of diamond like hydrocarbons from 0.2 to 0.6 atom fraction hydrogen. It is remarkable that this model, which is based on different assumptions, predicts a similar existence range as the constrained network model. **Figure 1.9** shows the proposed two dimensional model of DLC matrix.

1.7 Hydrogen Free DLC (a-C)

Hydrogen free diamond like carbon films (a-C) containing little hydrogen can be prepared by sputtering of a carbon target,[57] by direct ion beam deposition from carbon ion beams[58] or by condensation of carbon plumes produced by laser vaporisation.[59] The densities of the non-hydrogenated diamond like carbons have been reported[57] to be as high as 3.1 g/cm^3, which is closer to the density of diamond (3.51 g/cm^3) than that of graphite (2.26 g/cm^3). This unusually high density alone indicates an unusual structure. The density of the films and the fraction of sp^3 bonding increases as temperature of the substrate is decreased.[57] There are well documented

reports that indicate these films posses exceptional hardness, in some cases greater than that of diamond.[59]

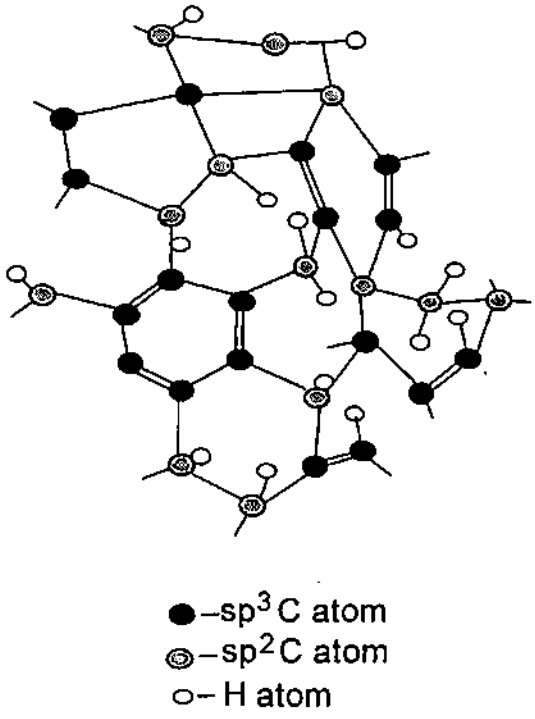

Fig. 1.9 A two dimensional representation of diamond like carbon films structure[22]

The constraint counting arguments used to describe the hydrogenated films show that a non-hydrogenated, non crystalline network made up solely of sp^3 and sp^2 carbon sites will be highly over constrained. Bonding constraints can be reduced by formation of clusters or microcrystallinity and this may be the source of stability for these unusual materials. In fact, recent molecular dynamics studies[60] show that several types of medium range order may be present in the non-hydrogenated amorphous carbons including five, six and seven membered rings and local clustering of sp^3 sites.[61] Tamor has concluded on the basis of his defected graphite model that it is unlikely if more than 10% of the carbon sites in non-hydrogenated diamond like carbons are four-fold coordinated.[56] However, recent k-edge absorption studies by Cuomo indicate upto 40 percent of the carbon atoms in a-C may be tetrahedral, sp^3 sites.[57]

1.8 Metal Containing a-C:H

Diamond like carbon films containing little amount of metal (e.g. W, Ta, Ru, Fe, Ti etc.) in their matrix are termed as metal containing a-C:H or M-C:H. The films were been prepared by codeposition of hydrocarbon/carbon and various metals, e.g. by sputtering a metal target in a hydrocarbon atmosphere. These materials have been found to be of great interest due to their favourable mechanical and tribological properties.[62] The friction coefficient of metal containing M-C:H films were much less dependent on humidity. Iron containing films exhibited reduced friction (0.04) while R_u-containing films exhibited increased friction (0.7). Incorporation of tungsten was found to increase the wear resistance. Incorporation of Si upto 30% reduced the coefficient of friction to 0.05 and further they were found to be independent of humidity.[63]

1.9 Diamond Like Nanocomposite (DLN)

Diamond like nanocomposite (DLN) is a new class of amorphous material similar to DLC. Drofman *et al.*[64] first grew this material and have shown that the structure of these films consist of atomic scale composites of two interpenetrating diamond like (a-C:H) and quartz like (a-Si:O) random network. The diamond like network is stabilised by hydrogen and quartz like network is stabilised by oxygen resulting in a purely amorphous structure[64-66] as shown in **Fig. 1.10**. The mutual stabilisation of these interpenetrating atomic scale filaments and the common random network structure prevents the growth of graphitic carbon at high temperature, serving to enhance adhesion and to reduce the internal stress in these films. Such self-stabilised C-Si amorphous structure form an ideal matrix for the introduction of the metal (W, Ti, Zr, Ni etc.). These metals are distributed as separate atoms or as separate networks, and all these networks (the carbon matrix, a-Si and a-MeO) are bonded to one another by weak chemical forces.

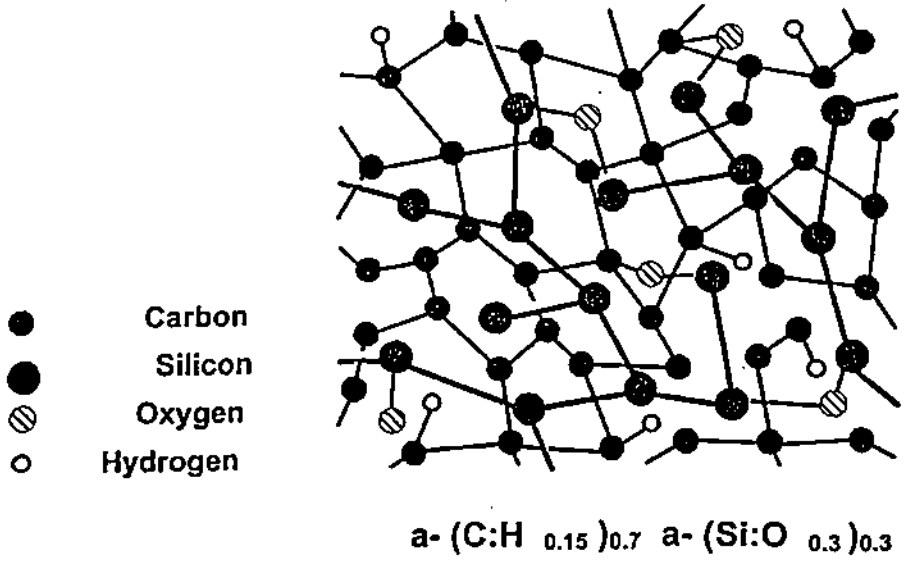

Fig. 1.10 Proposed DLN structure[65]

DLN films are grown by plasma polymerisation of silicon organic precursors of carbon and silicon (viz. polyvinylsiloxanes).[65-67] DLN synthesis involves codeposition of cluster less beams of

C-containing and Si-containing radicals and, optionally, ions and/or atoms of the transition metals. The methods of pure amorphous DLN synthesis involves the exclusion or minimisation of cluster formation in the sources, in the primary plasma, in the deposition region and during film growth. Radicals are formed via glow discharge plasma breakdown of the precursor using a quasi closed plasmatron and DC (0.3 - 5.0 kV) or high frequency (90-450 kHz, 0.3-5.0 kV) fields are used to transport the radicals to the substrate. Incorporation of metallic elements into the diamond like network is achieved by coevaporation. Substrate temperature is in the range of 150-200°C. Typical deposition rate is 1.0 to 3.0 μm/hour.

DLN films shows some improved properties as compared to DLC as listed in the **Table 1.5.**

Table 1.5 Some properties of DLN films[65]

Property	**Range of obtainable values**
Coefficient of friction	0.03-0.2
Adhesion	10^7-10^9 N/m^2 Adhere to a wide range of substrates including metals, plastics and ceramics; no interlayers required
Thermal stability	Stable to 400-600°C in air; capable of 1000-1200°C in absence of oxygen
Physical flexibility	Very flexible; does not crack while beak
Corrosion and erosion	Resistance to acids, alkalis and particulates due to pore free structure
Electrical conductivity	~10^{-4}-10^{-14} Ω^{-1} cm^{-1}
Dielectric breakdown strength	10^6-10^8 volt/cm
Hardness	10-22 GPa
Modulus of elasticity	150-200 GPa
Residual stress	200-300 MPa
Index of refraction	1.7-3.1
Infrared transmission	80-95% at 2-25 μm
Ultraviolet transmission	Opaque

The applications of DLN films are similar to DLC films and offer more flexibility than DLC films. Some of the important applications of DLN films are listed below:

* Thin films, wear resistant electrical heaters
* Thermal and chemical diffusion barriers
* Electrochemical contacts
* Catalyst supports for fuel cells
* Thin film capacitors
* Window coatings for thermal management
* Microwave applications: fine frequency tuning
* Coatings for magnetic/optical media
* Protection against ablation in laser devices
* Low friction coatings on moving parts
* Protection against corrosion at high temperature
* Biocompataible wear resistant coatings
* Protection of lenses, controlled opticals
* UV protection
* Protection against salt water and abrasion

1.10 Definition of the Problem

As discussed earlier in **section 1.3**, that a large number of techniques have been used to grow DLC films. On the basis of different review articles describing DLC deposition techniques, there are probably more than seven hundred techniques or variants of techniques being used throughout the world. In Japan alone, over 200 patents have been filed in this area over the last 15 years.[68] However, none of these techniques can be treated as perfect enough to eliminate all the drawbacks of DLC deposition. It has also been found that the DLC films deposited by the conventional techniques possess very high compressive stress, of the order of several Giga Pascal (GPa), resulting sometime in the delamination of the film from the substrates. Various investigations that have been conducted by the researcher and an account of which is embodied in this thesis are, therefore, to identify the specific reasons which cause such high compressive stress in DLC films and then to develop technique(s) which would be easy to implement and the DLC films so formed should show lower stress values and should not readily age.

To achieve the above goal, first a very systematic study of DLC films grown by the conventional RF asymmetric self bias technique has been carried out. The effect of operating at VHF frequencies has been subsequently explained. The limitations of these techniques are then discussed. It is this appreciation of the limitations of the RF asymmetric PECVD technique that forms the basis of all that have been suggested and implemented by the researcher subsequently.

The search for a suitable technique meeting requirements of low stress and ease of operation, lead the researcher to consider saddle field fast atom beam (FAB) technique. The reasons to concentrate research efforts on FAB produced DLC films are as stated below. Grill *et al.*[69] pointed out that perhaps presence of significant amount of unbound hydrogen plays an important role in the formation of high built-up stress in the DLC films. DC discharge technique has been found by them to be better suited rather that RF asymmetric self bias technique. However, DC technique has certain inherent limitations for depositing insulating DLC films. FAB is one technique which though operates on a DC power supply but the potential profile is like that obtained in a RF discharge.

The FAB source, therefore, has the attributes both of the RF and DC glow discharge and none of their shortcomings. Insulating DLC films can therefore be deposited easily on insulating substrates by this technique.

The main objective of the present investigation is to find in what specific ways saddle field fast atom beam deposition technique deviates from the more conventional RF asymmetric PECVD technique. This is accomplished by carrying out a detailed optimisation study of the process and an extensive characterisation of the films produced by this technique.

Further the *"lost memory effect"* i.e. the absence of dependence of the DLC film properties on the nature of hydrocarbon source gases/vapours used need to be confirmed (this was earlier believed to exists in the case of RF self bias deposition technique). The scaling of deposition rate with the variation of the ratio of C/H in the starting material for the films grown by this specific method of deposition needs also to be established.

To understand fully the operation of a FAB source the detailed characterisation of the beam coming out of the FAB source needs to be analysed by measuring beam current density and the neutralisation coefficient. An attempt to filter out the ionic radicals of the beam coming out from the FAB source using a deflector arrangement appeared to led to interesting possibilities. Using this technique it should be possible to grow DLC films simultaneously by neutral and ionic radicals. A detailed characterisation study of these two type of films then needs to be carried out.

Finally an assessment of the relative merits of this technique vis-à-vis more conventional RF self bias and ion beam techniques needs to be made in respect of the following

(i) The simplicity of the method of deposition

(ii) The stress behaviour of the DLC films so deposited

(iii) Suitability of the technique for realising various industrial applications of DLC

(iv) Upscaling of the process for commercialisation.

1.11 References

1. M.N. Yoder in *Diamond and Diamond-Like Films and Coating*, eds. R.E. Clausing *et al.* (Plenum, New York) (1991) p. 1.
2. A.V. Bogdsanov, I.M. Vikulin and T.V. Boddoanovas, *Sov. Phys Semicond.*, **16** (1982) 720.
3. M.W. Geis, *Proc. IEEE*, **79** (1991) 669.
4. F.J. Himpsel, J.A. Knapp, J.A. VanVechten and D.E. Eastmen, *Phys. Rev. B*, **20** (1979) 624.
5. M.W. Geis, J.A. Gregory and B.B. Pate, *IEEE Trans. Electron Devices*, **38** (1991) 619.
6. M.W. Geis, N.N. Efremow, J.D. Woodhouse, M.D. McAleese, M. Marchywka, D.G. Socker and J.H. Hochedez, *IEEE Electron Device Lett.*, **12** (1991) 456.
7. M.W. Geis, *Thin Solid Films*, **216** (1992) 134.
8. G.S. Gildenblat, S.A. Grot and A. Badzian, *Proc. IEEE*, **79** (1991) 647.
9. D. S. Hoover, S. Lynn and D. Garg, *Solid State Technol.*, **Feb.** (1991) 89.
10. M.W. Geis and M.A. Tamor, *Encylopedia of Applied Physics*, Vol. **5**, p. 1
11. C.V. Deshpandey and R.F. Bunshah, *J. Vac. Sci. Technol.* A, 7 (1989) 2294.
12. P. Koidl, C. Wild, R. Locher and R.E. Sah in *Diamond and Diamond-Like Films and Coating*, eds. R.E. Clausing *et al.* (Plenum, New York) (1991) p. 243.
13. S. Aisenberg and R. Chabot, *J. Appl. Phys.*, **42** (1971) 2953.
14. J.C. Angus, P. Koidl and S. Domitz in *Plasma Deposited Thin Films,* eds. J. Mort and F. Jansen (CRC Press, Boca Raton, FL) **Chapter 4** (1986) p. 89.
15. J.C. Angus and C.C. Hayman, *Science*, **241** (1988) 913.
16. L. Holland and S.M. Ojha, *Thin Solid Films*, **38** (1976) L17.
17. Y. Catherine in *Diamond and Diamond-Like Films and Coating*, eds. R.E. Clausing *et al.* (Plenum, New York) (1991) p. 193.
18. H. Kersten and G.M.W. Kroesen, *J. Vac. Sci. Technol.* A, **8** (1990) 38.
19. E.G. Spencer, P.H. Schmidt, D.C. Joy and F.C. Sansalone, *Appl. Phys. Lett.*, **29** (1976) 118.
20. C. Weissmantel, *J. Vac. Sci. Technol.*, **18** (1981) 179.
21. J.C. Angus, F. Jansen, *J. Vac. Sci. Technol.* A, **6** (1988) 1778.

22. J.C. Angus and Y. Wang in *Diamond and Diamond-Like Films and Coating*, eds. R.E. Clausing *et al.* (Plenum, New York) (1991) p. 173.
23. Y. Lifshitz, R.R. Kasi and J.W. Rabalais, *Phys. Rev. B,* **41** (1990) 10468.
24. H.J. Steffen, D. Marton and J.E. Rabalais, *Phys. Rev. Lett.*, **68** (1992) 1726.
25. J. Koike, D.M. Parkin and T.E. Mitchell, *Appl. Phys. Lett.*, **660** (1992) 1450.
26. J. Robertson, *Diamond and Related Mater.*, **2** (1993) 984; *Phil. Trans. Roy. Soc. A,* **342** (1993) 277, *J. Non-Crst. Solids*, **164-166** (1993) 1115.
27. N. Moller, *Appl. Phys.* A, **56** (1993) 527: *Appl. Phys. Lett.*, **62** (1993) 937.
28. B. Meyerson and F.W. Smith, *J. Non-Cryst. Solids,* **35-36** (1980) 435.
29. S. Lin and B.J. Feldman, *Philos. Mag.* B, **47** (1983) 113.
30. Information Brochure, *Diamonex Performance Products*, USA.
31. A. Bubenzer, B. Dischler, G. Brandt and P. Koidl, *J. Appl. Phys.*, **54** (1983) 4590.
32. T.J. Moravec and J.C. Lee, *J. Vac. Sci. Technol.* A, **20** (1982) 829.
33. A.R. Nyaiesh and W.B. Nowak, *J. Vac. Sci. Technol.* A, 1 (1983) 308.
34. J. Zelez, *J. Vac. Sci. Technol.* A, 1 (1983 305.
35. T. Mori and Y. Namba, *J. Vac. Sci. Technol.* A, **1** (1983) 23.
36. K. Enke, H. Dimigen and H. Hubsch, *Appl. Phys. Lett.*, **36** (1980) 291.
37. J.C. Angus, C.C. Hayman and R.W. Hoffman in *Diamond Optics*, Proceedings of SPIE, **969** (1988) 2.
38. F. Jansen, M. Machonkin, S. Kaplan and S.J. Hask, *J. Vac. Sci. Technol.* A, **3** (1985) 605.
39. B. Dischler, A. Bubenzer and P. Koidl, *Solid State Commun.*, **48** (1983) 105.
40. F. Demichelis, C.F. Pirri and T. Tagliaferro, *Phys. Rev. B*, **45** (1992) 15364.
41. R.H. Jarman, G.J. Ray, R.W. Standley and G.W. Zajac, *Appl. Phys. Lett.*, **49** (1986) 1065.
42. J.C. Lascovich, R. Giorgi and S. Scaglione, *Appl. Surf. Sci.*, **47** 17 (1991).
43. C. Weissmantel, K. Bewilogua, K. Breuer, D. Dietrich, U. Ebersbach, H.J. Erler, B. Rau and G. Reisse, *Thin Solid Films*, **96** (1982) 31.
44. S. Craig and G.L. Harding, *Thin Solid Films*, **97** (1982) 345
45. D.R. McKenzie, R.C. McPhedran, N. Savvides, L.C. Botten, *Philos. Mag.* B, **48** (1983) 341.
46. F.W. Smith, *J. Appl. Phys.*, **55** (1984) 674.

47. J.L. Bredas and G.B. Street, *J. Phys.* C, **18** (1985) L651.
48. J. Robertson, *J. Non. Cryst. Solid*, **198-200** (1996) 615.
49. J. Robertson and E.P. O'Reilly, *Phys. Rev.* B, **35** (1987) 2946.
50. J. Robertson, *Adv. Phys.*, **35** (1986) 317.
51. M.F. Thrope, *J. Non-Cryst. Solids*, **57** (1983) 355.
52. H. He and F. Thrope, *Phys. Rev. Lett.*, **54** (1985) 2107.
53. J.C. Angus and F. Jansen, *J. Vac. Sci. Technol.* A, **6** (1988) 1778.
54. J.C. Phillps, *Phys. Rev. Lett.*, **42** (1979) 153.
55. G.H. Dohler, R. Dandaloff and H. Bilz, *J. Non-Cryst. Solids*, **42** (1980) 87.
56. A. Tamor and C.H. Wu, *J. Appl. Phys.*, **67** (1990) 1007.
57. J.J. Cuomo, Proceeding of workshop on the science and technology of *Diamond Thin Films* (American Carbon Society), May 20-24 (1990).
58. P.J. Martin, S.W. Filupczuk, R.P. Netterfield, J.S. Field, D.F. Whitnall and D.R. Mckenzie, *J. Mat. Sci. Lett.*, 7 (1988) 410.
59. F. Davanloo, E.M. Juengerman, D.R. Jander, T.J. Lee and C.B. Collins, *J. Appl. Phys.*, **67** (1990) 2081.
60. J.C. Angus, C.C. Hayman and R.W. Hoffman, in *Diamond Optics proceeding of SPIE*, **969** (1988) 2.
61. G.Galli, R.M. Martin, R. Car and M. Parrinello, *Phys. Rev. Lett.*, **62** (1989) 555.
62. H. Dimigen, H. Hubsch and R. Memming, *Appl. Phys. Lett.*, **50** (1987) 1056.
63. K. Oguri and T. Arai, *J. Mater. Res.*, **5** (1990) 2567.
64. V.F. Dorfman and B.N. Pyokin, *Surf. & Coatings Technol.*, **48** (1991) 193.
65. V.F. Dorfman, *Thin Solid Films*, **212** (1992) 267.
66. V.F. Dorfman, A. Bozhko, B.N. Pypkin, R.T. Borra, A.R. Srivatsa, H. Zhang, T.A. Skotheim, I. Khan, D. Rodichev and G. Kirpilenko, *Thin Solid Films*, **212** (1992) 274.
67. J. H. Lee, D. S. Kim, Y. H. Lee and B. Farouk, *Thin Solid Films*, **280** (1996) 204.
68. D. Tither, A. Matthews, P. John and J. Wilson, *Surf. & Coatings Technol.*, **38** (1989) 251.
69. A. Grill, Patel and B.S. Meyeroson in *Diamond and Diamond-Like Films and Coating*, eds. R.E. Clausing *et al.* (Plenum, New York) (1991) p. 417.

Chapter II

Growth and Characterisation of Diamond Like Carbon Films

2.1 Introduction

The chapter begins with a brief review of the different innovations that have been made and the techniques that have been developed to reduce stresses in diamond like carbon (DLC) films to date. Details of the plasma reactors used for the present investigations are subsequently given. This is followed by brief descriptions of different characterisation techniques used during the present investigation. Finally a brief description of the model used to determine the carbon bonding ratio (sp^3/sp^2) in DLC films has been presented.

2.2 A Review of the Stress Reduction Efforts

Zelez[1] first reported the growth of low stress ($<10^8$ dyne/cm^2 i.e. <0.01 GPa) DLC films using a hybrid process involving reactive bias sputtering of ultrapure carbon targets together with plasma decomposition of normal butane. The films, reported by Zelez,[1] indeed, had some superlative properties including low hydrogen content, high IR and visible transmission and high bandgap. Robertson[2] in his review made a special mention of this work. However the researcher could not reproduce the said results in the experiments undertaken in this laboratory. This therefore requires further investigation.

Substrate temperature at the time of the film deposition may affect the built up stress in the DLC films. Yamada *et al.*[3] found a linear relationship between the internal stress of DLC films and the deposition temperature over the range 0 to 150°C. An increase in the internal film stress from 0.48 to 1.5 GPa has been reported by them against the increase of deposition temperature of the above mentioned range. Y. Catherine[4] has also mentioned that in order to obtain hard and nearly transparent DLC films, it is necessary to keep the substrate temperature as low as possible because the electron and ion fluxes cause considerable substrate heating.

The other important effort towards reduction of residual stress includes annealing of DLC films. Grill *et al.*[5] reported that annealing at 440°C reduced the stress in their films. It was found that DLC films deposited by DC excited technique exhibit smaller stress values than the films deposited by RF PECVD technique.[6] On further investigation Grill *et al.*[6] could find a correlation between the high residual stress and unbound hydrogen in these films. Inherent in the way DC plasma excited films are grown is the feature that less unbound hydrogen gets incorporated in them as compared to the films grown by RF excitation technique. Stress values in DLC films, for a particular deposition technique adopted, was also found to depend on the type of hydrocarbon gases or vapours used. This was traced to be due to their different dissociation energies and corresponding production of varying degrees of unbound hydrogen.

The attempt to dope DLC films lead to some interesting results. Among the various dopants like nitrogen, fluorine etc., N_2 has been found to be particularly good for the reduction of stress in these films. Torng *et al.*[7] reported that nitrogen incorporation in amorphous carbon (a-C) films produced by sputtering in the argon/nitrogen plasma helped to overcome delamination problems to a great extent. Franceschini *et al.*[8] have also reported internal stress reduction by nitrogen incorporation in hard amorphous carbon thin films. Nitrogen atom admits a co-ordination equal to 3 at most (sp^3 hybridised nitrogen). Therefore, the replacement of carbon by nitrogen in a-C:H films implies a reduction of the average co-ordination number and hence the degree of over constraining. This change in co-ordination number could be responsible for the internal stress reduction in a-C:N:H films.[8]

From the above review it becomes abundantly clear that, though the RF self bias technique is very common, it often fails to grow low stress DLC films. In the RF self bias technique to achieve sufficient self bias voltage one needs to input high RF power which, in turn, increases the unbound hydrogen. Secondly, application of higher power leads to an increase in the energy of the ions/radicals responsible for the growth of DLC films. The ions/radicals after being stabilised, release energy to the growing surface, resulting in an increase in the temperature of the growing films. This again plays an important role in the increase of the built up stress in the films being grown.

The other techniques which are reported to be capable of producing low stress DLC films are **A.** Very High Frequency (VHF)-PECVD, **B.** Dual frequency PECVD, **C.** Laser ablation etc.

In VHF discharge sheath thickness and potential drop at the sheaths are significantly small and ions do not accelerate considerably while being attracted towards the substrates kept on the cathode, resulting in a decrease in the substrate temperature and consequently low stress in the films. However, the films so grown may not have the requisite hardness. Dual frequency (Microwave/RF) discharge extensively investigated by Martinu *et al.*,[9] is a remote plasma technique and substrates do not undergo a high degree of ion bombardment. Pulsed laser ablation technique is essentially a thermal evaporation technique and substrates are kept far from the plasma and the plume created by the laser ablation.

From the above observation it becomes abundantly clear that it is perhaps the substrate heating during growth that somehow is implicated in the phenomena of occurrence of high residual (compressive) stress in DLC films. It is, therefore, very clear that any technique which does not allow the substrates to heat up during the growth process and, thus, allows only a low level of unbound hydrogen to be incorporated in the films are attractive.

2.3 System Description and the Methodology Employed for the Deposition of DLC Films

The most common technique to grow good DLC films is the RF self bias method. Here, the two most important process parameters are the self bias voltage and the pressure of the hydrocarbon gases. The advantages of RF self bias technique are the following:

(1) Uniform coatings on different substrates.

(2) Insulating substrate can be coated without difficulty.

(3) Higher deposition rates as compared to DC glow discharge technique.

(4) The process parameters can be tailored to achieve desired deposition.

(5) The interaction between the plasma and its surroundings is "*focussed*" to the small powered electrode; i.e., deposition and sputtering is almost totally restricted to the electrode with the substrate on top. Contamination from the reactor walls as well as undesirable coating of the vacuum system are minimised.

(7) Due to the high negative self bias voltage, the acceleration potential, which determines the average kinetic energy per positive ion impinging on the electrode, is at least one order of magnitude lower for the electrons in comparison to the positive ions. Therefore, the electrons contribution to the power dissipated on the substrate is negligible.

(8) Larger particles (e.g. dust), like any electrically floating probe in contact with the plasma, charge up negatively. They are thus repelled from the negatively biased substrates, one prerequisite for pinhole-free coatings.

2.3.1 Plasma Enhanced Chemical Vapour Deposition (PECVD) System

The first set of DLC films for the present investigation was prepared using plasma enhanced chemical vapour deposition (PECVD) technique. The plasma glow discharge deposition system designed and fabricated for the present study, employs a four way stainless steel cross (150 mm). The electrode system consisted of a cathode (area $\cong$ 100 cm^2) on which substrates were placed

while the rest of the reactor body acted as anode and was kept at ground potential. The cathode was connected to a RF (Radio Frequency, 13.56 MHz)/VHF (Very High Frequency, 100 MHz) power supply. The deposition system used in this study is shown in **Plate 2.1** and also schematically in **Fig. 2.1**.

Plate 2.1 Photograph of the PECVD deposition system

An electrode, capacitively coupled to a RF generator, develops a negative self bias if the electrode area is smaller than the area of the grounded part of the system.[10] This bias arises from the large difference in the mobilities of the electrons and ions. Since the powered electrode is capacitively coupled, the steady state DC current must be zero. A surplus of electrons accumulates on the electrode until a sufficient negative potential develops to ensure that the net current flow over a full cycle is zero. The result is ion bombardment of the substrates, which is placed on the powered electrode, during the film growth.

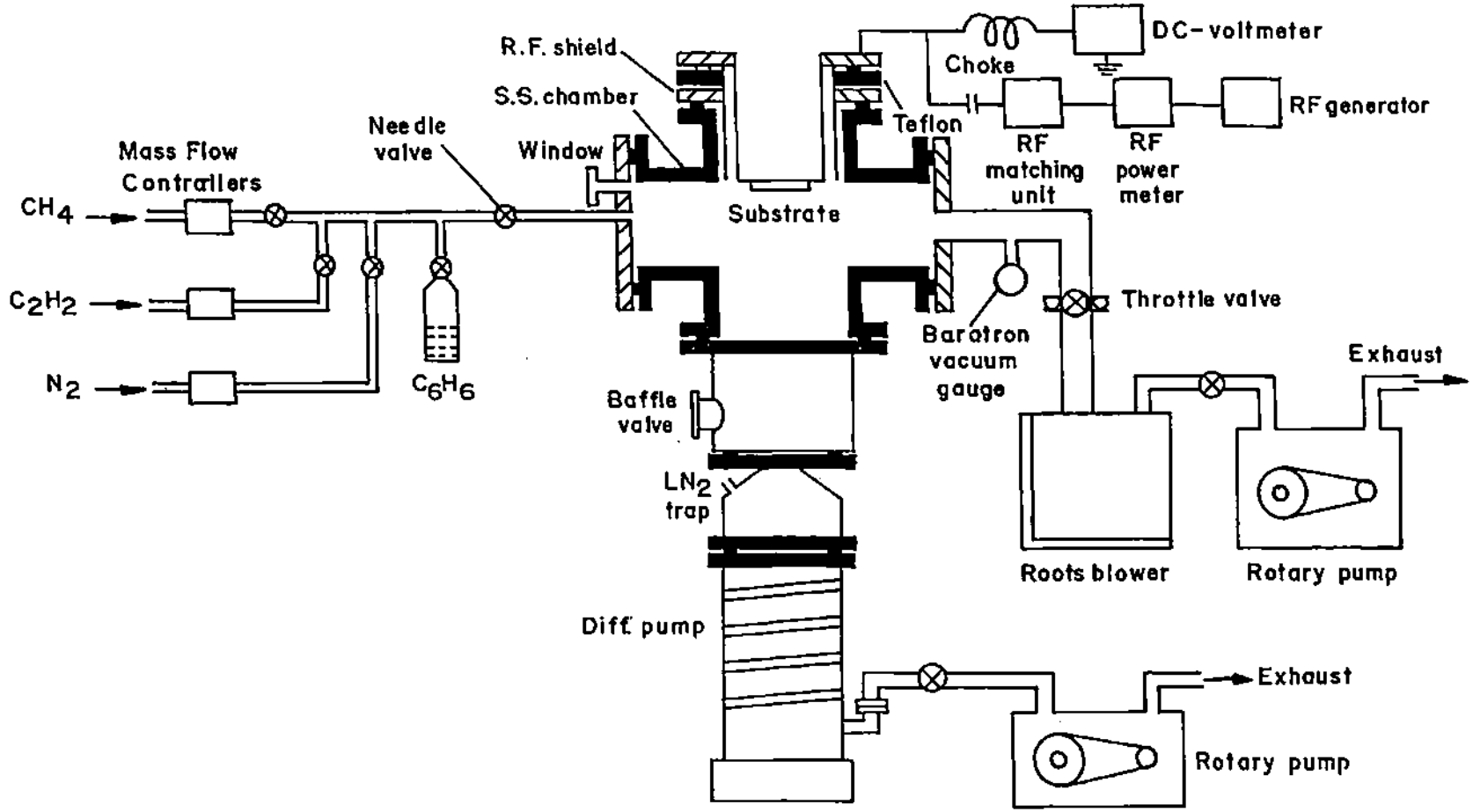

Fig. 2.1 Schematic diagram of the PECVD deposition system

The reactor geometry, i.e. basically the ratio of the capacitively coupled electrode surface (cathode, A_c) to the grounded part of the system, (anode, A_a), is of importance for the potential distribution.

The ratio of the sheath potential over the cathode and anode dark space ($V_{s,c}$ and $V_{s,a}$ respectively) depends on the ratio of the electrode areas as[11]

$$\frac{V_{s,c}}{V_{s,a}} = \left(\frac{A_a}{A_c}\right)^m \qquad 1 < m < 4$$

Thus, a large asymmetric system as shown in **Fig. 2.1** is characterised by a large self bias potential at the powered cathode of slightly less than half the RF peak to peak voltage V_o.

2.3.2 Saddle Field Fast Atom Beam (FAB) Technique

The main research effort documented in this thesis is related to the study of DLC films formed by a saddle field fast atom beam (FAB) source. It may be noted that, in the present thesis, at times, a comparison will be made to the properties of the films deposited by other innovative techniques to the one obtained by RF self bias method. The FAB source[12] (M/s Ion Tech Ltd., FAB-110) used in the present research work is shown in **Fig. 2.2.** It is a cold cathode device and consists of two anode rods (graphite) surrounded by a rectangular cathode also made of carbon (graphite). The source used is of twin (double) cell construction but designed as a modular unit for multiple combination in a linear or matrix array. When a DC positive voltage is applied to the source (anode) by a power supply (Ion Tech Ltd., Model B50-50) the electrons originate from a sector of the cathode and travel through the anode region towards the opposite cathode sector. While travelling, they are retarded, return and continue to oscillate about a central saddle field under the action of a DC electrostatic field. The electrons, therefore, travel long oscillatory paths before being captured by the anode. This increases the efficiency of ionisation. When a hydrocarbon gas or vapour is introduced, the probability of ionisation is high because of the long electron paths and this unique feature of the source provides the ability that the discharge can be

maintained at a pressure approaching two orders of magnitude lower than that normally associated with cold cathode sources. Typical operating pressure can be 10^{-4} - 10^{-3} mbar. The positive ions formed in the discharge travel radially towards the cathode and emerge along straight paths when an aperture is introduced. Another unique feature of the source is the neutral nature of the particle beam produced. The energetic atoms of the supply gas or the fast atoms originate as energetic ions (energy nearly corresponding to the applied voltage) which are positive within the body of the plasma but while coming out of the source they are neutralised. The two proposed mechanism of neutralisations are: **(i)** The ions are neutralised by colliding with residual gas molecules before passing through the aperture of the source, and **(ii)** The electrostatic field close to the output grid helps electrons to recombine with ions with little loss of energy.

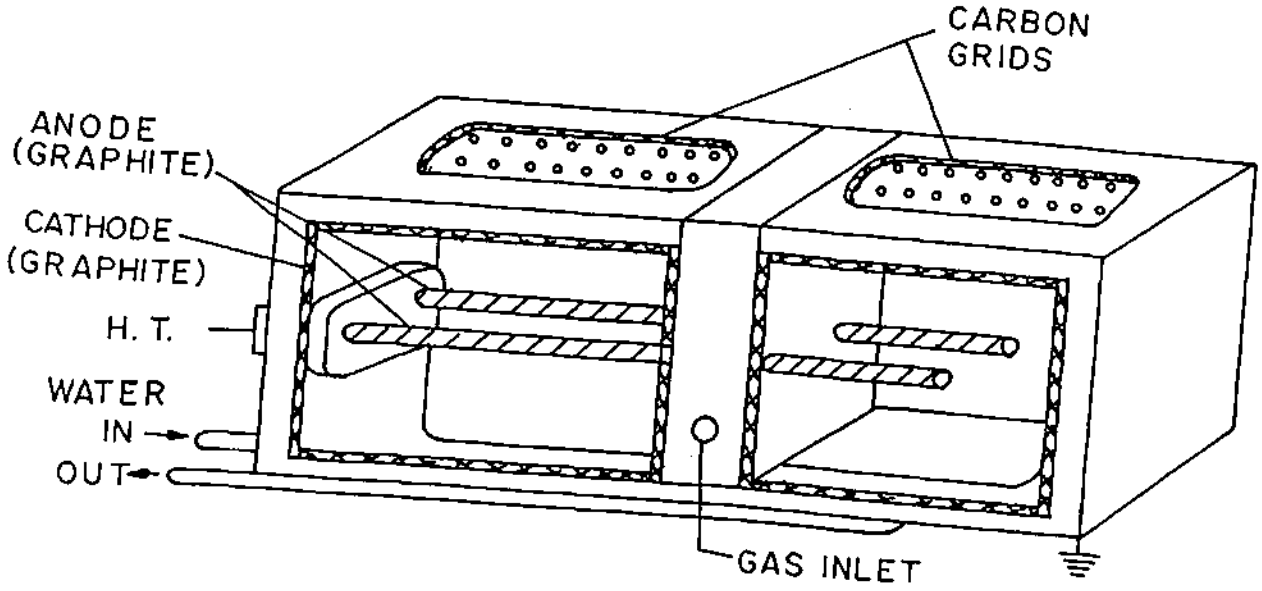

Fig 2.2 Schematic of the saddle field fast atom beam (FAB) source

The plasma chamber of the source and electrodes are made of carbon and coupled with the cold cathode operation, this construction allows the source to be used with gases other than inert gases, such as hydrocarbon gases for producing DLC films. The operation of the source is dependent only on two parameters. These are the regulated current output from the power supply and the discharge voltage which is determined by the gas flow (pressure) and consequently by setting of the needle valve used etc.

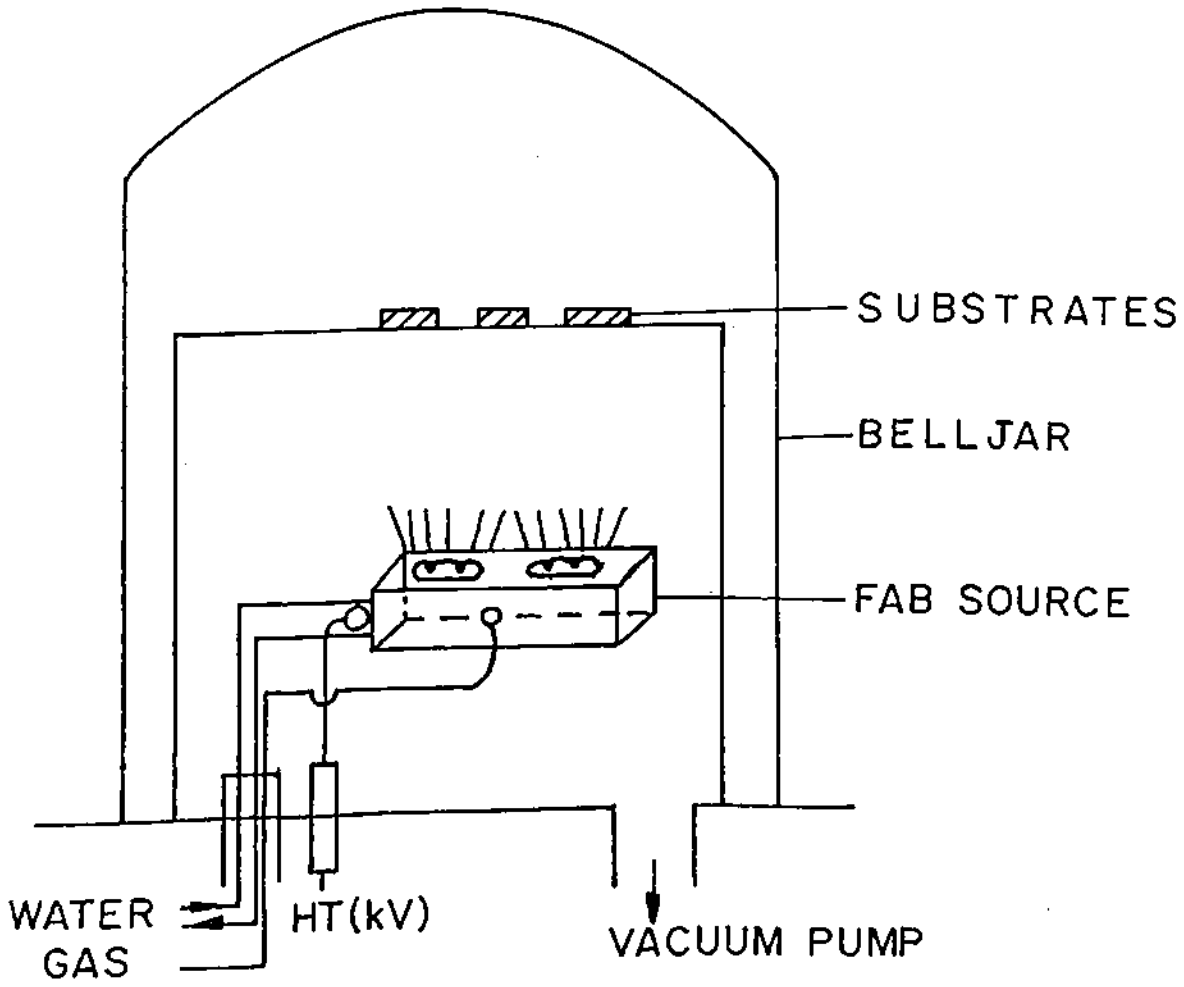

Fig 2.3 Schematic of the FAB experimental setup to grow DLC films

The FAB source used in the present investigation, FAB 110-2 (double cell), was mounted inside a 30 cm in diameter vacuum system as shown in **Plate 2.2** and also schematically in **Fig. 2.2**. The source was cooled by forced water circulation and hydrocarbon gases/vapours were aspirated through gas regulator and needle valve combinations. **Plate 2.3** shows the typical beam coming out from the FAB source.

In earlier experiments, a diffusion pump backed with the rotary pump was used as a pumping stack. Later on to increase the pumping speed and thereby the deposition rate of the films so grown, a turbomolecular pump backed with a rotary pump system was employed.

Plate 2.2 Photograph of the FAB deposition system

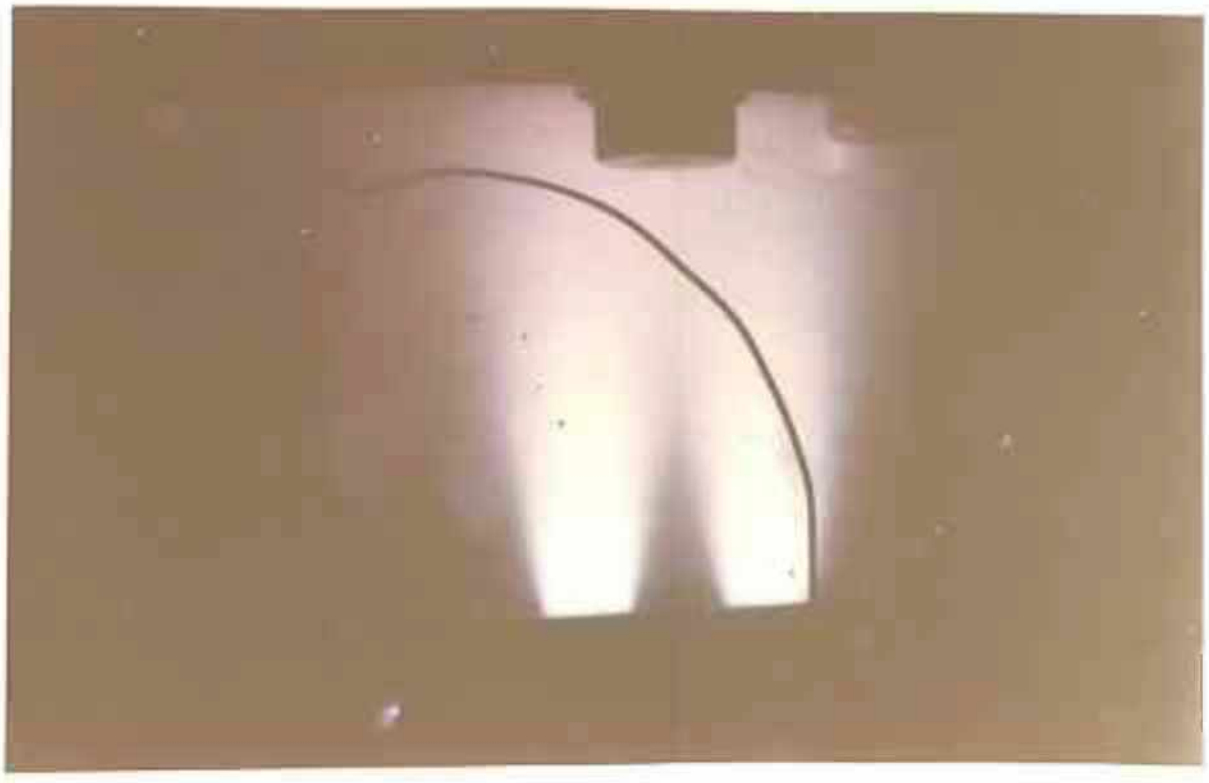

Plate 2.3 Photograph of the typical beam coming out from the FAB source.

2.4 Preparation of the Substrates to Deposit DLC Films

This was found to be a very important step and proper cleaning of the substrates before being introduced into the deposition chamber has been paid particular attention in order to deposit high quality DLC films. The substrates used for the deposition of DLC (a-C:H) films were Corning 7059 glass, single crystalline silicon wafer (5-10 Ω cm, p-type), well polished germanium, optically polished stainless steel pieces and quartz plates. The procedure for cleaning the glass, quartz and stainless steel substrates was simple, comprising an initial wash with soap solution and double distilled water followed finally by an ultrasonic cleaning for 15 minutes in pure alcohol. The Si wafers were, however, given an HF etch to remove the native oxide layer and then an ultrasonic cleaning in distilled water was carried out. The Ge pieces were additionally boiled in trichloroethylene. The substrates were dried by blowing with dry nitrogen gas.

2.5 Experimental Procedure for the Deposition of DLC Films

2.4.1 PECVD System

The cleaned substrates were fixed to the powered electrode. The chamber as well as the gas lines were evacuated to a vacuum of the order of 10^{-5} mbar in a system that used a diffusion pump fitted with a liquid nitrogen trap, backed by a rotary pump. For pumping the process gas, there was a separate pumping line which was connected with an ON-OFF valve, throttle valve, roots blower and rotary backing pump. Before starting the actual process, an argon discharge was maintained, at RF power of 50 W for 10 min. This helps the loose surface impurities on the substrates to be taken out by the energetic argon ion bombardment. This way of cleaning the substrates was found to provide good adhesion of the films to the substrates. After cleaning the substrate(s), the system was again evacuated to a high vacuum. Then the hydrocarbon gas/vapour (usually Matheson Gas Products, USA) was introduced into the chamber and the flow rate and pressure were adjusted using the mass flow controller (Sierra Instruments, Inc.) and throttle valve controller (MKS, Type 252C). The process gas was pumped out by a roots-rotary combine. The RF (13.56 MHz, RF 5S, RF Plasma Products Inc.) or an indigenously developed VHF (100 MHz, Nuclear Science Center, New Delhi) generators were used as sources for plasma excitation. They were turned on and plasma was excited after the pressure and flow of the gas were stabilised. The matching network was tuned to minimise the reflected power.

2.5.2 FAB System

The substrates cleaned as indicated earlier were fixed on the substrate holder located normal to the FAB source at a particular distance. First the vacuum system was evacuated to a base pressure of less then 10^{-5} mbar by a diffusion pump backed by a rotary pump (alternatively a turbo pump backed by a rotary pump). By slow adjustment of the needle valve, argon gas was allowed to

enter the saddle field source in order to clean the substrates. This was done at a pressure of ~1.0 × 10^{-3} mbar. After stabilisation of the argon pressure inside the chamber, the FAB power supply was switched on and the high voltage was set to ~2.5 kV using the current limit control knob of the power supply. Initiation of the plasma discharge was indicated by a drop in voltage to ~ 1 kV and the resulting plasma current was read on the current meter provided on the power supply. The plasma current was controlled with the current control knob and the voltage drop was controlled largely by adjusting the flow rate of the gases which in turn determined the pressure. Flow rate of the particular hydrocarbon gas was controlled by the use of a needle valve. The discharge cleaning was done for about half an hour. This is considered an important step in getting highly adherent DLC films particularly on a non carbide forming substrate, such as glass. After discharge cleaning of the substrates, the system was again evacuated to the base pressure and subsequently a particular hydrocarbon gas was introduced. The aspirated gas/vapour is largely fragmented and the fragments emerge as a beam (aperture size ≅ 1.5 mm) which is directed towards the substrates held at nearly room temperature, to form DLC films.

2.6 Thickness Measurement

Thickness of the thin films is one of the first important parameters to be evaluated. Initial estimation of the thickness was done by using a Talystep (Rank Taylor and Hobson, UK) profilometer. The instrument, equipped with a diamond stylus, measures the height of the step and it is amplified and recorded on a magnetic chart paper. It is very difficult to form a step after depositing DLC films on the substrates. Therefore, before loading the substrates in the deposition chamber a dot mark was made on the substrate using a marker pen, which acts as a step after the dot is erased, using for instance, acetone. The thicknesses of the films were also verified by ellipsometry. Both thickness values were found to be within the experimental error. The deposition rate was estimated by dividing the observed thickness of the films by the deposition time.

2.7 Hardness Measurement

To qualify the DLC films as a protective coating it is very important to evaluate the hardness of the films. Hardness is also expected to reflect the other related properties of thin films, like porosity, density or surface quality.[13] Again the hardness of a material is a parameter describing its ability to withstand penetration by a surface contact. The determination of the hardness of a material is normally made by driving a sharp indenter of a defined geometry into the surface under specified conditions for a fixed time. Usually a pressure, termed the hardness, H, is calculated from the applied load P and the contact area A of the loaded indenter: H = P/A.

A Knoop hardness indenter equipped with Zwick 3212 instrument (Germany) has been used to evaluate hardness of the DLC films. The Knoop hardness (HK) is defined as the applied load *P* divided by the projected area of the impression, and can be calculated by the formula HK = 14229 P/l^2, where *l* is the length of the diagonal of the indenter. The Knoop hardness gives better results than Vicker hardness for films having thickness less than 0.3 nm because of its small indentation depth.[13] DLC films deposited on to the Si substrates were used for this purpose.

2.8 Stress Measurement

Residual stress formation in the film and the film to substrate adhesion determine the stability of the film/substrate composite and, thus, the lifetime of the devices that incorporate the DLC coatings. It is, therefore, very important to deposit well adhering and low stress films for better performance. Thus measurement of stress is a very important characterisation study.

A laser scanning based technique has been used in the present investigation to determine the residual stress in the DLC films. The laser scanning stress measurement setup, developed indigenously, and used extensively in this study is shown in **Plate 2.4** and also schematically in **Fig. 2.3**. The entire arrangement was laid on a heavy metallic table.

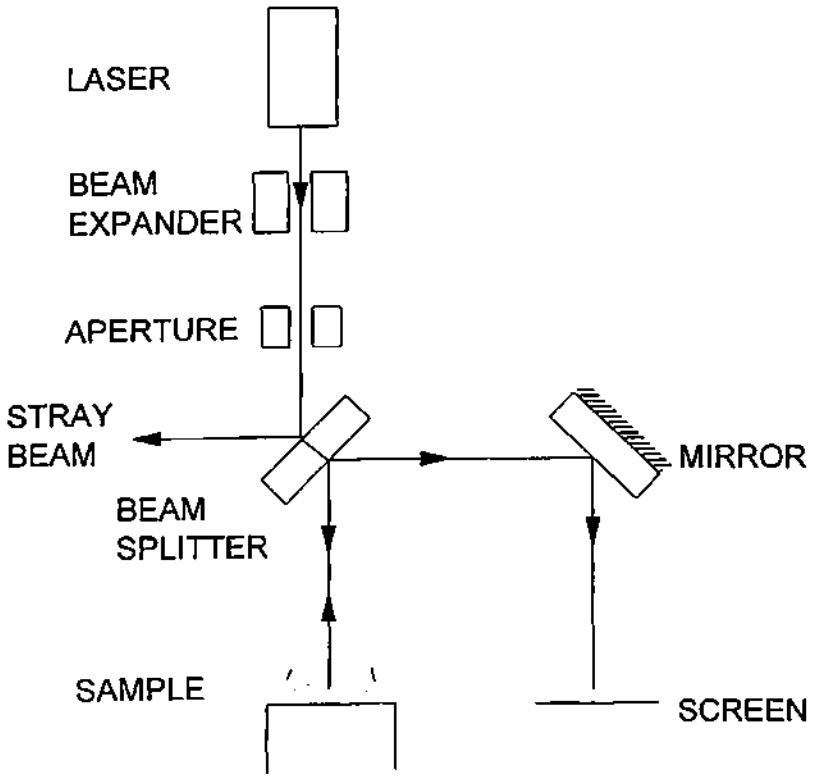

Fig. 2.3 Schematic diagram of the stress measurement setup

Stress measurements were carried out on DLC films deposited on (20 × 20) mm^2 glass slides ~0.15 mm thick. The film stress was estimated from the change in the radius of curvature of the glass substrate caused due to the deposited film. This setup is similar in design to that of Sinha *et al.*[14] A semiconductor diode laser was used to direct a light beam on the sample. Before reaching the sample, the beam passed through a beam expander, aperture and beam splitter. The beam expander and apertures focussed the beam such that the beam traversed a large distance with minimal divergence. The beam splitter reflected a part of the incident laser beam to the sample, and the reflected beam from the sample was directed to a mirror. The beam splitter reflected 30% and transmitted 70% of the incident light and had an optically flat surface. The beam was reflected from the mirror to a location where the change in position of the reflected beam was measured.

Radius of curvature measurements were made by translating the sample a known distance X, along a direction perpendicular to the incident beam and measuring the displacement, d, of the reflected beam. The reflected beam movement was measured by measuring the displacement of the reflected beam spot on the screen. Measurement of the reflected beam displacement was performed at a distance L from the sample. Using the values of X, d and L, the radius of curvature, R, of a sample may be calculated by the relation

$$R = \frac{2XL}{d}$$

The precision of the system described above was tested by measuring the radius of curvature of a commercially available concave spherical mirror, with radius of curvature 33 m.

Plate 2.4 Photograph of the laser scanning stress measurement setup

The residual stress in a film is related to the radius of curvature of the substrate and is given by[15]

$$\sigma = \frac{Et_s^2}{6(1-\mu)t_f}\left(\frac{1}{R} - \frac{1}{R_0}\right)$$

where E and μ are Young's modulus and Poisson's ratio of the substrate, respectively; t_s is the substrate thickness, t_f is the film thickness and R_0 and R the radii of curvature of substrate before and after film deposition. Values of $E = 1.03 \times 10^{11}$ kg/m^2, μ=0.22 and t_s=0.15 mm have been used in the present investigation.

The stress values obtained from a measurement involving the above setup was compared with a commercially available setup available at the Solid State Physical Laboratory, Delhi (SMSi 8900 TC, Scientific Measurement Inc. System, USA). The values of these two results were found to differ within 20%.

2.9 Optical Properties

2.9.1 Optical Bandgap

The optical bandgap of amorphous semiconductors can be found from the dependence of the absorption coefficient α on the photon energy $h\nu$. The forms of α as a function of $h\nu$ are determined by the energy dependence of the density of state N(E) for the bands containing the initial and final states.

The absorption edge is very different in shape and in position from the Urbach type edge observed in diamond. It is well documented that except for the lowest tail, the absorption follows the Tauc's relation[16]

$$\alpha h\nu = B\left(h\nu - E_g\right)^2$$

where B is a constant and E_g the optical bandgap.

Although the assumptions leading to the above relation may not be fulfilled, plots of $\sqrt{\alpha h\nu}$ vs. $h\nu$, provide a simple parametrisation of the electronic absorption edge. The optical bandgap is taken from the extrapolation of the linear portion of the curves towards abscissa.

The optical measurements were carried out, both in transmission and in reflection mode, on a Shimadzu 3101 PC Spectrophotometer in the wavelength range 400 to 900 nm.

2.9.2 Ellipsometry

Ellipsometry is a convenient and accurate technique for the measurement of thickness and refractive indices of very thin films on solid surfaces and for the measurement of optical constants on reflecting surfaces. Ellipsometry technique can also be used for quantitative microstructural information of the film by analysing ε_1 vs. $h\nu$ and ε_2 vs. $h\nu$ trace.

In ellipsometry, the change in the state of polarisation of elliptically polarised light due to reflection is measured and interpreted in terms of properties of the reflecting surface. Two characteristic parameters measured in ellipsometry are the change in the relative amplitude $tan\psi$ and phase difference Δ, of two orthogonal components of the incident light due to reflection. From these two measured quantities, two parameters of the reflecting surface can be determined. For a surface covered with a absorbing film, thickness and refractive index of the film can be determined, if the optical constants of the substrate are known.

A Rudolph research ellipsometer (Model 43603-200 E), with a tungsten iodine lamp and a line filter (546.1 nm) and with an variable angle of incidence was used in the present investigation to evaluate the refractive index (n) and the extinction coefficient (k). The samples used for this characterisation were films deposited on Si substrates. A Fortran computer program has been used employing a two phase model (substrate/absorbing film/air) to compute the complex refractive index from ellipsometer measurements.

Spectroscopic ellipsometry data were also acquired using a rotating polariser spectroscopic ellipsometer (SOPRA, Model ES2G, France) in the spectral range 2.5 - 5.0 eV and the optical constants [viz. refractive index (n) and extinction coefficients (k)] of the deposited DLC films were determined employing two phase model (substrate\film\air) for the analysis of the data. The values of dielectric constants (ε_1 and ε_2) were evaluated from the values of optical constants (n, k) by the well known relation viz. $\varepsilon_1 = n^2 - k^2$ and $\varepsilon_2 = 2nk$.

2.9.3 Subgap Absorption

Any technique through which one can measure low absorption can also be used as a technique to characterise impurities, defects, etc. The distribution of states within optical bandgap is believed to be exponential and is characterised by a slope E_o, an important parameter in deciding the quality of the material. The parameter, E_o determines the broadness of the states distribution; higher the value of E_o, more will be the disorder in the amorphous network.

As shown in **Fig.2.4**, the absorption edge spectrum of a typical amorphous semiconductor can be roughly divided into three regions:

A. *High absorption region* A ($\alpha > 10^3$ cm^{-1})

The optical transition of this region is usually described by the Tauc expression

$$\alpha h\nu = B\left(h\nu - E_g\right)^2$$

where B is a constant and E_g is the optical bandgap.

B. *Exponential edge* B ($10^1 < \alpha < 10^3$ cm^{-1})

In this region, the variation of α with $h\nu$ follows the equation,

$$\alpha = \alpha_0 \exp\left(\frac{-h\nu}{E_0}\right)$$

where α_o is a constant and E_o the characteristic energy representing the slope of the exponential tail state distribution and reflects the randomness of an amorphous network.

C. *Weak absorption tail* C ($\alpha < 10^{1}cm^{-1}$)

The weak absorption tail of region C is attributed to the deep defect states in the mid-gap, mostly originating from dangling bonds and impurities.

Therefore, measurement of α in the appropriate wavelength regions provides useful information about the electronic states within the bandgap of the material. The optical transitions responsible for each region are shown in the simplified gap-state profile of **Fig. 2.5**.

For the low absorbing films, transmission measurements on a spectrophotometer is not suitable for obtaining the required absorption spectra. Photothermal Deflection Spectroscopy (PDS) can be used to acquire absorption spectra accurately. In the present investigation a transverse PDS setup has been adopted.

2.9.3.1 Transverse Photothermal Deflection Spectroscopy

Transverse photothermal spectroscopy is based on the commonly observed "*mirage*" effect during a hot day. The magnitude of refraction/deviation Φ of a beam of light, such as a laser beam, propagating close to the sample surface which is absorbing the incident monochromatic light flux (pump beam) under investigation is related to the optical absorption coefficient of the material in the following manner:

$$\Phi = k\left[1 - \exp(-\alpha t)\right]$$

where t is the film thickness. The proportionality constant k depends on various system parameters such as the diameter of the probe beam in relation to the pump beam and its closeness to the sample surface, the thermophysical properties of the fluid medium in contact with the sample, the modulation frequency of the pump beam etc. In order to increase the sensitivity of the technique it is advantageous to have a medium with higher temperature coefficient of refractive index in contact with the sample. Carbon tetrachloride (CCl_4) for which $dn/dT = 5 \times 10^{-4}/K$ (for air $dn/dT = 5 \times 10^{-6}/K$) has been found to possess such a property. The deflection is measured using a position sensitive detector.

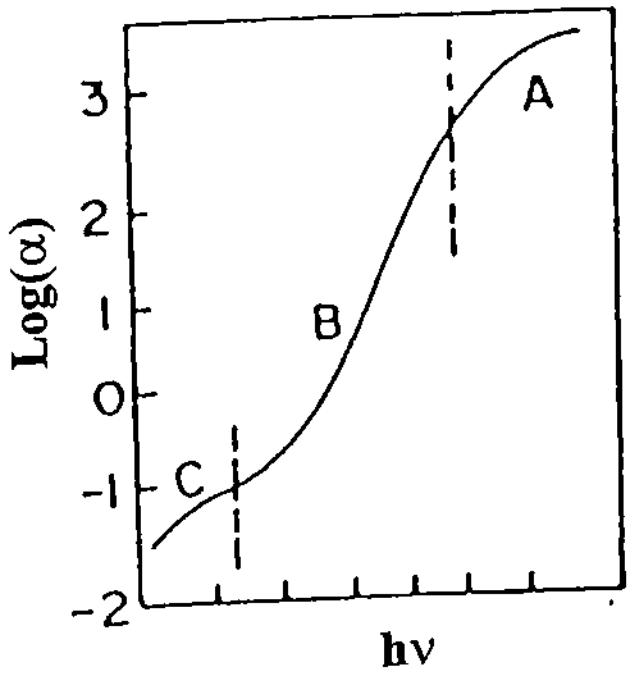

Fig 2.4 The absorption edge spectrum of a typical amorphous semiconductor

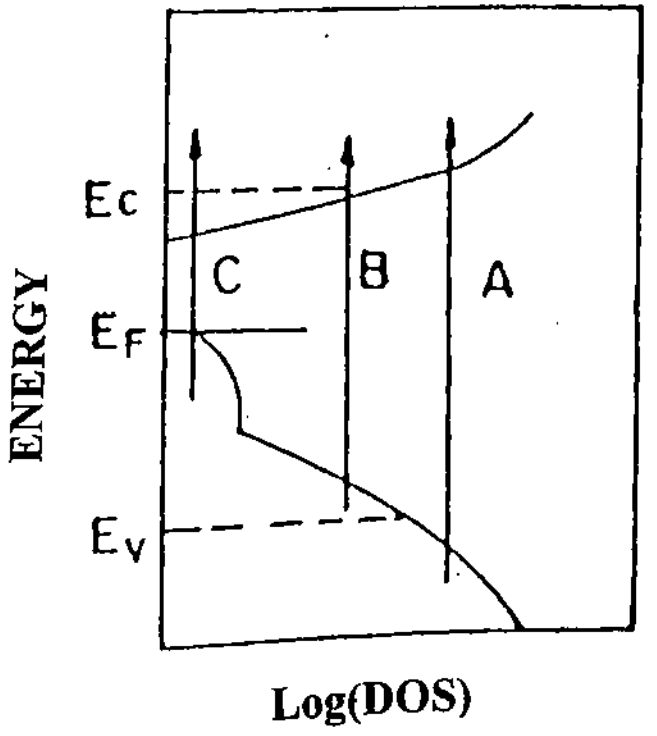

Fig. 2.5 The optical transitions of a typical amorphous semiconductor

The PDS setup used for this study is shown in **Plate 2.5** and also schematically in **Fig 2.6**. The whole arrangement was made on a vibration damping optical table (M/s Holo optics Ltd., New Delhi). The table consists of aluminium honeycomb structure in between thick stainless steel plates and is supported on three air filled cylinders to damp out low frequency vibrations.

Plate 2.5 Photograph of the PDS setup used in the present investigation

The broad band light source used in this experiment is an air cooled 350 W tungsten-halogen lamp. The beam is focused on the entrance slit of a 0.25 meter monochromator (Thermo Jarrell Ash Corporation, Model 82-410). The monochromatic beam coming out of the exit slit of the monochromator is chopped at a low frequency, typically 12 Hz, by a mechanical chopper (Stanford Research Systems, Model 540) and is focussed on the sample surface by means of a combination of lenses. The sample is immersed in doubly distilled CCl_4 in a cuvette of 10×10×70 mm size. The top of the cuvette is tightly closed to prevent the escape of CCl_4 vapour

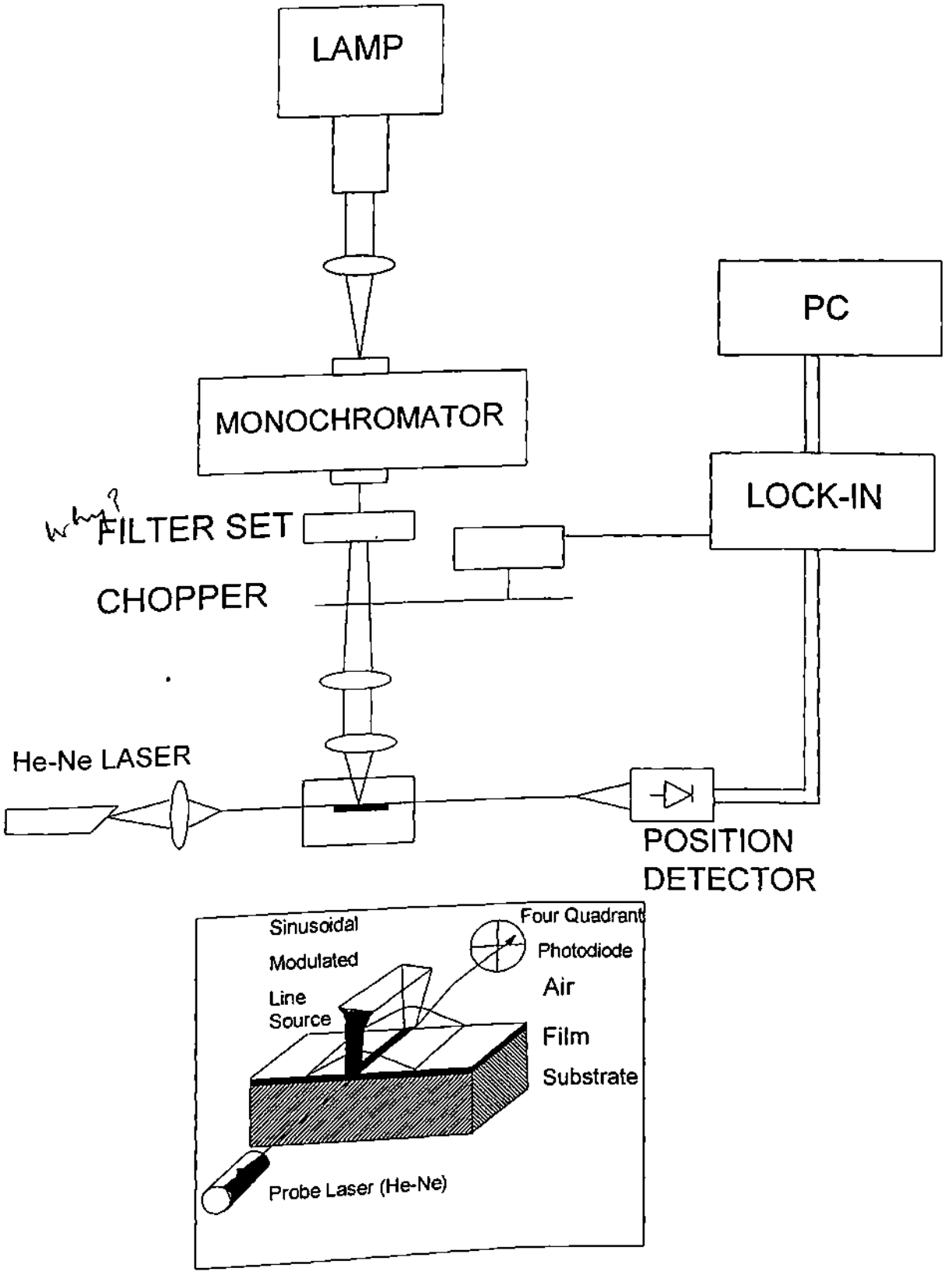

Fig. 2.6 Schematic diagram of transverse PDS setup

into the atmosphere. The cuvette is mounted on a tilting stage attached to a manipulator capable of three axis i.e., X, Y & Z translation. The sample's position was manipulated so that the 5 mW He-Ne laser probe beam travels close to and parallel to the surface of the sample. The position of the quadrant detector mounted on an X, Y & Z translation stage was adjusted so that the laser beam falls perpendicularly on the active area of the quadrant position detector (Silicon Detector Corporation Ltd., USA). The analog signal (A-B)/(A+B) is fed to a lock-in-amplifier (Stanford Research Systems, SR-530) after computing it electronically. The reference signal to the lock-in amplifier is provided by the mechanical chopper driver. By varying the wavelength of the incident (pump beam) radiation, the PDS signal and its phase with respect to the probe beam were recorded using the lock-in amplifier at various wavelengths. The raw PDS spectra is matched with the α values obtained by reflection and transmission measurements beyond 1000 cm^{-1} and finally this matched curve is normalised with respect to standard carbon black sample.

2.10 Electrical Properties

2.10.1 Electrical Conductivity

Conductivity measurements were performed on samples deposited on 7059 glass substrates having aluminium or silver contacts above the a-C:H film in a coplanar configuration with a gap of about 0.078 cm, after annealing at 300°C for an hour in vacuum. A DC voltage was applied to the electrodes and the current passing through the film was measured by a electrometer (Keithley, Model 610C or 617). Measurements were carried out under a vacuum of better than 10^{-4} mbar.

The value of conductivity (σ) was calculated from the relation

$$= \frac{I \times L}{V \times t \times w} \quad \Omega^{-1} \text{ cm}^{-1}$$

Where V is the applied voltage in volts, I is measured current in amperes, t is thickness in cm, w is width of film in cm, and L is the distance between the electrodes in cm.

Electronically, a-C:H would be best described as a composite of very small conducting islands captured in an insulating matrix. Studies of the temperature dependence of the conductivity indicate that conduction is via thermally activated hopping of charge carries between localised states. This localisation is presumed to occur on graphitic clusters.

2.10.2 Current-Voltage (I-V) Measurements (SCLC)

I-V characteristics were investigated on sandwiched specimens which were prepared by depositing DLC films on silicon substrates and aluminium dots were made as a top electrode by thermal evaporation in $\approx 10^{-6}$ mbar pressure. The active area of the devices was 7.85×10^{-3} cm^2 and a programmable Keithley 617 electrometer was used for I-V measurements.

2.11 Surface Morphology, Composition and Structure

2.11.1 X-ray Photoelectron Spectroscopy (XPS) and X-ray Auger Electron Spectroscopy (XAES) Studies

XPS is a chemical sensitive technique and the XPS chemical shift has been proven to be a valuable method for understanding the local environment of an atom in a solid and to investigate whether a carbon film is sp^3 or sp^2 bonded.[17] Apart from the chemical shift, the XPS technique can provide other useful information such as film composition, plasma loss for conducting materials, valence band density of states etc.

A relatively sensitive analysis of the sp^3 and sp^2 bonding in the DLC films is provided by AES or XAES.[17] XAES has further advantage of not damaging the samples under investigation.

XPS and XAES measurements were carried out on a multi technique surface analytical instrument (M/s Perkin Elmer, Model 1257) capable of attaining a vacuum level ~ 10^{-11} mbar. MgKα (1253.6 eV) was used as a X-ray source for irradiating the sample. The spectra were recorded before and after cleaning the top surface by using argon beam at 3 keV at a pressure of ~10^{-8} mbar for 2 min. The system is calibrated with respect to contaminant free Ag 3d line using MgKα as the incident photon. The XPS survey scan was obtained at 100 eV pass energy at a step of 1.0 eV and the XPS C(1s) core level spectra was acquired at 0.1 eV step with a pass energy of 25 eV. The XAES spectra were obtained at a step of 0.1 eV with a pass energy of 100 eV. The first derivative spectra (dN/dE) of the XAES data were obtained by first eliminating the effect of X-ray satellite from the measured spectra and the spectra were differentiated to obtain dN/dE using programme supplied with the spectrophotometer.

2.11.2 Scanning Electron Microscopy Studies

Scanning electron microscopy (SEM) is a widely used technique for studying surface topography as well as cross-sectional features of thin films. In SEM, a finely focussed electron beam is scanned over the surface of the specimen. The secondary electrons emanating from about 10 A° from film surface are extracted by a high potential applied to a scintillator-detector system. Secondary electron images are generated by synchronising the optical output of the detector with raster of the electron probe across the sample. SEM of some of the DLC films were studied on JEOL, JSM -35CF scanning electron microscope.

2.11.3 IR Studies

IR spectroscopy is a non-destructive method capable of providing a lot of information about the material without having to form contacts. Difference in the structure and the composition show

up in the IR absorption spectra. The absorption in the IR below the optical gap is characterised by an absorption tail extending towards lower energy, as well as C-H and C-C vibrational bands, the latter becoming allowed due to the lack of translational symmetry in the amorphous materials.

IR spectroscopy technique has been used in the present investigation to determine the bonded hydrogen content. The number N of bonds per unit volume contributing to IR-active vibrational bond is given by[18]

$$N = A\int\frac{\alpha(\omega)}{\omega}d\omega$$

where A is a normalisation factor proportional to the inverse of the absorption strength and $\alpha(\omega)$ is the frequency dependent absorption coefficient. The integration is performed over the absorption band of 2700-3100 cm^{-1}, $\alpha(\omega)$ was determined from the film thickness and IR spectra. For hard a-C:H films, A is about 8.5×10^{20} cm^{-2} for C-H vibration.[18] IR spectra of the DLC films grown on Si wafer were recorded in a BIO-RAD, FTS40 FTIR spectrophotometer.

2.12 Hydrogen Content Estimation

Hydrogen in DLC films plays a important role and influences the material quality a great deal. It is, therefore, very essential to estimate the hydrogen content. The total hydrogen content of the DLC films has been estimated using Elastic Recoil Detection Analysis (ERDA). In the present investigation the estimation of hydrogen content of some of the DLC films has been carried out at Nuclear Science Centre, New Delhi, using their facility 15 UD NSC Pelletron. 50 MeV ^{28}Si ions were used for this purpose. The hydrogen content of the DLC films were estimated using standard procedure published in the literature.[19]

2.13 Evaluation of sp^3/sp^2 Ratio

2.13.1 Introduction

The physical, optical and electrical properties of DLC films appear to be determined by the relative amount of sp^3/sp^2 sites. For this reason, evaluation of sp^3/sp^2 ratio in these films is important. Quantitative information on the relative concentration of sp^3, sp^2 and sp^1 hybridised carbon has been estimated through the use of different experimental techniques, viz. Infra-red (IR) spectroscopy,[20] Electron energy loss spectroscopy (EELS),[21] Nuclear magnetic resonance (NMR, CNMR),[22] Raman spectroscopy,[23] X-ray photoelectron spectroscopy (XPS),[19] X-ray Auger electron spectroscopy (XAES).[19] But all of these techniques have some inherent limitations.

Infra-red spectroscopy provides information through the deconvolution of the C-H stretching peak (2900-3100 cm^{-1}) into individual contributions correlated to the different bonding environment of C-H bonds. This method does not allow one to extract information on the sites where C is not bonded to H.

EELS is a highly sensitive technique for the surface microstructure and gives information on very small region near the surface.

NMR is a precise and bulk-sensitive method. The information on hydrogen bonding to different sites can be obtained through this technique if large amounts (>50 mg) of materials are used.

Raman spectroscopy can only be used to obtain a qualitative indication of the amount of graphitisation in the film. Thus this technique individually can not give information about the sp^3/sp^2 ratio if both C-C and C-H bonds are present.

XPS and XAES are sensitive techniques. The ratio of sp^3/sp^3 is determined by the deconvolution of XPS C(1s) spectra and by measuring the Auger width in XAES derivative spectra. But diamond sample (100% sp^3) and graphite sample (100% sp^2) are needed as reference spectra.

However, most of these techniques are not available for a routine measurement of sp^3/sp^2 ratio particularly during a material development programme for some specific device application. A simple technique involving measurements on a readily available equipment like a spectrophotometer or a ellipsometer could, therefore, be most appropriate. In fact such techniques have already been developed and a brief account of these efforts will be presented in the following:

Savvides[24] determined sp^3/sp^2 ratio using a method based on energy dependence of the imaginary part of the dielectric constant (ε_2) of the DLC films. The effective number of π electrons is evaluated by comparing the ε_2 first moment for a-C:H to that of graphite. However, no information on sp^3 sites or on σ bonds is obtained, and knowledge of ε_2 values up to at least 8 eV is needed, since the energy dependence of ε_2 for graphite and a-C:H at energies below 7 eV is quite different.

Similarly, F. Demichelis *et al.*[25] analysed real (ε_1) and imaginary (ε_2) components of dielectric constant of DLC or a-C:H films for obtaining what they claimed was more reliable information on the sp^3/sp^2 ratio. In this method the contribution to $\varepsilon_1(E)$ of $\pi \rightarrow \pi^*$ transition is taken into account through Kramers-Kronig relationships and the contribution of $\sigma \rightarrow \sigma^*$ transition to $\varepsilon_1(E)$ is analysed within the frame work of Wemple-Didomenico model.[26]

2.13.2 A Simple Technique to Estimate sp^3/sp^2 Ratio

The technique developed in this laboratory during the present investigation is in many ways similar to that proposed by Demichelis *et al.*,[25] but with some differences which are described below:

2.13.2.1 Wemple-Didomenico Model

In this model, the real $\varepsilon_1(E)$ and imaginary part $\varepsilon_2(E)$ of the dielectric constant $\varepsilon(E)$ of an a-C:H film are analysed, for estimating the Plasmon energy of carriers. It is important to see how it follows from the basic relation given in *Principles of the Theory of Solids* by J.M. Ziman, Cambridge (1964), Ch. 8, which is written as,

$$\varepsilon(\omega) = 1 + \frac{4\pi Ne^2}{m} \sum_j f_j \{ \frac{1}{\omega_j^2 - \omega^2} + i \frac{\pi}{2\omega} \delta(\omega - \omega_j) \} \tag{2.1}$$

where ω is the frequency of radiation incident upon a solid having fixed assembly of N independent neutral atoms and each atom contains only one electron of mass m (single electron approximation), f_j equals the electric dipole oscillator strength associated with transition at frequency ω_j. In the single oscillator approximation (j=1), and f_j=1, therefore, one can write the energy dependence of dielectric constants $\varepsilon_1(E)$ and $\varepsilon_2(E)$ as

$$\varepsilon_2(E) = \frac{\pi}{2} \frac{E_P^2}{E} \delta(E - E_o) \tag{2.2}$$

$$\varepsilon_1(E) = 1 + \frac{E_P^2}{E_o^2 - E^2} \tag{2.3}$$

where, $\hbar\omega = E$, $\hbar\omega_j = \varepsilon_j - \varepsilon_o = E_o$ is the spacing between bands and Plasmon frequency ω_p, Plasmon energy E_p are given by

$$\omega_P = \frac{4\pi Ne^2}{m}, \quad E_P = \hbar\omega_P \tag{2.4}$$

Equation 2.3 can be rewritten as

$$\frac{1}{\varepsilon_1(E) - 1} = \frac{E_o^2}{E_P^2} - \frac{E^2}{E_P^2} \tag{2.5}$$

A plot of $1/[\varepsilon_1(E)-1]$ vs. E^2 yields a straight line whose slope and intercept gives E_P and E_o. At E=0, it follows from equation (2.5) that

$$E_P^2 = (\hbar\omega_P)^2 = E_o^2 [\varepsilon_1(0) - 1] \tag{2.6}$$

This equation also enables the determination of Plasmon energy (E_P) of carriers.

2.13.2.2 Dielectric Constants

The real $\varepsilon_1(E)$ and imaginary $\varepsilon_2(E)$ parts of dielectric constant $\varepsilon(E)$ of an insulator are inter-related by Kramers-Kronig relations

$$\varepsilon_1(E) = 1 + \frac{2}{\pi}\int_0^{\infty} \frac{E'\varepsilon_2(E')}{(E')^2 - E^2} dE' \tag{2.7}$$

$$\varepsilon_2(E) = \frac{2}{\pi} E \int_0^{\infty} \frac{\varepsilon_1(E')}{(E')^2 - E^2} dE' \tag{2.8}$$

Assuming independent contributions of $\sigma \rightarrow \sigma^*$ and $\pi \rightarrow \pi^*$ transitions to $\varepsilon_2(E)$ one can write

$$\varepsilon_2(E) = \varepsilon_{2\pi}(E) + \varepsilon_{2\sigma}(E) \tag{2.9}$$

In view of this, equation (2.7) can be rewritten as

$$\varepsilon_1(E) = 1 + \frac{2}{\pi}\int_0^{\infty} \frac{E'\varepsilon_{2\pi}(E')}{(E')^2 - E^2} dE' + \frac{2}{\pi}\int_0^{\infty} \frac{E'\varepsilon_{2\sigma}(E')}{(E')^2 - E^2} dE' \tag{2.10}$$

Further the real $\varepsilon_{1\pi}(E)$, $\varepsilon_{1\sigma}(E)$ and imaginary parts $\varepsilon_{2\pi}(E)$, $\varepsilon_{2\sigma}(E)$ are related by Kramers-Kronig relation as

$$\varepsilon_{1\pi}(E) = 1 + \frac{2}{\pi}\int_0^{\infty} \frac{E'\varepsilon_{2\pi}(E')}{(E')^2 - E^2} dE' \tag{2.11}$$

$$\varepsilon_{1\sigma}(E) = 1 + \frac{2}{\pi}\int_0^{\infty} \frac{E'\varepsilon_{2\sigma}(E')}{(E')^2 - E^2} dE' \tag{2.12}$$

Elimination of integrals as expressed by equations (2.10) to (2.12) results:

$$\varepsilon_1(E) - 1 = \left[\varepsilon_{1\pi}(E) - 1\right] + \left[\varepsilon_{1\sigma}(E) - 1\right] \tag{2.13}$$

The aim is to extract $\varepsilon_{1\sigma}(E)$ from experimentally observed $\varepsilon_1(E)$ using equation (2.13). Once this is achieved, Wemple-Didomenico model[26] (as outlined in Section 2.13.2.1) can be used to determine Plasmon energy for σ electrons. For this task, information about $\varepsilon_{1\pi}(E)$ or $\varepsilon_{2\pi}(E)$ (as discussed below) is required.

The imaginary part of the dielectric constant $\varepsilon_{2\pi}(E)$ is found to be related with the density of states (DOS) in these materials. Das Gupta *et al.*[25] proposed a pair of broad Gaussian like distributions of DOS, lying above and below the Fermi-level, arising out of the π-states. Their detailed analysis predict the contribution of $\pi \rightarrow \pi^*$ transitions to $\varepsilon_2(E)$, given by

$$\varepsilon_{2\pi}(E) = \frac{A}{E^2}\,\mathrm{erf}\left(\frac{E}{2\sigma_\pi}\right)\exp\left[-\left(\frac{2E_\pi - E}{2\sigma_\pi}\right)^2\right] \qquad (2.14)$$

where A denotes scale factor and E_π and σ_π are known as Gaussian parameters. Using Kramers-Kronig relation equations (2.11) and (2.14), one can estimate $\varepsilon_{1\pi}(E)$ and hence $\varepsilon_{1\sigma}(E)$ via equation (2.13).

2.13.2.3 Procedure for Determination of sp^3/sp^2 Ratio

(a) Estimate the parameters E_π, σ_π of Gaussian like bands and the scale factor *A* of the formula obtained from the convolution of the Gaussian bands, (Equation (2.14), assumed valid for all energies), by fitting the low energy region (E < 4eV) of the experimentally observed $\varepsilon_2(E)$ spectra, i.e.

$$\left[\varepsilon_{2\pi}(E)\right]_{\text{equation}} = \left[\varepsilon_2(E)\right]_{\text{experimental}}$$

(b) Evaluation of $\varepsilon_{1\pi}(E)$ using Kramers-Kronig relation (equation (2.11)) and hence $\varepsilon_{1\sigma}(E)$ from equation (2.13) in the same energy range in which optical measurements have been performed.

(c) Apply Wemple-Didomenico model[26] to $\varepsilon_{1\sigma}(E)$ spectra, for the estimation of Plasmon energy of σ electrons (i.e. plot $1/[\varepsilon_{1\sigma}(E)-1]$ vs. E^2) from

$$E_{P_\sigma}^2 = \left(\hbar\omega_P\right)_\sigma^2 = E_o^2\left[\varepsilon_{1\sigma}(0) - 1\right]$$

Since Plasmon energy is proportional to the number of valence electrons, therefore,

$$n_{v\sigma} = k^{-1}E_{P\sigma}^2 = k^{-1}E_o^2\left[\varepsilon_{1\sigma}(0) - 1\right] \tag{2.15}$$

(d) Estimate Plasmon energy of electrons by evaluating

$$n_{v\sigma} = k^{-1}E_{P\sigma}^2 = k^{-1}M_{1\pi} \tag{2.16}$$

where
$$M_{1\pi} = \frac{2}{\pi}\int_0^\infty E'\varepsilon_{2\pi}(E')dE' \tag{2.17}$$

$M_{1\pi}$ is known as the first moment of $\varepsilon_{2\pi}(E)$ (equation (2.14)). Now dividing equation (2.16) by equation (2.15), one gets

$$\frac{n_{v\pi}}{n_{v\sigma}} = \frac{M_{1\pi}}{E_o^2\left[\varepsilon_{1\sigma}(0) - 1\right]} = \alpha \text{ , say} \tag{2.18}$$

Therefore, the ratio of sp^3/sp^2 can be calculated as follows:

Let X, Y, Z denote the number of sp^3, sp^2 and H atomic sites/volume.

So
$$X+Y+Z = N = \text{atomic density} \tag{2.19}$$

Now each sp^2 site give rise to 3 σ states and 1 π state, whereas each sp^3 site give rise to 4 σ states, and each H atom to a single σ state, then

Total number of π state = Y

Total number of σ states = 3 Y + 4 X + Z

Therefore,
$$\frac{n_{\pi^*}}{n_{\sigma^*}} = \frac{Y}{3Y + 4X + Z} = \alpha \qquad (2.20)$$

Now from equation (2.19)
$$\frac{X}{N} + \frac{Y}{N} + \frac{Z}{N} = 1$$

and from equation (2.20)
$$\frac{\frac{Y}{N}}{3\frac{Y}{N} + 4\frac{X}{N} + \frac{Z}{N}} = \alpha$$

Further if
$$\frac{X}{N} = f_3 \text{ (atomic fraction of } sp^3 \text{ atoms)},$$
$$\frac{Y}{N} = f_2 \text{ (atomic fraction of } sp^2 \text{ atoms) and}$$
$$\frac{Z}{N} = f_H \text{ (atomic fraction of H atoms)}$$

it follows from the above equations that

$$f_H + f_2 + f_3 = 1 \qquad (2.21)$$
$$\frac{f_2}{3f_2 + 4f_3 + f_H} = \alpha \qquad (2.22)$$

Simplification of equations (2.21) and (2.22), results

$$f_2 = \frac{(4 - 3f_H)\alpha}{(1 + \alpha)} \qquad (2.23)$$

$$f_3 = \frac{(1-3\alpha)-(1-2\alpha)f_H}{(1+\alpha)} \tag{2.24}$$

Dividing equation (2.24) by equation (2.23), one gets

$$\frac{f_3}{f_2} = \frac{(1-3\alpha)-(1-2\alpha)f_H}{\alpha(4-3f_H)} \tag{2.25}$$

Knowing the H content in DLC films the values of sp^3/sp^2 can be estimated from equation (2.25). Block diagram for the entire analysis is given in **Fig. 2.7.**

2.13.2.4 Example

The scale factor A and Gaussian parameters E_p, σ_p for a typical a-C:H film deposited by RF PECVD technique[28,29] have been estimated by least square fit of experimental $\varepsilon_2(E_i)$ spectrum (over a small energy range with equation (2.4), described above) as

A = 28.572,

E_π = 1.999 and

σ_π = 0.715

and further following above steps, one gets

sp^3 atoms = 42.49 %,

sp^2 atoms = 32.51 % and

sp^3/sp^2 ratio = 1.307 for DLC films having H-content = 25 %.

The details of this technique and corresponding computer programmes have already been published as a report.[30]

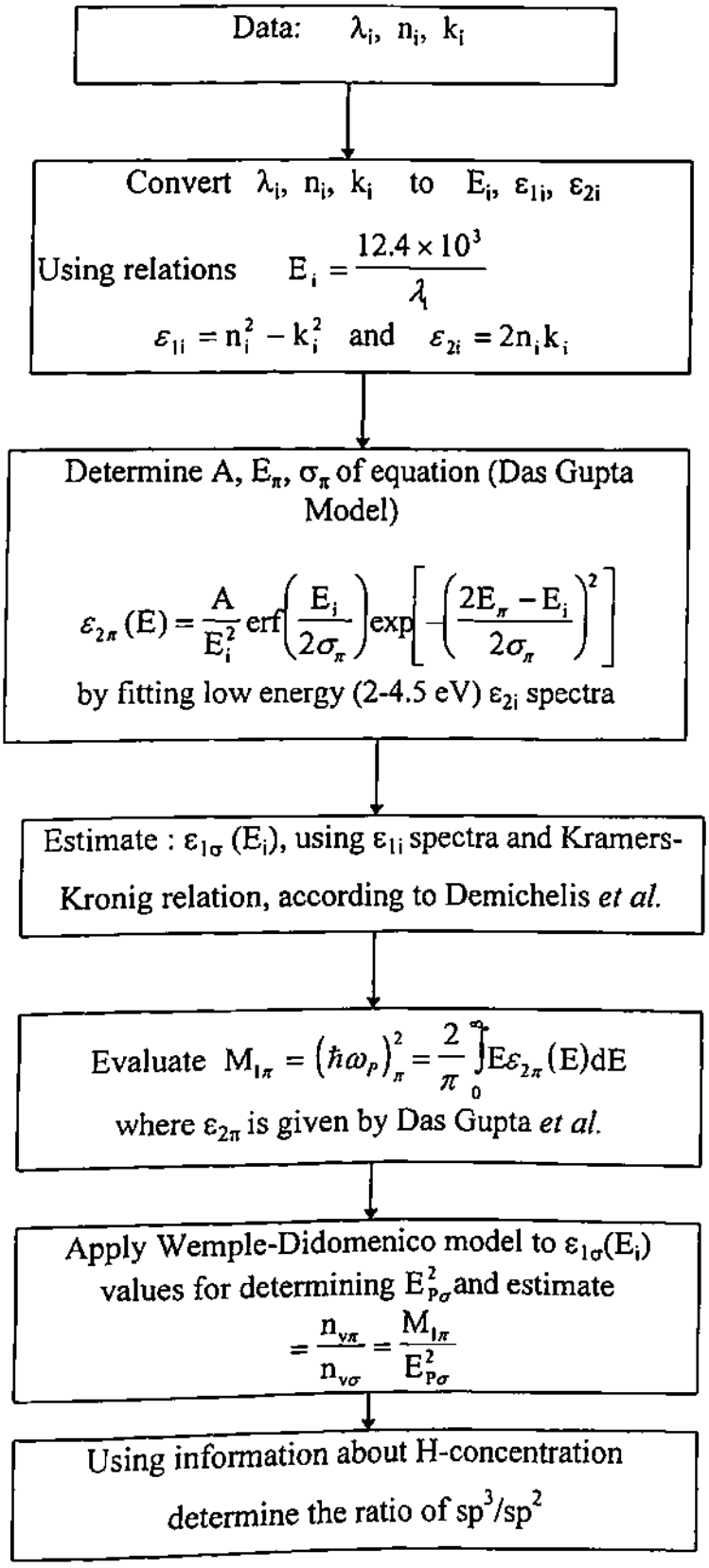

Fig. 2.7 Block diagram showing steps to evaluate sp^3/sp^2 ratio

2.14 Part Summary

A brief review of the different innovations that have been made to reduce stresses in DLC films has been presented in this chapter. The experimental setup used to grow DLC films during the present investigation and the different techniques used to characterise DLC films so formed have been discussed. Subsequently a brief description of the model used to determine the carbon bonding ratio (sp^3/sp^2) has been presented which is essentially an improvement of the analysis technique proposed by Demichelis *et al.*[25] This is followed by a brief review of the other techniques in use to determine the sp^3/sp^2 ratio. In recent published literature,[31] relating to the determination of sp^3/sp^2 ratio combining various features of Savvides[24] and Demichelis *et al.'s*[25] method, ~3 times enhancement of sp^3/sp^2 ratio has been estimated as compared to the estimation made by Savvides's[24] method. Thus, the estimation of the ratio of sp^3/sp^2 has been found to be something which requires a lot of care and, therefore, values of sp^3/sp^2 of DLC films grown in different laboratories and estimated differently should be difficult to compare. A brief review of other established techniques for the estimation of sp^3/sp^2 ratio are also presented as some of these techniques have been adopted during the present investigations to compare DLC films grown by the saddle field fast atom beam technique.

2.15 References

1. J. Zelez, *J. Vac. Sci. Technol.* A, **1** (1983) 305.
2. J. Robertson, *Adv. in Phys.*, **35** (1986) 317.
3. H. Yamada, O. Tsuji and P. Wood, *Thin Solid Films*, **270** (1995) 220.
4. Y. Catherine in *Diamond and Diamond-Like Films and Coatings*, eds. Clausing *et al.* (Plenum, New Work), (1991) p. 193.
5. A. Grill, V. Patel and B.S. Meyerson, in *Diamond and Diamond-Like Films and Coatings*, eds. Clausing *et al.* (Plenum, New Work), (1991) p. 417.
6. A. Grill and V. Patel, *Diamond and Related Materials*, **2** (1993) 1519.
7. C.J. Torng, J.M. Sivertsen, J.H. Hudy and C. Chang, *J. Mater. Res.*, **5** (1990) 2490.
8. D.F. Franceschini, C.A. Achete and F.D. Freire Jr., *Appl. Phys. Lett.*, **60** (1992) 323.
9. L. Martinu in *Diamond and Diamond-Like Films and Coatings*, eds. Clausing *et al.* (Plenum, New Work), (1991) p. 475.
10. J.L. Vossen, *J. Electochem Soc.*, **126** (1979) 319.
11. B. Chapman, *Glow Discharge Process* (John Wiley & Sons, New York), (1980).
12. J. Franks, *Vacuum*, **34** (1984) 259.
13. S. Scaglione and G. Emiliani, *J. Vac. Sci. Technol.* A, **7** (1989) 2303.
14. A.K. Sinha, H.J. Levinstein and T.E. Smith, *J. Appl. Phys.*, **49** (1978) 2423.
15. G.G. Stoney, *Proc. R. Soc. London Ser.* A, **82** (1990) 172.
16. J. Tauc, R. Grigorovici and A. Vancu, *Phys. Status Solidi,* **15** (1966) 627.
17. J.C. Lascovich and S. Scaglione, *Appl. Surf. Sci.*, **78** (1994) 17.
18. M.H. Brodsky, M. Cardona and J.J. Cuomo, *Phys. Rev.* B, **16** (1977) 3556.
19. D.K. Avasthi, D. Kabiraj, Jaipal, G.K. Mehta, H.C. Barshilia, S. Sah, and V.D. Vankar, *Vacuum*, **46** (1995) 633.
20. B. Dischler, A. Bubenzer and P. Koidl, *Solid State Commun.*, **48** (1983) 105.
21. D.R. Mckenzie, R.C. Mc Phedra, N. Saddides and D.J.H. Cockayne, *Thin Solid Films,* **108** (1983) 247.
22. R.H. Jarman, G.J. Ray, R.W. Standley and G.W. Zajax, *Appl. Phys. Lett.*, **49** (1986) 1065.

23. R.O. Dilion, J.A. Woollam and V. Katkanant, *Phys. Rev.* B, **29** (1984) 3482.

24. N. Savvides, *J. Appl. Phys.*, **59** (1986) 4133.

25. F. Demichelis, C.F. Pirri and A. Tagliaferro, *Phys. Rev.* B, **45** (1992) 14364.

26. S.H. Wimple and M. Didomenico, Jr., *Phys. Rev.* B, **3** (1971) 1338.

27. D. Dasgupta, F. Demichelis, C.F. Pirri and A. Tagliaferro, *Phys. Rev.* B, **43** (1991) 2131.

28. B.S. Verma, A. Basu, O.S. Panwar, P.N. Dixit, D. Sarangi, M. Kar and R. Bhattacharyya, *NPL Technical Bulletin*, **July** (1994) 8.

29. B.S. Verma, A. Basu, O.S. Panwar, P.N. Dixit, D. Sarangi, M. Kar and R. Bhattach
in *Semiconductor Devices*, ed. K. Lal (Narosa Pub. House, New Delhi) (1996) p. 430.

30. B.S. Verma, A. Basu, O.S. Panwar, P.N. Dixit, D. Sarangi, M. Kar and R. Bhattacharyya, *NPL Technical Report*, No. NPL/94-C1.5-0005.

31. S.S. Mahajan, H.C. Barshilia, B.R. Mehta and V.D. Vankar, *Thin Solid Films*, **302** (1997) 250.

Chapter III

Growth of Diamond Like Carbon Films by Plasma Enhanced Chemical Vapour Deposition Techniques

3.1 Introduction

In this chapter an attempt has been made to show how the conventional technique of RF self bias, which is widely used,[1-9] has many limitations and is inadequate to realise many potential applications of diamond like carbon (DLC) material. It is felt that by treating this as a starting point all subsequent efforts made in pursuit of a benign and versatile technique of growth of DLC films, which is also easy to implement, will be better appreciated.

The most popular technique to grow DLC films appears to be the asymmetric RF self bias PECVD. This can be easily setup in many laboratories and depends largely on the characteristics of a RF discharge in a hydrocarbon gas. Ion energies in the range of a few hundred eV can be conveniently generated at reasonable RF power densities (~ 200-300 mW/cm^2). This technique thus avoids the use of expensive ion beam sources which would otherwise be preferred to grow such films. However, RF self bias technique has certain limitations which will be subsequently brought out during the discussion of the results of the present investigation. It is the appreciation of these limitations that lead the researcher to find new ways to grow DLC films.

The RF self bias technique has the ability to grow highly insulating DLC films on equally insulating substrates. In this process the impact energy of the precursor radical is found to be physically the most important parameter in the deposition of dense DLC film and has been estimated to be in the range of several tens to few hundreds of eV.[10] Since the ion energy is not directly measurable in RF systems, most workers used the discharge power and hydrocarbon

pressure to control the deposition process and, thereby, the film properties. Alternatively, the negative self bias voltage and partial pressure of the hydrocarbon gas in question have been used as independent deposition parameters. Bubenzer *et al.*[3] demonstrated the dependence of the mean impact energy (E) on self bias voltage (V_B) and pressure (P). In their experiments involving RF discharge in benzene, the proportionality $E \approx V_B P^{-1/2}$ was found. Also Dischler *et al.*[9] have shown that the film properties can be reproducibly varied by changing V_B and P. Enke[10] has painstakingly mapped a *"landscape"* which vividly depicts the variation of refractive index, bandgap, hardness, stress etc. with self bias voltage and hydrocarbon pressure.

As the impact energy increases, one goes from plasma polymers to dense hydrocarbons to dense carbon, and at very high energies of about 1000 eV, degradation to a graphitic structure is observed.[11] Increasing amounts of graphitic character are also noticed when the substrate temperature is increased.[11] Enke[10] also reported that carbon films can be made hard at sufficiently high bias voltages and low pressures and in the remaining parameter space films produced remain largely soft. At high pressures, inelastic collisions in the ion sheath tend to reduce the average ion energy.[12]

The organisation of the chapter is as follows: In a RF self bias reactor setup in this laboratory, DLC film growth process was first optimised. DLC films were grown at varying power densities, gas pressure and the dependence of film properties on these variables studied. Subsequently plasma excitation frequency was changed and these experiments repeated. Through these studies it became abundantly clear that RF asymmetric self bias growth has many limitations as far as scale up of the process for industrial application and reliable deposition of low stress DLC films are concerned. This appreciation of the limitations of this technique provided the researcher certain guidelines about the appropriate techniques for the production of low stress DLC films.

For the attainment of a higher rate of deposition of a-C:H films, having a denser network structure, growth experiments should be performed by means of a higher generation rate of the radicals and by allowing them to land on the surface of the substrate at a high enough energy. In

order to obtain a higher radical generation rate, the electron density and/or the partial gas pressure should be increased. However, the application of a high power density to the hydrocarbon plasma at 13.56 MHz leads to the enhancement of stresses and operating at high pressures may lead to gas phase polymerisation, etc. Thus it becomes necessary to find out an alternate method to enhance growth rates. In other words, one is looking for more efficient plasma deposition processes that can provide low residual stress DLC films deposited at high deposition rate.

In recent years, there has been an increased interest in the use of very high frequency (VHF) plasma processing compared with the conventional radio frequency (RF) discharge at 13.56 MHz. Earlier it was believed that increase of the excitation frequency above 13.56 MHz would not have a major influence on the growth and the properties of films, because one is already above ion plasma frequency.[13] Above this frequency, the ions are considered to remain stationary in the alternating electrical field and thus any further increase of the excitation frequency was earlier assumed to have no beneficial influence on the process performance.

Despite these doubts, VHF (30-300 MHz frequency band) plasma processing was demonstrated by several groups,[13-31] and convincing evidence was generated that the excitation frequency indeed influences the deposition rate significantly. Subsequently, more subtle effects of excitation frequency became known for silicon processing, such as ease of inducing microcrystallisation,[27,28] improved uniformity,[15] reduced stress[13,30] etc. More recently large area processing of a-Si:H at VHF frequencies, despite the earlier doubt of the existence of a finite wavelength effect at these frequencies, has been demonstrated by the Neuchatel[32] group. It would therefore, be interesting to grow a-C:H films by similar technique and judge how far this technique meets the requirements mentioned above.

Again by operating a discharge at VHF one has an access to yet another process parameter i.e. frequency (in addition to power density and gas pressure) to independently control the ion flux and ion energy to tailor the material property indicators.

Because of the experimental limitations, the present study focusses on the effect of varying the applied power to the cathode, at a fixed frequency of 100 MHz.

3.2 Experimental Details

The samples were deposited in a plasma CVD laboratory type reactor assembled during the early part of the present research programme. For the plasma decomposition of the various hydrocarbon source gases/vapours RF power was applied to the cathode of the reactor by using a RF (13.56 MHz) generator (RF5S, RF Plasma Products Inc.) or alternatively an indigenously developed (at Nuclear Science Center, New Delhi) VHF (100 MHz) generator. At each applied power, the matching network was adjusted for minimum (almost zero) reflected power. A high voltage regulated power supply (M/s Aplab) with a LC filter was used to apply externally a negative DC voltage together with the required VHF power to the cathode. The a-C:H films thus, deposited with varying applied power density, pressure and frequency were subsequently characterised for properties like deposition rate, stress, hardness, optical bandgap, refractive index etc. as per procedure already outlined in **Chapter II**.

3.3 Effect of Process Parameters

3.3.1 Effect of Self Bias Voltage

3.3.1.1 RF Power vs. Self Bias Voltage

The negative self bias voltage (V_B) was measured as a function of RF power density for glow discharge decomposition of methane, acetylene and benzene, as shown in **Fig. 3.1**. It is clear from this figure that self bias voltage has a linear dependence on the applied power density and this trend is identical for all the three hydrocarbons. However, for similar conditions, the self bias voltage is dependent on the type of hydrocarbon used. Koidl *et al.*[33] found that the average energy

of ions impinging on the substrate, in case of benzene discharge by RF self bias technique, is 0.4 times the self bias voltage. With this knowledge, the self bias voltage can be varied to tailor the ion energy.

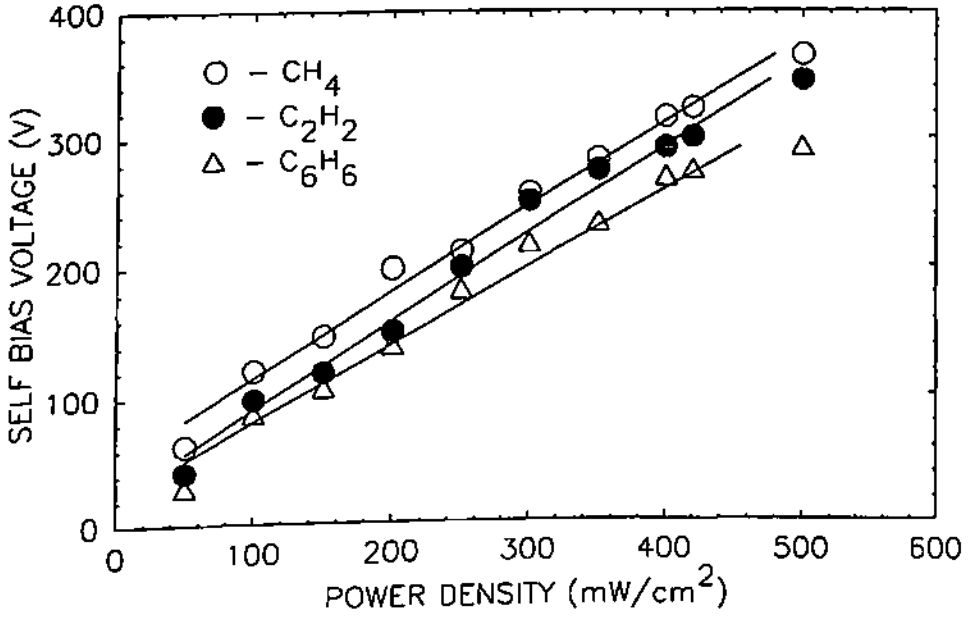

Fig. 3.1 Self bias voltage as a function of RF power density for glow discharge decomposition of CH_4, C_2H_2 and C_6H_6 at 25×10^{-3} mbar of pressure

3.3.1.2 Deposition Rate vs. Self Bias Voltage

In **Fig. 3.2** the variation of the deposition rate, obtained as a function of self bias voltage, has been graphically shown for all the three hydrocarbon grown films i.e. CH_4, C_2H_2 and C_6H_6. It is evident from this figure that the deposition rate (r_d) increases with the increase in the self bias voltage and this trend is identical for all the three hydrocarbons. However, for similar deposition conditions, the values of r_d was found to be dependent on the type of hydrocarbon used to grow DLC films. With the increase of power applied to the cathode, the generation of ions and neutrals also increases, which helps to increase the value of r_d. The observed results of the increase of r_d with the increase of applied power agrees with the results obtained by Koidl *et al.*[33] and Anderson *et al.*[34] The value of r_d increases when one changes from CH_4 to C_2H_2 gas or C_6H_6 vapours. It may

be observed that the carbon to hydrogen ratio is the same for C_2H_2 and C_6H_6 but the observed values of r_d are quite different in these two cases. The value of r_d for C_6H_6 vapour is about half that for C_2H_2 gas. It is not very clear why r_d is lower in case of C_6H_6, though there exists a report which

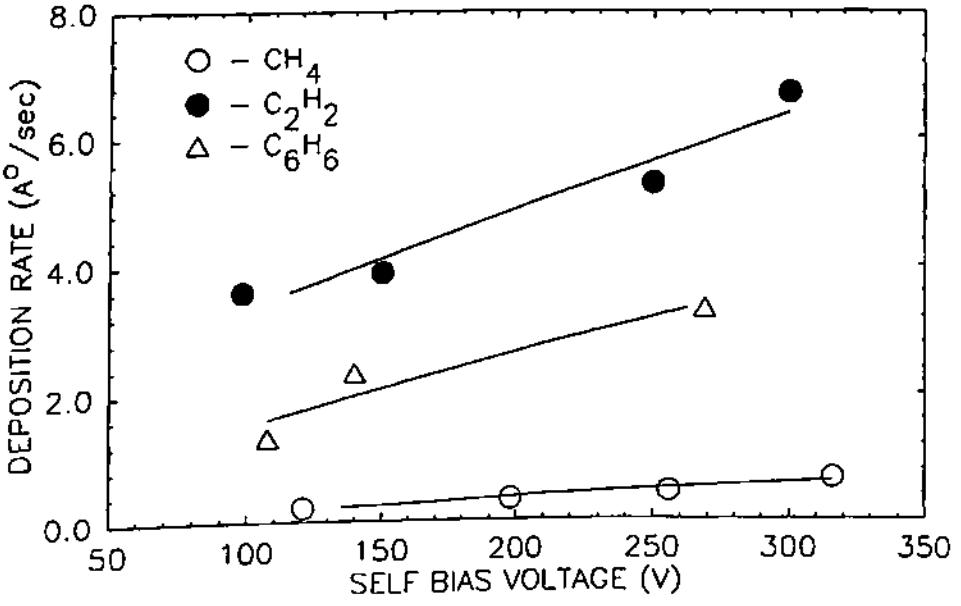

Fig. 3.2 Variation of the deposition rate as a function of self bias voltage for films grown at 25×10^{-3} mbar pressure of CH_4

says that the voltage scale for the benzene deposited films should be halved for comparison to films deposited from aliphatic hydrocarbons.[35] A simple explanation would be that the tendency for benzene to fragment into ions composed of two carbon atoms effectively halves the kinetic energy per carbon atom.

3.3.1.3 Stress vs. Self Bias Voltage

Assessment of the residual stress in DLC films is of paramount interest for practical applications of such films. Stress in a DLC film is most conveniently measured by the change in the curvature of the film-substrate combination. In this laboratory this is estimated by a laser scanning technique which was specifically set up for such measurements. **Figure 3.3** shows the

variation of internal stress as a function of the negative self bias voltage. It is evident from this figure that the stress in these films increases with the increase of self bias voltage. It is interesting

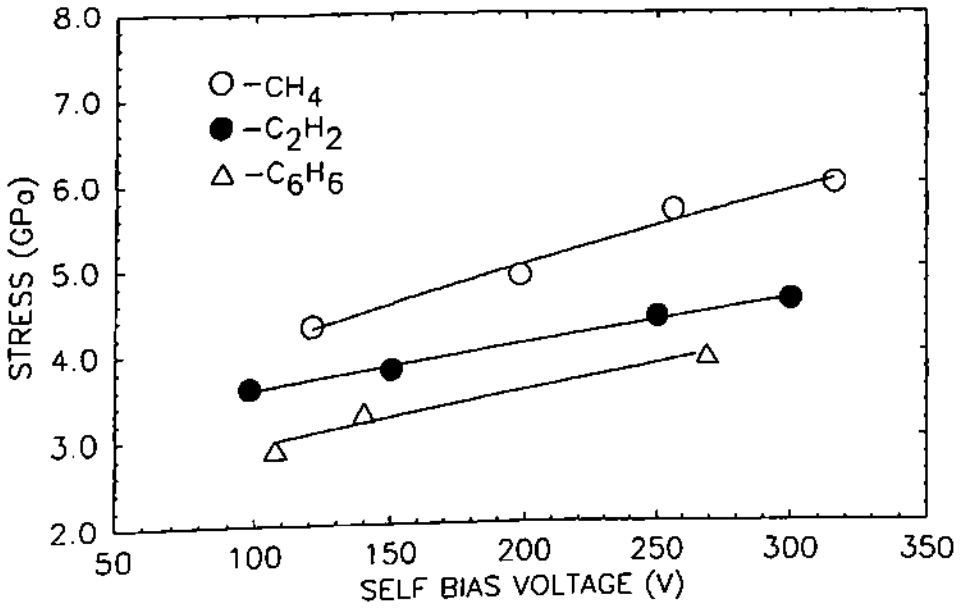

Fig. 3.3 Dependence of stress as a function of self bias voltage at 25×10^{-3} mbar gas pressure of CH_4

to note that the behaviour of stress, as a function of negative self bias voltage, correlates completely with the variation of hardness with the self bias voltage (**Fig. 3.4**). It can also be noticed from a study of **Fig. 3.3** that the value of stress decreases when one switches from CH_4 gas to C_2H_2 gas and then to C_6H_6 vapours. Several reports exist which specifically mention that stresses in DLC films are strongly dependent on the nature of the precursor used.[36-38] Different reasons have been assigned to explain this behaviour and a studied attempt has been made in this thesis to understand the same.

3.3.1.4 Hardness vs. Self Bias Voltage

Diamond like behaviour of DLC films entails that they are hard and rigid. Hardness of these films was estimated as per procedure outlined under **section 2.7** in **Chapter II**. **Figure 3.4**

shows the variation of hardness of these films with the self bias voltage. Hardness values are found to increase with the increase of self bias voltage systematically. Specifically, for self bias voltages in the range $0<V_b<100$ V, soft polymerised carbon films were obtained and these observations are not recorded in **Fig. 3.4**. These polymer like films easily scratched with a steel point and also were damaged easily on the application of a load during hardness measurement. Only those films that are grown on application of self bias voltage of 100 to 325 V were found to be hard and reasonably of low residual stress. Again the films that were grown with a significantly high value of the self bias voltage delaminated from the substrates after they were brought out of the reactor. Such stress relief

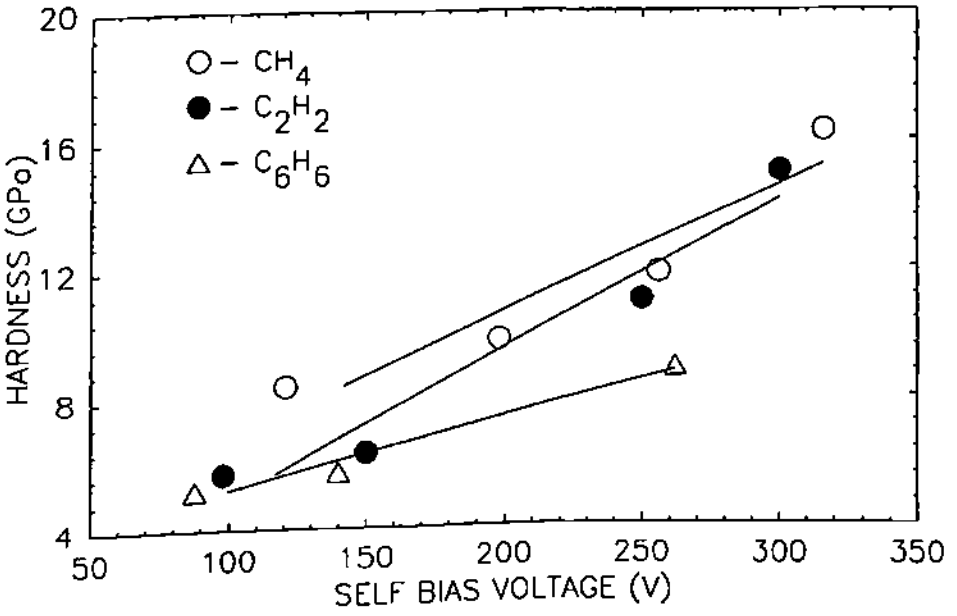

Fig. 3.4 Variation of hardness as a function of self bias voltage at 25×10^{-3} mbar pressure of CH_4

patterns of DLC films grown on glass substrates are discussed in detail under **section 4.10** in **Chapter IV**. **Figure 3.5** has been specifically drawn to illustrate the intimate relation that exists between the built-up residual stresses and hardness values of these films. It is observed from this figure that with the increase of hardness, the internal stresses of these films also increase. It endorses the observations reported by several other groups[39,40] that ***high hardness is always accompanied by high internal compressive stress***. From **Fig. 3.5** one can also see that slopes of

hardness vs. stress curves for CH_4 and C_6H_6 are nearly equal but for C_2H_2 it is quite different. In other words, C_2H_2 grown films show low incremental increase in the stress values compared to CH_4 and C_6H_6 grown films for the same amount of increase in the hardness value.

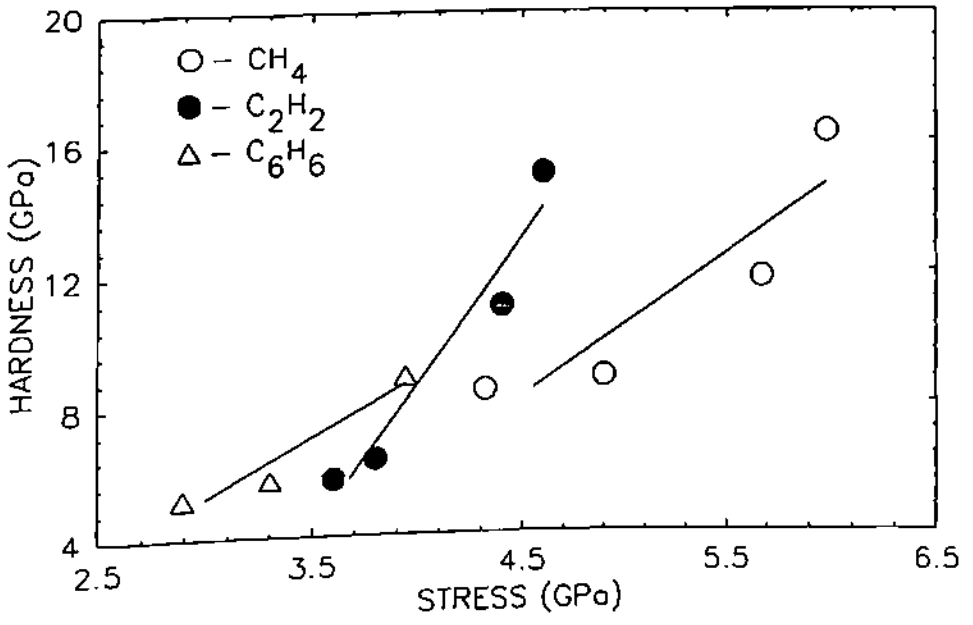

Fig. 3.5 Relation of stress and hardness of DLC films grown using CH_4, C_2H_2 and C_6H_6

3.3.1.5 Optical Bandgap vs. Self Bias Voltage

Optical bandgap has been determined from Tauc plots ($\sqrt{\alpha h\nu}$ vs. hν) as explained under **section 2.9.1** in **Chapter II**. The change in the optical bandgap of DLC films with the negative self bias voltage is shown in **Fig 3.6**. From this figure it is evident that the value of E_g decreases with the increase of self bias voltage. Optical bandgap values are found to depend strongly on the negative self bias voltage. Films deposited with a high V_b exhibit lower transmission, higher absorption, especially in the near-UV region, and a lower optical bandgap. The increase of V_b means an increase in the energy of the bombarding species during the DLC film growth, which

helps to remove the weakly bonded hydrogen from the film, and this presumably leads to reduced E_g values. It may be recalled that Dischler *et al.*[9] reported a linear increase of E_g of plasma deposited a-C:H films with the increase of hydrogen content.

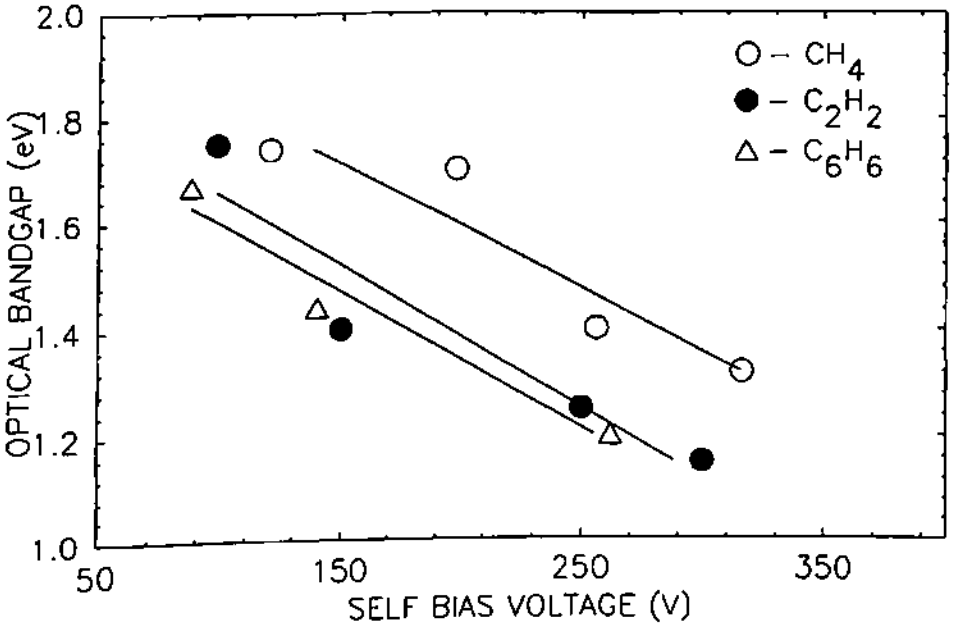

Fig. 3.6 The variation of the optical bandgap as a function of negative self bias voltage

3.3.1.6 Refractive Index vs. Self Bias Voltage

Figure 3.7 shows the variation of refractive index with the self bias voltage. It is evident from this figure that the value of *n* increases with the increase of self bias voltage. It is observed that the dense and hard, reasonably scratch resistant, carbon films are characterised by large values of *n* and soft carbon films by low values of *n*. This is consistent with the results published in the literature.[41,42] The observed refractive index values are found to depend strongly on the negative self bias voltage, similar to optical bandgap dependence, as discussed in **section 3.3.1.5** and shown in **Fig. 3.6.**

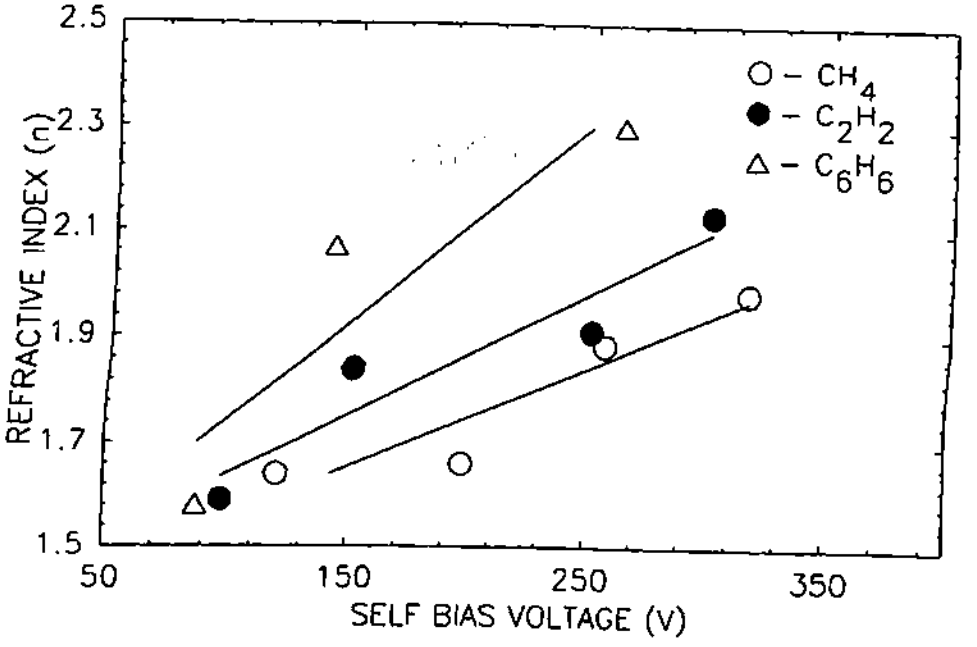

Fig. 3.7 The variation of refractive index with self bias voltage

3.3.2 Effect of Pressure

3.3.2.1 Self Bias Voltage as a Function of Gas Pressure

Figure 3.8 shows the measured self bias voltage (V_B) as a function of the RF power density for different C_2H_2 gas pressures. From this figure it is evident that the V_B increases as the RF power density increases, but decreases slightly as the gas pressure increases. Therefore, it is reconfirmed that V_B depends strongly on the RF power density and weakly on the gas pressure, as reported by several other workers.[43]

3.3.2.2 Deposition Rate as a Function of Gas Pressure

Figure 3.9 shows the variation of deposition rate with CH_4 gas pressure. It is found from this figure that the deposition rate increases with the increase of CH_4 pressure. With the increase of

gas pressure the generation rates of ions and neutrals increase which helped to increase the deposition rate.

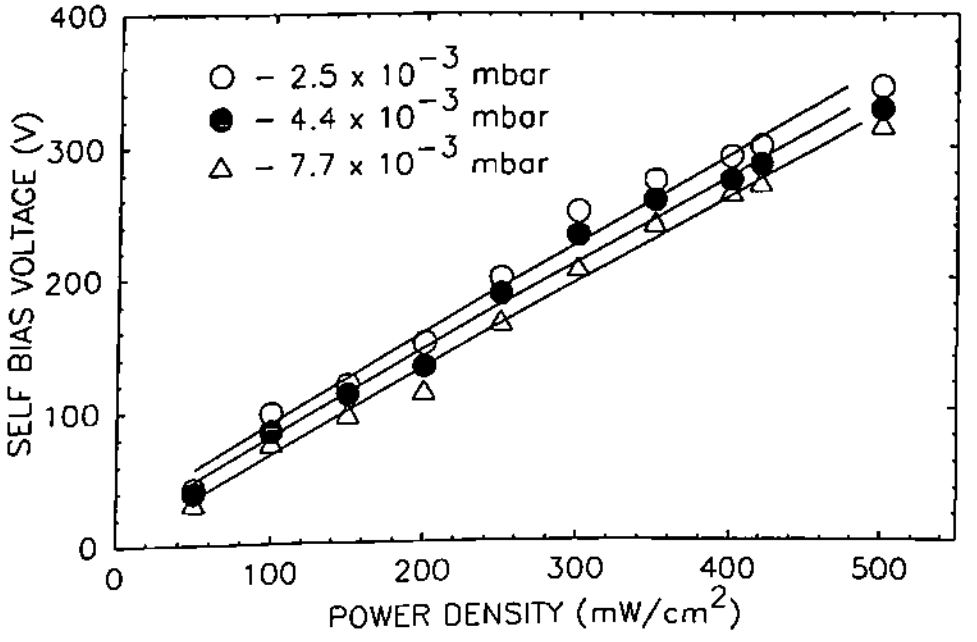

Fig. 3.8 Self bias voltage as a function of RF power density at different gas pressure

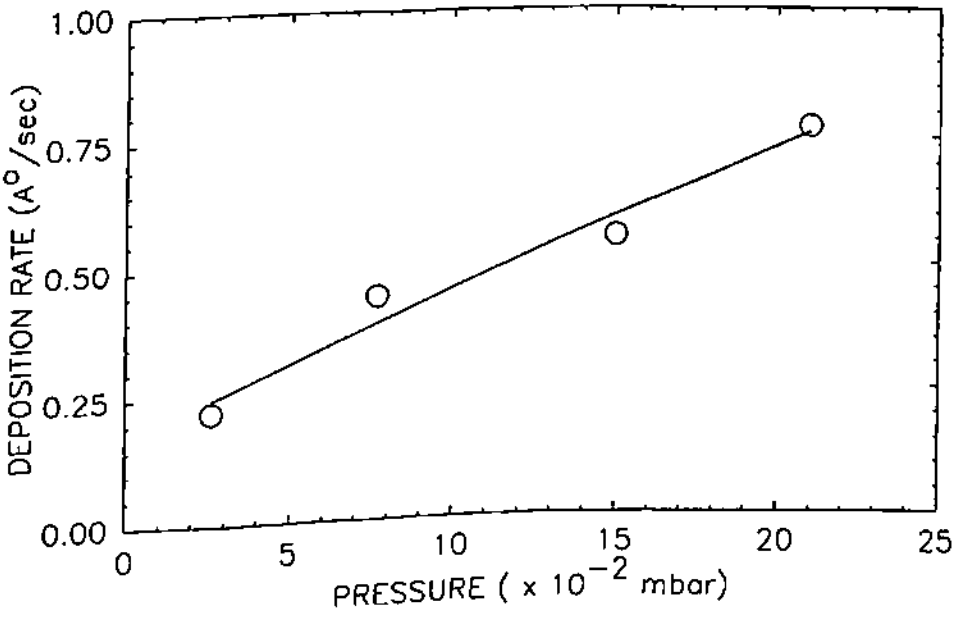

Fig. 3.9 Variation of the deposition rate with the gas pressure at 120 V self bias voltage

3.3.2.3 Stress as a Function of Gas Pressure

Figure 3.10 shows the variation of stress values as a function of CH_4 partial pressure at 120 V self bias voltage. It is evident from the figure that the stress values decrease with the increase of pressure. It has been well established that the stresses in DLC films depend largely on the impact energy of ions/neutrals. This has been confirmed during the present investigation as well as shown in **Fig. 3.3**. The stress values have been found to decrease with the increase of self bias voltage, or effectively the ion energy. With the increase of gas pressure the average energy of the film forming precursors (ions) reduces due to the more frequent collision with the residual gas molecules and thereby the residual stress in these films show a lower value.

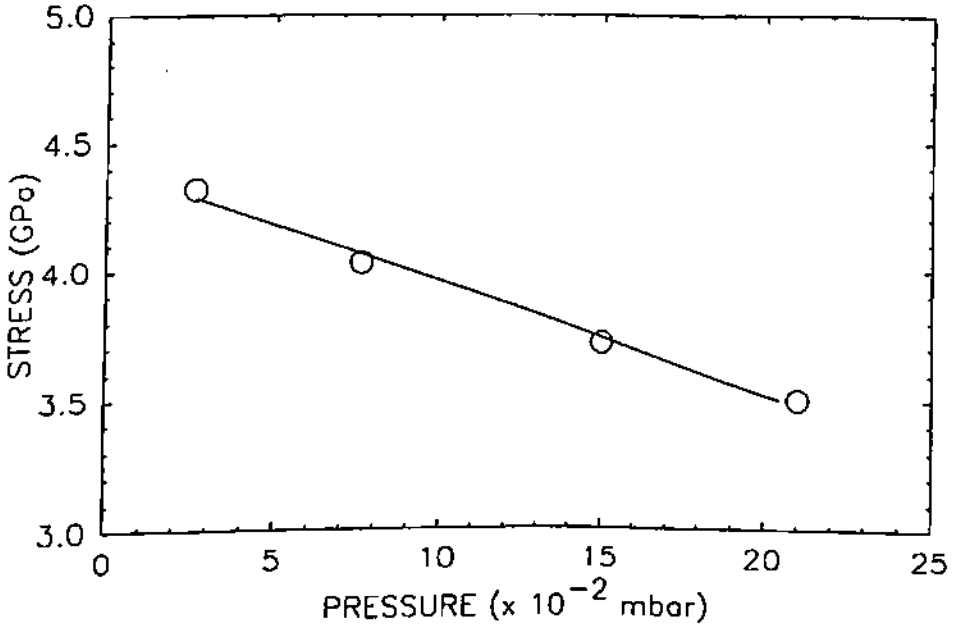

Fig. 3.10 Dependence of stress as a function of gas pressure at 120 V self bias voltage of CH_4

3.3.2.4 Hardness as a Function of Gas Pressure

Figure 3.11 shows the variation of hardness of DLC films with pressure when CH_4 is used as the feed gas, at 120 V self bias voltage. From this figure, it is seen that the values of film

hardness decreases with the increase of gas pressure. It may be noted that with increasing pressure, the effect of ion energy on the growing film surface will be reduced because of the frequent collisions with other atoms/molecules i.e. reduction of the mean free path, and this in turn will affect the hardness of the films.

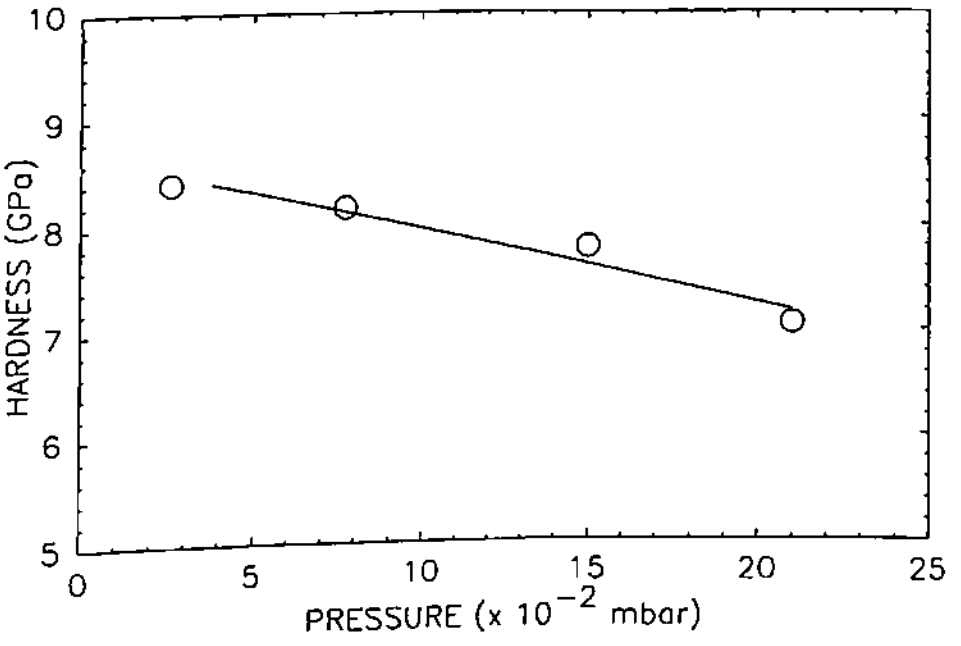

Fig 3.11 Variation of DLC film hardness as a function of gas pressure of CH_4 at 120 V self bias voltage

3.3.2.5 Optical Bandgap as a Function of Gas Pressure

Figure 3.12 shows the variation of optical bandgap with the CH_4 partial pressure at a fixed self bias voltage of 120 V. It is found that the values of optical bandgap increases with the increase of gas pressure. It is to be noticed that the dependence of optical bandgap on CH_4 partial pressure is not as strong as on self bias voltage as reported earlier (**Fig. 3.6**).

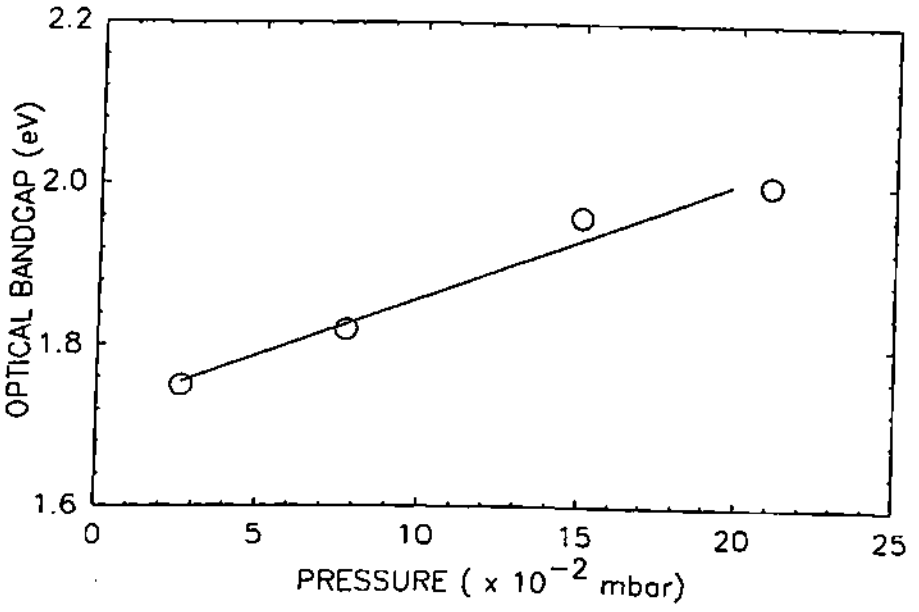

Fig. 3.12 The variation of the optical bandgap as a function of gas pressure of CH_4

3.3.2.6 Refractive Index as a Function of Gas Pressure

Figure 3.13 shows the variation of refractive index (n) with the CH_4 pressure. The values of refractive index are found to decrease with the increase of CH_4 pressure. This again weakly correlates with the dependence of optical bandgap on CH_4 partial pressure.

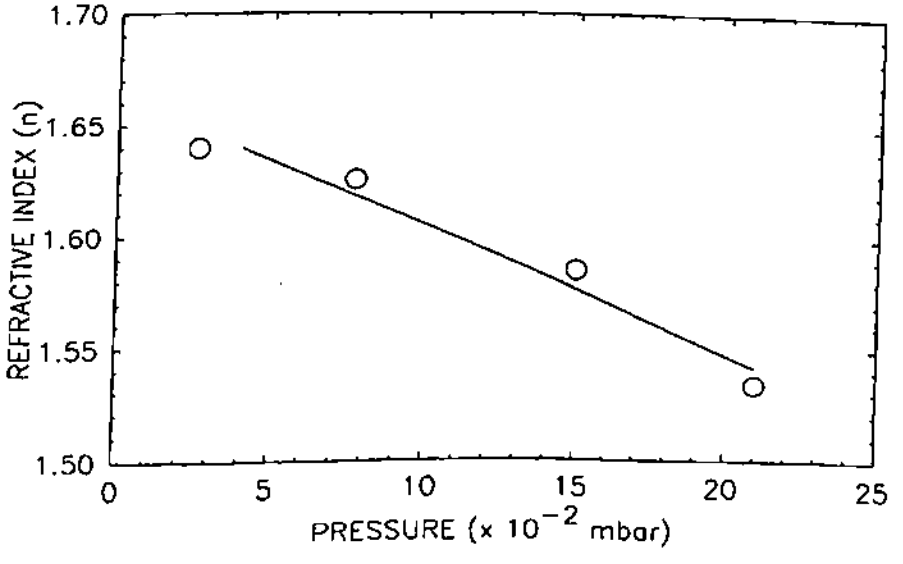

Fig. 3.13 The variation of refractive index with gas pressure of CH_4

3.3.3 Effect of Plasma Excitation Frequency

3.3.3.1 Negative Self Bias Voltage at 100 MHz

Figure 3.14 shows the variation of self bias voltage for VHF (100MHz) plasma discharge in CH_4 as a function of power density. A comparative study of **Fig. 3.1** and **Fig. 3.14** shows that self bias voltage (V_B) for VHF plasma is very low compared to RF plasma. This observation is similar to the one made by Kuske *et al.*[17]

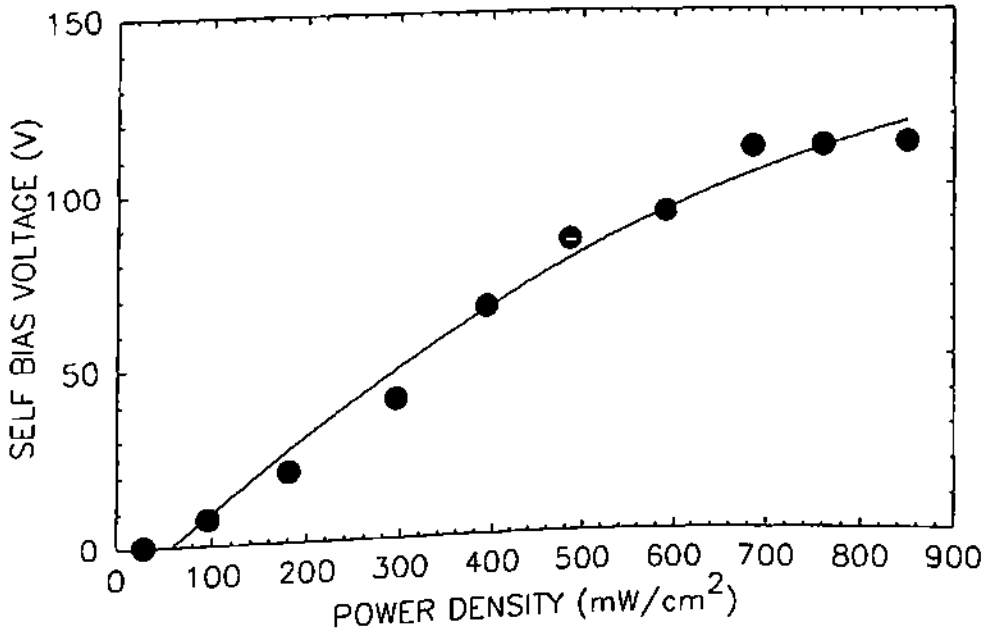

Fig. 3.14 The variation of self bias voltage for VHF (100 MHz) excitation of the plasma as a function of applied power density

The occurrence of low V_b is case of VHF plasma discharge appears to be understandable in view of the fact that at VHF frequencies the sheath impedance is reduced considerably.[20] This can be seen as a consequence of the decrease of the sheath thickness d_s, with the excitation frequency.[15] This in turn increases the cathode sheath capacitance $C = \varepsilon_o/d_s$ (per unit electrode area), where ε_o is the permittivity of the free space. In such situations self bias voltage decreases considerably,[17] as at high enough frequencies sheath capacitance is short circuited by the bulk plasma impedance.[20]

Indeed, measurements of the peak to peak voltage[15] and plasma impedance show that the potential drop across the sheath and the fraction of power dissipated in the sheath[21] decreases with frequency.

3.3.3.2 Variation of Deposition Rate for VHF (100 MHz) Discharge

It is found that the deposition rate increases with the applied power density (corresponding self bias voltages are given in **Table-3.1**) as shown in **Fig. 3.15**. It is evident from **Fig. 3.2** and **Fig. 3.15** that the r_d is about 5-6 times higher in VHF plasma grown films as compared to RF grown films (where all other parameters are kept constant). This may be because in VHF plasma large number of ions/neutrals of low energy are available, at the growing surface of the films, which help to increase deposition rate. It was also shown by H. Keppner[44] that the bulk plasma absorbs more power for plasma excitation frequencies in the range of 50-100 MHz. As a direct effect of this power transfer is an increased electron impact dissociation rate of the gas molecule (also called by him *"breeding effect"*). This naturally provides sufficient reactive species that are required for an enhanced deposition rate. The existence of such breeding effect has been confirmed by several other groups[23,31] to be frequency dependent i.e. if the plasma excitation frequency comes close to

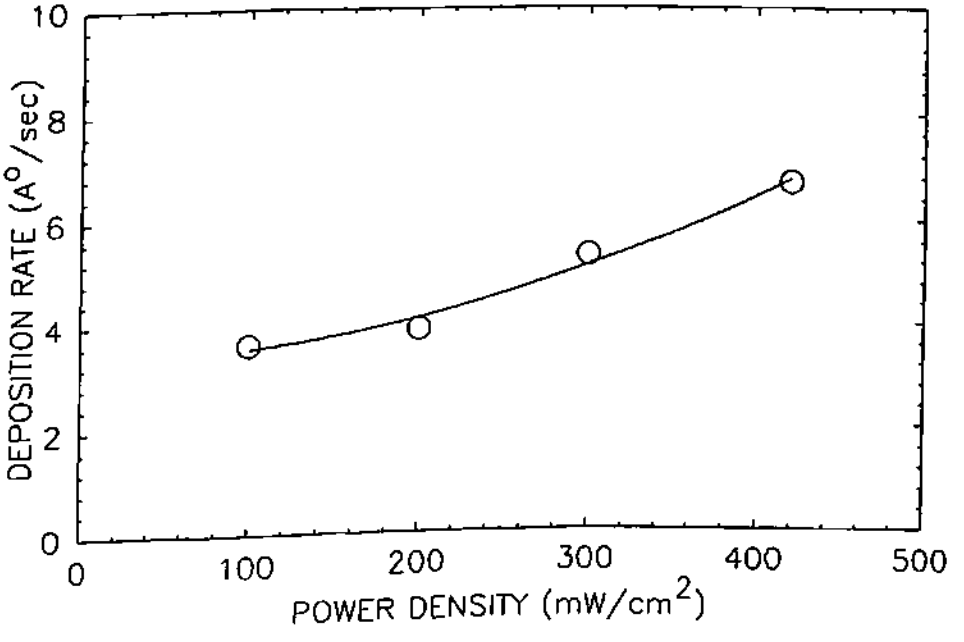

Fig. 3.15 The deposition rate as a function of applied power density for VHF glow discharge grown DLC films

the characteristic frequency (50-100 MHz) the most effective power transfer from the source occurs. Also it may be noted that Chatham *et al.*[19,45] studied the effect of excitation frequencies in the range of 13.56 to 110 MHz, using silane and disilane as source gases. In both these cases they found that growth rate r_d increase with the increase of excitation frequency. Oda and co-workers[16,46] have also prepared a-Si:H and μc-Si:H films at 13.56 and 144 MHz frequencies and found higher r_d for the higher excitation frequency. There is, therefore, convincing evidence that the excitation frequency also influences the growth of a-C:H like a-Si:H films.[47] It is evident from **Table-3.1** that there is a slight reduction in the deposition rate with externally applied negative DC voltage, though it remains quite high as compared to RF plasma produced films.

3.3.3.3 Stress for 100 MHz Grown Films

Figure 3.16 shows the variation of stress with bias voltage for VHF and RF grown films. It is to be noted here that bias voltage for the VHF case is the sum of self produced voltage of the VHF discharge and the externally applied negative DC voltage, whereas in the RF case bias voltage is only the self produced voltage of the RF discharge at the cathode. Stresses in the films produced

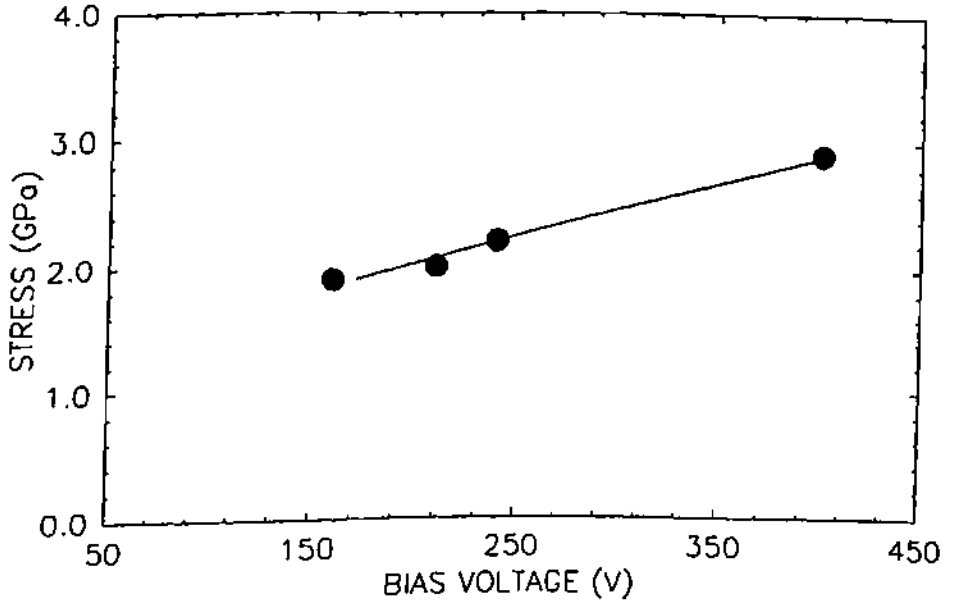

Fig. 3.16 The variation of the built-up stress with bias voltage for VHF glow discharge grown DLC films

by RF excitation are found to be more than in the case of VHF deposited films. They fall in the range 1.7-2.9 GPa for VHF and 3.6-4.6 GPa for RF grown films. The behaviour of stress as a function of bias voltage correlates completely with the behaviour of hardness (as shown in **Fig. 3.17**). In the case of VHF plasma grown films, the chance for stress buildup is very low as self bias voltage is quite low (as shown in **Fig. 3.14**). At such low biases ion bombardment on the surface of the growing film also reduces. Even in the case of externally applied negative DC voltage with VHF power, stress values may not increase in a manner similar to that seen in RF deposited films. Indeed, Grill *et al.*[38] have reported that DC plasma grown DLC films contain low stresses compared to RF grown films. For this to happen they argued that in DC plasma usually low power densities are used, compared to RF plasma. The higher power density causes stronger dissociation of the source gases in the plasma and thus higher incorporation of unbound hydrogen. This correlation of unbound hydrogen with increase in stress values has been confirmed during the present investigations and will be reported subsequently. Thus it is believed that the combined effect of self bias voltage produced by VHF plasma and the applied negative DC voltage does not enhance stress values much, though these values are quite high.

3.3.3.4 Hardness for VHF Plasma Grown Films

Figure 3.17 shows the variation of hardness with bias voltage (here also bias voltage means what has been explained earlier) for VHF grown films. Films deposited without negative DC voltage with VHF power were quite soft and while measuring hardness at 50 gm load they often crumbled and one could at best roughly estimate hardness of these type of films. They were found to be in the range of 20-40 MPa. In the case of RF deposited films the values of hardness increased from 5.7 GPa to 15 GPa with the increase of self bias voltage from 98 V to 300 V (**Fig. 3.4**). However, in case of VHF deposited films, corresponding to 10 V self bias voltage (i.e. the self bias developed by VHF discharge alone), the value of hardness of the film was approximately 4 GPa. As the externally applied negative DC voltage increased from 150 V to 390 V, the values of hardness of film also increased from 5 to 9 GPa.

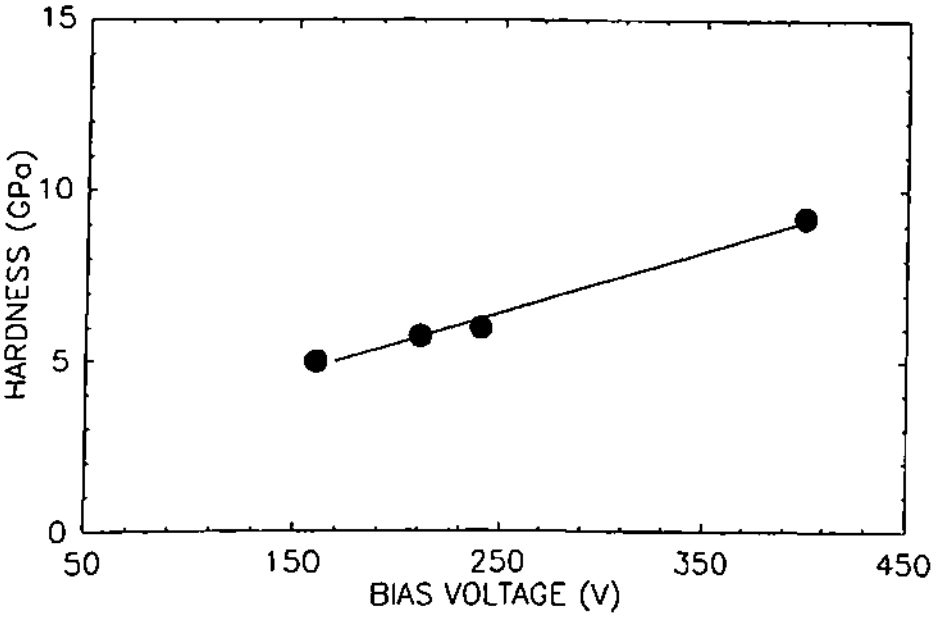

Fig. 3.17 The variation of hardness with bias voltage for VHF glow discharge grown DLC films

A study of **Table-3.1** reveals that for the RF plasma at 300 V self bias voltage, the hardness of the resulting DLC film is close to 15 GPa as compared to only 9 GPa for the films grown by VHF plasma, with externally applied negative DC voltage of 390 V. The reason why a VHF hydrocarbon plasma requires a higher negative DC voltage to be externally applied, to produce the same degree of hardness in DLC films that is otherwise realised at lower self bias values in case of RF excitation, is not very clear.

3.3.3.5 Optical Bandgap for VHF Plasma Grown Films

The changes in the optical bandgap (E_g) as a function of applied power density for VHF grown films are shown in **Fig. 3.18**. It is evident from **Fig. 3.6** and **Fig. 3.18** that the value of E_g decreases with the increase of power density for both RF and VHF deposited films. The change in E_g for RF grown films is large compared to VHF grown films for the same range of applied power. Self bias voltage variation with applied power of 100 to 300 mW/cm^2, is from 98 to 250 V for RF discharge grown films, whereas it was only 7.43 to 39.67 V for VHF discharge grown films. Thus,

this small variation in the self bias voltage in VHF discharges may be the reason for small variations in E_g values. Low self bias voltage is not able to provide sufficient energy to the bombarding ions on the growing surface of the film to make much difference to the microstructure. Also from **Table-3.1**, it is clear that with externally applied negative DC voltage to the VHF discharge, not much change in E_g occurs and values almost remain constant throughout the range of DC bias voltages studied.

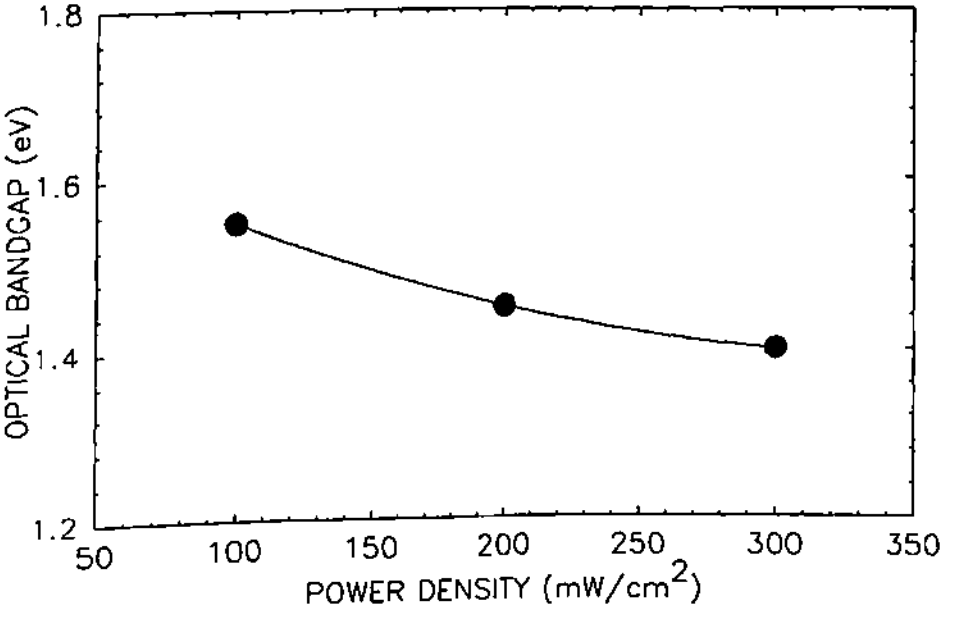

Fig. 3.18 The optical bandgap as a function of power density for VHF glow discharge grown DLC films

3.3.3.6 Refractive Index for VHF Plasma Grown Films

To calculate refractive index of these films ellipsometry measurements were performed on a rotating analyser/polariser instrument with an angle of incidence 70° when measured with a monochromatic light beam of 546.1 nm wavelength. **Figure 3.19** shows the variation of the refractive index as a function of applied power density for VHF grown films. The change in values of refractive index (n) lies between 1.8 to 1.9 for the VHF deposited films with different applied power. This change of refractive index is similar to the small changes observed in the optical bandgap of these films (**Fig. 3.18**). As the accuracy of determining the value of n is about 0.01, one

can say that this change in n falls within the range of experimental errors and there is hardly any change in n values. In case of RF plasma deposited films, however, this variation was between 1.59 to 2.13. From **Table-3.1** it may be noted that there is only a marginal change of refractive index values (a trend similar to optical bandgap even with externally applied negative DC voltage). Basu *et al.*[48] also reported invariant refractive index values for their a-C:H films deposited at different DC bias voltages using acetylene as the feed gas. They, however, did not assign any specific reason for their observation. In the present investigation also, no specific reason can be found for hardly any variation in the refractive index values. One possible explanation may perhaps be the difference in the electron energy distribution function at 100 MHz.

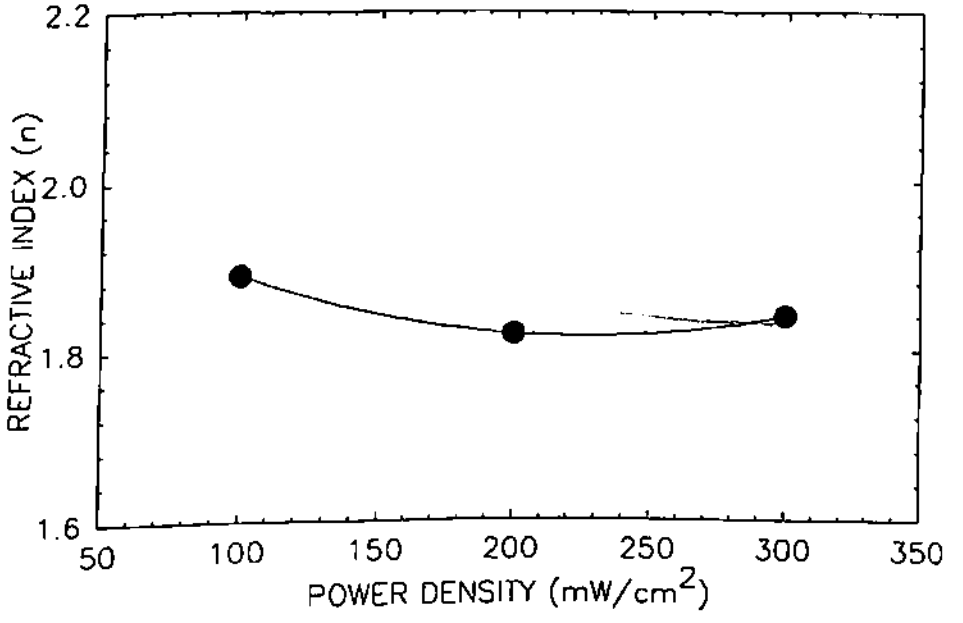

Fig. 3.19 The refractive index as a function of power density for VHF glow discharge grown DLC films

The most efficient breeding zone within the bulk plasma is the sheath edge region which comes close to the substrates at higher excitation frequencies. As the sheath thickness and, therefore, the distance from the sheath edge to the substrate is reduced, the short lifetime radicals can now directly contribute to the growth of the DLC film. The sheath, therefore, is not able to influence the precursors in the same fashion as happens at lower frequencies. This may be the reason for no change observed in optical bandgap and refractive index values for VHF grown films.

Furthermore, Koidl *et al.*[33] observed differences in refractive index values for ion beam and RF plasma deposited films, whereas values of optical gap remained unchanged. They assigned the reason for their observation as an influence of the high energy portion of the ion energy distribution (IED).

It is observed that as the value of n increases (though it is marginal), the optical bandgap decreases. This agrees with Koidl *et al.*'s[33] observations.

Table-3.1

Parametric variation of DLC film properties produced by RF and VHF plasma excitation.

Power density (mW/cm^2)	Self bias (V)	Applied -ve DC voltage	Dep. rate (A^0/s)	Bandgap (eV)	Ref. index	Hardness (GPa)	Stress (GPa)
100	98	0	3.60	1.75	1.59	5.71	3.6
200	150	0	3.89	1.40	1.84	6.32	3.8
300	250	0	5.28	1.25	1.91	10.97	4.4
420	300	0	6.70	1.15	2.13	15.00	4.6
100	7.43	0	20.0	1.55	1.55	-	-
200	19.95	0	22.2	1.45	1.45	-	-
300	39.67	0	26.7	1.40	1.40	-	-
100	10.00	0	19.4	1.60	1.60	4.00	1.7
100	10.00	150	18.5	1.65	1.65	5.00	1.9
100	8.00	200	18.0	1.60	1.60	5.75	2.0
100	7.43	230	17.8	1.55	1.55	6.00	2.2
100	8.00	390	11.7	1.60	1.60	9.02	2.9

3.4 Limitations of RF Self Bias Technique

It has become abundantly clear during the discussion of the various results, documented in this chapter of the thesis, that for the growth of low stress hard DLC films at a high rate, the RF self bias technique has many limitations. An ideal deposition process should satisfy at least the following requirements, so that the particular technique can be scaled up for mass production in industry:

(i) A high deposition rate on large areas with required thickness uniformity.

(ii) A good control of desired properties such as optical transparency, smooth surface topography.

(iii) Low stresses.

At first sight, it appears that a higher rate of deposition of DLC films having a denser network structure would be achieved by means of a higher generation rate of radicals and allowing them to land on the surface of the substrate at high enough energy. In order to obtain a higher radical generation rate, the electron density and/or the partial gas pressure should be increased. However, the application of a high power density to the hydrocarbon plasma at 13.56 MHz leads to an enhancement of residual stresses, and high pressures lead to polymerisation reactions. It is at this point an inspiration was derived from experiences in high rate processing of a-Si:H and VHF-PECVD experiments designed for a-C:H growth. It may be appreciated that changes in the plasma excitation frequency provide additional opportunities to tailor a-Si:H film properties. However during the initial experiment that has been reported in this thesis, the VHF processing in case of a-C:H has not yielded similar results as have been obtained in case of a-Si:H. One reason for this is perhaps due to necessity of obtaining a reasonable hardness in a-C:H films, substrates have been kept on the cathode, whereas, so far all VHF-GD have been processed on the anode of a PECVD reactor for a-Si:H growth. A VHF plasma excitation of hydrocarbon accompanied by the RF bias may perhaps provide a different result. It may be noticed that enhancement of hardness of DLC films in VHF-PECVD experiment has been achieved by providing additional DC bias[47,50]. This in some way resembles the experimental setup of Grill *et al.*[38]

3.4 Limitations of RF Self Bias Technique

It has become abundantly clear during the discussion of the various results, documented in this chapter of the thesis, that for the growth of low stress hard DLC films at a high rate, the RF self bias technique has many limitations. An ideal deposition process should satisfy at least the following requirements, so that the particular technique can be scaled up for mass production in industry:

(I) A high deposition rate on large areas with required thickness uniformity.

(ii) A good control of desired properties such as optical transparency, smooth surface topography,

(iii) Low stresses.

At first sight, it appears that a higher rate of deposition of DLC films having a denser network structure would be achieved by means of a higher generation rate of radicals and allowing them to land on the surface of the substrate at high enough energy. In order to obtain a higher radical generation rate, the electron density and/or the partial gas pressure should be increased. However, the application of a high power density to the hydrocarbon plasma at 13.56 MHz leads to an enhancement of residual stresses, and high pressures lead to polymerisation reactions. It is at this point an inspiration was derived from experiences in high rate processing of a-Si:H and VHF-PECVD experiments designed for a-C:H growth. It may be appreciated that changes in the plasma excitation frequency provide additional opportunities to tailor a-Si:H film properties. However during the initial experiment that has been reported in this thesis, the VHF processing in case of a-C:H has not yielded similar results as have been obtained in case of a-Si:H. One reason for this is perhaps due to necessity of obtaining a reasonable hardness in a-C:H films, substrates have been kept on the cathode, whereas, so far all VHF-GD have been processed on the anode of a PECVD reactor for a-Si:H growth. A VHF plasma excitation of hydrocarbon accompanied by the RF bias may perhaps provide a different result. It may be noticed that enhancement of hardness of DLC films in VHF-PECVD experiment has been achieved by providing additional DC bias[47,50]. This in some way resembles the experimental setup of Grill *et al.*[38]

In RF self bias technique during the deposition of DLC films positive ions from the plasma bombard the substrate surface due to the negative DC self bias voltage that they experience while travelling towards cathode. As a result of the ion impact, the substrate temperature increases, which may cause increase of stress in these DLC films.

It may be appreciated that RF self bias technique, as initially suggested by Holland and Ojha[1,2] is something which can be easily hooked up in a laboratory having modest vacuum apparatus and a RF supply. For small size specimens it has some inherent advantage as all the reactions are focussed on a small size electrode (cathode) and walls do not contaminate the growing films. Again the substrates placed on a high negative potential are immune to the influence of dust particles, which like any floating object in the plasma also acquire a negative charge and are repelled. Highly cross linked and pin-hole free coatings are thus obtained by this simple technique.

However upscaling of this process for industrial applications has many inherent difficulties. Further the process is often difficult to control. Most importantly the residual stress in the films so grown is very high (4-6 GPa). DC discharge on the contrary may provide low stress films, but are difficult to sustain and highly resistive nature of DLC films leads to a charging effect which may often result in electrical breakdown of the films.

Ideally one could therefore like to have a system which has all the attributes of a DC discharge but without its limitations. At the first sight it appears utopian. However in the subsequent chapters it will be shown how this is indeed realisable.

Another serious limitation of the RF asymmetric PECVD system is its limited throwing power and the difficulties of matching the impedance at different varying loads at all times. It may be recalled Aisenberg and Chabot[49] first experimented with the ion guns for growing DLC films which have the required throwing power.

It is again fortuitous that the technique that has been discussed in a subsequent chapter of the thesis has this capability.

3.5 Part Summary

In this chapter an account of a systematic study that was conducted to understand the properties of DLC films grown by RF-PECVD technique, with varying process parameters and using methane, acetylene and benzene as hydrocarbon sources, has been presented.

Negative self bias voltage and gas pressure were reconfirmed to be two significant parameters for obtaining a degree of control of the deposition process. It was found that sufficiently high self bias voltage (more than 100 V) and low gas pressure (~33 × 10^{-3} mbar) are suitable parameters for the deposition of hard a-C:H films. It was also observed that at very high self bias voltages (greater than 325 V in the present investigation) films deposited spontaneously delaminated from the substrates due to high internal stresses present in these films. The stress in these films was estimated to be in the range of 2-4 GPa.

The deposition rate (r_d), in case of films grown using CH_4 gas was found to vary from 0.22 to 0.66 A°/sec when the applied power was increased from 100 to 400 mW/cm^2 at a pressure of ~33 × 10^{-3} mbar . For the same range of power, the deposition rate varied from 3.6 to 6.7 A°/sec in case of C_2H_2 and from 1.33 to 3.33 A°/sec in case of C_6H_6 at a pressure of ~25×10^{-3} mbar.

It is observed that almost invariably hard DLC films are also under large amount of compressive stress, and the magnitude of stress also depends on the type of hydrocarbon used for the CVD experiment. Benzene grown films showed low stress values compared to methane and acetylene for the same deposition parameters, but unfortunately hardness values were also low. For this reason, in the present investigation special attention has been paid to specify stress per unit hardness or vice versa as a figure of merit. Slopes of stress vs. hardness curves have been calculated and it is found that acetylene grown films show higher hardness per unit increase of stress than methane or benzene grown films. It is another matter altogether the benzene grown films survive delamination in most cases.

It was found that optical bandgap decreases and refractive index increases with the increase of self bias voltage. These results are identical for all the three hydrocarbon grown films.

Just by changing excitation frequency from 13.56 MHz to 100 MHz deposition rate of a-C:H films was enhanced by about 5 times in a PECVD reactor. The process is far from optimised and one really does not know what are the limits of the scaling up of the deposition rate. Since self bias potential developed in a VHF plasma is very low, sufficiently high negative DC voltage was applied to the substrates in order to make a-C:H films being grown reasonably hard. Thus, the results of VHF-PECVD process of a-C:H, with externally imposed DC bias, is capable of producing reasonably hard films at respectably high growth rates. Further, residual stress in the VHF grown films was found to be marginally less than RF deposited films. Stress values were in the range of 1.7 GPa to 2.9 GPa for VHF grown films. The variation of the optical bandgap (E_g) with applied power was very small for VHF compared to RF deposited films. It was found that values of refractive index (n) lie between 1.8-1.9 for VHF deposited films and in the case of RF deposited films this variation was between 1.59-2.13. It has also been found that as the value of n increases, the E_g decreases for both RF and VHF deposited films.

Finally, limitations of RF self bias technique were identified. These were essentially the following

(I) Difficulty of upscaling due to its dependence on a geometrical factor of the reactor

(ii) High stress in the films so grown

(iii) Low throwing power because of small gap geometry.

Further, a technique which has both the attributes of DC and RF discharge appeared to be the one which may be the answer to the above limitations.

3.6 References

1. L. Holland and S.M. Ojha, *Thin Solid Films*, **48** (1978) L15.
2. L. Holland and S.M. Ojha, *Thin Solid Films*, **58** (1979) 107.
3. A. Bubenzer, B. Dischler, G. Brandt and P. Koidl, *J. Appl. Phys.*, **54** (1983) 4590.
4. T.J. Moravec and T.W. Orent, *J. Vac. Sci. Technol.*, **18** (1981) 226.
5. S. Berg and L.P. Anderson, *Thin Solid Films*, **58** (1979) 117.
6. K. Enke, H. Dimigen and H. Hubsch, *Appl. Phys. Lett.*, **36** (1980) 291.
7. D. Jones and A.D. Stewart, *Philos. Mag. B*, **46** (1982) 423.
8. R.J. Gambino and J.A. Thompson, *Solid State Commun.*, **34** (1980) 15.
9. B. Dischler, A. Bubenzer and P. Koidl, *Appl. Phys. Lett.*, **42** (1983) 636.
10. K. Enke, *Thin Solid Films*, **80** (1981) 227.
11. J.C. Angus, P. Koidl and S. Domitz, Chapter 4 in *Plasma Deposition of Thin Films*, eds. J. Mort and F. Jansen (CRC Press, Inc., Florida) (1986) p. 89, .
12. V.D. Davis, T.A. Vanderslice, *Phys. Rev*, **131** (1963) 219.
13. A. Matsuda, T. Kaga, H. Tanaka and K. Tanaka, . *J. Appl. Phys.*, **23** (1984) L567.
14. T. Ohmi and T. Shibata *et al.*, *Thin Solid Films*, **241** (1993) 159.
15. A.A. Howling, J.L. Dorier, Ch. Hollenstein, U. Kroll and F. Finger, *J. Vac. Sci. Technol.* A, **10** (1992) 1080.
16. Shunri Oda and Masahiro Yasukawa, *J. Non-Cryst. Solids*, **137** (1991) 677.
17. J. Kuske, U.Stephan, K. Schade and W. Fuhs, *Mater. Res. Soc. Symp. Proc.*, **258** (1992) 141.
18. F. Finger, U. Kroll, V. Viret, A. Shah, W. Beyer, X.M. Tang, J. Weber, A. Howling and Ch. Hollenstein, *J. Appl. Phy.*, **71** (1992) 5665.
19. H. Chatham and P. Bhat, *Mater. Res. Soc. Symp. Proc.*, **149** (1989) 447.
20. W. Schwarzenbach, A.A. Howling, M. Fivas, S. Brunner and CH. Hollenstein, *J. Vac. Sci. Technol.* A, **14** (1996) 132.
21. C. Beneking, *J. Appl. Phys.*, **68** (1990) 446.
22. M. Surendra and D.B. Graves, *IEEE Trans. Plasma Sci.*, **19** (1991) 144.
23. M. Moisan, C. Barbeau, R. Claude, C.M. Ferreira, J. Margot, J. Paraszczak, A.B. Sa, G. Sauve and M.R. Wertheimer, *J. Vac. Sci. Technol.* B, **9** (1991) 8.

24. M. Heintze, R. Zedlitz and G.H. Bauer, *J. Phys. D*, **26** (1993) 1781.
25. K.M. Kalpakjian, M.A. Lieberman and W.G. Oldham, *J. Vac. Sci. Technol.* B, **12** (1994) 1351.
26. U. Kroll, Y. Ziegler, J. Meier, H. Wagner and M.Scheib, *Appl. Phys. Lett.*, **65** (1994) 2588.
27. F. Finger, P. Hapke, M. Luysberg, R. Carius, H. Wagner and M. Scheib, *Appl. Phys. Lett.*, **65** (1994) 2588.
28. J. Meier, R. Fluckiger, H. Keppner and A. Shah, *Appl. Phys. Lett.*, **65** (1994) 860.
29. D.L. Flamm, *J. Vac. Sci. Technol.* A, **4** (1986) 729.
30. J. Dutta, U. Kroll, P. Chabloz, A. Shah, A.A. Howling, J.L. Dorier and Ch. Hollenstein, *J. Appl. Phys.*, **72** (1992) 3220.
31. C.M. Ferreira and J. Loureiro, *J. Phys. D: Appl. Phys.*, **1** (1984) 1175.
32. L. Sansonnens, A. Pletzer, D. Magnni, A.A. Howling, C. Hollenstein, U. Kroll, J. Meier and A. Shah, in *14th European Photovoltaic Solar energy Conference and Exhibition*, Barcelona (Catalunya), Spain, 30 June-4 July, 1997.
33. P. Koidl, C. Wild, R. Locher and R.E. Sah in *Diamond and Diamond -Like Films Coating* eds. R.E. Clausing *et al.* (Plenum, New York) (1991) p. 243.
34. L.P. Anderson, S. Berg, H. Norstrom, R. Olaison and S. Towta, *Thin Solid Films*, **63** (1989) 155.
35. M.A. Tamor and W.C. Vassell, *J. Appl. Phys.*, **76** (1994) 3823 .
36. D. Nir, *Thin Solid Films*, **146** (1987) 27.
37. A. Grill and V. Patel, *Diamond Films Technol.*, **1** (1992) 219.
38. A. Grill and V. Patel, *Diamond and Related Materials*, **2** (1993) 1519.
39. J.W. Zou, K. Schmidt, K. Reichelt and B. Dischler, *J. Appl. Phys.*, **67** (1990) 487.
40. J.W. Zou, K. Reichelt, K. Schmidt and B. Dischler, *J. Appl. Phys.*, **65** (1989) 3914.
41. J.C. Angus, P. Koidl and S. Domitz in *Plasma Deposited Thin Films*, eds. J. Mort and F. Jansen (Chemical Rubber, Boca Raton, FL (1988) p. 89.
42. *Diamond and Diamond like Films and Coatings*, eds. R.E. Clausing, L.L. Horton, J.C. Angus and P. Koidl (Plenum, New York) (1991).
43. K. W. Whang and H.S. Tae, *Thin Solid Films*, **204** (1991) 49.

44. H. Keppner, Ph.D. Thesis, University of Neuchatel, Switzerland.

45. H. Chatham, P. Bhat, A. Benson and C. Matovich, *J. Non-Cryst. Solids*, **115** (1989) 201.

46. S. Oda, J. Noda and M. Matsumusa, *Mater. Res. Soc. Symp. Proc.*, **118** (1989) 117.

47. Sushil Kumar, P.N. Dixit, D. Sarangi and R. Bhattacharyya, *Appl. Phys. Lett.*, **69** (1996) 49.

48. M. Basu, A.B. Maity, B. Maity, S. Choudhuri and A.K. Pal, *Vacuum*, **47** (1996) 1047.

49. S. Aisenberg and R. Chabot, *J. Appl. Phys.*, **42** (1971) 2953.

50. Sushil Kumar, P.N. Dixit, D. Sarangi and R. Bhattacharyya in *Semiconductor Devices*, ed. K. Lal (Narosa Pub. House, New Delhi) (1996) p. 433.

Chapter IV

Saddle Field Fast Atom Beam Deposited DLC Films

4.1 Introduction

The development of saddle field fast atom beam (FAB) sources opened a new era of material processing of amorphous thin films in a very uncomplicated manner. Glow discharge decomposition by either DC or RF excitation, of the hydrocarbon gases, are the more conventional techniques. Both these methods of plasma excitations have certain draw backs and one would prefer to have advantages specific to both these techniques and none of their inherent disadvantages. It may, at the first sight, appear to be a rather strange idea. However saddle field source deposition does indeed come very close to this ideal. The combined attributes of DC and RF discharges make it a novel technique for thin film growth applications. The potential profile[1] of the saddle field FAB discharge together with that of a DC and RF PECVD discharges are shown in **Fig. 4.1**. From this figure it is clear that the potential distribution in a FAB source is similar to RF PECVD (GD) technique though DC voltages are used to operate such FAB sources. Earlier FAB sources were used for cleaning, milling, etching, thinning (the specimen preparation for TEM) and sputtering applications and also for a variety of surface analytical techniques. Franks[2] first used it to deposit diamond like carbon (DLC) films. His attempts to deposit DLC films using methane (CH_4) as the source gas lead to the etching of the substrates. Propane (C_3H_8), butane (C_4H_{10}) and acetylene (C_2H_2) have been used as source gases to grow DLC films and deposition rates in these cases were found to increase with the increase of carbon to hydrogen ratio of the hydrocarbon source gases/vapours used.

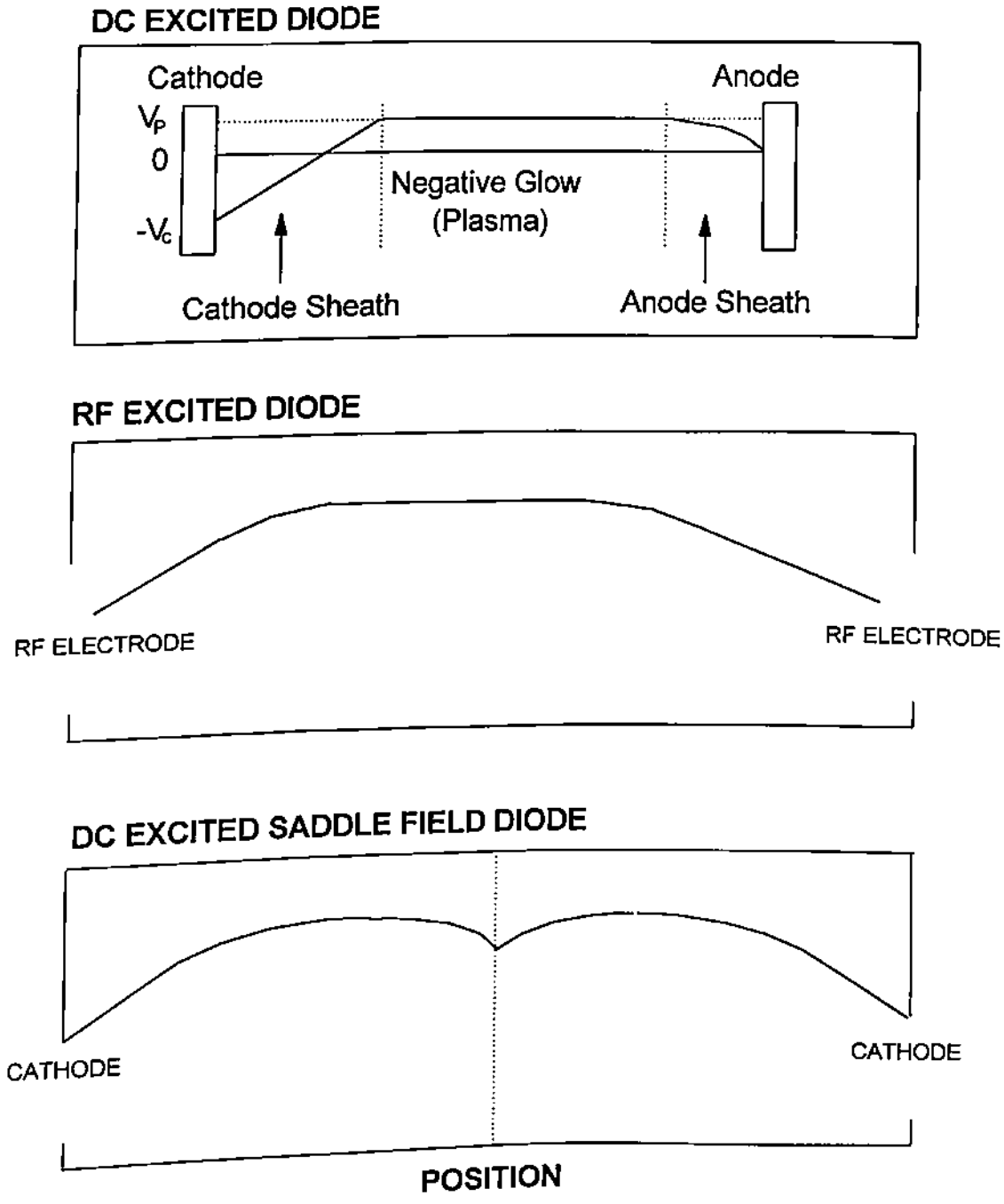

Fig 4.1 Potential profile of saddle field FAB discharge together with that of DC and RF PECVD discharges[1]

To understand fully the growth of DLC films using FAB sources it is very essential to understand the basic principle involved in the FAB technique. The next section discusses the discovery and mechanism involved in the operation of a FAB source.

4.2 Discovery of the Saddle Field Fast Atom Beam (FAB) Source

4.2.1 A Charge Particle Oscillator

The concept of the saddle field fast atom beam (FAB) source came after the discovery of the charge particle oscillator by McIlraith[3] in 1966. Taking the example of the rubber gravitational model he proved that it is possible to confine the charged particle of a particular sign to a limited volume solely by means of electrostatic forces. This system was named as a ***charge particle oscillator.***

The working of this oscillator can be fully understood by resolving different force field contributions. The force field resulting from a pair of equally charged poles is shown in **Fig. 4.2.** The poles A and A′ could be a pair of equally charged rods, a pair of equally charged spheres or charged rings. The field has a saddle point at O. In the vicinity of the origin the lines of forces are strongly curved, elsewhere they are essentially straight and radiate from O. D is the locus of

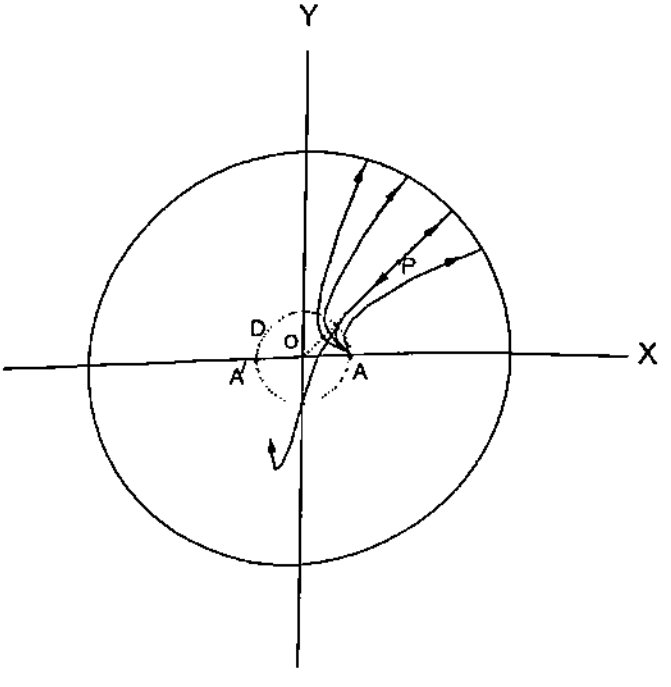

Fig 4.2 Force field resulting from a pair of equal poles A and A′[3]

points for which the electric field component along X-direction (E_x) is zero. Outside D, E_x is directed away from the Y-axis while inside D it is directed towards the Y-axis. The shape of D depends upon the shape of the electrode system. D always passes through the poles. For a set of parallel rods D is a circle.

A negatively charged particle, released from a point (P), initially follows a line of force but, owing to its momentum, it fails to follow the sharp bend to A and its trajectory crosses the X-axis. The negatively charged particle after having been retarded from the conducting boundary wall again crosses the X-axis and starts to oscillate back and forth between the two electrodes.

The trajectories of the charged particle may be stable or unstable depending upon its starting position. McIlraith[4] computed and provided a contour as shown in **Fig. 4.3**, within which all stable trajectories start from rest. If a charged particle starts from x = 0.8, y = 2 it follows the stable oscillating path as shown in **Fig. 4.4(a)**. Similarly charged particle follows stable oscillating path

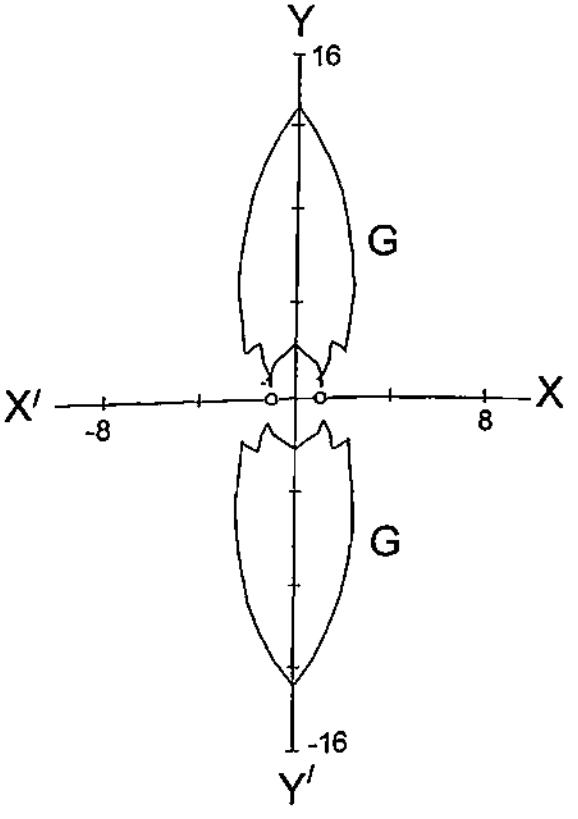

Fig 4.3 Contours of the regions G, within which all stable trajectories start from rest[4]

as shown in **Fig. 4.4(b)** if it starts from x =1.3, y =10. But the charged particle that starts from x =1.5, y =10, follows an unstable trajectory as shown in **Fig. 4.4(c)**. So if the oscillating electrons are to follow long paths, their source must lie in one of the regions G (**Fig. 4.3**). The point midway between the poles is called *"saddle point"* and it is a point of unstable equilibrium. So the motion of the oscillating particle is intrinsically stable. ***Therefore, it is a class of motion in which particles of one sign perform stable oscillations about a point of unstable equilibrium.***

It was found that if the diameter of the cylinder (cathode) is more than 13 times the separation of the charged rods or wires, none of the secondary electrons will have stable trajectories and it will be impossible to produce a discharge.[4] The performance of the oscillator is not practically dependent on its dimensions or on the exact alignment of its parts. Lateral displacement of the charged rods or wires has a negligible effect provided they are equidistant from the axis of the cylinder to within about 25% of their mutual separation. The charged rods or wires should be kept under spring tension to prevent bowing. Otherwise kinks will form and the resultant strong local disturbance field will not allow the electrons to follow stable oscillatory paths.

4.2.2 Saddle Field Ion Source

Ion sources are generally used for specimen cleaning, polishing and etching of surfaces, for sputtering and for thinning specimen for electron microscopy. In most of the existing ion sources, ions are generated thermally and also operate at high pressure (~ 0.1 mbar) in order to obtain adequate current density. These disadvantages of these ion sources make the specimen surface contaminated.

Using the concept of electrostatic charge particle oscillator, discovered by McIlraith[3], Fitch *et al.*[5] first developed a positive ion source. This ion source consisted of a stainless steel tube (200 mm long and 54 mm internal diameter) as a cathode and two tungsten wires (0.3 mm diameter and separated by 5 mm) as a anode. The wires were spring loaded to avoid bowing. In such a source when a high positive voltage (~ 1 - 10 kV) is applied to the anode (wires), an electron starting from

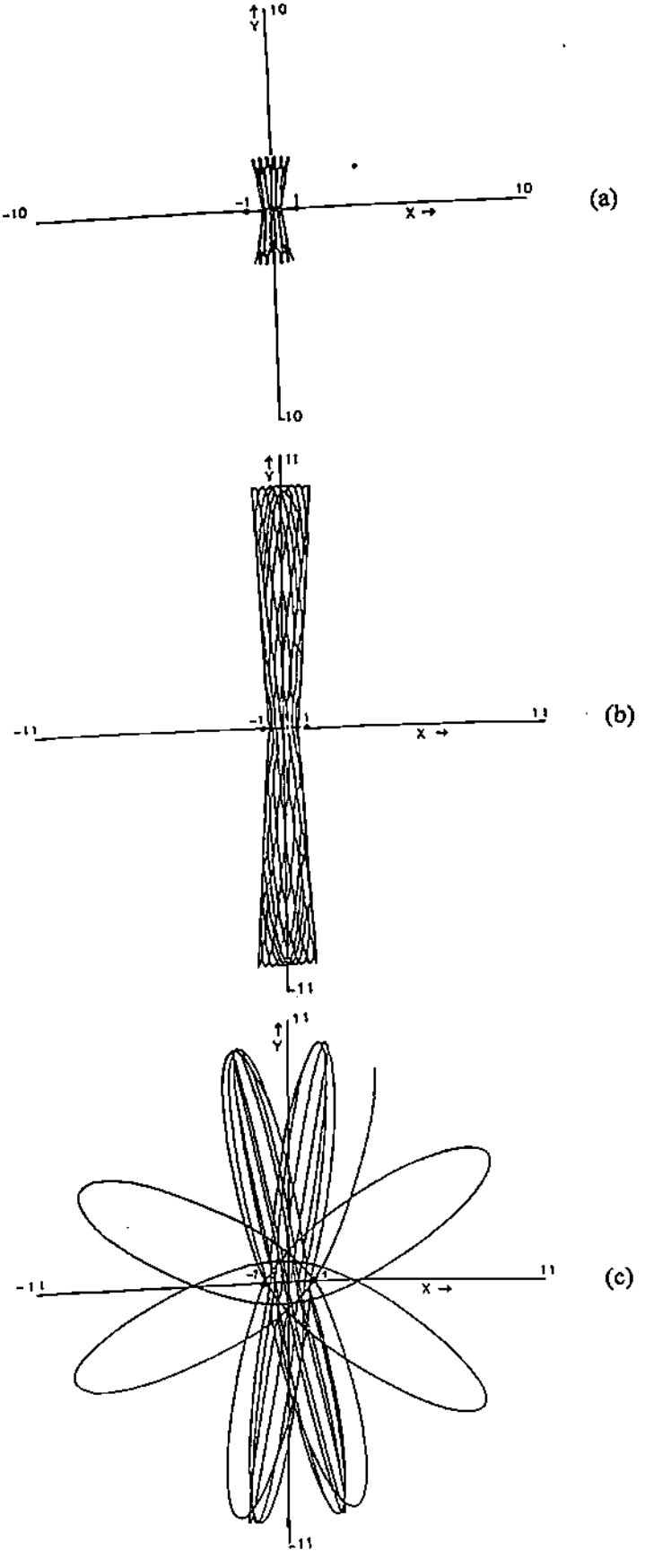

Fig 4.4 Computer trajectories of a charged particle attracted by a pair of equal line poles[4]

rest within a specified region follows a long oscillatory path between the anode wires. Thus, a cold cathode discharge can be maintained down to about 10^{-6} mbar without the application of a magnetic field. The discharge is concentrated about an axial plane normal to the plane of the anode wires. Ions generated in the discharge were allowed to escape from the oscillator through a rectangular slot in the cathode positioned above the plane of the anode wires. A highly directional beam of positive ions was obtained.

Later Fitch and Roushton[6] slightly modified the above source. They found that the performance of the source was critically dependent on the anode separation. So they reconstructed the ion source using 2 mm diameter tungsten rods (to avoid the burning of wires due to sudden rise in pressure) as anode, separated by 8 mm (optimum separation found after tube current measurement). The rods were not spring-loaded but were free to move in ceramic insulator bushes during thermal expansion caused by secondary electron bombardment (easy to scale up). The ion beam was found to be reasonably well colliminated and the ions coming out of the source were found to have a broad energy.

In all the ion sources, described above, gas was admitted into the vacuum chamber and not directly into the source to get the positive ionised beam. Rushton *et al.*[7] modified the source and they allowed the gas to admit directly into the source through a stainless steel tube. This produces a pressure difference inside and outside of the ion source, the value depends on the conductance of the exit aperture and the pumping speed of the pumping stack. This has the advantage that the specimen stage in the vacuum chamber can be maintained at a lower pressure for a given ion density, thus reducing the contamination of the specimen and the scattering of the ion beam. In this process a greater ion beam current density is obtained at a given chamber pressure and the quantity of gas used is also less.

Ghander and Fitch[8] modified the above source as a twin ion source by providing two apertures on the cathode in the two opposite directions. The two beams coming out from such a

source were found to have similar intensity and energy. This source obviously has a lot of commercial potential and, in fact, its improved version is being produced by M/s Atom Tech. Ltd.

The cylindrical ion source described above was found to have certain disadvantages:

(1) The ion aperture is in the region of the cylinder where the axial component of the field (i.e. parallel to the anodes) is small compared with the radial field. However, it is essential that the electrode geometry be such that at the ends of the cylinder, the axial field is large and of a sense to confine the ionising electrons to the central region. To achieve this, the length of the cylinder must be several times the cylinder diameter, so that the dimensions of the source remain large even when a narrow ion beam is required. With the small cathode aperture, a small fraction of available ions are utilised, this geometry is, therefore, inefficient both from the dimensional and the power consumption (i.e. heating) considerations.

(2) With the cylindrical geometry the emerging beam is highly divergent and needs to be focussed, if a narrow beam is required.

These disadvantages could be overcome by using a spherical ion source geometry.[9,10] In the spherical ion source the cathode cylinder was replaced by a sphere and the anode rods by a ring. This way an axially symmetric geometry was ensured and this compact ion source was found to produce a narrow intense beam with a small angle of divergence. The beam coming out from this type of source was found to contain only a small fraction of neutrals.

The energy distributions of ion beams were found to be different in cylindrical and spherical type sources.[11] In case of cylindrical ion source, the energy distribution was broad and contained two peaks at energies equivalent to 35% and 75% of the anode potential. But for the spherical type of ion source, only one comparatively narrower peak was observed at energies approximately 75% of the anode potential. This difference could be attributed to the axial symmetry of the spherical source. Thus, from the application point of view, the cylindrical source should be used if a wide

ion beam with a broad energy spread is required but if a fine ion beam of much lower energy spread is necessary, then the spherical source is more suitable.

From the above discussion it is abundantly clear that the saddle field ion sources have a number of advantages over other sources. (1) ***It doses not require a magnetic field, thermoionic emitter or supplementary beam focussing facilities.*** (2) ***Its operating pressure is low ($\sim 10^{-4}$ mbar), avoiding contamination in the films produced using such sources.*** (3) ***It is also possible to build such sources into existing equipments like electron microscope.***

4.2.3 Fast Atom Beam (FAB) Source

An ion beam source has many applications such as in ion cleaning, ion milling, ion etching, thinning the specimen, sputtering and a variety of surface analytical techniques. The ion beam bombardment, however, can give rise to substantial chemical and structural disruption. It was found that the surface damage, both physical and chemical, is very much reduced when a neutral beam of exactly the same energy and associated momentum replaces the beam consisting mostly of charge particles.

An analysis of the beam coming out from a spherical type source[9,10] reveals that the beam contains not only ions but also some neutrals as well. This leads to the development of the atom beam source[12,13] or the saddle field fast atom beam (FAB) source.

The working model of a FAB source is shown in **Fig. 4.5** and the working principle is the following:

1. Electrons are induced to oscillate between cathodes under the action of a DC field.
2. Electrons originating from a sector of the cathode travel through the anode region towards the opposite cathode sector, are retarded, return and continue to oscillate about a central saddle point in the potential field.
3. The electrons, therefore, describe long trajectories before being captured by the anode.

4. A positive ion sheath exists near the cathode (**Fig. 4.5**) which carries most of the discharge voltage, apart from the relatively small drop in the potential at the cathode(s) and the plasma. The injected gas atoms are ionised and positive ions are formed. The positive ions are accelerated towards the cathode as a result of the potential difference between the ion sheath and the cathode. Thus the cathodes allow self extraction of the ions in the form of a beam when an aperture is introduced.

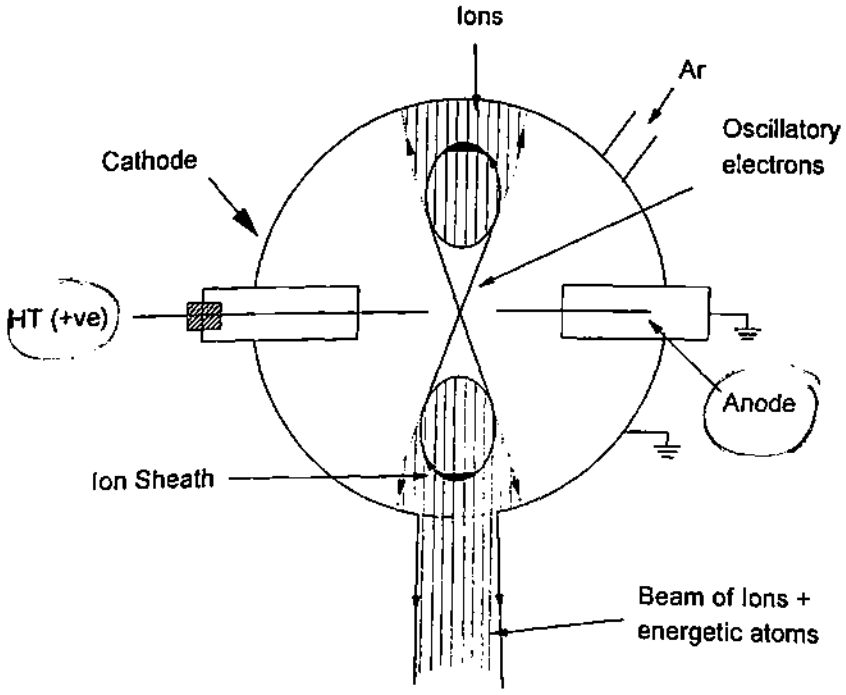

Both are anode cathode is properly insulated

Fig 4.5 Schematic of the saddle field FAB source[13]

The two mechanism of neutralisation of such ion beams that have been proposed are :

A. The inherent arrangement of the electrostatic field close to the output grid helps electrons to recombine with the ions with little loss of energy (***resonance charge exchange***).

B. The ions are neutralised by colliding with the residual gas molecules before passing through the aperture of the source.

A considerable amount of work has been carried out by Shimokawa *et al.*,[14-16] relating to high energy FAB sources and related source characterisation.

Very few groups are working internationally in the area of DLC film deposition using FAB sources. Frank's[2] attempt to deposit DLC films using CH_4 as feed gas lead to the etching of the substrates. The researchers at the University of Hull, UK, characterised the DLC films grown by the FAB technique[17-23] involving film deposition rate, density and morphology. The success of growing transparent DLC films by the saddle field technique was also reported by them.[23] The structural and compositional properties of FAB grown DLC films have been investigated using neutron diffraction,[24-28] neutron scattering,[28,29] IR spectroscopy,[28,30] NMR spectroscopy,[28,31] X-ray diffraction,[26,27] X-ray scattering,[32] neutron compton scattering[33] etc. Using these investigations they were able to satisfactorily explain the high values of hardness observed in these films. The effect of annealing[34] and N_2 dilution[26] have also been reported. The researchers at the University of Toronto, Canada, used a five electrode saddle field configuration[1] in their deposition system and were able to grow DLC films using CH_4.[35] They also found good photoluminescence efficiency[35] and very high sp^3/sp^2 ratio in these films.[36,37] Using neutron compton scattering Mayers *et al.*[33] found that the mean kinetic energy (103.9±0.9 meV) of the individual carbon atoms in DLC films deposited using FAB source with C_2H_2 as the feed gas is the same within statistical limit with carbon atoms in graphite (108.3±3.0 meV) and slightly less than diamond (120.7±3.2 meV). They also inferred from this statistics that the samples contained molecular hydrogen.

Inspite of the above listed references that have been reported on the structure and the composition of the DLC films grown by the FAB technique, still there appears to be a dearth of information regarding possible correlation between the macroscopic properties of the films grown this way, like hardness, stress, refractive index, optical bandgap and the microscopic properties like amount of bound and unbound hydrogen, density and nature of voids etc.

In undertaking the experiments to be reported in the following a conscious attempt has been made to answer the following:

1. In what ways increasing carbon to hydrogen ratio, in the hydrocarbon source material, influences the properties of the films formed by this technique as compared to more conventional RF self bias growth method as documented in **Chapter III** ?

2. Is there indeed a marked difference in the nature of the DLC films produced by this technique than the films produced by the RF self bias method ? A very detailed film characterisation study has, therefore, been undertaken to find the specific differences.

3. The effect of nitrogen dilution on the properties of DLC films so grown has also been investigated.

4.3 Experimental Details

DLC films have been grown on Corning 7059 glass and silicon substrates held at nearly room temperature at a distance of ~ 6 cm by aspirating hydrocarbon gases (CH_4 and C_2H_2) and C_6H_6 vapours into a saddle field fast atom beam source (Ion Tech. Ltd., presently Atom Tech. Ltd., FAB 110 - 2) mounted in a 30 cm diameter vacuum system. The source operates at 0.5 - 2.0 kV in the pressure range 10^{-4} - 10^{-3} mbar and is of modular design to cover increasingly larger areas. The operation of the source is dependent only on the regulated current output from the power supply and the discharge voltage which is decided by the gas flow (pressure and consequently by setting of the needle valve etc.). Other details of the experimental setup and the saddle field FAB source have already been described in **Chapter II**.

4.4 Results and Discussion

4.4.1 Deposition Rate

Figure 4.6 shows the variation of the deposition rate of a-C:H (DLC) films grown using C_2H_2 gas at 4.0×10^{-4} mbar pressure (when the substrate is not intentionally heated) with varying power applied to the saddle field FAB source. The figure also shows the effect of varying power

while substrates are kept at different source to substrate distances. It is evident from the figure that the deposition rate increases with the increase of power applied to the saddle field source at all the distances of source to substrate investigated. **Figure 4.7** shows the variation of the deposition rate with varying source to substrate distance of DLC films using C_2H_2 gas in the saddle field source, at 4.5 W power and at 4.0×10^{-4} mbar pressure. The maximum deposition rate is found to occur at a distance of 6 cm. At shorter distances (~ 4 cm) it is observed that the deposition is not uniform and there may be errors in estimating correct thickness using a profilometer of limited span.

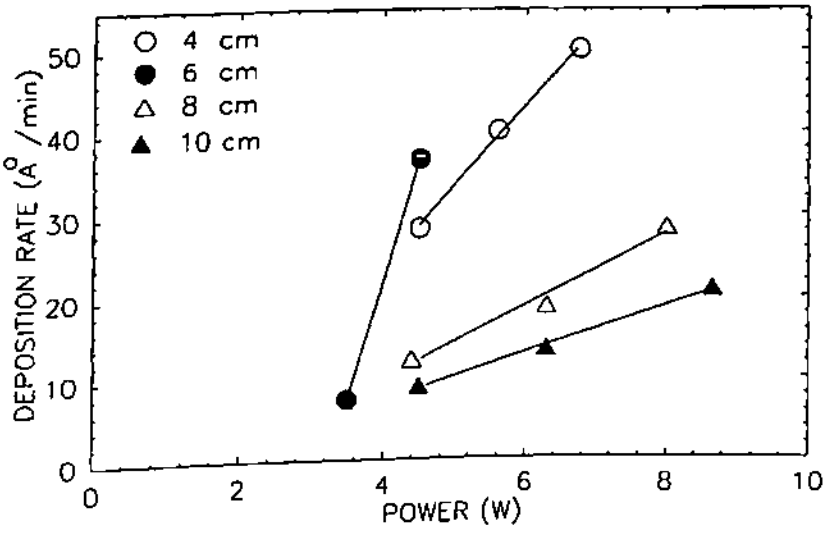

Fig. 4.6 Variation of deposition rate of DLC films grown using C_2H_2 gas at 4.0×10^{-4} mbar pressure vs. power, at different source to substrate distance

One possible reason for the observed nonuniformity could be that at short substrate to source distances the flux of film forming precursors is highly ionised and, as one goes away from the source, the degree of ionisation is drastically reduced. Langmuir probe investigations of the ion current density and plasma potentials in similar situations (C_2H_2 discharge in a saddle field source), corroborate such views.[17] Source to substrate distance was subsequently kept 6 cm in the case of DLC films grown using CH_4 and C_2H_2 gases and C_6H_6 vapours. The deposition rate of DLC films using CH_4 gas was found to vary only from 11.7 to 16.7 A°/min when the power was increased from 7.2 to 12.6 W, at a pressure of 8.0×10^{-4} mbar. The deposition rate of DLC films using C_2H_2 gas varied from 7.4 to 50 A°/min at different distances of source to substrates, when the applied power was increased from 3.5 to 8.6 W, at a pressure of 4.0×10^{-4} mbar. The deposition rates of a

few DLC films obtained using C_6H_6 vapours were in the range of 21.0 - 23.0 A°/min, at a pressure of 2.0×10^{-4} mbar, when the applied power increased from 4.5 to 5.0 W. C_6H_6 vapours were found to pose a problem during pump out. They contaminated the rotary pump oil. This affected the performance of the vacuum system after a few runs were made. This could be largely remedied by replacing the pump with one working at higher temperature. The increase of deposition rate with the increase in power and with the increase in carbon to hydrogen ratio in the hydrocarbon gas is in general agreement with the fact that the growth rate depends upon the process gas used and the energies (or power) applied to the source and it increases when one goes from CH_4 to C_2H_2 gas or C_6H_6 vapours.[38,39]

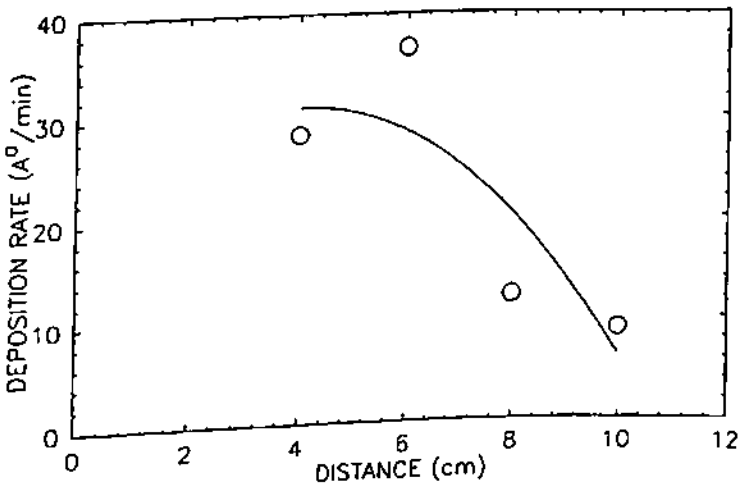

Fig. 4.7 Variation of deposition rate of DLC films grown using C_2H_2 gas at 4.5 W power and 4.0×10^{-4} mbar pressure with varying source to substrate distance.

4.4.2 Hardness

The most important characteristic of dense carbon films is their unusual hardness. Hardness is defined as resistance to local plastic deformation. Qualitatively one finds the films difficult to scratch with a steel point. The hardness of the film was determined using a Knoop hardness indenter as discussed in **Chapter II** under **section 2.7**. In principle, the hardness is expected to be

independent of the applied load. However, the apparent indentation hardness can be a function of load at very light loads. An increase in the hardness with decreasing load has been observed.[39] The Knoop hardness values (HK) at 50 gm load for DLC films grown using CH_4, C_2H_2 gases and C_6H_6 vapours aspirated in the saddle field source, lie in the range 9-21 GPa. **Figure 4.8** shows the variation of hardness values with the power applied to the FAB source for the DLC films grown using C_2H_2 as source gas. The hardness values are found to increase with the increase of power, higher applied power leading to an enhancement of the energy of the radicals participating in the formation of DLC films. At such high energies a process of compaction (density increase) of the DLC films takes place with the consequent increase of hardness values.

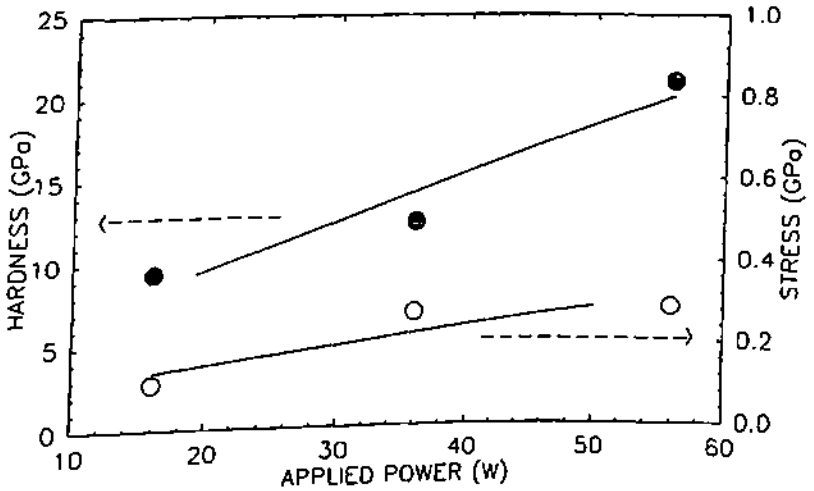

Fig 4.8 Variation of hardness and stress with the applied power for DLC films grown using C_2H_2 gas

4.4.3 Adhesion and Residual Stress

It was found that DLC films produced using a saddle field source adhere well to 7059 glass, quartz, Ge, silicon, Mo and mylar substrates. The adhesion of the films varies widely on different substrates and depends upon the method of preparation. These DLC films appear to have significant internal compressive stress. The hardest and thicker films peel off easily because such high internal stresses cause delamination of the films from the substrates.[40] The values of internal

stress have been evaluated using a laser based technique developed indigenously, as discussed in **Chapter II** under **section 2.8**. The values of internal stress of the DLC films so evaluated were found to be in the range of 0.1-0.5 GPa. This improved the ageing behaviour of the DLC films and the films were able to stay for a long period. It may be noted that the stress values reported here are very much less than the stress values obtained in films that are deposited using the RF self bias technique. **Figure 4.8** also shows the variation of stress values with the power applied to the FAB source for the DLC films grown using C_2H_2 as source gas. From this figure it is clear that the values of stress increases with the applied power. These observations reconfirmed that high hardness values are accompanied with high residual stress values, though in this case the dependence is not so marked as in the case of the RF self bias grown DLC films.

4.5 Electrical and Optical Properties

4.5.1 Electrical Conductivity

Figure 4.9 shows the variation of dark conductivity with the inverse of temperature in the range from 30 to 300°C for the DLC film grown using CH_4, C_2H_2 gases and C_6H_6 vapours. These films were annealed at 300°C before conductivity measurements commenced. The curves in **Fig. 4.9** consist of two straight lines having two different activation energies which follow a relation of the form

$$\sigma_D = \sigma_{01}\exp\left(-\frac{\Delta E_1}{kT}\right) + \sigma_{02}\exp\left(-\frac{\Delta E_2}{kT}\right)$$

The first term is dominant at high temperature and the second term assumes a significant value at lower temperature and there is a kink temperature between the two activated processes. Here the symbols used have their usual meanings. The values of dark conductivity (σ_D), activation energies (ΔE_1, ΔE_2), conductivity pre-exponential factors (σ_{01}, σ_{02}) and the kink temperature (T_K), derived from the conductivity data of DLC films grown using different hydrocarbons are

summarised in **Table-4.1**, along with the deposition rates and other properties to be discussed in the following sections. The values of dark conductivity lie in the range 10^{-9}-10^{-7} $\Omega^{-1}cm^{-1}$. The values of high and low temperature activation energies ΔE_1 and ΔE_2 lie in the range 0.38 - 0.46 eV and 0.22 - 0.32 eV, respectively. The kink temperature between the two processes occurs at around 155 ± 15°C. The values of high and low temperature conductivity pre-exponential factors σ_{01} and σ_{02} lie in the range 10^{-3}-10^{-1} $\Omega^{-1}cm^{-1}$ and 10^{-5} - 10^{-3} $\Omega^{-1}cm^{-1}$, respectively. The high temperature process suggests the conduction of carriers take place in the band tails and the lower temperature process could possibly be due to the conduction at Fermi level. It seems extended band conduction in these films could possibly occur at much higher temperature. In this case the values of activation energies are expected to be much higher, possibly in the range of 1.0-1.5 eV and that of the conductivity pre-exponential factor in the range of 10^{0} - 10^{2} $\Omega^{-1}cm^{-1}$ as reported in the literature.[41] Hauser[42] found a linear relationship between log σ vs. $T^{-1/4}$ in sputtered amorphous carbon (a-C) films indicating conduction by variable range hopping. However, for a-C:H films no such relationship has been found except for doped films.[43]

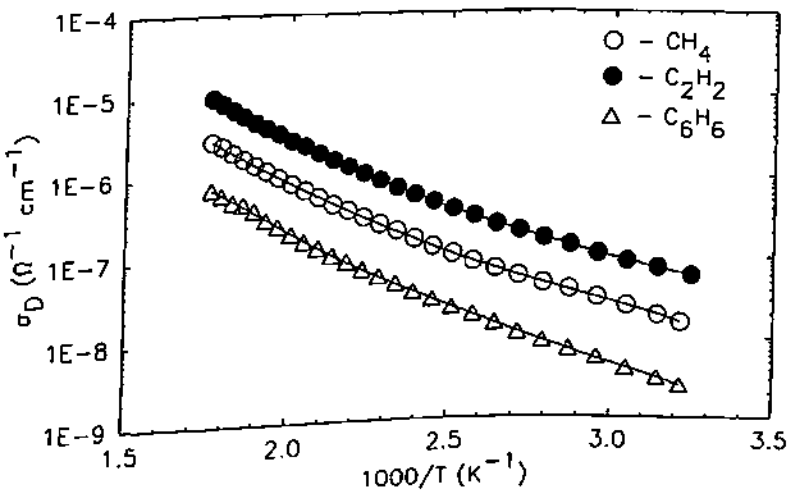

Fig. 4.9 Variation of dark conductivity with inverse of temperature in the range 30 to 300°C of DLC films annealed at 300°C.

Increase of the power applied to the saddle field source leads to a marginal increase in the values of σ_{01}, σ_{02} and T_K and decrease in the values of ΔE_1 and ΔE_2 without changing the dark conductivity values (σ_D) very much. Annealing the samples at 300°C marginally increases the

values of σ_D, σ_{01} and T_K and decreases the values of ΔE_1, ΔE_2 and σ_{o2}. If one goes from CH_4 to C_2H_2 gas and then to C_6H_6 vapours the values of deposition rate, σ_D, σ_{01}, σ_{02} and T_K marginally increase and the values of ΔE_1 and ΔE_2 decrease. Inspite of the observed dependence of the deposition rate on the type of hydrocarbon gases, the properties of hard a-C:H (DLC) films were found to be relatively precursor independent which is in agreement with the results reported in the literature[38] for films grown using the RF self bias technique. It should be mentioned that because of the fundamental difference in the nature of precursors involved in these two techniques one would expect some difference in the behaviour of these films. However, in the absence of precise knowledge concerning the mechanism of growth of DLC films by the saddle field technique, no further comments will be made. Finally, the decrease in the values of activation energy with the increase of power and carbon to hydrogen ratio can be explained by a possible movement of the Fermi level towards the conduction band edge leading to an increased density of states in the material.

4.5.2 Current-Voltage (I-V) Measurements (SCLC)

The current-voltage (I-V) characteristics of the sandwich structure of p-type silicon wafer/DLC films/aluminium have been used to derive information about the density of states in these DLC films. **Figure 4.10** shows typical logarithmic I-V characteristics recorded at room temperature for the structure of the type, p-type silicon wafer/DLC film/Al. The DLC films were grown using CH_4, C_2H_2 gases and C_6H_6 vapours in the saddle field FAB source. It may be noted that these curves begin with a linear ohmic region with a slope approximately unity, followed by a gradual transition to a steeper curve with slope $m>2$ indicating the onset of space charge limited conduction (SCLC) followed by a third region with slope $m<2$. No V^2 dependence is observed as reported by Mackenzie and co-workers.[44] This form of I-V characteristics can not be explained by a single trap model.[45] DLC films grown on the silicon substrates have slope, *m*, larger than 2 owing to the presence of traps in the films. The density of states $N(E_F)$ was calculated from I-V curves by

the differential method of Nespurek and Sworakowski.[46] In this analysis $N(E_F)$ is related to the voltage V and the slope m ($=\frac{\partial \ln I}{\partial \ln V}$) of the experimental I-V curve by the expression,[46,47]

$$N(E_F) = \left(\frac{a\varepsilon}{ed^2kT}\right)\frac{V}{m-1}$$

where a is a process dependent constant that accounts for the non-uniformity of charge carrier distributions and electric field within the space charge region, which is taken to be 0.75, ε is the permittivity of the material which is taken as 4.0×10^{-12} CV cm^{-1} for DLC films,[19] e is the electronic charge, d is the thickness of the films, k is the Boltzman constant, T is the temperature in Kelvin and V is the voltage at which SCLC sets in. There is a sharp increase in the current with slope $m > 2$. The position of quasi-Fermi level relative to $E_c = 0$ is found by the relation,

$$E_F = kT \ln\left(\frac{eN_C\mu_o b}{d}\right) + kT \ln\left(\frac{V}{J}\right)$$

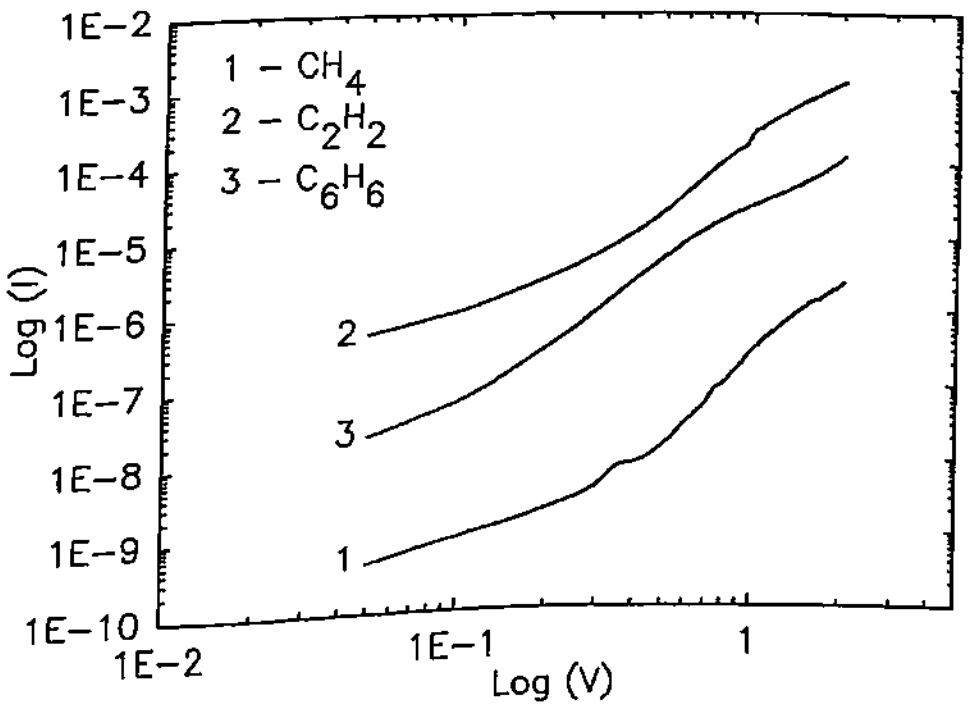

Fig 4.10 Logarithmic I-V characteristics of DLC films

where the factor $eN_C\mu_o$ is a pre-exponential factor, μ_o obtained from the temperature dependence of the DC conductivity in the ohmic region, *b* is the process constant with a value 1.5, this is assigned to account for the non-uniformity of the internal space charge field, N_c being the density of states at the conduction band edge, m_o is the carrier mobility. The values of $N(E_F)$ near the Fermi level calculated for a large number of samples lie in the range 4.1 - 6.4 × 10^{17} eV^{-1} cm^{-3} for the DLC films grown using CH_4 gas and 1.2 - 3.3 × 10^{17} eV^{-1} cm^{-3} for the DLC films grown using C_2H_2 gas and for the DLC films grown using C_6H_6 vapours this comes out to be 3.5 - 4.5 × 10^{17} eV^{-1} cm^{-3}. The values of $N(E_F)$ are found to decrease with the increase of carbon to hydrogen ratio in the hydrocarbon gases/vapours used. However, the $N(E_F)$ in the films grown using C_6H_6 vapours, having the same carbon to hydrogen ratio, shows marginally higher value than those for films grown using C_2H_2 gas. The values of $N(E_F)$ evaluated from SCLC measurements on DLC films grown using CH_4, C_2H_2 gases and C_6H_6 vapours in the saddle field FAB source are found to be 2 - 3 times lesser than the DLC films grown using CH_4 gas in a RF plasma CVD system, as reported by Silva and Amartunga[47] who reported a value of the density of mid gap states ~ 8 - 9 ×10^{17} eV^{-1} cm^{-3}. The values of characteristics energy of band tails (Urbach energy, E_o) evaluated from PDS measurements for DLC films grown using CH_4, C_2H_2 gases and C_6H_6 vapours are found to lie in the range 180 - 280 meV and this value decreases with the increase of carbon to hydrogen ratio in the hydrocarbon gases/vapours used (**section 4.5.5**). Thus, the sharpness of band tails (E_o) is closely related to the density of states $N(E_F)$ in DLC films grown using hydrocarbon gases in the saddle field FAB source and the values of E_o and $N(F_F)$ are found to decrease with the increase of carbon to hydrogen ratio in the hydrocarbon gases/vapours used.

4.5.3 Optical Bandgap

The variation of the absorption coefficient (α) was calculated from the spectral dependence of optical reflection and transmission using Tauc's expression.[48] **Figure 4.11** shows the variation of αhν vs. hν curve for the DLC film grown using CH_4, C_2H_2 gases and C_6H_6 vapours. The curves follow the well known Tauc's relation. The intercept on the X-axis of the plot of $\sqrt{\alpha h\nu}$ vs. hν gives the value of the optical bandgap (E_g) of the material. The values of E_g and constant B derived

from the slope of $\sqrt{\alpha h\nu}$ vs. hν plot, together with the values of α at 2.756 eV for DLC films grown using different hydrocarbons, are included in **Table-4.1**. It is found that

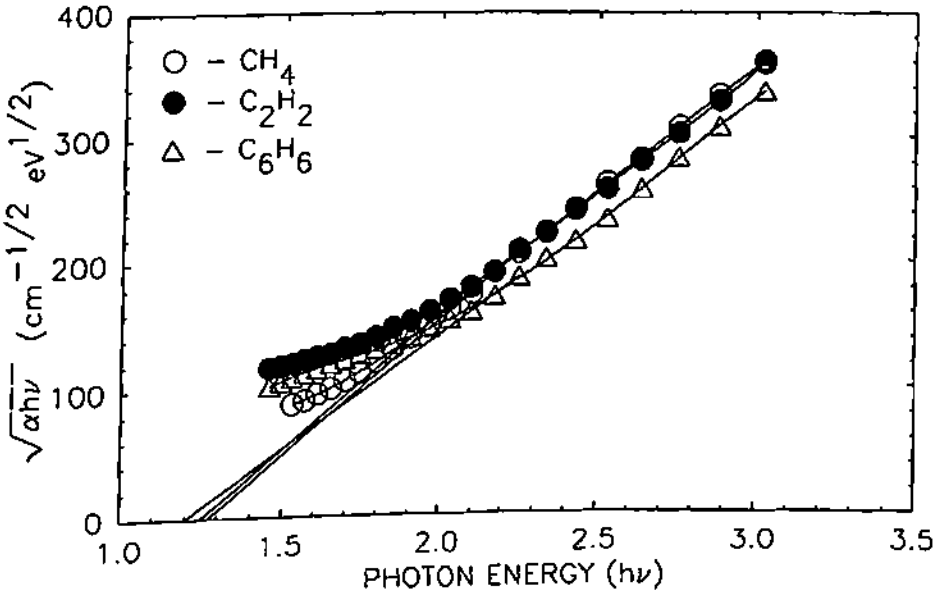

Fig. 4.11 Variation of $\sqrt{\alpha h\nu}$ vs. hν of DLC films grown using CH_4, C_2H_2 gases and C_6H_6 vapours

the values of E_g and constant B decrease marginally with the increase of power, whereas, the values of α seem to remain constant. The values of E_g and constant B decrease marginally when one goes from CH_4 gas to C_2H_2 gas and then to C_6H_6 vapours. The decrease in the values of constant B with the increase of power applied to the saddle field source indicates an increase in the density of states in the material. Further more, the decreased values of constant B in C_2H_2 gas and C_6H_6 vapour grown DLC films as compared to CH_4 grown DLC films suggest a decreased density of states in these films. The decreased value of E_g with the increase of power applied to saddle field source is consistent with the decreased value of activation energy obtained from the conductivity data as reported under **section 4.5.1.**.

Table-1.1

Properties of DLC films grown using different hydrocarbons in a saddle field source

Serial No.	Properties	CH_4	C_2H_2	C_6H_6
1.	Deposition rate at 6 cm. distance at specific power (A°/min.)	11.7 (7.2 W)	37.7 (4.5W)	21.7 (4.5 W)
2.	σ_D at 35°C (Ω^{-1} cm^{-1})	10^{-9}-10^{-8}	10^{-8}-10^{-7}	10^{-9}-10^{-8}
3.	ΔE_1 (eV)	0.44-0.45	0.38-0.46	0.44-0.45
4.	ΔE_2 (eV)	0.27-0.32	0.22-0.29	0.26-0.27
5.	σ_{01} (Ω^{-1} cm^{-1})	10^{-3}-10^{-2}	10^{-2}-10^{-1}	10^{-3}-10^{-2}
6.	σ_{02} (Ω^{-1} cm^{-1})	10^{-5}-10^{-3}	10^{-4}-10^{-3}	10^{-5}-10^{-4}
7.	T_K (°C)	145-155	140-170	145-150
8.	α at 2.756 eV (cm^{-1})	2.2-2.6×10^4	2.0-3.6×10^4	1.5-1.6×10^4
9.	E_g (eV)	1.0-1.30	1.0-1.30	1.20-1.30
10.	Constant B (cm^{-1} $eV^{-1/2}$)	185-220	120-200	200-210
11.	n at 546.1 nm.	2.10-2.29	1.80-2.57	2.50-2.52
12.	k at 546.1 nm	0.07-0.45	0.05-0.50	0.49-0.50
13.	ϵ_1 at 546.1 nm.	4.22-5.16	3.10-6.62	6.07-6.10
14.	ϵ_2 at 546.1 nm.	0.30-1.98	0.22-3.43	2.53-2.55
15.	Knoop hardness at 50 g load (GPa)	9 - 15	10-21	12.5-13

4.5.4 Ellipsometric Studies

4.5.4.1 Refractive Index and Extinction Coefficient

The values of the refractive index (n), extinction coefficient (k) derived from the ellipsometric measurements made at 546.1 nm wavelength of light together with the dielectric constants (ε_1 and ε_2) of DLC films grown using different hydrocarbons are summarised in **Table-4.1**. The values of n and k lie in the rage 1.80 - 2.57 and 0.05 - 0.50, respectively. One

observes, as compared to films grown by RF self bias technique,[38] it is possible to achieve higher values of refractive index in this case. The corresponding values of ε_1 and ε_2 lie in the range 3.10 - 6.62 and 0.22 - 3.43, respectively. The values of n and ε_1 decrease and that of k and ε_2 increase in the case of DLC films grown using CH_4 gas with the increase of power applied to the saddle field source. On the other hand the values of all these parameters seem to increase with the increase of power applied to the saddle field source in the case of DLC films grown using C_2H_2 gas and C_6H_6 vapours. It is observed that the dense and hard, reasonably scratch resistant carbon films are characterised by a large values of n and soft carbon films by low values of n.

4.5.4.2 Spectroscopic Ellipsometry (SE) and sp^3/sp^2 Ratio

Figures 4.12(a) and **4.12(b)** show the variation of refractive index (n), extinction coefficient (k) for the DLC films grown using CH_4 and C_2H_2 gases and C_6H_6 vapours over the photon energy range from 2.5 - 5.0 eV. **Figures 4.13(a)** and **4.13(b)** show the corresponding variation of real and imaginary part of the dielectric constants ε_1 and ε_2 for the DLC films grown. In the case of DLC films grown using CH_4 and C_2H_2 gases almost similar trend in the dispersion of the values of optical constants (n, k, ε_1 and ε_2) with photon energy is observed whereas DLC films grown using C_6H_6 vapours show somewhat different trend in the dispersion of optical constants. The values of n ranges from 1.74 to 2.19, k ranges from 0.28 to 0.59, ε_1 ranges from 2.75 to 4.63 and ε_2 ranges from 1.10 to 2.35. The maximum values of n and ε_1 are found to be 2.19 and 4.63 at 3.07 eV for films grown using CH_4 gas, whereas, for films grown using C_2H_2 gas the corresponding maximum values are found to be 2.04 and 4.06 at 3.14 eV. DLC films grown using C_6H_6 vapours show the maximum values of n and ε_1 as 2.10 and 4.24, respectively at 3.74 eV. However, in this case the variation of n and k with energy appears to be rather slow and one observes almost flat response at higher energies. The values of n and ε_1 decrease on both sides of this peak value. The values of k and ε_2 increase with the increase of photon energy and approach towards saturation at the energy greater than 3.7 eV in the case of DLC films grown using CH_4 gas and at an energy greater than 3.9 eV for the DLC films grown using C_2H_2 gas, whereas, the saturation occurs at much higher energy ~ 4.5 eV in the case of DLC films grown using C_6H_6 vapours.

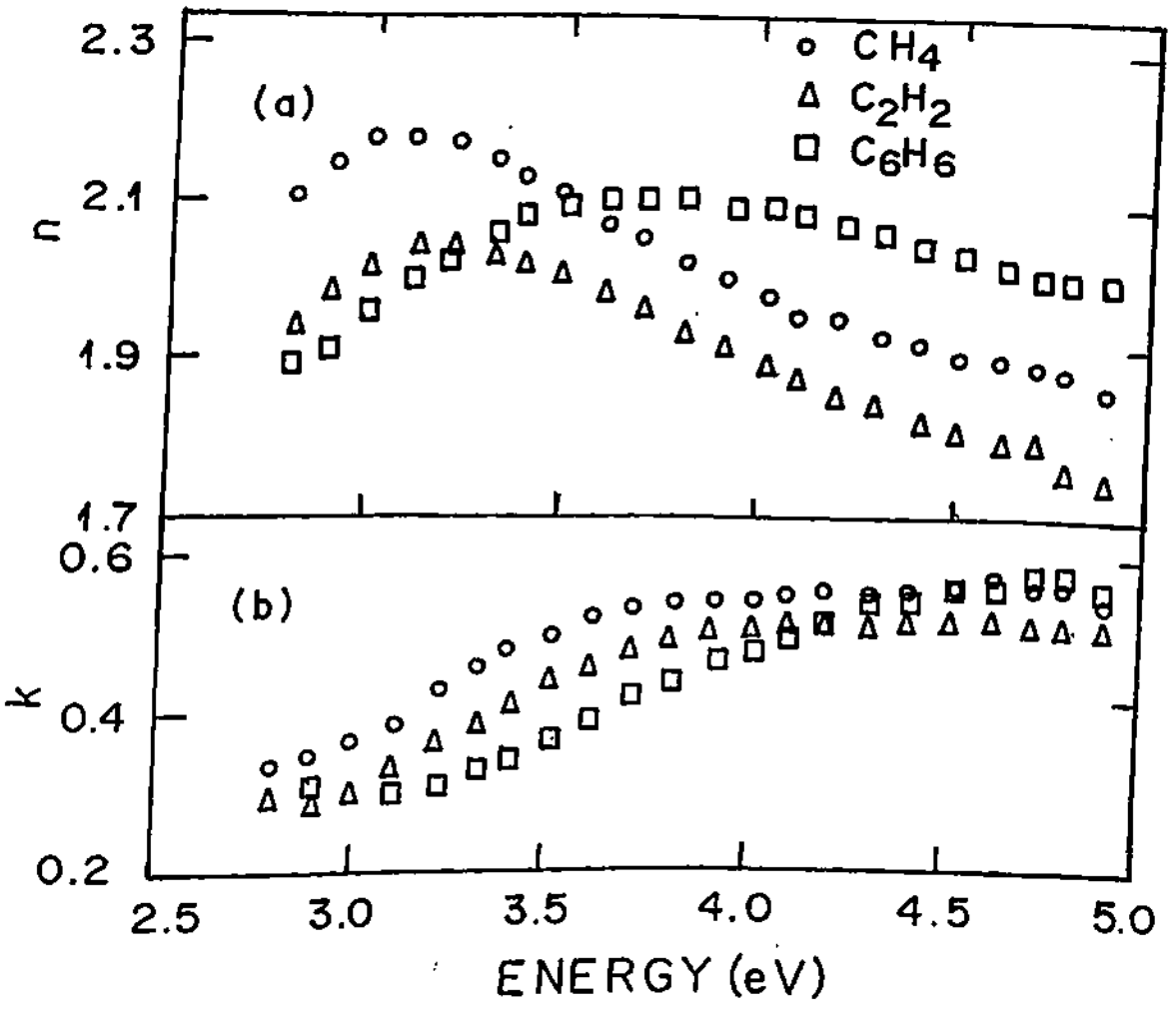

Fig. 4.12 Variation of (a) refractive index (n) and (b) extinction coefficient (k) vs. photon energy for DLC films grown using CH_4 and C_2H_2 gases and C_6H_6 vapours.

The maximum values of k are found to be 0.54 and 0.50 and that of ε_2 are found to be 2.20 and 1.90 for films grown using CH_4 and C_2H_2 gases, respectively, when measured at a wavelength corresponding to 3.7 eV, whereas DLC films grown using C_6H_6 vapours show the maximum value of k and ε_2 as 0.51 and 2.30, respectively at ~4.5 eV. The values of optical constants decrease with the increase of carbon to hydrogen ratio of the hydrocarbon gases/vapours used. The shift of the peak position in the values of optical constants towards higher energy with the increase of carbon to

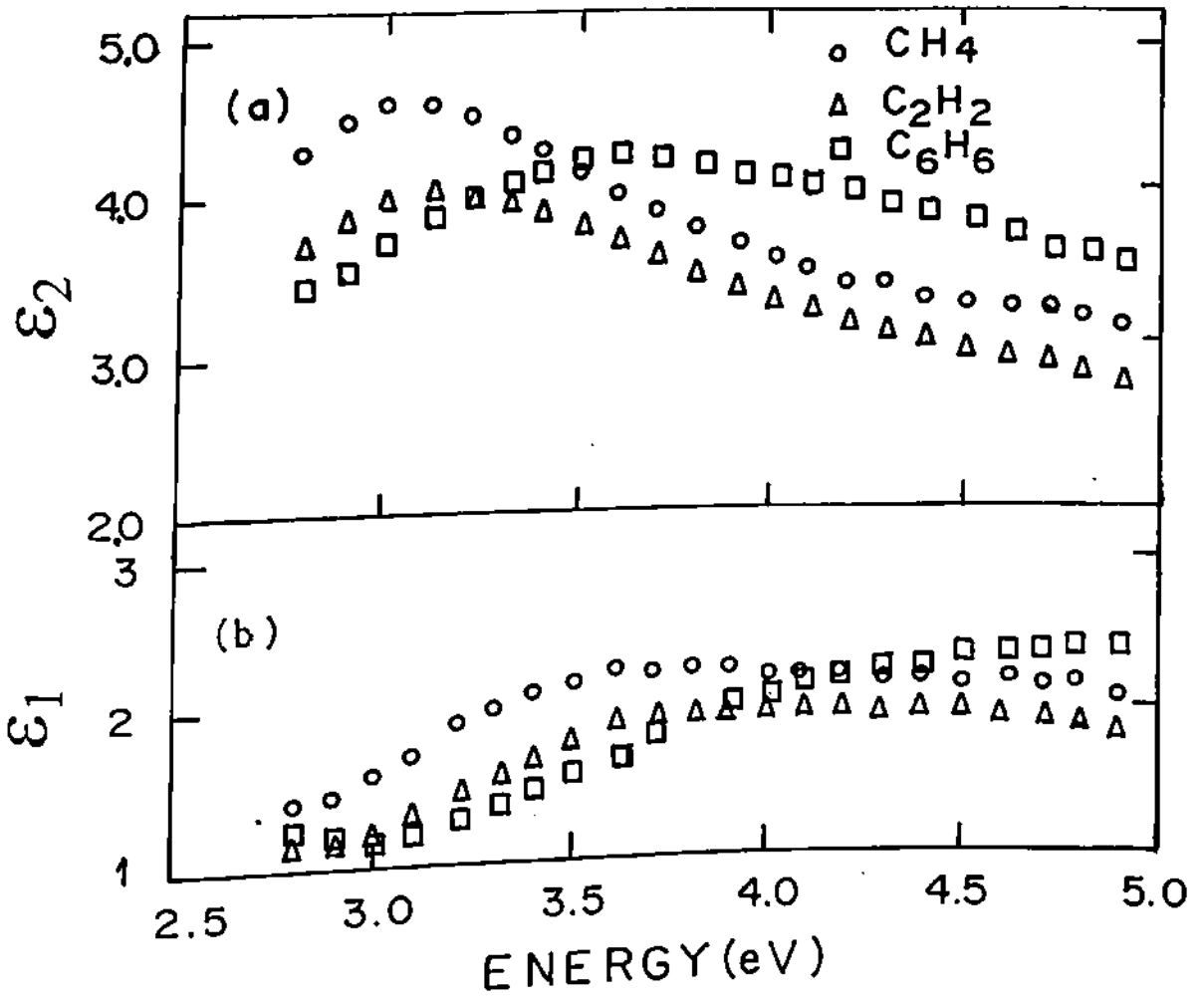

Fig. 4.13 Variation of dielectric constants (a) ε_1 and (b) ε_2 vs. photon energy for DLC films grown using CH_4 and C_2H_2 gases and C_6H_6 vapours.

hydrogen ratio in hydrocarbon gas/vapour used indicate stronger bonding of C-C bonds which leads to a higher sp^3/sp^2 ratio and more diamond like a-C:H films. Further, DLC films grown using C_6H_6 vapours which show significant shift of peak position in the values of optical constants towards higher energies compared to the peak position in the values of optical constant of DLC films grown using C_2H_2 gas, having the same carbon to hydrogen ratio, indicate much more stronger bonding of carbon atoms leading to still larger sp^3/sp^2 ratio. Dense carboneous films are

characterised by large refractive index with relatively low dispersion and hydrogen appears to lower the refractive index. Typical a-C:H films are reported to cover the range $1.8 \leq n \leq 2.3$ and polymer like hydrocarbon films deposited at low energy have refractive index values less that 1.8. The values of optical constants depend weakly on the precursors of hydrocarbon gases used and the values decrease with the increase of carbon to hydrogen ratio in the hydrocarbons used in growing DLC films by the saddle field FAB source.

The sp^3/sp^2 ratio for some of the DLC films were evaluated using the technique describe in **Chapter II** under **section 2.13**. The values of this ratio is found to be in the range of 9 to 11, more than for the DLC films grown by RF self bias technique. A trend in the increase of sp^3/sp^2 ratio is observed as one goes from CH_4 to C_2H_2 gases to C_6H_6 vapours.

4.5.5 Photothermal Deflection Spectroscopy (PDS)

Figure 4.14 shows the variation of absorption coefficient (α) vs. photon energy (E) (PDS data) for DLC films grown by introducing CH_4 and C_2H_2 gases and C_6H_6 vapours into the saddle field FAB source. The variation of α with the photon energy, in the energy range studied, consists of two distinct regions. One is the high energy region above ~ 1.8 eV which is due to a direct band to band transition and where Tauc type behaviour is evidenced. The second region is an exponential Urbach edge region which extends down to ~1.0 eV and can be expressed as $\alpha = \alpha_o \exp(-h\nu/E_o)$, where α_o is a constant. The exponential portion of α is referred to as the Urbach tail and E_o is the characteristic energy of the band tail (Urbach edge) which is related to the thermal and the structural disorder in the material. The lowest energy region where the subgap tail is superimposed on the Urbach edge and involve absorption due to gap states, is however not visible due to monochromator grating limitations. The values of α are found to be consistently higher for DLC films grown using CH_4 gas than the values of α for DLC films grown using C_2H_2 gas and C_6H_6 vapours above ~1.65 eV and lower below this energy. The values of E_o were found to be ~280 meV, 260 meV and 180 meV for DLC films grown using CH_4 and C_2H_2 gases and C_6H_6 vapours, respectively. These values of α and E_o reported here for DLC films indicate that the

properties are found to be precursor dependent whereas the results reported in the literature for the films grown using the RF self bias technique[38] are found to be relatively precursors independent. Broad band tails are usually found in a-C:H and the values of E_o is frequently over 500 meV[49] but some what narrower tails ($E_o \approx 300$ meV) have been seen in a-C:H by Dischler *et al.*[50] The values of E_o in highly tetrahedral hydrogenated amorphous carbon (ta-C:H) are found to be ~ 350 meV.[51] Thus, the values of E_o evaluated for DLC the films grown using CH_4, C_2H_2 gases and C_6H_6 vapours by a saddle field FAB source in the present study are found to be significantly lower than the values of E_o (300 - 500 meV) for DLC films reported in the literature[49-52] and more than the values of E_o (~50 meV) of hydrogenated amorphous silicon (a-Si:H) films usually mentioned.[52]

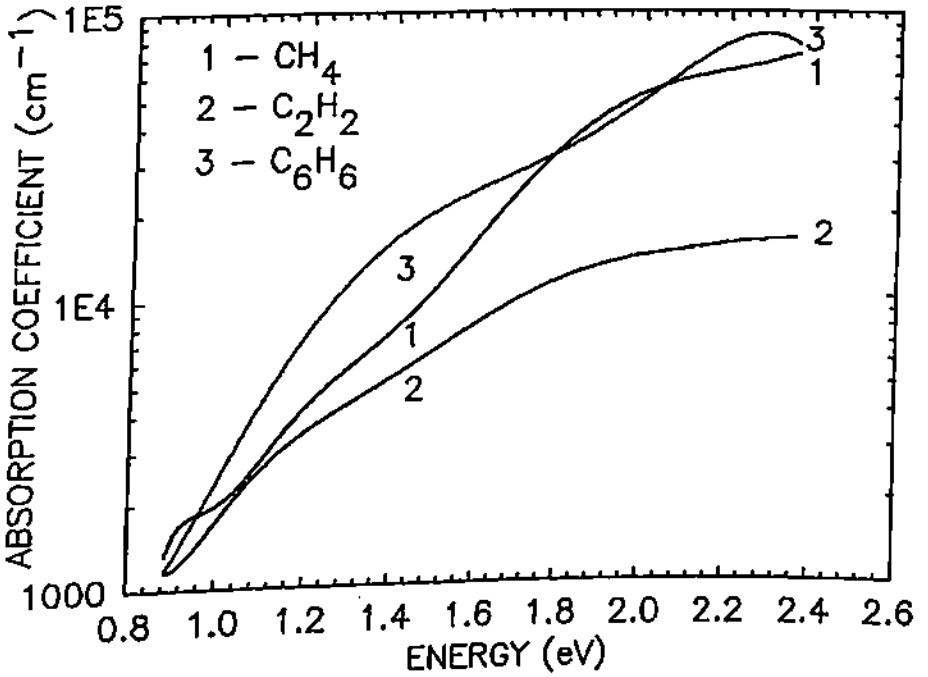

Fig. 4.14 Variation of absorption coefficient (α) obtained from PDS data vs. photon energy for DLC films grown using CH_4 and C_2H_2 gases and C_6H_6 vapours

4.6 Surface Morphology and Structural Analysis

It was felt that it would be rewarding to undertake a detailed structural analysis of the DLC films grown by the saddle field fast atom beam technique and find correlation, if any, of the structure related information and the data collected thus for by the other measurements.

4.6.1 Scanning Electron Microscopy (SEM)

Figure 4.15 shows the typical SEM monographs (at normal angle) of DLC films grown by using (a) CH_4, (b) C_2H_2 gases and (c) C_6H_6 vapours, respectively. It is evident that all the micrographs show the films to have some agglomerates and the number of agglomerates are found to decrease when one goes from CH_4 to C_2H_2 gas. The number of agglomerates are again found to increase with the increase of power applied to the source. The number of agglomerates diminishes in DLC films grown using C_6H_6 vapours. The surface morphology is found to be smoother in DLC films grown using C_6H_6 vapours than the DLC films grown using C_2H_2 gas having the same carbon to hydrogen ratio in the hydrocarbons used. This probably reveals that the stress present in the films grown using C_6H_6 vapours is less than the stress present in DLC films grown using C_2H_2 gas. A similar type of smoother surfaces were recorded by SEM studies of DLC films grown using RF self bias decomposition of C_6H_6 vapours. The surfaces of DLC films grown using RF decomposition of CH_4 and C_2H_2 gases were again found to be not all that smooth. Process gas (vapour) dependence of DLC films properties inspite of the method of formation is, thus, again reconfirmed.

4.6.2 X-ray Photoelectron Spectroscopy (XPS)

XPS is a chemical sensitive technique and the XPS chemical shift has proven to be a valuable method for understanding the local environment of an atom in a solid and to investigate whether a carbon film is sp^3 or sp^2 bonded. Apart from the chemical shift, the XPS technique can provide other useful information such as film composition, Plasmon loss for conducting materials, valence band density of states etc.

Representative XPS spectra for DLC films grown using (a) CH_4, (b) C_2H_2 gases and (c) C_6H_6 vapours are shown in **Fig. 4.16**. The XPS spectra shows only oxygen as a surface contaminant in addition to main peak of C in all the DLC film grown using these gases/vapours and

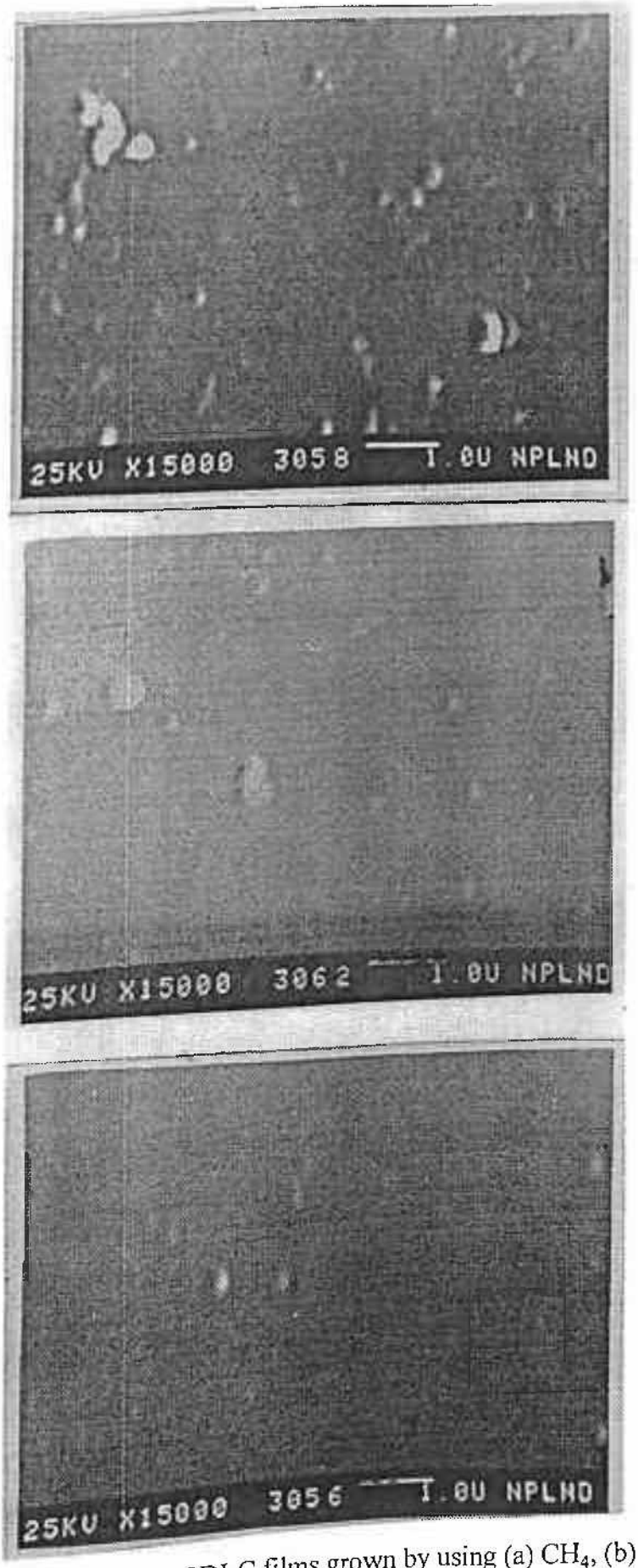

Fig. 4.15 SEM monographs of DLC films grown by using (a) CH_4, (b) C_2H_2 gases and (c) C_6H_6 vapours

it may be mentioned that no other important peaks were found. The spectra were recorded before and after cleaning the top surface using argon (Ar) ion beam at 3 keV, at a pressure of ~10^{-8} mbar, for 2 minutes. The oxygen peak was found to diminish after cleaning of the top surface by Ar ion beam in all the DLC samples which indicates that the oxygen is present only on the surface and not throughout the bulk of the film. **Figure 4.17** shows the typical C1s spectra of DLC films grown using CH_4, C_2H_2 gases and C_6H_6 vapours. The position of C1s peak is found to occur at 286 eV, 286.7 eV and 287.1 eV respectively, in DLC films grown using CH_4, C_2H_2 gases and C_6H_6 vapours. It is evident that there is a shift in C1s peak towards higher energy by ~ 0.7 eV in DLC

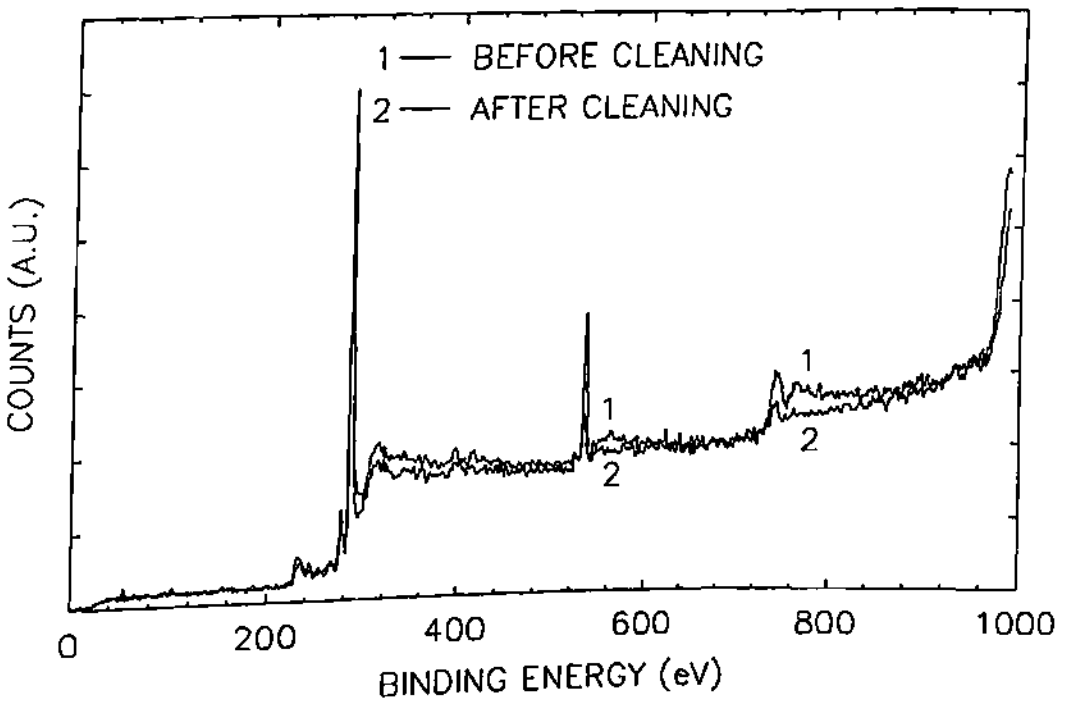

Fig. 4.16 XPS spectra of DLC films grown by using CH_4 gas before and after Ar ion bombardment at 3 keV for 2 min

films when one goes from CH_4 to C_2H_2 gas i.e. with the increase of carbon to hydrogen ratio in the hydrocarbons used. Again the peak position of C1s peak shifts by ~0.6 eV towards higher energy in case of DLC films grown using C_6H_6 vapours as compared to DLC films grown by C_2H_2 gas having the same carbon to hydrogen ratio in hydrocarbon gases/vapours used. The peak position of

C1s is also found to shift towards lower energy by 0.3 eV, 1.0 eV and 2.3 eV in DLC films grown using CH_4, C_2H_2 gases and C_6H_6 vapours, respectively, as recorded after the surfaces of the films were cleaned by Ar ion beams. XPS has been used earlier[53,54] to analyse DLC films and the photoelectron peaks located at binding energies of 284, 285 and 287 eV are assigned to graphite, hydrocarbon and diamond (with cubic symmetry). Thus, it is evident that the photoelectron peaks observed in DLC films grown by the saddle field FAB source in the present study indicates that the films are more diamond like and such diamond like behaviour increases with the increase of carbon to hydrogen ratio in the hydrocarbon used for growing DLC films.

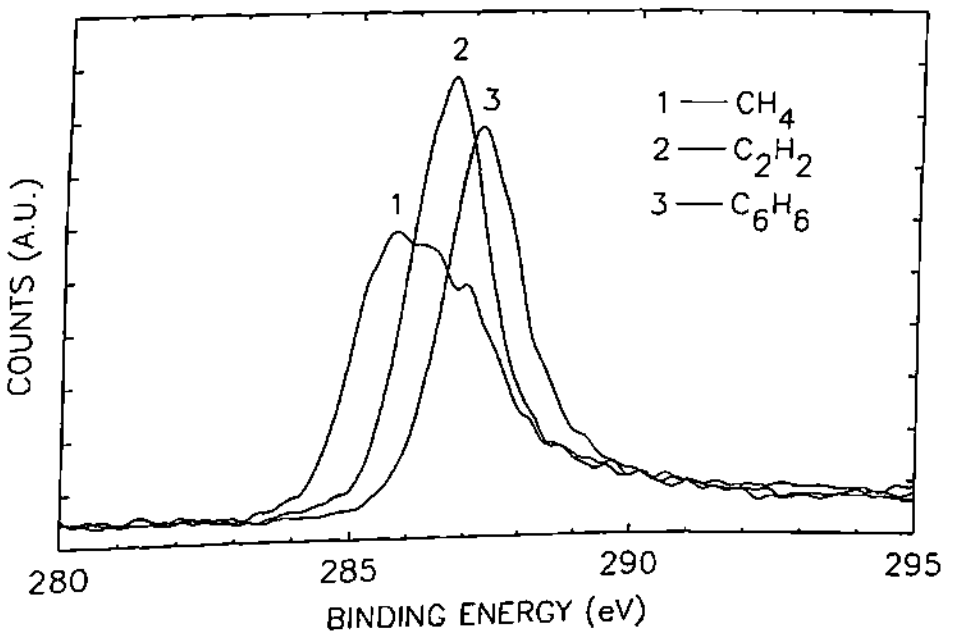

Fig 4.17 C1s spectra of DLC films grown by using CH_4 and C_2H_2 gases and C_6H_6 vapours

4.6.3 X-ray Auger Electron Spectroscopy (XAES)

A relatively sensitive analysis of the sp^3 and sp^2 bonding in the DLC films is provided by AES or XAES. XAES has further advantage that it does not damage the samples under investigation. **Figure 4.18(a)** and **4.18(b)** show the measured N(E) and dN/dE C KLL spectra of

DLC films grown using CH_4, C_2H_2 gases and C_6H_6 vapours, in the saddle field FAB source. The energy of the main feature in N(E) DLC spectra ranges from 250 - 280 eV being 260 eV for DLC films. It is known that the main feature for graphite occurs at 269 eV and those for diamond occurs at 262 eV. A comparison of N(E) spectra of a number of DLC films shows that the main feature of the overall structure are similar to one another and films are more diamond like in nature and similar to those reported by other workers.[58] There are differences, however, in the fine structure which are made more pronounced in the dN/dE spectra. The fine structure provides sort of a finger

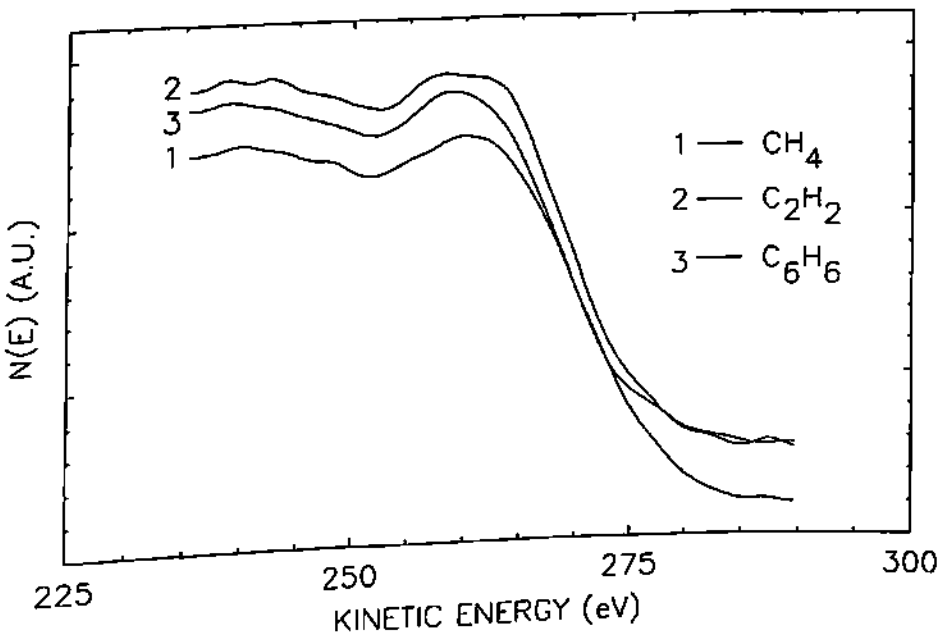

Fig 4. 18 (a) N(E) spectra studied by XAES vs. kinetic energy (E) of DLC films grown by using CH_4, C_2H_2 gases and C_6H_6 vapours.

print to distinguish different states of diamond and graphite in these materials. The main contributions in these spectra are localised at 262.5±0.5 eV which are close to diamond feature with peak at 262.0 eV as reported by several workers.[55,56] dN/dE spectra are often characterised by the energy separation between two major excursions. For carbon specimens, this energy separation indicates whether the carbon is involved in sp^2 or sp^3 bonding.[56,57] Carbon with sp^2 bonding gives a wide energy separation of ~ 22.5 eV and with sp^3 bonding yields a narrow energy separation of ~14.3 eV, which agree with the values reported by Lascovich *et al.*[55] and also by Mizokawa *et al.*[57] The assumption made here is that the DLC films present a sp^3 (i.e. tetrahedral bonding as in

diamond) and sp^2 (i.e. trigonal bonding as in graphite) hybridisation and the method proposed by Lascovich *et al.*[55] to calculate the ratio of the two has been adopted. Specifically they define a parameter *D*, the distance between the maximum of positive going excursion and the minimum of negative going excursion in the derivative XAES spectra. The maximum at positive going excursion occurs at 255.5 ± 0.5 eV and minimum of negative going excursion occurs at 269.7 ± 0.7 eV in DLC films grown during the present study. The values of D are found to be 14.8, 14.5 and 13.5 eV for DLC films grown using CH_4, C_2H_2 gases and C_6H_6 vapours, respectively, which are close to the *D* value obtained with sp^3 bonding in the DLC films. It is evident that the value of *D*

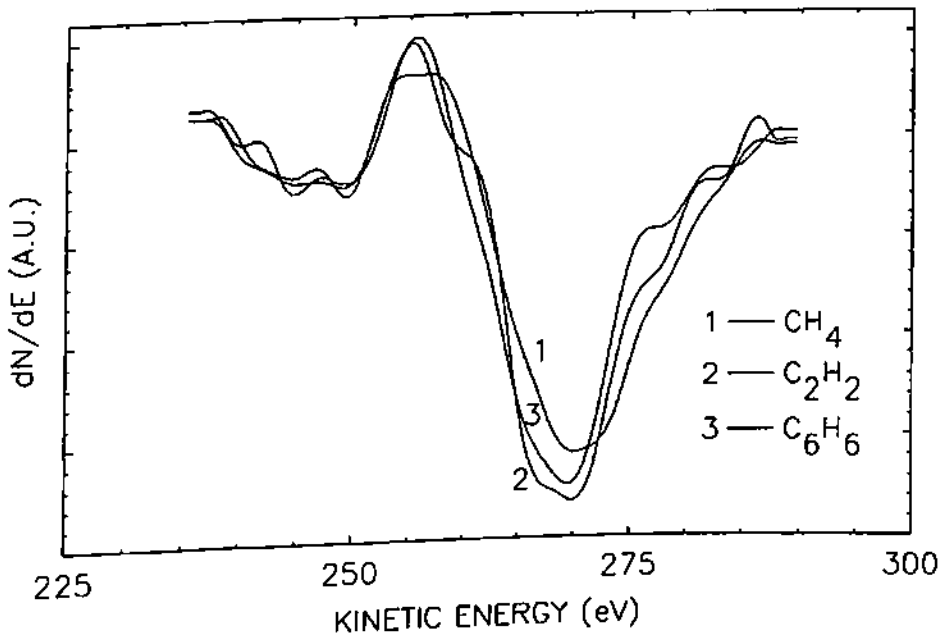

Fig 4.18 (b) dN/dE spectra studied by XAES vs. kinetic energy (E) of DLC films grown by using CH_4, C_2H_2 gases and C_6H_6 vapours

decreases marginally with the increase of carbon to hydrogen ratio in the hydrocarbon gases/vapours used in the present study, which implies that the films are more diamond like in nature. The sp^2 percentage are evaluated using *D* values by the relation[55]:

$$sp^2\ \% = \left(\frac{D_{DLC} - D_{Diamond}}{D_{Graphite} - D_{Diamond}} \right) \times 100$$

where D_{DLC}, $D_{Diamond}$ and $D_{Graphite}$ are the D values of DLC films, Diamond and Graphite respectively. Taking into consideration that in the DLC matrix only sp^2 and sp^3 sites contribute, the sp^3 percentage for DLC films grown can be easily calculated. The sp^2 percentage in the DLC films are found to be low and lie at 15, 12.5 and 10 for films grown using CH_4, C_2H_2 gases and C_6H_6 vapours and the values decrease with the increase of carbon to hydrogen ratio in the hydrocarbons used. Thus the sp^3 percentage comes out to be 85, 87.5 and 90 yielding the values of sp^3/sp^2 ratio as 5.67, 7.0 and 9.0 for DLC films grown using CH_4, C_2H_2 gases and C_6H_6 vapours, respectively. Thus, it is evident that the sp^3 percentage (85 - 90 %) and the sp^3/sp^2 ratio (5.67 - 9.00) of DLC films grown are found to be significantly high which indicates that the films grown by saddle field FAB technique exhibit more diamond like behaviour and this behaviour increases with the increase of carbon to hydrogen ratio in hydrocarbon gases/vapours used. It has been reported by Lascovich *et al.*[55] that an increase in the hydrogen content in the film corresponds to an increase in the sp^3 percentage. Nothing much can be said about this at this stage unless DLC films are grown with different hydrogen content. After the bombardment of these DLC films by the argon ion beam for 2 min the value of D increased to 20.2 ± 0.3 and the sp^2 percentage was found to increase significantly which indicates that the samples start showing graphitic nature. Similar observations have been made by various other workers[53,55] and they concluded that the argon ion beam irradiation changes the diamond like bonding in DLC films to graphitic like bonding.

The sp^3/sp^2 ratio for DLC films grown using RF self bias technique using hydrocarbon gases are reported to be less (1.5-3) in the literature[40] than the sp^3/sp^2 ratio (6 - 9) evaluated for DLC films grown using the saddle field FAB technique in the present study. The trend in the sp^3/sp^2 ratio evaluated from XAES study are consistent with the trend of sp^3/sp^2 ratio reflected from spectroscopic ellipsometry (SE) results on these DLC films which increases with the increase of carbon to hydrogen ratio in hydrocarbon gases/vapours used. The results of XPS studies reported under **section 4.6.2** are in conformity with XAES results being reported here. It may be emphasised here that main objective of the present investigation has been to find a method of growth of DLC films which is easy to implement as also that produces superior DLC films for many device application. A high value of sp^3/sp^2 that was obtained during these investigations, first

came as a surprise to the investigator, raising doubts about the accuracy of the particular technique used. That is the reason different techniques were employed to asses the same. However, in view of the recent report of as high a value as ~96 % sp^3 in DLC films grown by similar technique by Lim *et al.*[36] It appears that the initial observation of high sp^3/sp^2 in saddle field grown DLC films may perhaps be correct.

4.7 IR Studies of DLC Films

IR measurement were performed using a Fourier transform infrared spectrometer (Model BIO-RAD, FTS40). The details about FTIR method is already given in **Chapter II,** under section **2.12.3. Figure 4.19** shows IR transmission spectra of DLC films grown by inputting different power to the FAB source using C_2H_2 as the feed gas. Analysis of the spectra is carried out on the basis of the peak assignment published in the available reports.[59-60] But as may be noticed in these spectra there is no well defined peaks. This may be because of the low incorporation of hydrogen in these films. Low hydrogen content in these films is again confirmed from ERDA analysis. However weak CH_2 stretching and bending vibration modes are observed at 1450 and 2930 cm^{-1}. In these spectra Si bands are also seen as measurements were carried out on films deposited on silicon substrates. It has also been observed form **Fig. 4.20** that with the increase of power applied to the FAB source, CH_2 stretching vibration mode diminishes. This indicates a decrease of hydrogen in the films with the increase of applied power. This can be explained in terms of more efficient etching of hydrogen in the films by higher energy incident particle. Similar behaviour was observed by Walters *et al.*[30] in their FAB grown DLC films using C_2H_2 gas.

4.8 Hydrogen in the DLC Films

Incorporation of hydrogen in the DLC films decides a number of properties of these films. In the present investigation hydrogen in these films has been estimated using FTIR and ERDA techniques, as discussed in **Chapter II** under **section 2.12**. FTIR provides the information about

the bound hydrogen in DLC films and ERDA the total hydrogen. From these measurements unbound hydrogen in these films was calculated and a characteristic relation has been found to exist in the stress behaviour of the films and amount of unbound hydrogen.

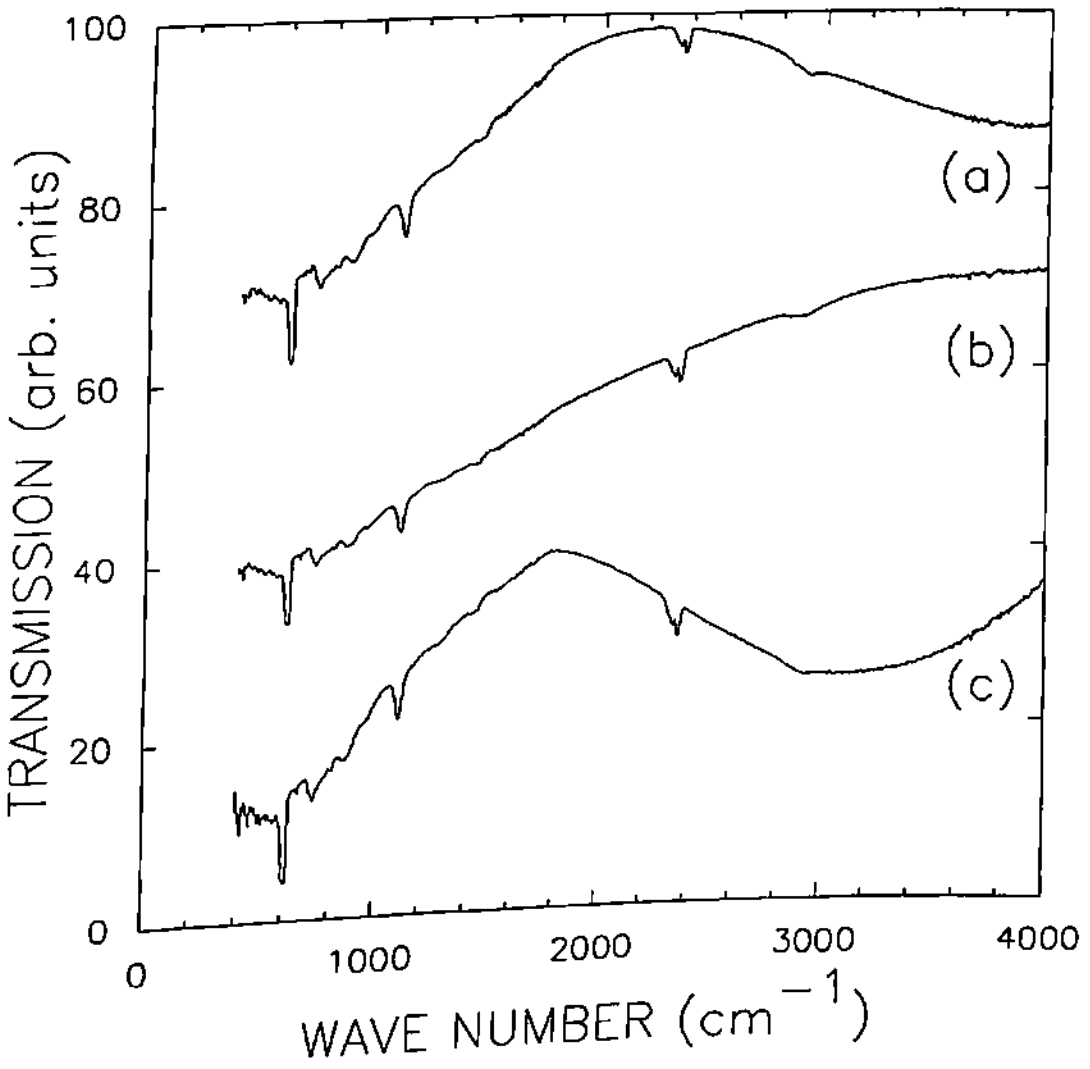

Fig. 4.19 Infrared transmission spectra of DLC films grown using C_2H_2 gas at (a) 16 W, (b) 36 W and (c) 56 W power applied to the FAB source

For these studies, a set of DLC films were grown at different power applied to the FAB source using C_2H_2 as the feed gas. The total hydrogen concentration in these films was found to be very low and a maximum of ~ 8 at. % has been observed. In the published literature[28,30] FAB deposited DLC films using C_2H_2 as the feed gas, a minimum 22 at. % of hydrogen has been

reported when beam energies of ~0.8 kV were used to form these films. However, during the present investigations beam energies used to deposit DLC films were in the range of 1 kV to 2.0 kV, which maybe the reason for the low hydrogen incorporation (as revealed by the FTIR measurements, discussed in earlier section). Similar results were also reported by Walters *et al.*[30] in their DLC films grown by FAB and PECVD techniques.

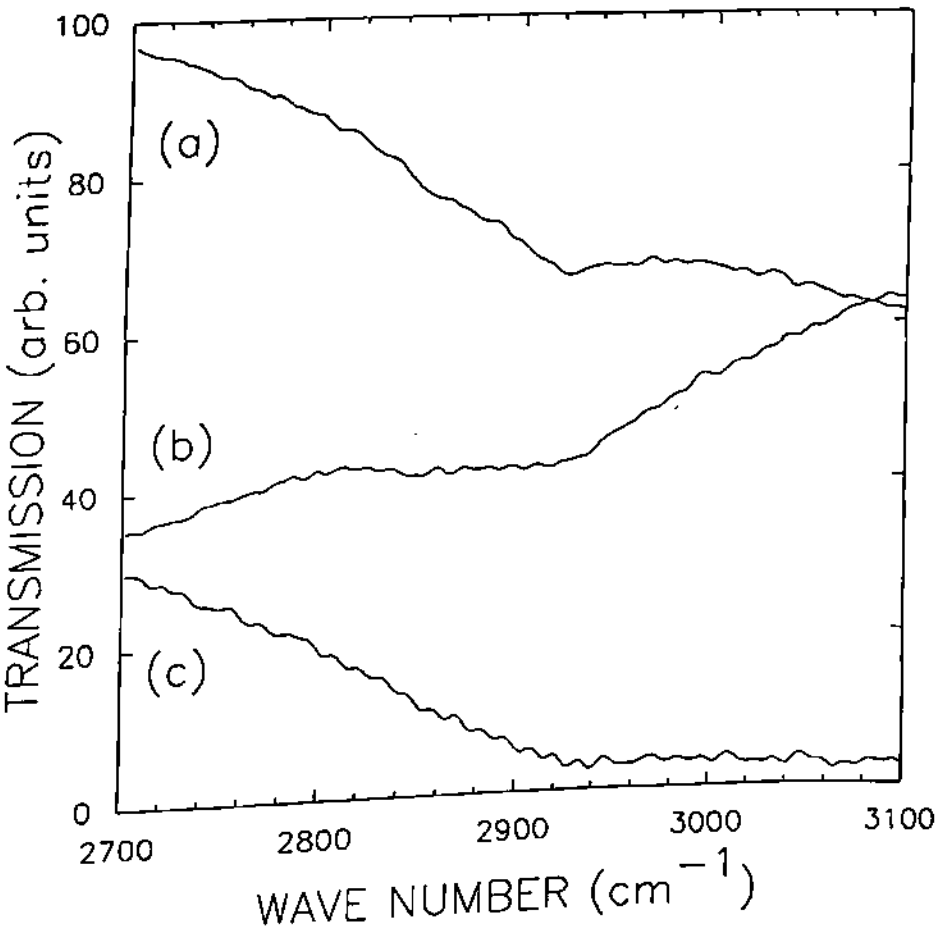

Fig. 4.20 The infrared transmission spectra showing diminishing of CH_2 stretching vibration mode with the increase of power applied to the FAB source

From **Table-1.2** it is evident that the hydrogen concentration decreases with the power applied to the FAB source. This is because an increasing bombardment of the films during growth with rising energy appears to remove the weakly bound hydrogen from the films. From the

Table-1.2 it is also evident that the hydrogen concentration increases in case of CH_4 deposited DLC films.

Table-1.2

Hydrogen concentration of the DLC films

Gas Used	Pressure (mbar)	Power (W)	Total H_2 (at %)	Bound H_2 (at %)	Unbound H_2 (at %)
C_2H_2	5×10^{-3}	16	5.62	3.11	2.51
C_2H_2	5×10^{-3}	36	5.31	2.65	2.66
C_2H_2	5×10^{-3}	56	3.4	0.48	2.9
CH_4	5×10^{-3}	30	7.86	6.24	1.62

Grill *et al.*[61,62] were first to find a correlation between the amount of unbound hydrogen in DLC films and degree of residual stress in the films. System used for growing DLC films in their case had RF (13.56 MHz) power applied to the cathode and a varying negative DC voltages were also added through a RF choke. In the present study a saddle field fast atom beam source was used to grow such films and a similar correlation was found. It, thus, appears that the relation between the unbound hydrogen and stress in DLC films is of a fundamental nature. In this laboratory an attempt is being made to further confirm this trend in DLC films grown by a variety of other techniques like pulse plasma, VHF glow discharge etc. It may be worth mentioning here that in a-Si:H system, particularly for films grown by hot filament technique, a similar correlation between the void density and stability of the a-Si:H films against Stabler-Wornski type degradation has been confirmed.[63] Without doubt confirmation of the existence of a correlation amongst the density of voids, unbound hydrogen, stress in a-Si:H films and their stability could indeed be a rewarding exercise.

4.9 Effect of Nitrogen Dilution

There exist many reports which state that incorporation of nitrogen into the DLC films reduces the residual stress without any significant change in the hardness values.[64,65] Shrinkage of the optical bandgap and the enhancement of conductivity are the other two related effects of nitrogen incorporation in DLC films. In the present investigation few films were deposited by introducing N_2 in the FAB source along with C_2H_2. These films were deposited at different applied power to the FAB source keeping other parameters (N_2 partial pressure, chamber pressure, gas flow rates) unchanged. **Figure 4.21** shows the properties of N_2 diluted DLC films as also those grown without any dilution at different powers. It is evident from this figure that the stress, hardness, unbound H_2 and carbon co-ordination numbers are more for the undiluted DLC films than N_2 diluted DLC films. From this figure it is also becoming clear that with the increase of the applied power to the FAB source, different properties under consideration are enhanced for N_2 diluted films, similar to the behaviour that is observed for undiluted films. For N_2 diluted films the hydrogen content has been found to be low as observed from both ERDA and FTIR measurements.

4.10 Stress Relief Behaviour of DLC Films

During the present investigation it has often been observed that films grown on the glass substrates which were more than 0.5 μm thick started delamination soon after they were brought out of the reactor or soon afterwards. This was more pronounced for RF self bias grown films. The stress relief behaviour of DLC films has been reported to have the characteristic morphology of sinusoidal buckling propagation. Weissmantel and co-workers[66,67] first reported sinusoidal stress relief patterns in DLC films on glass and NaCl substrates. Nir[68] investigated the shapes of stress relief patterns such as *sinusoidal buckling, straight cracking, strings of beads* and *cracking after buckling*. A qualitative dependence of the dimension of the buckling pattern with the film thickness has also been established. Estimating the elastic energy of the wrinkled films it is possible to determine the Young's modulus, internal strain and adhesion energy between the films and the

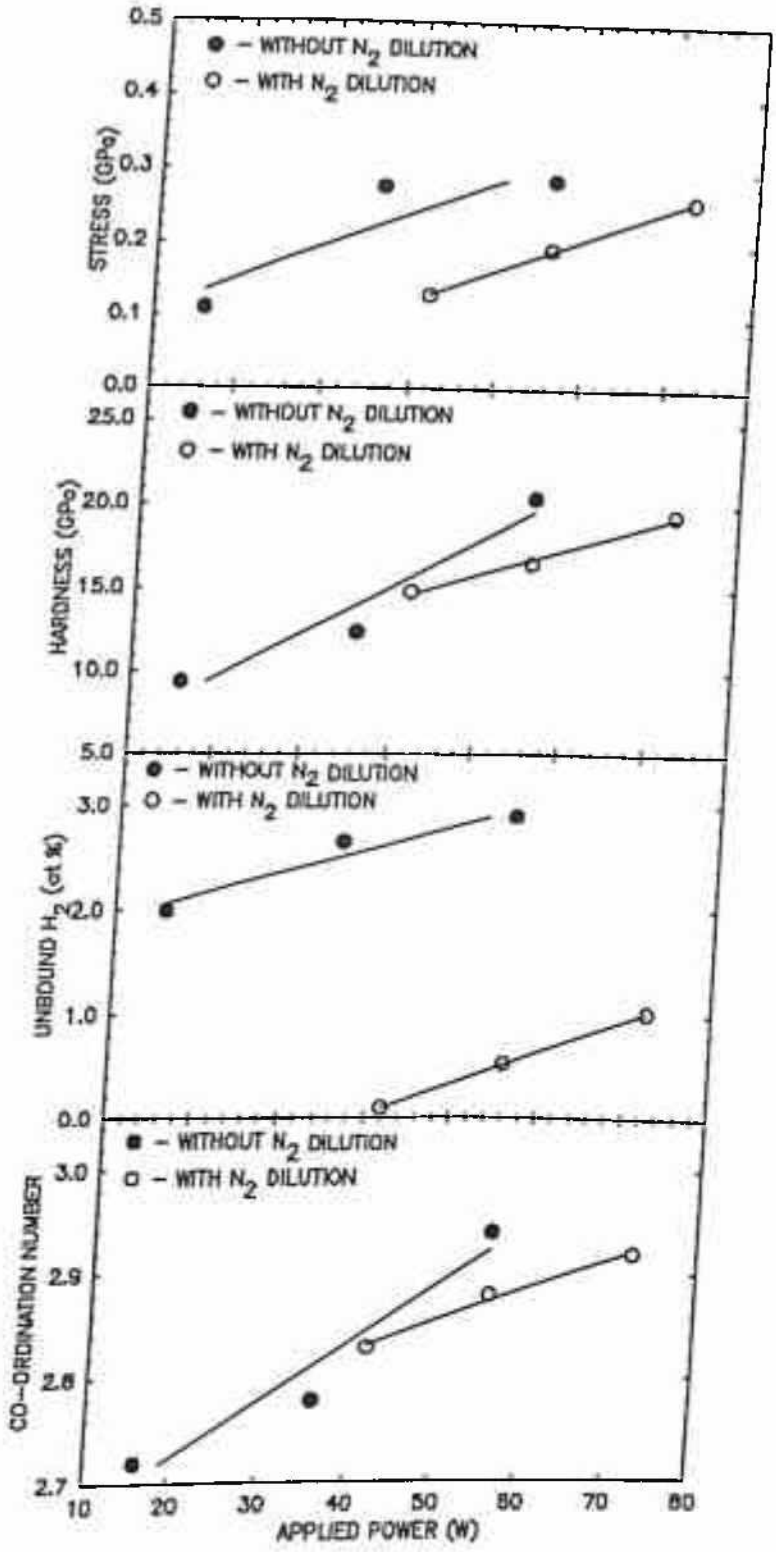

Fig. 4.21 Properties of N_2 diluted DLC films as also those grown without any dilution at different power applied to the FAB source

substrate from the size and shape of the wrinkles.[69,70] J. Seth *et al.*[71] also observed stress relief behaviour in DLC films. They observed that soft films buckle and terminate via wavy wrinkles while harder films crack after buckling. Two new stress relief patterns for DLC films, namely *flaking* and *blistering*, were observed by them. This type of behaviour has also been observed in the present study for FAB grown films as shown in **Plate 4.1 - 4.6**. Stress relief patterns have also been studied for nitrogen diluted films during the present investigation.

Plate 4.1 Sinusoidal buckling wave stress relief pattern of DLC film

The evolution of the stress relief pattern during the present investigation was observed on DLC films with an optical microscope and the following general behaviour was found.

(i) Stress relief and the buckling or cracking process usually begin some time after exposure to air at atmospheric pressure and are accelerated greatly by a high humidity.

(ii) In most cases, buckling or cracking starts at the film edge or at defects. It has been mentioned that at the film edge stress values are about four times higher than in the bulk of the film.[72]

(iii) The buckling propagates by spreading from a new centre and not by generation of new buckling defects.

(iv) The buckling usually develops in a direction perpendicular to the scratches on the film and other defects.

(v) The buckling propagates with a characteristic width.

(vi) After propagating a characteristic distance, the buckling undergoes a change in the propagation direction and branching.

Plate 4.2 Total delamination of DLC film

Plate 4.1 shows the sinusoidal buckling wave, observed on the DLC films on glass substrates having thickness ~0.5 μm. As shown in the plate the buckling waves start at the defects.

A clear tendency of the branching of the waves has also been observed. As the films became thicker and time elapsed, the distinct buckling wave could not be seen and the failure mode proceeded via branching-buckling '*fronts*', which lead to the total delamination and wrinkling of the films, as shown in **Plate 4.2**. **Plate 4.3** shows that the sinusoidal cracking is mixed with sinusoidal buckling, which is coarsened after it covers the whole area of the substrate. However, the cracking morphology of thicker films are different as shown in **Plate 4.4**. **Plate 4.5** shows the higher magnified view of the contents of the previous plate. **Plate 4.6** shows the stress relief behaviour of N_2 diluted DLC film (>2 μm thick), which reached a hardness value of ~20 GPa. This particular stress relief pattern shows hexagonal cracking propagation, having same branching and mixing behaviour like buckling wave. The cracking behaviour appears to be related to the high hardness of the films but the reasons behind the occurrence of this type of pattern has not yet been well understood. Again, so far it has not been reported in any DLC films as per the information available.

Plate 4.3 The sinusoidal cracking is mixed with sinusoidal buckling

The wavelength of the sinusoidal buckling was measured and an increase of wavelength with the thickness was also found, which is consistent with the reported literature.[73] The variation of wavelength from ~40 μm to ~60 μm with the increase of thickness from 0.5 μm to 0.8 μm have been observed.

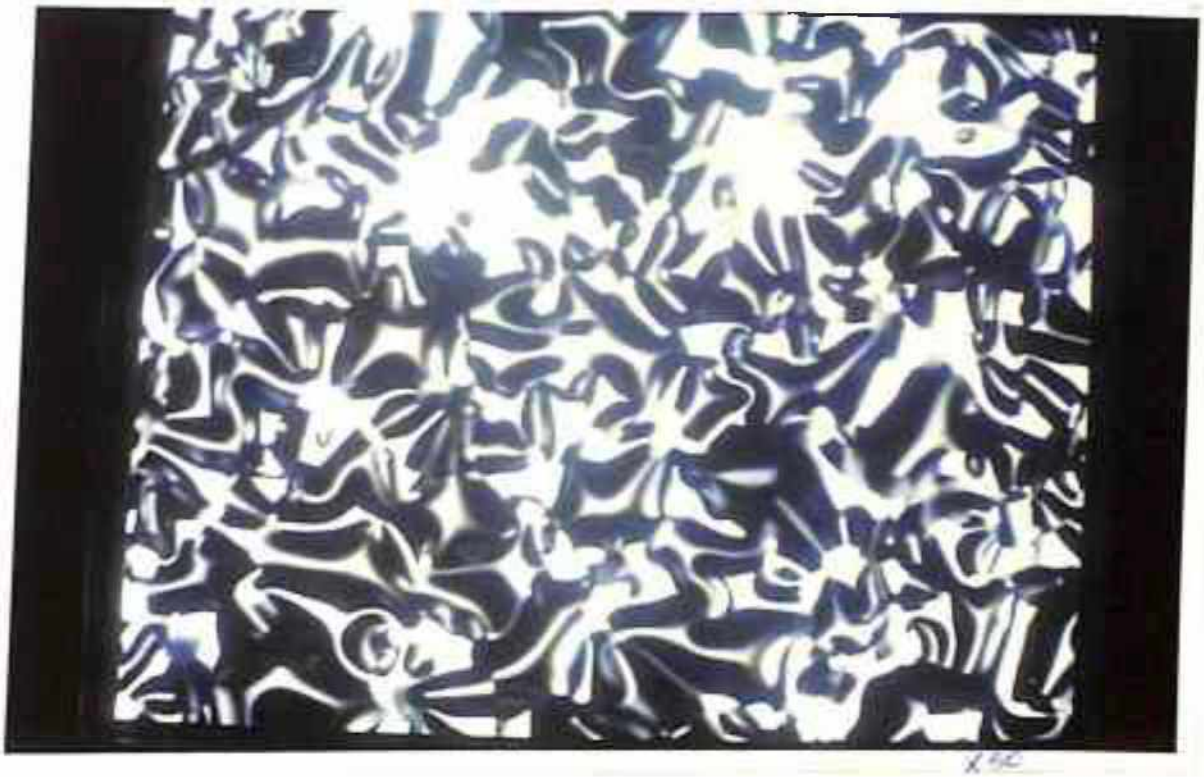

Plate 4.4 Stress relief pattern of DLC films having cracking morphology

The elastic modulus (Young's modulus) of these films has been estimated using the following relation[70]

$$\lambda^2 = \left(\frac{E\, 5\pi^2 t_f^2}{(1-\mu^2)\, 3\sigma} \right)$$

where λ is the wavelength of the sinusoidal buckling, E is the elastic modulus of the films, μ is the Poisson ratio of the film, σ is the internal stress and t_f is the film thickness. This relation basically

follows from Nir's[68] phenomenological analysis using plate theory and Lee *et al.*'s[73] experimental observation that the amplitude of the buckling wave is one fourth of the wavelength, regardless of the deposition conditions. This equation shows that the wavelength of sinusoidal buckling is proportional to the film thickness and is inversely proportional to the square root of the internal stress.

Plate 4.5 Magnified view of plate 4.4

For films thicker than 0.1 μm the residual stress of the film is generally found to be independent of the film thickness.[74] Hence the rate of increase of the wavelength with respect to the film thickness, $d\lambda/dt_f$, is proportional to the square root of $E/(1-\mu^2)\sigma$. The term $d\lambda/dt_f$ has been evaluated to be in the range of 66 to 82 for the DLC films grown at different applied power to the FAB source using C_2H_2 as the source gas. Using the corresponding stress value the elastic constant

$E/(1-\mu^2)$ was estimated to increase with the increase of applied power to the FAB source from ~1306 GPa at 16 W power to ~1530 GPa at 42 W power. Because the Poisson ratio is positive, these values are the lower limits of the elastic modulus E. These values are less than those reported by Lee *et al.*[73] and close to that of the diamond, 900 GPa.[75]

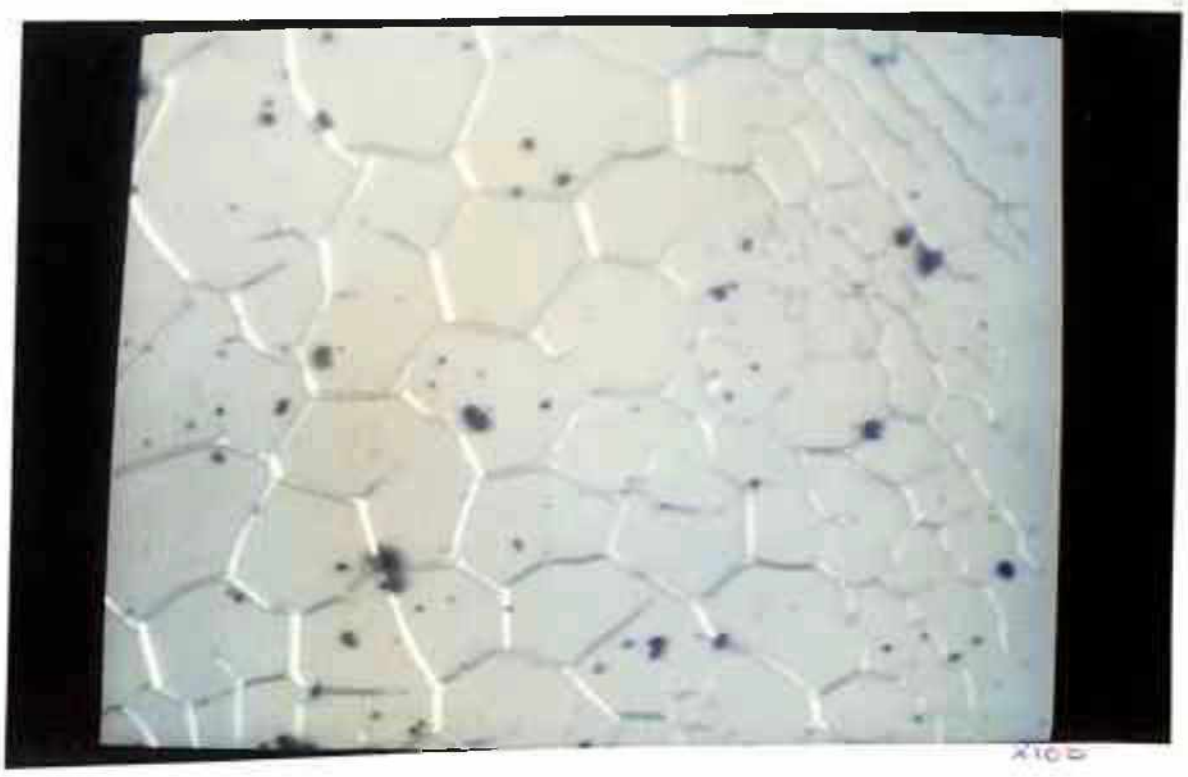

Plate 4.6 Stress relief pattern showing hexagonal cracking (N_2 diluted)

4.11 Part Summary

DLC films, were formed by a saddle field fast atom beam source to which various hydrocarbon gases (CH_4, C_2H_2) and vapours (C_6H_6) were introduced with different C/H ratio. The following important observations were made:

(1) Sufficiently thick DLC films could be formed by CH_4 as the feed gas utilising a saddle field source.[76]

(2) In films formed by CH_4, C_2H_2 and C_6H_6 as source gases/vapours, scaling of the deposition rate as expected, i.e. 4 to 8 times, which is observed is the case of RF self-bias deposition technique, could not be observed.

(3) For films grown at low source to substrate distance non-uniformity of the film thickness was observed. The reasons for that could be the following:

(i) Geometrical effect of low source to substrate distance and comparatively lower pressure of the chamber.

(ii) Change in the ratio of ions/neutrals at lower source to substrate distances.

(4) The values of characteristics energy of band tails (Urbach energy, E_o) evaluated from PDS measurements for DLC films grown using CH_4, C_2H_2 gases and C_6H_6 vapours are found to lie in the range 180 - 280 meV and this value decreases with the increase of carbon to hydrogen ratio in the hydrocarbon gases/vapours used.[77]

(5) The sharpness of band tails (E_o) is closely related to the density of states $N(E_F)$ in DLC films grown using hydrocarbon gases in the saddle field FAB source and the values of E_o and $N(F_F)$ are found to decrease with the increase of carbon to hydrogen ratio in the hydrocarbon gases/vapours used.[78]

(6) The sp^3/sp^2 ratio evaluated using two different techniques give different values. However, a clear trend indicating an increase in sp^3/sp^2 ratio is noticed when one goes from CH_4 to C_2H_2 gases and to C_6H_6 vapours.[79,80]

(7) The hydrogen concentration in these films determined from ERDA and IR analysis are found to be low and a correlation of the increase in the value of stress with unbound hydrogen is found to exist, as earlier predicted by Grill *et al*.[61,62]

(8) The elastic constant (Young's modulus) of the DLC films were evaluated from the sinusoidal buckling stress relief patterns and found to be in the range of ~1305 to ~1530 GPa.

It may be appreciated that the present exhaustive investigation study has clearly established the efficacy of the saddle field fast atom beam deposition technique over the more conventional RF asymmetric PECVD growth technique. The films by this technique are grown in an uncomplicated manner and indeed found to possess superior properties as far as the reduced stress values and maximisation of sp^3/sp^2 content is concerned. It may be mentioned here that Kruzelecky *et al*[35] in a related study found significant PL efficiency in DLC films grown by the saddle field technique. This together with Robertson's[81] theoretical analysis which shows that PL efficiency in DLC system can be significantly high, even with a high degree of defect density as compared to a-Si:H, indeed makes further detailed investigations, specifically involving PL studies, imperative.

4.12 References

1. R.V. Kruzelecky, and S. Zukotynski, in *Plasma Properties Deposition and Etching, Materials Science Forum*, eds. J.J. Pouch, and S. Alterovitz (Trans Tech, Aedermannsdorf, Switzerland) Vol. **140 - 142** (1993) p. 89.
2. J. Franks, *J. Vac. Sci. Technol.* A, 7 (1989) 2307.
3. A.H. McIlraith, Nature, **212** (1966) 1422.
4. A.H. McIlraith, *J. Vac. Sci. Technol.*, **9** (1972) 209.
5. R.K. Fitch, T. Mulvey, W.J. Thatcher and A.H. McIlraith, *J. Phys.* D, **3** (1970) 1399.
6. R.K. Fitch and G.J. Rushton, *J. Vac. Sci. Technol.*, **9** (1972) 379.
7. G.J. Rushton, K.R. O'Shea and R.K. Fitch, *J. Phys.* D, **6** 1167 (1973).
8. A.M. Ghander and R.K. Fitch, *Vacuum*, **23** (1973) 269.
9. J. Franks and A.M. Ghander, *Vacuum* **24** (1974) 489.
10. J. Franks, *J. Vac. Sci. Technol.*, **16** (1979) 181.
11. M. Khorossary and R.K. Fitch, *Vacuum*, **27** (1979) 159.
12. J. Franks, *Int J. Mass Spect. Ion Phys.*, **46** (1983) 343.
13. J. Franks, *Vacuum*, **34** (1984) 259.
14. F. Shimokawa and K. Nagai, *Nuclear Inst. & Methods in Phys. Res.* B, **33** (1988) 867.
15. F. Shimokawa and H. Kuwano, *J. Appl. Phys.*, **72** (1992) 13.
16. F. Shimokawa and H. Kuwano, *J. Vac. Sci. Technol.* A, **12** 194 (2739).
17. A.A. Voevodin, J.M. Schneider, C. Caperaa, P. Stevenson, and A. Matthews, *Vacuum*, **46** (1995) 299.
18. A. Dehbi-Alaoui, A.S. James and A. Matthews, *Surf. & Coat. Technol.*, **43/44** (1990) 88.
19. J. Smith, P. Holiday, A. Dehbi-Alaoui and A. Matthews, *Diamond and Related Materials*, **1** (1992) 355.
20. P. Holiday, A. Dehbi-Alaoui &A. Matthews, *Mat. Sci. Forum*, **102-104** (1992) 645.
21. Y. Bounouh, M.L. Theye, A. Dehbi-Alaoui, A. Matthews, J. Cernogora, J.L. Fave, C. Colliex, A. Gheorghiu and C. Senemaud, *Diamond and Related Materials*, **2** (1993) 259.
22. Y. Bounouh, M.L. Theye, A. Dehbi-Alaoui, A. Matthews, and J. P. Stoquert, *Phys. Rev.* B., **51** (1995) 9597.

23. A. Dehbi-Alaoui, B. Ollivier and A. Matthews, Proc. 11th Conf. *Vacuum* Metallurgy, Paris, 1992, p. 221.

24. J.K. Walters, P.J.R. Honeybone, D.W. Huxley, R.J. Newport and W.S. Howells, *J. Phys.:Condense. Matter*, **5** (1993) L387.

25. J.K. Walters, P.J.R. Honeybone, D.W. Huxley, R.J. Newport and W.S. Howells, *Phys. Rev.* B, **50** (1994) 831.

26. J.K. Walters, R.J. Newport, W.S. Howells and G. Bushnell-Wye, *J. Phys.:Condense. Matter*, **8** (1996) 4739.

27. J.K. Walters, C.D. Algar, T.M. Burke, J.S. Rigden, R.J. Newport, G. Bushnell-Wye, W.S. Howells, S. Sattel, M. Weiler and H. Ehrhardt, *J. Non-Cryst. Solids*, **197** (1996) 41.

28. J.K. Walters and R.J. Newport, *J. Phys.:Condens. Matter*, **7** (1995) 1755.

29. P.J.R. Honeybone, R.J. Newport, J.K. Walters, W.S. Howells and J. Tomkinson, *Phys. Rev.* B, **50** (1994) 839.

30. J.K. Walters, R.J. Newport, S.F. Parker and W.S. Howells, *J. Phys.:Condense. Matter*, **7** (1995) 10059.

31. C. Jager, J. Gottwald, H.W. Spiess and R.J. Newport, *Phys. Rev.* B, **50** (1994) 846.

32. T.M. Burke, D.W. Huxley, R.J. Newport, G. Bushnell-Wye and J. Franks, *Mat. Res. Soc. Symp. Proc.*, **270** (1992) 457.

33. J. Mayers, T.K. Burke and R.J. Newport, *Rutherford Appleton Laboratory Report*, RAL-93-052 (July 1993)

34. Y. Bounouh, M.L. Theye, A. Dehbi-Alaoui, A. Matthews and J.P. Stoquert, *Phys. Rev.* B, **51** (1995) 9597.

35. R.V. Kruzelecky, C. Wang and S. Zukotynski, *Mat. Res. Soc. Symp. Proc.*, **334** (1994) 537.

36. P.K. Lim, F. Gaspari, S. Zukotynski, T. Bilgildeyeva, in *BAPSMAR97* (Abstract).

37. T. Allen, W. Chan, F. Gaspari, E. Moreno and S. Zukotynski, in *BAPSMAR97* (Abstract).

38. P. Koidl, C. Wild, R. Locher, and R.E. Sah in *Diamond and Diamond-Like Films and Coatings*, eds. R.E. Clausing *et al.* (Plenum Press, New York) (1991) p. 243.

39. L.P. Anderson, S. Berg, H. Norstrom, R. Olaison and S. Towta, *Thin Solid Films*, **63** (1989) 155.

40. *Diamond and Diamond-Like Films and Coatings*, eds. R.E. Clausing *et al.* (Plenum Press, New York) (1991).

41. D.A. Anderson, Philos. Mag., **35** (1977) 17.

42. W. Paul, J. Non-Cryst. Solids, **35** (1980) 929.

43. B. Meyerson and F.W. Smith, *Solid State Commun.*, **34** (1980) 531.

44. K.D. Mackenzie, P.G. Lecomber and W.E. Spear, *Philos. Mag.* B, **46** (1982) 377.

45. M.A. Lampert and P. Mark, *Current Injections in Solids*, (Academic, New York) (1970).

46. G.W. Nespurek and J. Sworakowski, *J. Appl. Phys.*, **51** (1980) 2098.

47. S.R.P Silva, G.A.J. Amartunga, *Thin Solid Films*, **253** (1994) 146.

48. J. Tauc in *Optical properties of Solids*, ed. F. Abeles (North-Holland, Amsterdam, 1970).

49. D. Das Gupta, F. Demichellis, C.F. Pirri and A. Tagliaferro, *Phys. Rev.* B, **43** (1993) 2131.

50. B. Dischler, A. Bubenzer and P. Koidl, *Appl. Phys. Lett.*, **42** (1993) 636.

51. M. Weiler, S. Sattel, T. Giessen, K. Jung, H. Ehrhardt, V.S. Veeraswamy and J. Robertson, *Phys. Rev.* B, **53** (1996) 1594.

52. T. Datta, J.A. Woollam and W. Notohamiprodjo, *Phys. Rev.* B, **40** (1989) 5956.

53. O. Matsumoto and T. Katagiri, *Thin Solid Films*, **146** (1987) 283.

54. F. McFecly, S. Kwalezyk, L. Ley, R. Cavil, R. Pollak and D. Shriley, *Phys. Rev.* B, **9** (1979) 5268.

55. J.C. Lascovich, R. Giorgi and S. Scaglione, *Appl. Surf. Sci.*, **47** (1991) 17.

56. J.C. Lascovich and S. Scaglione, *Appl. Surf. Sci.*, **78** (1994) 17.

57. Y. Mizokawa, T. Miyasato, S. Nakamura, K.M. Geib and C.W. Wilmsen, *J. Vac. Sci. Technol.* A, **5** (1987) 2809.

58. P.K. Lim, F. Gaspari and S. Zukotynski, *J. Appl. Phys.*, **79** (1995) 1.

59. B. Dischler, A. Bubenzer and P. Koidl, *Solid State Commun.*, **48** (1983) 105.

60. M.P. Needler, T.M. Donovan and A.K. Green, *Thin Solid Films*, **116** (1984) 241.

61. A. Grill and V. Patel, *Diamond Films Technol.*, **1** (1992) 219.

62. A. Grill and V. Patel, *Diamond and Related Materials*, **2** (1993) 1519.

63. A.H. Mahan, Y. Chen, D.L. Willimson & G.D. Mooney, *J. Non-Cryst. Solids*, **137-138** (1991) 65.

64. C.J. Trong, J.M. Siverten, J.H. Judy and C. Chang, *J. Mater. Res.*, **5** (1990) 2590.

65. O. Stenzel *et al*, *Phys. Stat. Solidi*, **140** (1993) 179.

66. C. Weissmantel, C. Schure, F. Froglich, P. Grau and H. Lehmann, *Thin Solid Films*, **61** (1979) L5.

67. C. Weissmantel, G. Reisse, H.J. Erler, F. Henny, K. Bewilogua, U. Ebersbach and C. Schure, *Thin Solid Films*, **63** (1979) 315.

68. D. Nir, *Thin Solid Films*, **112** (1984) 41)

69. N. Matuda, S. Baba and A. Kinbara, *Thin Solid Films*, **81** (1981) 305.

70. G. Gille and B. Rau, *Thin Solid Films*, **120** (1984) 109.

71. J. Seth, R. Padiyath and S. V. Babu, *J. Vac. Sci. Technol.* A, **10** (1992) 284

72. J.H. Lee, D.S. Kim, Y.H. Lee, B. Faraok, *Thin Solid Films*, **280** (1996) 204.

73. K. Lee, Y. Baik and K. Eun, *Diamond and Related Materials*, **2** (1993) 218.

74. J.W. Hutchinson, M.D. Thouless and E.G. Liniger, *Acta Metall. Mater.*, **40** (1992) 295.

75. R. Kieffer and F. Benesovsky, in *Kirk-Othmer Encyclopedia of Chemical Technology*, ed. M. Grayson, (Wiley, New York) vol. 4, (1978) p. 480.

76. O.S. Panwar, D. Sarangi, Sushil Kumar, P.N. Dixit and R. Bhattacharyya, *J. Vac. Sci. Technol.*, **13** (1995) 2519.

77. D. Sarangi, O.S. Panwar, C. Mukherjee, Sushil Kumar and R. Bhattacharyya in *Thin Film Characterisation & Applications*, eds. Sa.K. Narayandas *et al.* (Allied Pub. Ltd., New Delhi) (1996) p. 314.

78. D. Sarangi, O.S. Panwar and R. Bhattacharyya in *Semiconductor Devices*, eds. V. Kumar *et al.* (Narosa Pub. House, New Delhi) vol. II (1998) p. 1251.

79. O.S. Panwar, D. Sarangi, B.R. Mehta and R. Bhattacharyya in *Semiconductor Devices*, ed. K. Lal (Narosa Pub. House, New Delhi) (1996) p. 424.

80. D. Sarangi, O.S. Panwar, Sushil Kumar and R. Bhattacharyya in *XX Nat. Conf. of the Microscope Soc. of India*, Calcutta, India, Dec. 1996 (Abstract).

81. J. Robertson, *J. Non-Cryst. Solids*, **198-200** (1996) 615.

Chapter V

Filtered Fast Atom Beam Deposition of DLC Films

5.1 Introduction

In the previous chapter (IV) a review of the saddle field fast atom beam (FAB) sources that are now available and their potential for use in growing smooth diamond like carbon (DLC) films has been presented followed by an account of further work undertaken by the researcher. In this chapter, first an analysis of the beam coming out from the FAB source will be made followed by a characterisation study of the films so grown. It will be seen through this characterisation study that a completely novel technique has been found to deposit DLC films, simultaneously by neutral and ionic radicals. The difference in the properties of the two types of films so formed has, subsequently, been carefully studied.

It is to be emphasised that the beam coming out of the FAB source is not fully neutral. A fraction of ionised species is also present along with the neutrals from the beam that comes out of the FAB source. Franks[1] in his experiment estimated the flux of the beam coming out of the FAB source to be of the order of 10 to 40 mA, under the source operation voltage of 0.8 kV to 3 kV. He also concluded, after etching rate study due to ion and neutrals, that neutral beams have energies and flux densities similar to ion beams. Atom Tech. Ltd. (Formerly Ion Tech. Ltd.) were the first to commercialise the atom beam sources. They now market different types of FAB sources, like B93, B95, FAB 110 series etc. with a range of capabilities.

Saied *et al.*[2] carried out a full characterisation study of the FAB source and the beam coming out of the FAB source used (FAB 11). The operation modes of a FAB source have been found to be similar to a saddle field ion source,[3] namely a *glow discharge mode* (~10^{-4} mbar), *transition mode* (lower than 10^{-4} mbar pressure) and *oscillation mode* (~10^{-5} mbar pressure). Anode current or discharge current increases linearly with the discharge voltage or anode voltage. Also they found an increase in the beam current density with decrease in pressure at a given value of discharge current. They found that the source operated more efficiently in the range 10^{-5} to 7×10^{-5} mbar. When operated in its most efficient mode, at low chamber pressure, the beam emitted from the source contained about 50% of the fast atoms. The source can be used to produce a beam composed almost entirely of fast atoms at higher chamber pressure, but this is of little consequence since under these conditions the atom beam flux is too low for most applications. The particle beam has a very broad energy distribution, typically producing 1100 eV FWHM (Full Width at Half Maximum) at 4 keV. They found the energy of the fast atoms measured from the spectra was the same as when a significant proportion of the beam consisted of ions.

Shimokawa *et al.*[4-7] made a series of characterisation studies of the beam coming out of a hollow cathode type FAB source. Using a magnetic field, perpendicular to the motion of electron, they were able to produce high power FAB sources. These types of FAB sources have large operating range (1×10^{-5} - 1×10^{-3} mbar). The beam coming out from this source has neutralisation coefficient ~ 95% and beam current density of ~0.1-1.0 mA/cm^2. The main results obtained by them are outlined below, as the may be subsequently referred to during the discussion of the experiments carried out in this laboratory.

A. <u>*Beam Current density*</u>: Beam current density increased with the increase of discharge current and was found to be 10 times higher with the application of a magnetic field. It

was also found by them that the beam current density increased with the increase of external magnetic field and operating pressure of the source.

B. *Beam energy*: The energy distribution of residual ions and fast atoms was studied by them using a retarding potential analyser (RPA). The comparison of these spectra showed that the energy distribution of the fast atoms was similar to the distribution obtained for the residual ions. The energy distribution of fast atoms was almost completely independent of the discharge voltage, discharge current, electrode configuration and feed gas. It was found to depend almost entirely on the gas pressure of the source. When the pressure was low, the main peak of the distribution coincided with the discharge voltage. When the pressure was high, the peak energy level was found to be about 25% of the discharge voltage and had a broader spectrum.

C. *Neutralisation coefficient*: The beam neutralisation coefficient found by them with the use of a magnetic field was more than 90%. The beam neutralisation coefficient was found to be almost independent of the magnetic flux density and source configuration. The neutralisation coefficient was found to be strongly dependent on the gas pressure and increased rapidly as gas pressure increased.

Voevodin *et al.*[8] found the flux coming out from the FAB source (B93) contains a significant percentage of ions. The ion composition of fluxes greatly depends on the distance from the source. In the near source region a level of ionisation of 80% was observed by them.

As documented in **Chapter IV**, during initial experiments using a FAB source the following two difficulties were encountered **1.** Non-uniformity in film thickness at lower source to substrate distances **2.** The deposition rate did not scale up for various source gases used, as reported by Zou *et al.*[9] for RF glow discharge deposited DLC films. It was speculated that the absence of uniformity in film thickness, observed at lower substrate to source distances, could as well be partly due to the different degree of neutralisation of

the beam coming out of the source. Some other reference was also found in the published literature in support of this hypothesis.[8] Subsequent experiments using Faraday cup measurements of neutralisation coefficient revealed that, indeed, inspite of what has been claimed by the manufacturer of the source, the degree of neutralisation is far from 100% and may vary a great deal depending upon the deposition conditions. In an attempt to filter the ionic radicals from the predominantly neutral flux, initial experiments with a stainless steel (S.S.) mesh (80% transparency) which was placed between the source and the substrate and to which a high positive voltage was applied, were performed. This arrangement appeared to filter out positive ionic radicals (believed to be the film forming precursors). However, a faint signature of the mesh could be seen on the films so deposited and these experiments were abandoned at this stage. Subsequently a deflector type arrangement to repel positive radicals (and, thus, filter the positive radicals) from the predominantly neutral beam was conceived. It may be mentioned at this stage that the application of a deflector to a saddle field source is not entirely new.[4-7] What is, however, novel about this approach is that an attempt to grow DLC films using the deflected beams has been made for the first time. This has allowed a comparison between the two types of films being grown this way to be made. Further careful investigations may possibly allow one to test the applicability of the models of growth of DLC which is discussed in terms of *subplantation*, *ion peening*, *ion stitching*[10,11] etc. The measured film properties suggest that basic mechanism of DLC growth, in these two cases, may, indeed, be different. At this point it would be pertinent to draw attention to a very important study by Sullivan *et al.*[12] who carried out a detailed investigation on ion and neutral beam treated TiO_2.

It is to be noted that this research was motivated by the desire to see whether saddle field fast atom beam growth of a-C:H can be optimised so as to produce a material of superior quality, i.e. to develop a benign process for the deposition of the active layers of electroluminescent (EL) devices capable of light emission in the visible spectral region, as reported by Zhang *et al.*[13] and Hamakawa *et al.*[14] Robertson's[15] theoretical treatment of the problem shows that photoluminescence (PL) intensity could indeed be

significant in a-C:H. This is because the PL of a-C:H follows basically the a-Si:H model, with gap states acting as non-radiative center, but PL occurs at much higher defect densities in a-C:H due to its shorter Bohr radius. The recent experiments[16,17] reporting as high as 97% sp^3 content of saddle field produced DLC films will, thus, go a long way in sustaining research efforts in this direction.

In the experiments documented in this chapter, both CH_4 and C_2H_2, having different carbon to hydrogen ratio in the feed gas, have been used. To access the material quality, systematic photothermal deflection spectroscopy (PDS) study and measurements of deposition rate, hardness and optical constants etc. were carried out.

It may be seen that no attempt has been made to investigate detailed structure and composition of the two type of films so formed by the surface analytical and other techniques as documented in **Chapter IV** for films grown under the normal operation of the source. One reason for this has been that such characterisation techniques are not readily available to the researcher. Most importantly since the researcher has been able to show significant difference in the macroscopic properties of these types of films, it is hoped that it will be taken up by some other researcher as a topic of research. It appears to be very rewarding to undertake photoluminescence studies of these films and to optimise the deposition process in a manner that one is able to get significant visible luminescence in these materials. These would, therefore, fall under the scope of future work to be done.

5.2 Experimental Procedure

The saddle field fast atom beam (FAB) source characterisation studies have been carried out using argon (Ar), methane (CH_4) and acetylene (C_2H_2) as source gases. The FAB source was mounted inside a 30 cm diameter conventional vacuum chamber having water cooling and gas feedthrough arrangements. The chamber was first evacuated to $\sim 10^{-5}$ mbar base pressure. Argon, CH_4 and C_2H_2 were allowed into the vacuum chamber

through a fine needle valve. The beam current (I) was measured using a Faraday cup made of Molybdenum target placed normal to the source at a distance of ~ 7 cm. The current density (J=I/S) was obtained by dividing the ion current (I) by the aperture area (S) of the Faraday cup. The schematic diagram of the Faraday cup used in the present investigation is shown in **Fig. 5.1**.

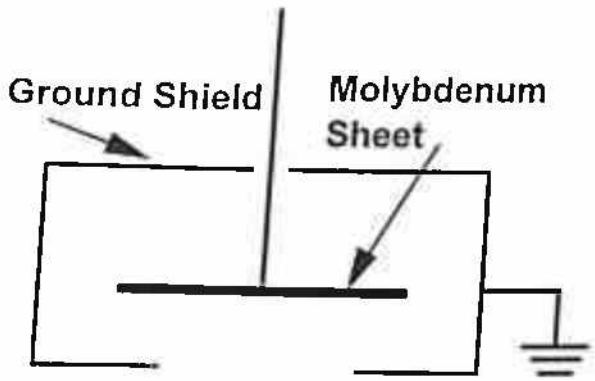

Fig. 5.1 Typical Faraday cup configuration

Deflector plates made of alluminium (5 cm × 14 cm) and separated by 4 cm were used to filter neutrals and ionic radicals as shown in **Fig. 5.2**. One deflector plate was grounded and a varying positive voltage was applied to the other deflector plate. The substrates were kept at position A, which is normal to the surface of FAB source (at a distance of 7.0 cm, r = 7.0 cm, $\theta = 90^{\circ}$) and also at position B, which was on the grounded plate of the deflector at a distance 2.7 cm from the FAB source (r = 3.4 cm, $\theta = 53^{\circ}$). It may be noted that with deflector OFF i.e. in the normal operation of FAB source, DLC films are formed in a mixed ion & neutral precursors environment.[18]

DLC films were prepared at different source voltages and current combinations i.e. at different power levels (discharge current × discharge voltage), keeping the pressure, distance and the applied deflection voltage constant, while using CH_4 and C_2H_2 as feed gases. Corning 7059 glass and both sides polished Si substrates were used to deposit DLC films. DLC films were deposited by applying 1.6 to 2.0 kV voltage to the deflector plate. (No glow discharge near the positive biased plate was observed at this voltage and

pressure). This enabled the ionic radicals to be deflected towards the grounded deflector plate, while the path of the neutral radicals remained unchanged.

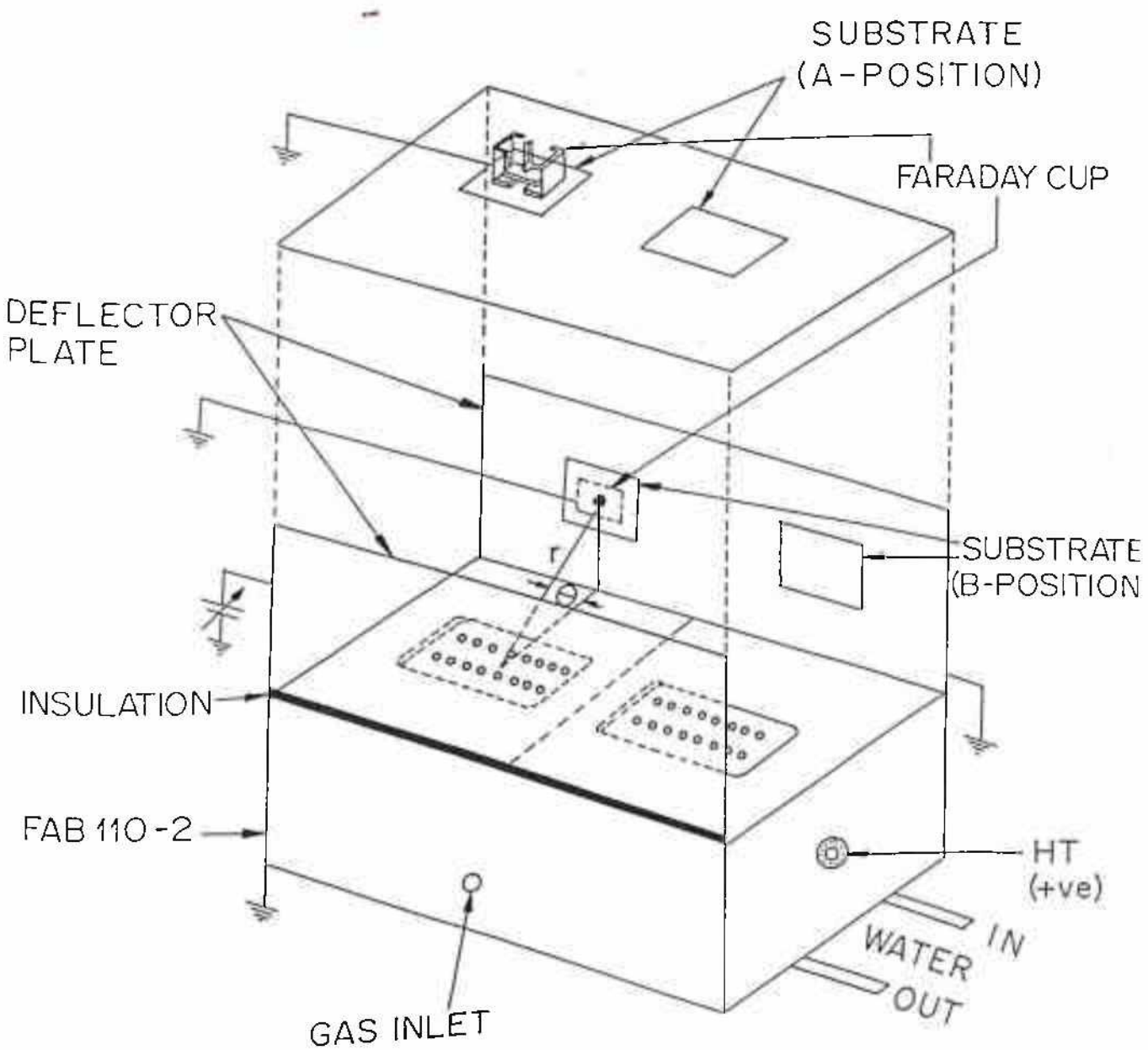

Fig. 5.2 Schematic diagram of the deflector arrangement used to separate out ion and neutral radicals coming out of a FAB source

5.3 FAB Source Characterisation

5.3.1 Operating Regions

The operational modes of the saddle field fast atom beam (FAB) source (FAB 110-2) studied in this present investigation are found to be similar to what has been reported by Saied *et al.*[2] namely a *glow discharge mode*, *transition mode* and *oscillation mode*.

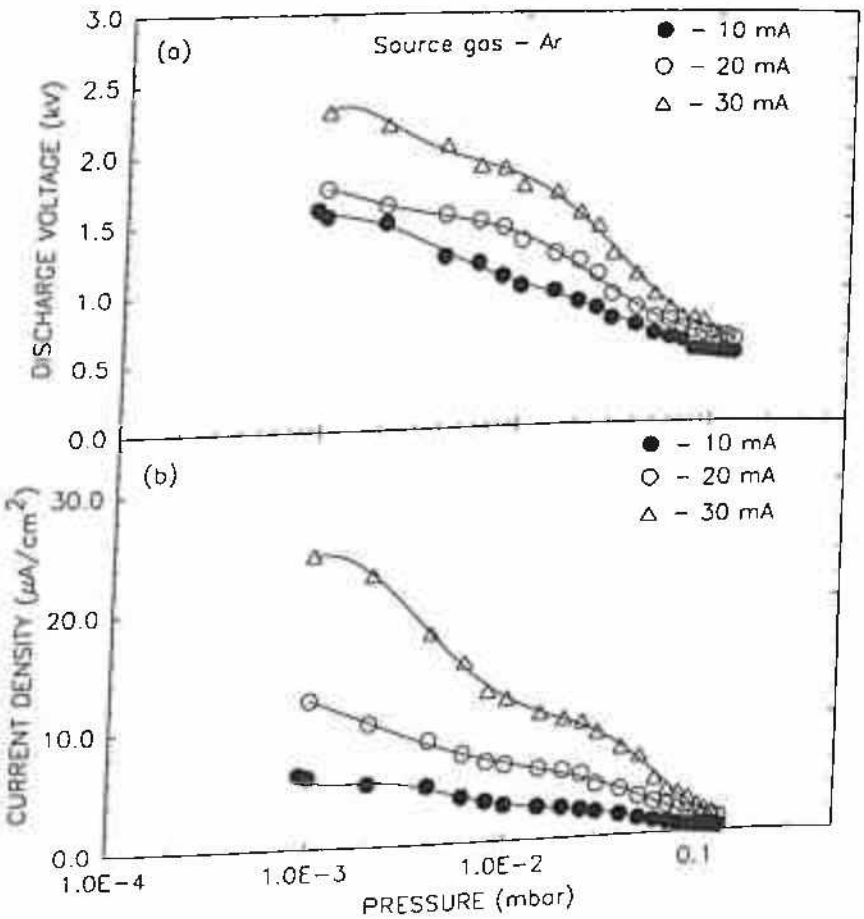

Fig. 5.3 Variation of (a) discharge voltage vs. chamber pressure and (b) beam current density vs. chamber pressure at a series of constant discharge current using Ar as source gas

The modes of operation of the FAB source have been studied as a function of pressure and are illustrated in **Fig. 5.3**. **Figure 5.3(a)** shows the variation of the discharge voltage with chamber pressure, for the three different discharge current settings

when Ar is used as the source gas. **Figure 5.3(b)** shows the variation of the beam current density with the chamber pressure for different discharge current settings for the same source gas.

The *glow discharge mode* was observed in the present experiments under low voltage (~0.5 kV) and high pressure (~10^{-1} mbar) condition, which is found to be higher than the pressure range reported by Saied *et al.*[2] for their experiments with a FAB-11 source. Electrons oscillations in the saddle field region, which is responsible for the efficient operation of the source, has been found to be reduced in this pressure range. This has predictably resulted in lower ionisation inside the source, and thus a lower beam current.

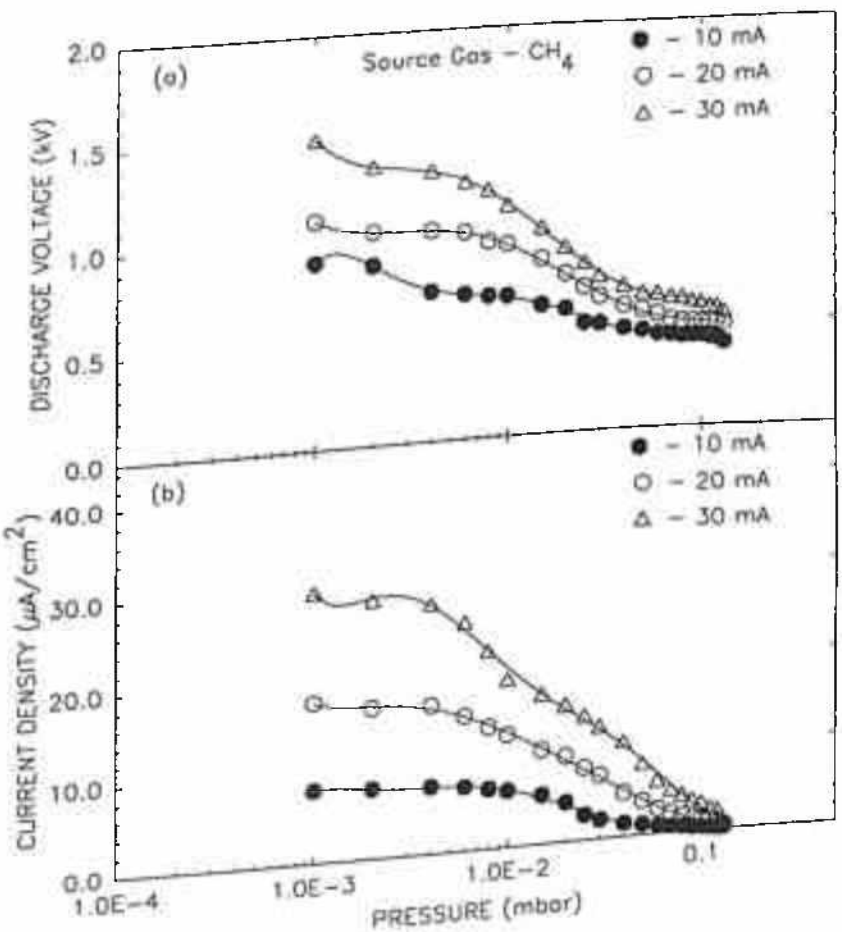

Fig. 5.4 Variation of (a) discharge voltage vs. chamber pressure and (b) beam current density vs. chamber pressure at a series of constant discharge current using CH_4 as source gas

The *transition mode* occurs at a slightly lower pressure (3-2 × 10^{-2} mbar), just below the glow discharge region. In this case the mean free path of the oscillating electrons increases, leading to a higher ionisation efficiency. This, in turn, results in an increase of the beam current density.

The *oscillation mode* has been found to occur in the pressure range below 10^{-2} mbar. In this case the oscillating mean free path and as well as the ionisation efficiency are high, leading again to an increase in the beam current density.

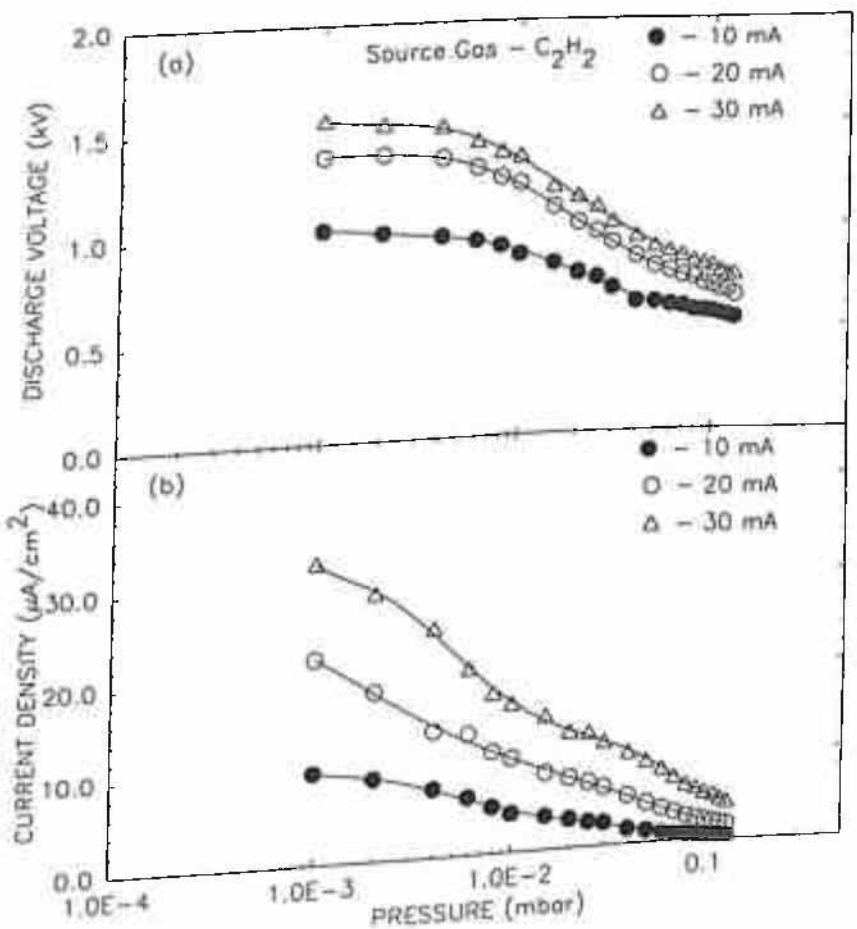

Fig. 5.5 Variation of (a) discharge voltage vs. chamber pressure and (b) beam current density vs. chamber pressure at a series of constant discharge current using C_2H_2 as source gas

Similar modes of operation were also observed when CH_4 and C_2H_2 were used as the source gases, as shown in **Fig. 5.4** and **Fig. 5.5**. Thus, selection of a suitable operating mode, on the basis of the desired application, is found to be a very important consideration.

5.3.2 Discharge Current vs. Discharge Voltage

In this section a detailed study of the variation of the discharge voltage (anode voltage, A_v) with the discharge current (anode current, A_c) of the FAB source used is reported. The variation of A_v with A_c is shown in **Fig. 5.6**. **Figure 5.6(a)** shows the variation of A_v with A_c when Ar gas was used as the source gas at 25×10^{-3} mbar pressure and at different flow rate conditions. It is evident from this figure that the value of A_v increased linearly with the value of A_c for all flow rate conditions and the value of A_v decreased with the increase of gas flow rate for a particular value of A_c. It is very important to mention at this stage that the power supply used to operate FAB source is a *current controlled device*. It, therefore, becomes possible, by keeping all other parameters constant, for the discharge voltage to be increased by suitably increasing the discharge current only. Therefore, the decrease of discharge voltage, at a particular discharge current, with the increase of gas flow rate is due to higher ionisation of the feed gas inside the FAB source. This can be seen to have effectively reduced the plasma resistance.

Figure 5.6(b) and **Fig. 5.6(c)** show the variation of A_v with A_c for CH_4 and C_2H_2 as source gases and having a similar set of operation conditions used in the case of argon discharge. The variation of A_v with A_c is also found to be linear in this case as well. However, in both these cases (CH_4, C_2H_2), dependence of discharge voltage on discharge current appears to have two distinct patterns, one for flow rates below 1 sccm and other above that. In case of argon discharge, the variations are distinct in all the three different flow rates. But in the above two cases of the hydrocarbon discharge, the discharge

voltage attains almost similar values for the flow rates of 2, 6 and 10 sccm. It seems that for gas flow rates above 2 sccm the ionisation of the gas inside the FAB source begins to saturate. It is, therefore, concluded that the FAB discharge using argon as a source gas and hydrocarbon gases as source gases are, indeed, different.

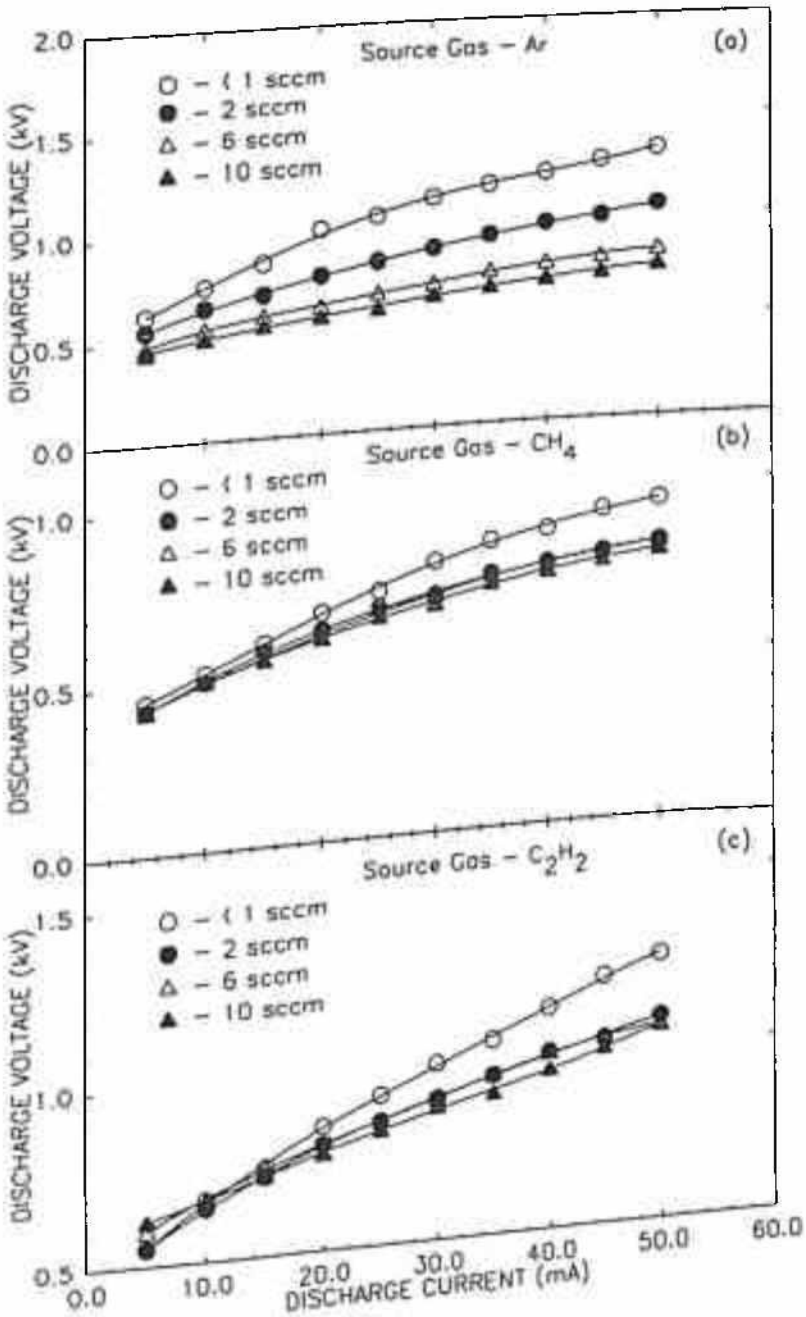

Fig. 5.6 Variation of discharge voltage vs. discharge current when (a) Ar was used as source gas, (b) CH_4 was used as source gas and (c) C_2H_2 was used as source gas at 25×10^{-3} mbar chamber pressure and at different gas flow rate conditions

Figure 5.7 (a) shows the variation of the discharge voltage with discharge current at gas flow rate less than 1 sccm and at two different pressures, 25×10^{-3} mbar and 5×10^{-3} mbar, using Ar, CH_4 and C_2H_2 as source gases. The value of A_v is strongly dependent on pressure and has been found to increase with the decrease of pressure. In this figure a clear distinction of the variation of A_v with A_c has been observed for the other source gases used. But as shown in **Fig. 5.7 (b-d)** any specific trend in this variation is not discernible. This indicates that, at higher flow rates, the variation is strongly dependent on the source gas used and it follows different trends for different sets of conditions.

From the above observations it is clear that discharge voltage not only depends on discharge current, it also depends on flow rate, pressure and type of source gas used. Therefore the term, applied power, which is equal to the product of discharge current and the corresponding discharge voltage, could be better used as a reference parameter to describe the properties of the films so made.

The variation of power developed with the discharge current is shown in **Fig. 5.8** in case of Ar, CH_4 and C_2H_2 as source gases at 2.5×10^{-2} mbar pressure and at different flow rates. From this figure it is clear that the developed power is limited by the flow rate. So, when Ar is used as source gas, a decrease in flow leads to a higher developed power (**Fig. 5.8 (a)**). But this is not true in case of hydrocarbons used as source gases as shown in **Fig. 5.8 (b)** and **Fig. 5.8 (c)** for CH_4 and C_2H_2 used as source gases. The power developed is found to be weakly dependent upon the flow rate at particular pressure and is almost similar at all flow conditions.

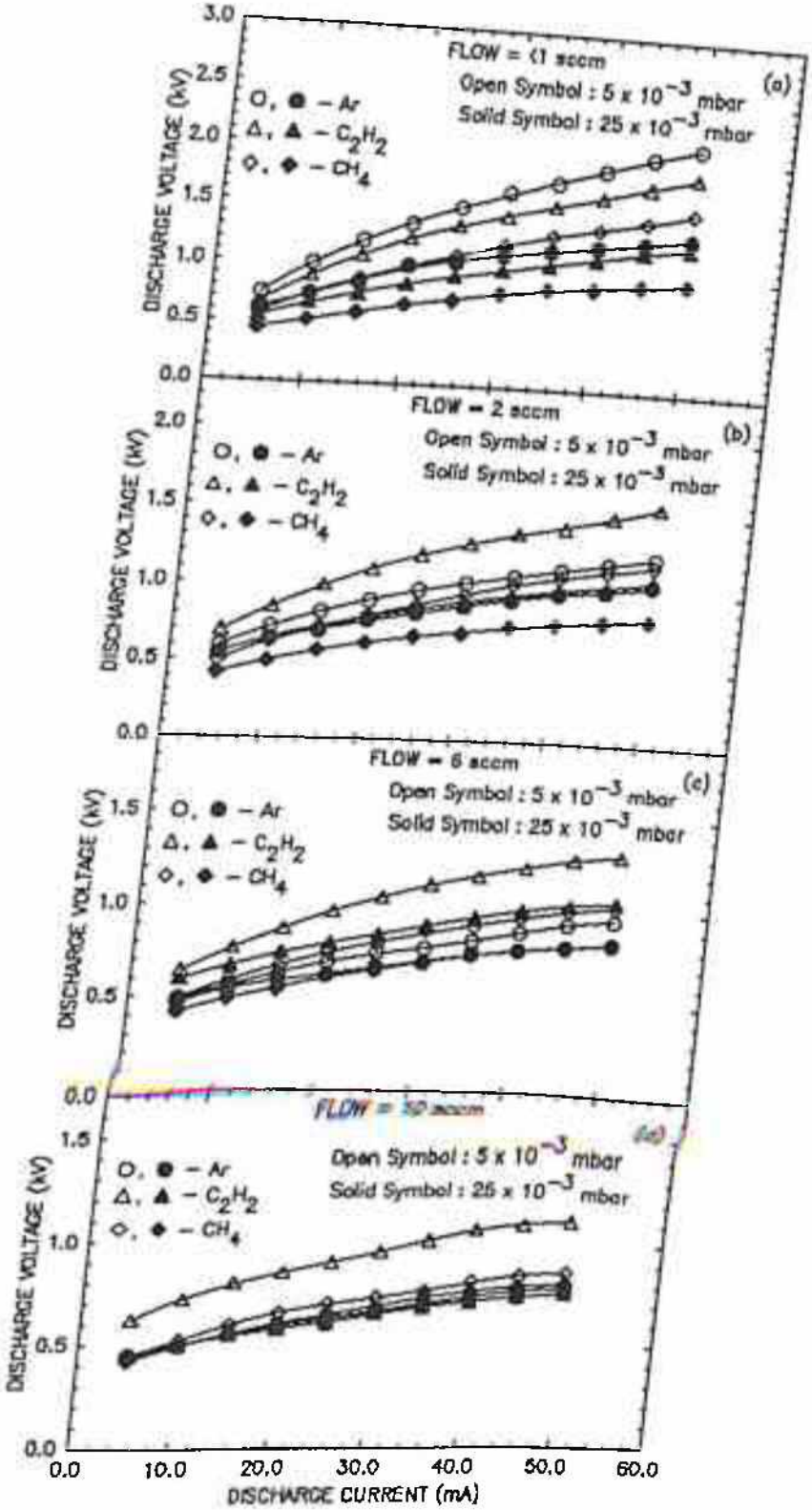

Fig. 5.7 *Variation of discharge voltage vs. discharge current at gas flow rate (a) < 1 sccm, (b) 2 sccm, (c) 6 sccm and (d) 10 sccm using Ar, CH_4 and C_2H_2 as source gases at two different chamber pressure*

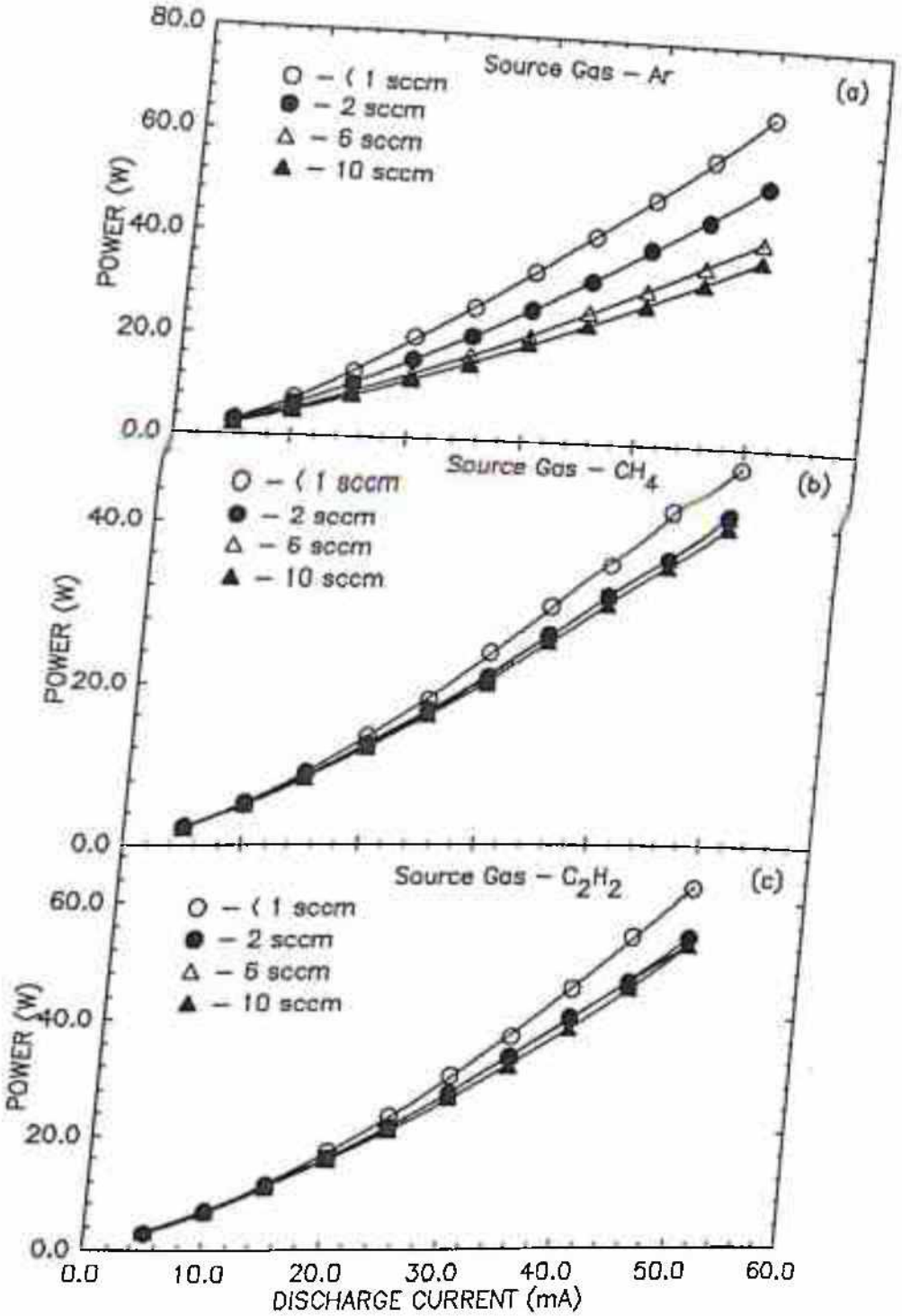

Fig 5.8 Variation of power developed vs. discharge current when (a) Ar was used as source gas, (b) CH_4 was used as source gas and (c) C_2H_2 was used as source gas at 25×10^{-3} mbar chamber pressure and at different gas flow rate conditions

5.3.3 Current Density Measurement

5.3.3.1 Normal Operation

The variation of current density (J) with the applied power for Ar as source gas is shown in **Fig. 5.9 (a)** for different set of flow conditions and at a pressure 2.5×10^{-2} mbar. The value of J depends on the applied power and is found to increase linearly with the power. The value of J was also found to increase with the decrease in flow of Ar, at particular power and Ar pressure used.

Fig 5.9 (b) and **Fig. 5.9 (c)** show the variation of J with the applied power when CH_4 and C_2H_2 are used as the source gases, at 25×10^{-3} mbar pressure and different flow rates of the hydrocarbon gases used. The value of J was also found to increase with the applied power. It is abundantly clear from these figures that, at a particular gas pressure condition, current density does not appear to depend so much on the flow rate of the hydrocarbon gas used. Therefore, while dealing with the hydrocarbon gases at a particular pressure, flow rate does not constitute a critical process parameter.

5.3.3.2 Measurements with a Deflector Arrangement

A deflector type arrangement was provided in front of the FAB source. Details about the deflector have been given under **section 5.2**.

The current density (J) of the beam carrying DLC film forming precursors was measured with the variation of deflector voltage using Faraday cups, which were placed at the two different positions inside the vacuum chamber. Specifically, these cups were placed at position A where r = 7.0 cm and $\theta = 90^{\circ}$ and at position B, where r = 3.4 cm and $\theta = 53^{\circ}$ from the center of the FAB source (**Fig. 5.2**). **Figure 5.10** shows the variation of beam current density (J) with the discharge current, in both deflector OFF and ON

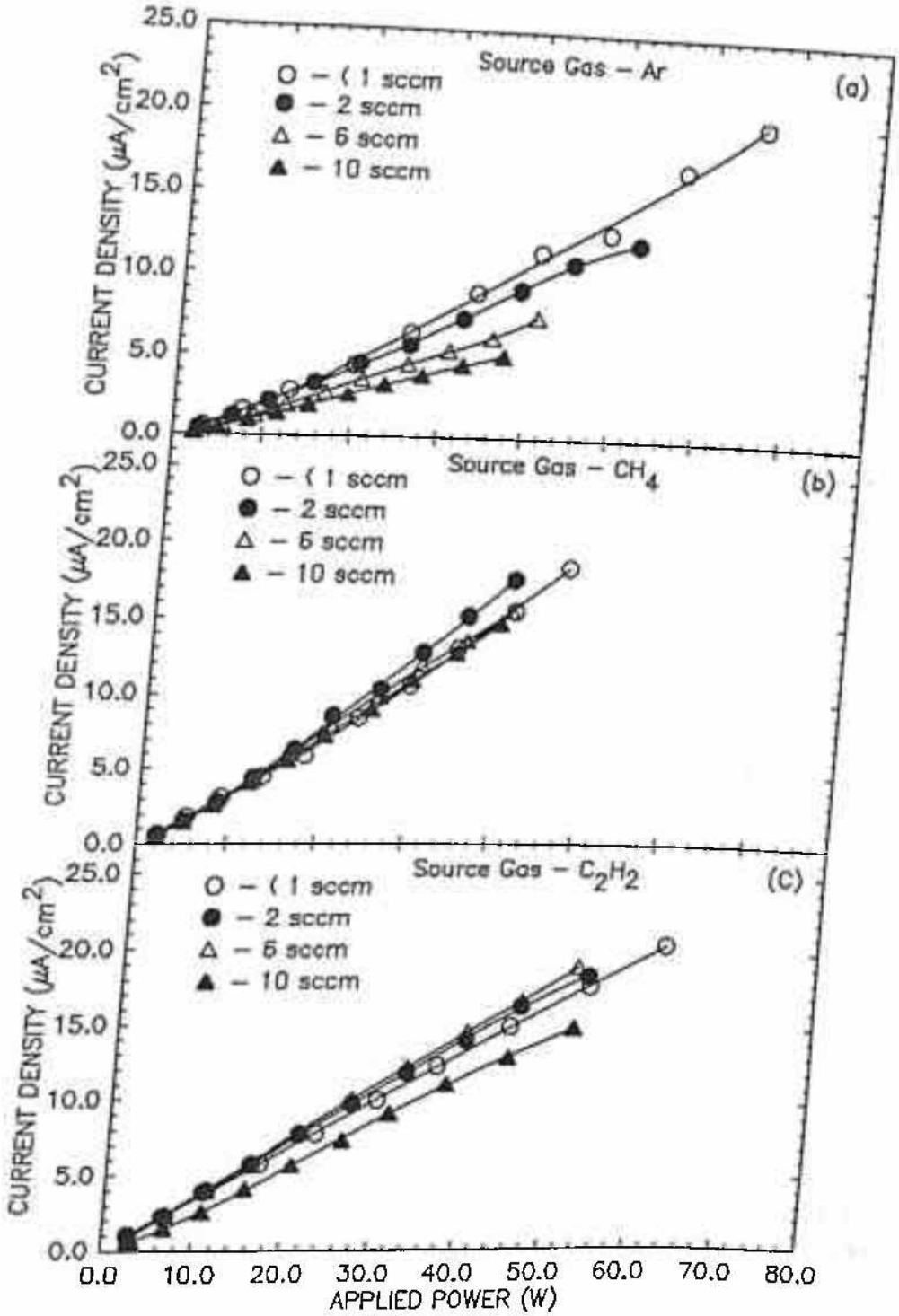

Fig 5.9 Variation of beam current density vs. applied power when (a) Ar was used as source gas, (b) CH_4 was used as source gas and (c) C_2H_2 was used as source gas at 25×10^{-3} mbar chamber pressure and at different gas flow rate conditions

conditions at two separate positions A and B. For this experiment Argon gas at 5×10^{-3} mbar pressure was fed to the FAB source. In all the cases studied, the value of J was found to increase with the increase of the discharge current. There was a sharp decrease in the value of J at position A when the deflector was switched ON. This implies that the beam coming out from the FAB source does not consist of neutrals alone, i.e., a fraction of ionised radicals are responsible for the formation of the beam. High positive deflector voltage (1.6 - 2.0 kV) deflects the positive ions away from A. Similarly, the value of J at position B increased sharply when the deflector was switched ON. In this case, the deflected ionic radicals contributed to the current. The position B was chosen after repeated search and it was found that only at that particular position the mean current density revealed a maximum.

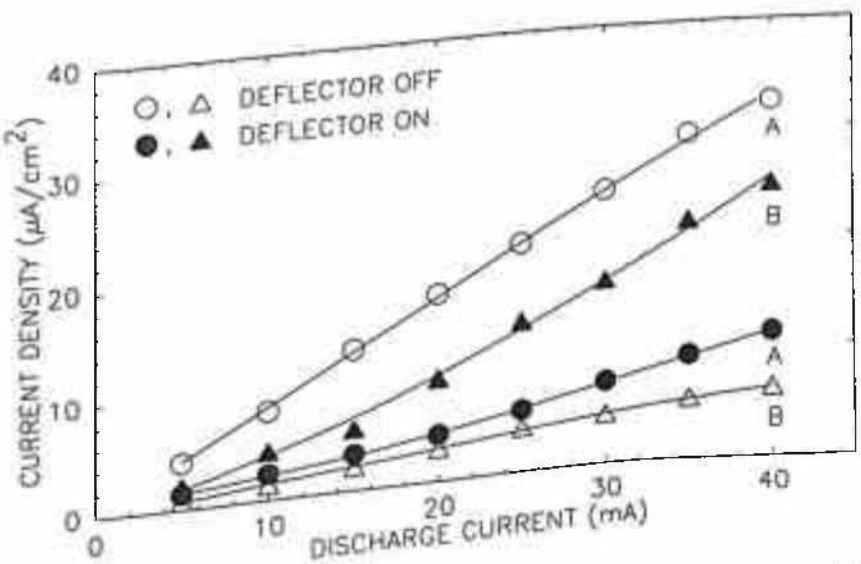

Fig. 5.10 Dependence of beam current density at positions A and B with deflector OFF and ON conditions and of discharge voltage with varying discharge current, using Argon beam at 5×10^{-3} mbar pressure

The variation of J vs. the deflector voltage at both A and B positions, using CH_4 as feed gas, at different applied powers to FAB source, is shown in **Fig. 5.11**. It was found that the value of J, in both the positions (A and B), increases with the increase of power applied to the FAB source, when the deflector is in the OFF condition. This current density is, however, small at position B and is believed to be primarily due to a

combination of ion and neutral precursors that may possibly be reaching position B at this pressure. At position A, the value of J is found to decrease with the deflector voltage, whereas, at position B, J increases with the deflector voltage. The value of J beyond 1.0 kV of the deflector voltage at position A is found to be small and this does not seem to change with the increase of deflector voltage, whereas, the value of J beyond 1.0 kV at position B increases with the increase of deflector voltage. This indicates that at position A, beyond 1.0 kV of deflector voltage, only neutral radicals are present, whereas, at position B only ionic radicals are present.

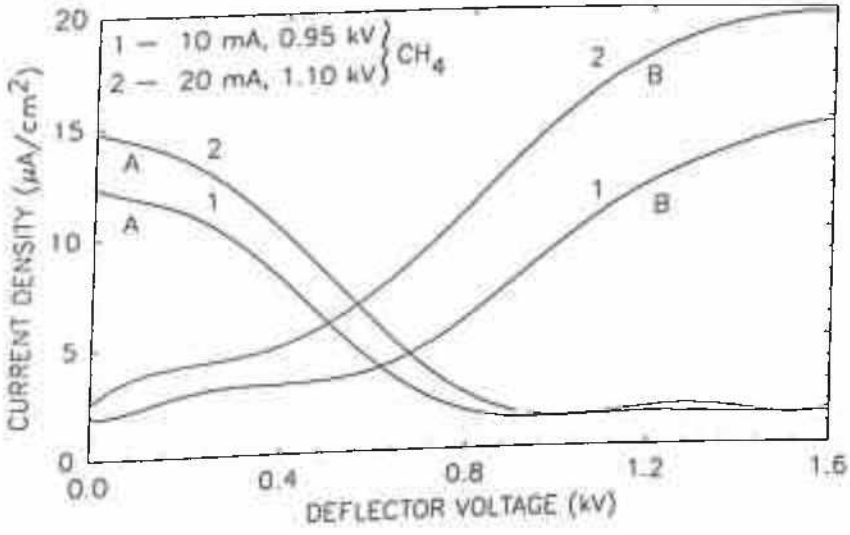

Fog. 5.11 Variation of beam current density vs. deflector voltage at position A and position B using CH_4 as the source gas, at two different conditions of source operation (CH_4 partial pressure ~ 5.0×10^{-3} mbar kept constant)

Figure 5.12 shows the variation of J with the deflector voltage at both A and B positions, using CH_4 and C_2H_2 gases, keeping almost similar conditions of discharge (10 mA, 0.95 kV and 4 - 5 $\times$ 10^{-3} mbar pressure). It was found that the value of J at position A increases at deflector OFF position when one switches from CH_4 to C_2H_2 gas. Similar behaviour was also observed at position B, but the value of J was found to be small during deflector OFF condition. Further, for both the gases the value of J was found to decrease with the deflector voltage. Also it was found to remain almost constant near the voltage (1.0 kV) applied to the FAB source. At high enough deflector voltage the current

recorded at A is most likely to be due to the secondary electrons emitted from Mo sheet due to the bombardment of energetic neutrals. The value of J at position B was found to increase with the deflector voltage for both the gases but when C_2H_2 gas was used, current density increased far more than when CH_4 gas was admitted to the FAB source. This, perhaps, is the direct evidence of an enhanced deposition rate for C_2H_2. Therefore, from the analysis of these data one can conclude that the DLC films deposited at position A is formed by neutral radicals and at position B by ionic radicals (at least under the deposition conditions of the present experiment).

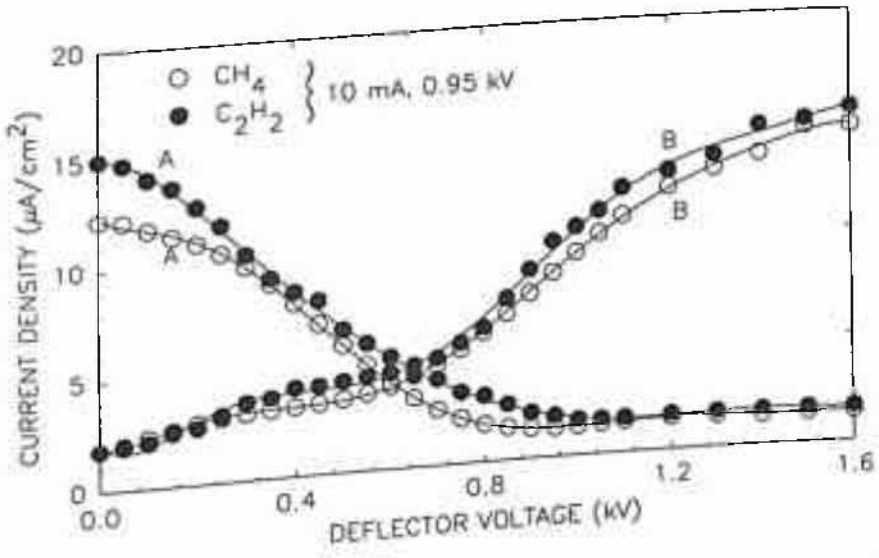

Fig. 5.12 Variation of beam current density vs. deflector voltage at position A and position B, using CH_4 and C_2H_2 as the source gases, at same conditions of source operation

5.3.4 Energy Distribution of Residual Ions

The energy distribution spectra (-dJ/dV) of residual ions was obtained by differentiating the current density (J) vs. deflector voltage (V) measured at position A. On comparing the energy distribution of ions so obtained with the published results of Shimokawa *et al.*,[5] for distribution of ions and neutrals coming out of their FAB source, it is speculated that the energy distribution of neutrals in the present case may also show a similar pattern to that obtained for ions.

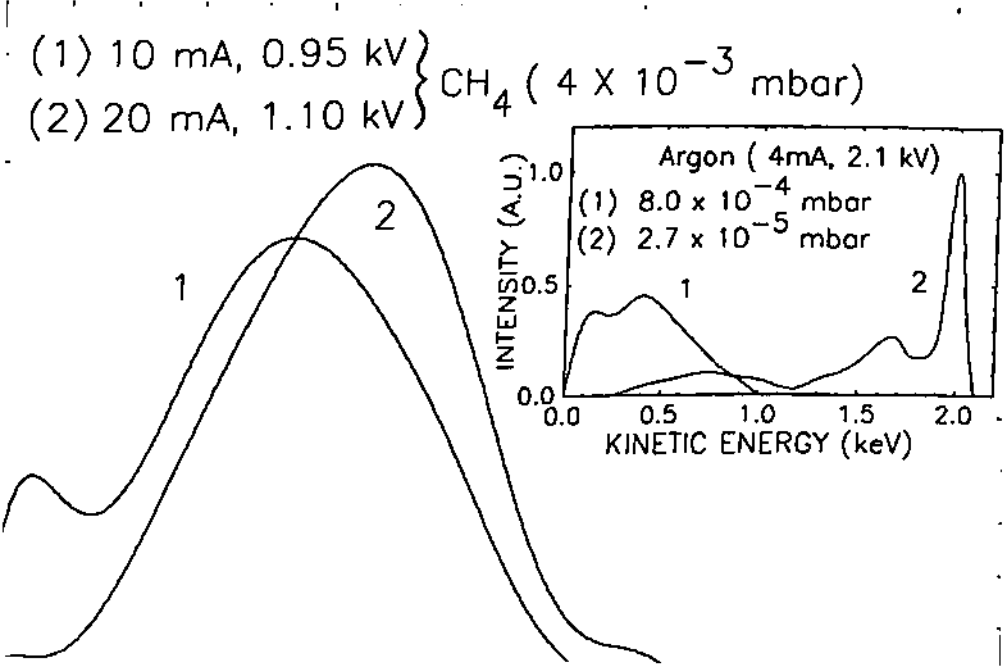
(1) 10 mA, 0.95 kV
(2) 20 mA, 1.10 kV
CH4 (4 X 10−3 mbar)
1
2
Argon (4mA, 2.1 kV)
(1) 8.0 x 10−4 mbar
(2) 2.7 x 10−5 mbar
INTENSITY (A.U.)
1.0
0.5
0.0
0.0
0.5
1.0
1.5
2.0
KINETIC ENERGY (keV)

experiment, it was not possible to operate the FAB source at elevated vacuum conditions, similar to that used by Shimokawa *et al*.[5] The important observation is that the beams coming out from the FAB source contains ions and neutrals of varying energies and maximum number are within the energy which is approximately half of the discharge voltage.

5.3.5 Beam Neutralisation Coefficient

The beam neutralisation coefficient of the FAB source was estimated by measuring the current in both the conditions i.e. deflector ON (deflector voltage = 1.6 kV) and deflector OFF (deflector voltage = 0 V) and assuming the following relation to be valid[7]

$$\eta = I_o(1+\gamma_i)/[I_o(1+\gamma_i)+\gamma_o(I-I_o)]$$

where η is the neutralisation coefficient, I and I_o are current recorded at position A when deflector voltage is 0 V (OFF) and 1.6 kV (ON), respectively (**Fig. 5.14**), γ_i is the yield of

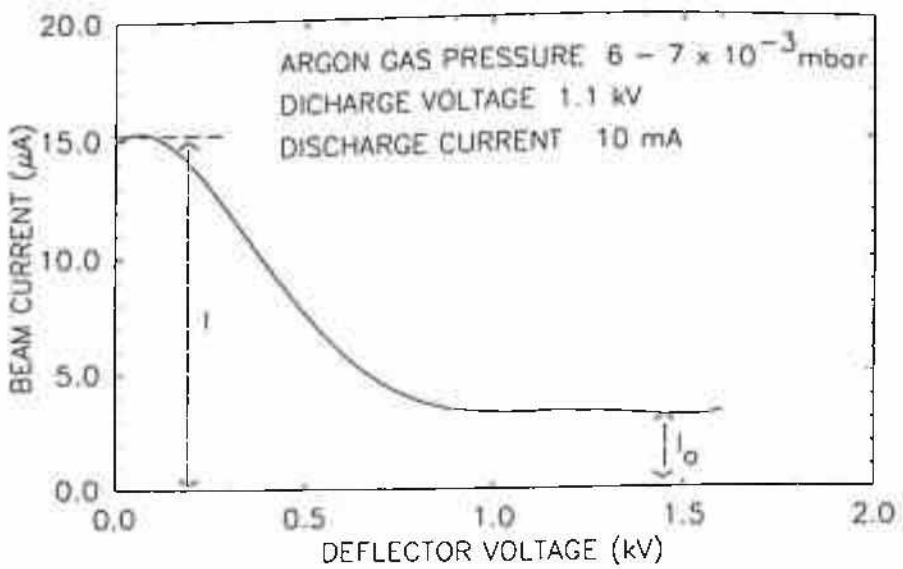

Fig. 5.14 Variation of the beam current vs. deflector voltage, I and I_o have been used to estimate beam neutralisation coefficient

the secondary electrons from the surface of the Mo target under the ion bombardment condition and γ_0 is the yield of the secondary electrons under energetic neutral particle bombardment. Argon was used for the estimation of beam neutralisation coefficient experiments. It may be mentioned that the energies of the ions and the neutrals coming out from the FAB source were assumed to be the same and this corresponds to the applied voltage of the FAB source. The neutralisation coefficient of the beam was estimated to be more than 90% and was found to be almost independent of the discharge current of the FAB source, as shown in **Fig. 5.15**.

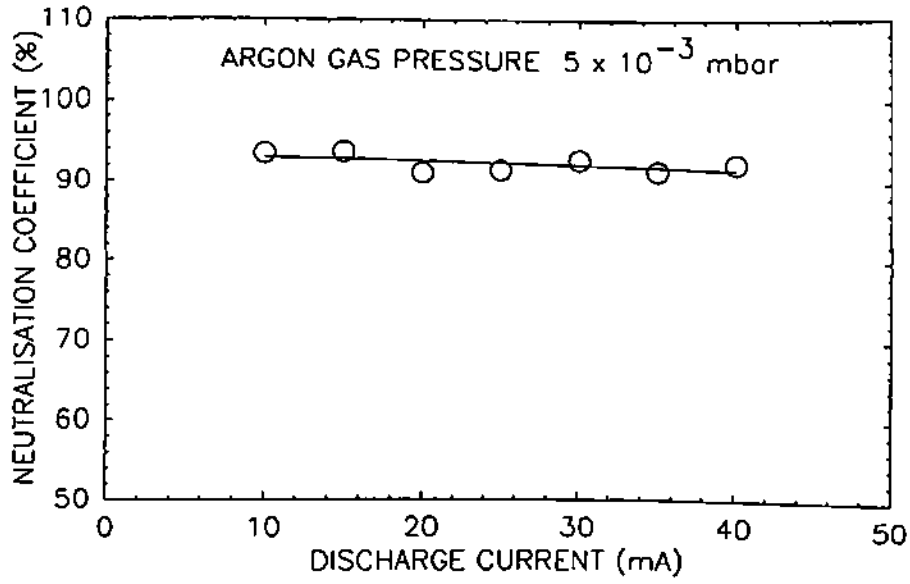

Fig. 5.15 Variation of the beam neutralisation coefficient vs. discharge current at chamber pressure 5×10^{-3} mbar

5.4 Filtered Saddle Field FAB Deposited DLC Films

In the preceding sections an analysis of the beams coming out of the FAB source to which a deflector was integrated, was carried out. It was found that ionic and neutral precursors could be filtered out and made to land at two different locations. The DLC films so formed were subsequently characterised. The results of these characterisation studies are presented below:

5.4.1 Deposition Rate

The variation of deposition rate (r_d) vs. power applied to the FAB source for the DLC films grown using ionic and neutral radicals of CH_4 and C_2H_2 gases is shown in **Fig. 5.16**. The r_d values of DLC films is found to increase with the increase of applied power to the FAB source, for both ionic and neutral radicals, and for both CH_4 and C_2H_2 deposited DLC films. The value of r_d as well as the rate of increase of r_d with increasing power, were found to be larger in the DLC films deposited by C_2H_2 gas than by CH_4 gas. As expected, the value of r_d is also found to be larger in the DLC films deposited by neutral radicals than the DLC films deposited by ionic radicals, assuming that both the sticking coefficient and dehydrogenation rates are comparable in case of neutral and ionised beam deposition processes. The value of r_d at position A (due to neutral radicals) was found to be ~ 3 times larger than that at position B (due to ionic radicals). This result appears to roughly correlate with the measured beam current density. It was found that beam current density at position B is nearly 2.6 times larger than the current density at position A. The current density measurements performed using these gases also confirms the difference in deposition rate of C_2H_2 and CH_4 deposited DLC films. The values of r_d for DLC film deposited using a mixture of ions and neutrals are found to be larger (discussed in **chapter IV**) than the values obtained using the filtered source of the present investigation, as expected.

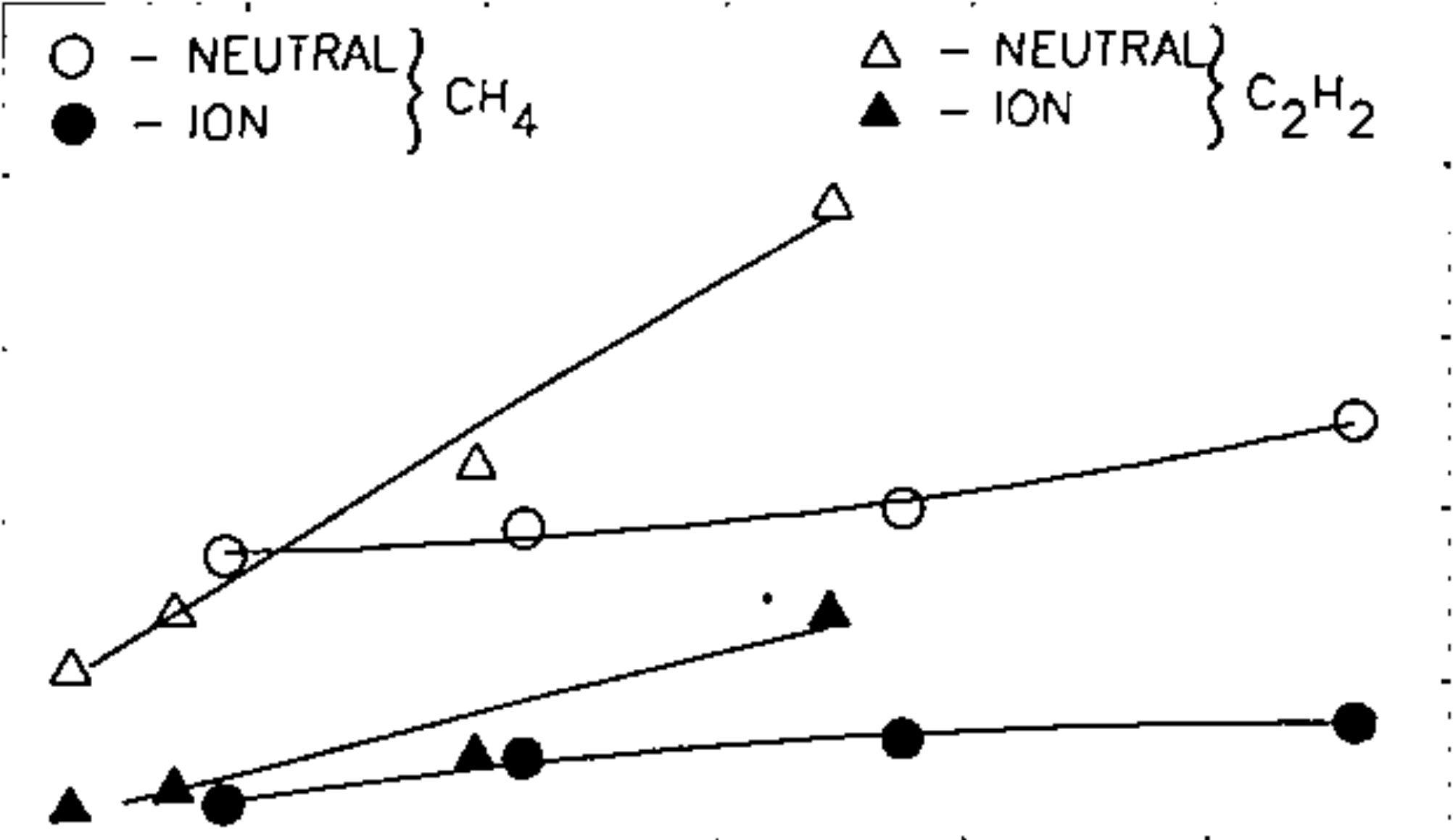
○ – NEUTRAL
● – ION
CH_4
△ – NEUTRAL
▲ – ION
C_2H_2

Earlier observations with FAB deposited DLC films by Franks[1] revealed that the deposition rate of C_2H_2 deposited films is 1.33 & 2 times more than C_4H_{10} and C_3H_8 deposited films, respectively. Similarly, Debli-Alaoui *et al.*[19] found that the r_d values of C_2H_2 deposited films are 1.28 times higher than C_4H_{10} deposited DLC films and 1.22 times less than C_3H_8 deposited DLC films. However, Zou *et al.*[9] found for DLC films formed by RF self bias deposition technique, four to seven times increase of r_d when C_2H_2 was used as feed stock as compared to CH_4. It may be noticed that carbon to hydrogen ratio of C_2H_2 is 4 times higher than CH_4. Therefore, based on this observations and similar observations of other workers in their experiments with FAB sources, the conclusion may be drawn is that in case of FAB based growth the scaling of r_d is considerably lower as compared to RF self bias technique, where one uses similar source gases. The reasons for this, however, is not at all clear and needs to be further investigated.

5.4.2 Hardness

Knoop hardness indenter equipped with Zwick 3212 instrument, at 50 gm load, has been used for evaluating the hardness values. **Figure 5.17** shows the variation of hardness vs. power applied to the FAB source, for the DLC films grown using ionic and neutral radicals of CH_4 and C_2H_2 gases. The hardness values are found to increase in both the cases with the applied power to the FAB source. The rate of increase is higher for the C_2H_2 deposited films than for the CH_4 deposited one. C_2H_2 deposited films show larger hardness values than CH_4 deposited films, which can not be explained at the present time. Again, the values of hardness is found to be less in case of ionic radicals deposited films than those using neutrals. It may be mentioned that the mean value of energy of the neutral radicals, participating in the formation of the DLC films, is estimated to be higher than those of the ionic radicals participating in the formation of the DLC films. This may account for the difference in the values of hardness in these two types of DLC films. The observation of harder films being formed by high energy beams

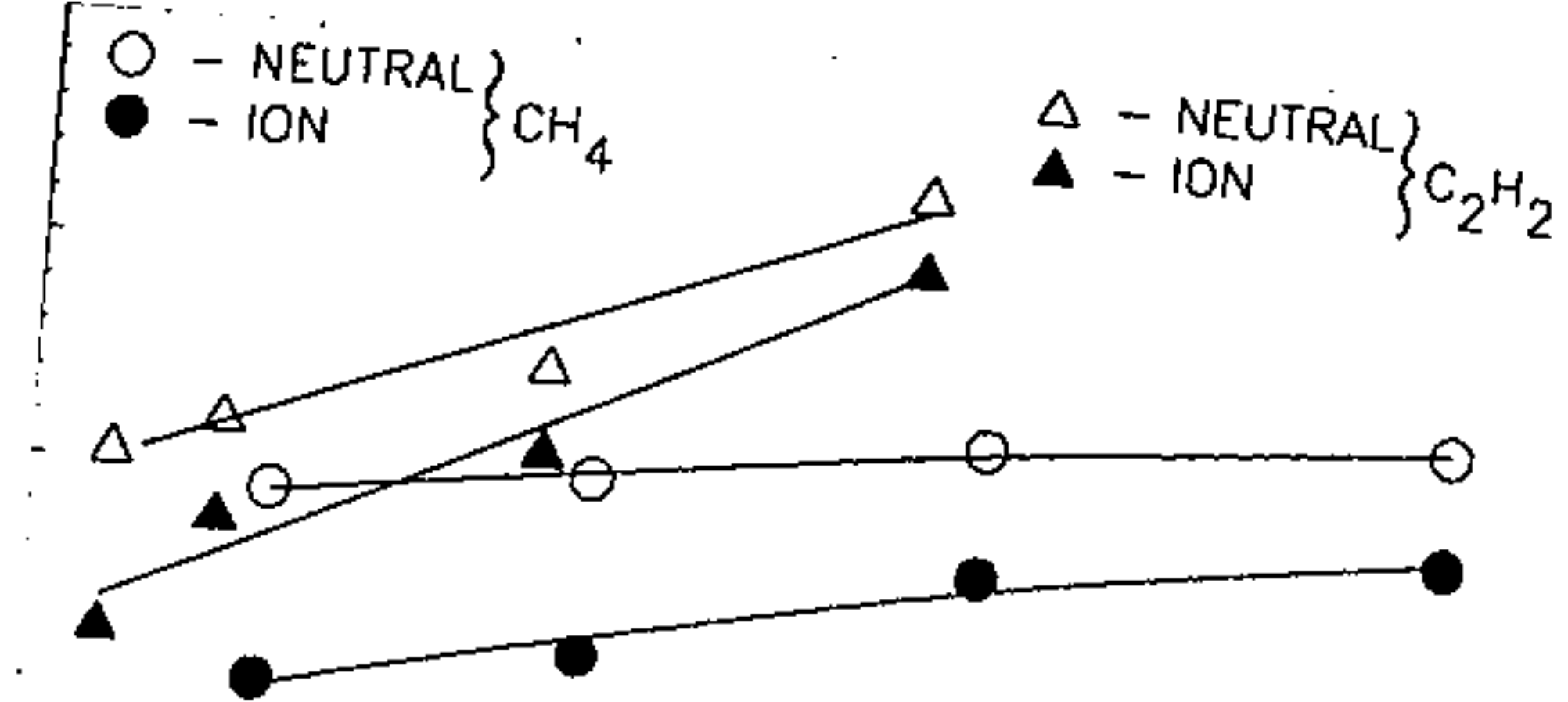
○ – NEUTRAL
● – ION
CH4
△ – NEUTRAL
▲ – ION
C2H2

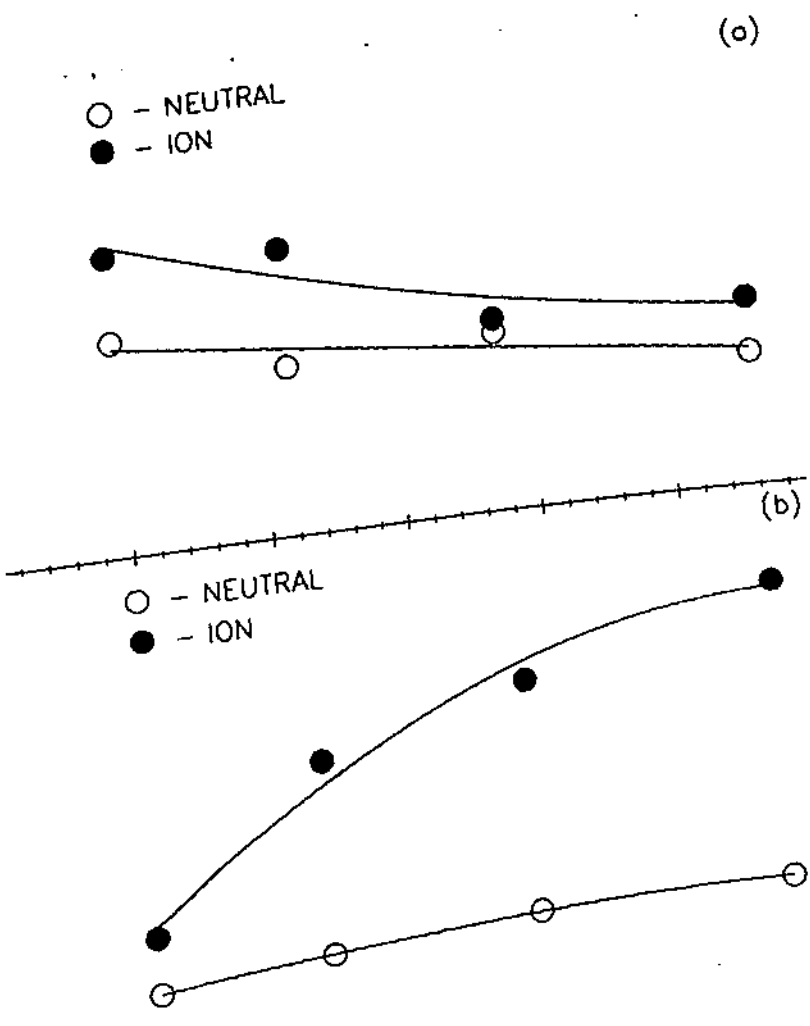
(a)
○ – NEUTRAL
● – ION
(b)
○ – NEUTRAL
● – ION

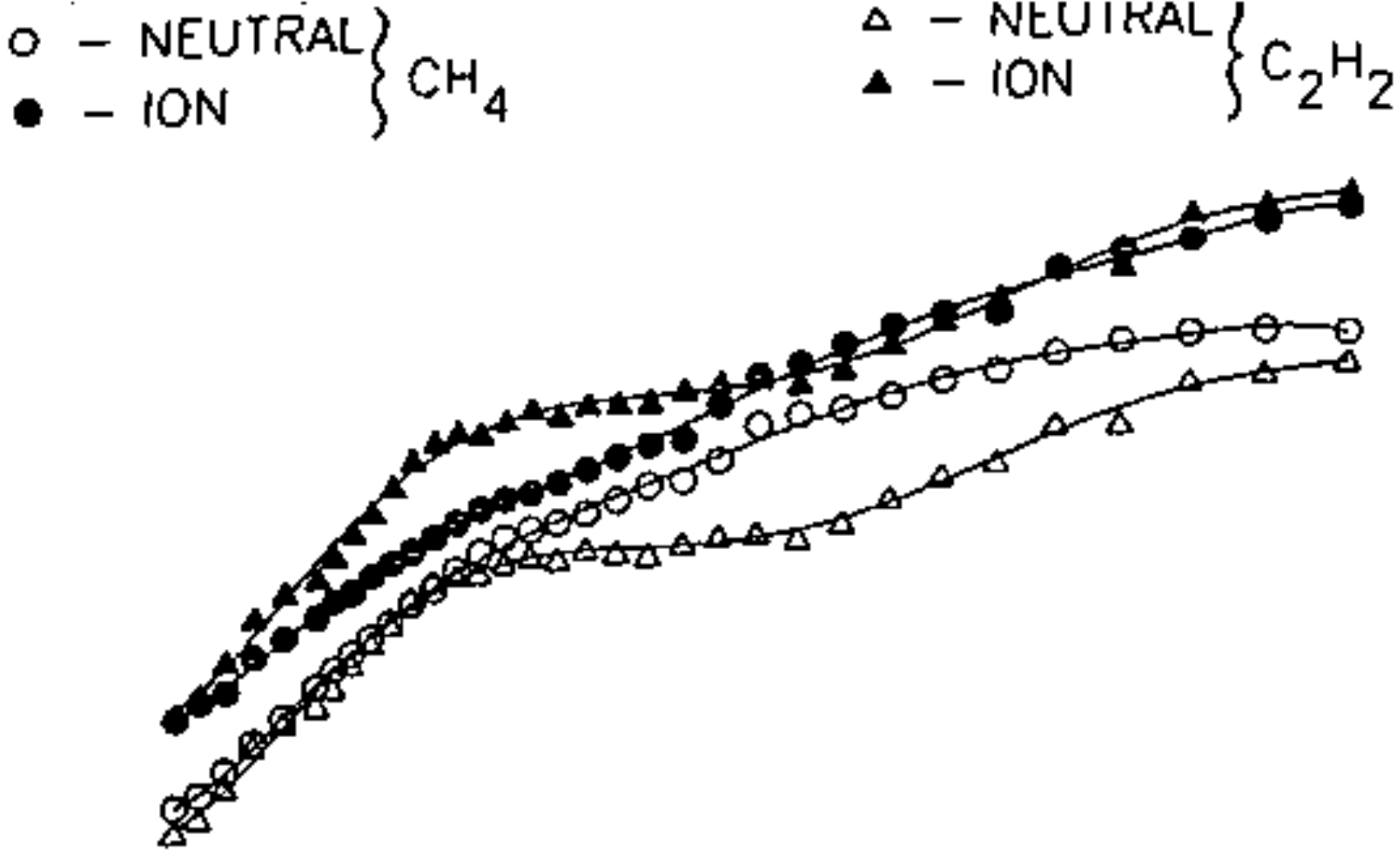
○ – NEUTRAL
● – ION
CH4
△ – NEUTRAL
▲ – ION
C2H2

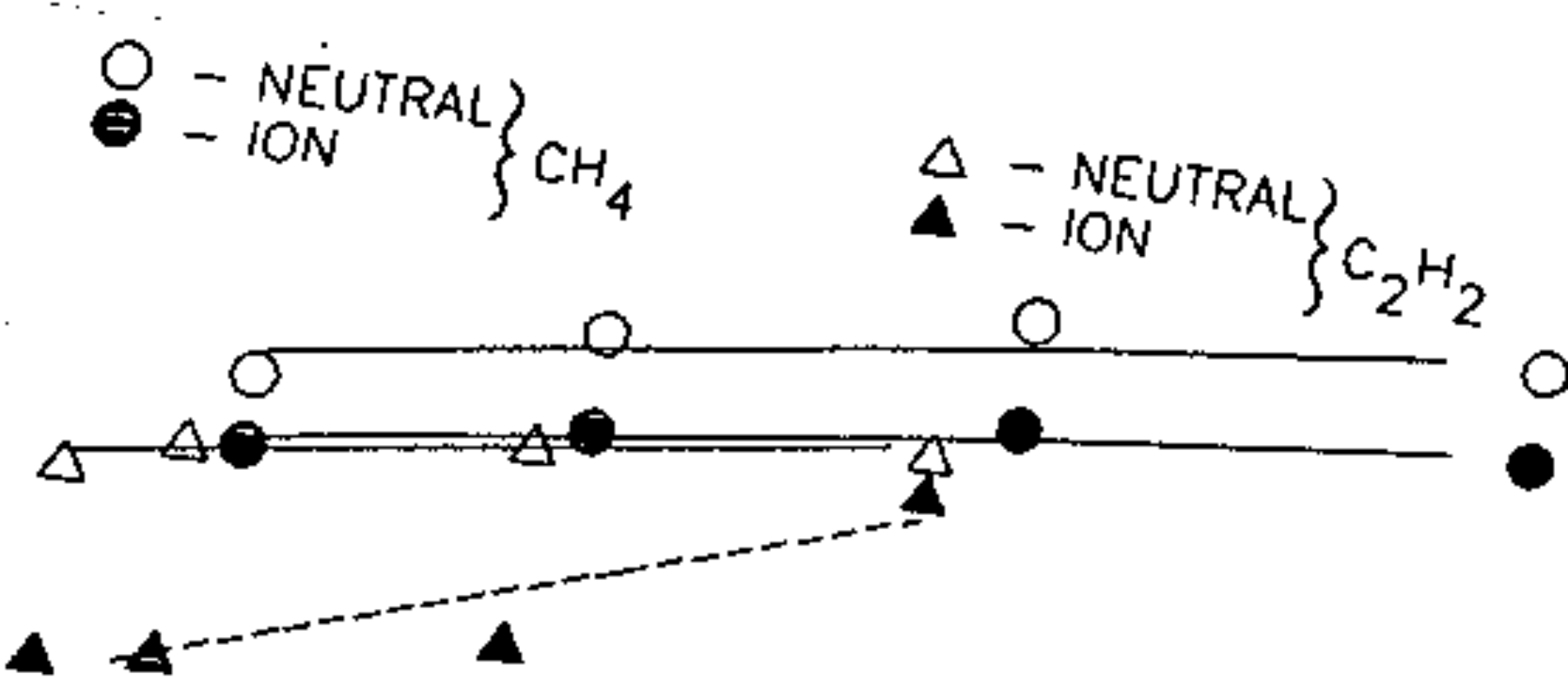
– NEUTRAL
– ION
CH_4
– NEUTRAL
– ION
C_2H_2

5.5 Part Summary

The operational modes of the saddle field fast atom beam (FAB) source (FAB 110-2) investigated in this present study are found to be the same as reported by Saied *et al.*,[2] namely a *glow discharge mode*, *transition mode* and *oscillation mode*. But in all these cases it has been found that the pressure range where the modes appeared are lower than the pressure range reported by Saied *et al.*[2] for their experiments with a FAB-11 source.

During the operation of the FAB source the discharge voltage was not only found to depend on the discharge current but also on chamber pressure and the gas flow rate. So the term applied power, which is a product of discharge current and discharge voltage has been used as a process parameter.

A deflector placed in front of a saddle field fast atom beam source filters out positive ions from the beam coming out of the source. These separated ions impinging on a earthed substrate, kept at a distance, allowed hard DLC films to be formed. The filtered neutral radicals were used to deposit another set of films simultaneously at a 90° position to the source. These two types of films were compared for their properties and found to be significantly different in some respects.[22,23] The normal operation of the saddle field source i.e. one without a deflector arrangement appears to have certain advantages in as much as films grown under these condition appear to be harder. A role of ion assistance is, thus, seen in hardening the films.

5.6 References

1 J. Franks, *Vacuum*, **34** (1984) 259.

2. S.O. Saied, J.L. Sullivan and R.K. Fitch, *Vacuum*, **38** (1988) 11.

3. G.J. Rushton, K.R. O"Shea and R.K. Fitch, *J. Phys. D:Appl. Phys.*, **6** (1973) 1167.

4. Shimokawa and K. Nagai, *Nucl. Instrum. Methods. Phys. Res. Sec. B*, **33** (1988) 867.

5. F. Shimokawa and H. Kuwano, *J. Appl. Phys.*, **72** (1992) 13.

6. F. Shimakawa, *J. Vac. Sci. Technol. A*, **10** (1992) 1352.

7. F. Shimokawa and H. Kuwono, *J. Vac. Sci. Technol. A*, **12** (1994) 2739.

8. A.A. Voevodin, J.M. Schneider, C. Caperaa, P. Stevenson, and R. Matthews, *Vacuum*, **46** (1995) 299.

9. J. W. Zou, K. Schmidt, K. Reichelt and B. Dischler, *J. Appl. Phys.*, **67** (1990) 487.

10. J. Robertson, *Phil. Trans. Soc. Lond. A*, **242** (1993) 277.

11. J. Robertson, *J. Non-Cryst. Solids*, **164** (1993) 1115.

12. J.L. Sullivan, S.O. Saied, and N.S. Xu, *Vacuum*, **42** (1991) 849 .

13. F. Zhang, G. Chen, Y. Zhang and Y. Li, *J. Non-Cryst. Solids*, **115** (1989) 87.

14. Y. Hamakawa, T. Toyama and H. Okamoto, *J. Non-Cryst. Solids*, **115** (1989) 180.

15. J. Robertson, *J. Non-Cryst. Solids*, **198-200** (1996) 615.

16. P.K. Lim, F. Gaspari, S. Zukotynski, T. Bilgildeyeva, *BAPSMAR97.*

17. T. Allen, W. Chan, F. Gaspari, E. Moreno and S. Zukotynski, *BAPSMAR97.*

18. O.S. Panwar, D. Sarangi, Sushil Kumar, P.N. Dixit and R. Bhattacharyya, *J. Vac. Sci. Technol.*, **13** (1995) 2519.

19. A. Dehbi-Alaoui, A.S. James and A. Matthews, *Surf. Coat. Technol.*, **43-44** (1990) 88.

20. T. Mori, and Y. Namba, *J. Vac. Sci. Technol. A*, **1** (1983) 23.

21. T. Datta, J.A. Woollam and W. Notohamiprodjo, *Phys. Rev. B*, **40** (1989) 5956.

22. D. Sarangi, O.S. Panwar, Sushil Kumar, P.N. Dixit and R. Bhattacharyya, *Surf. & Coat. Technol.*, **94-95** (1997) 356.

22. D. Sarangi, O.S. Panwar, Sushil Kumar, P.N. Dixit and R. Bhattacharyya, *J. Vac. Sci. Technol.*, **16** (1998) 203.

Chapter VI

Conclusions and Future Scope

6.1 Important Conclusions of the Present Investigation

In the thesis, which embodies the results of investigations carried out over a period extending 5 years, a conscious attempt has been made to identify the specific reasons which cause high compressive stress in diamond like carbon (DLC) films. This requires one to develop technique(s) which would be easy to implement and the DLC films so formed should show lower stress values and should not readily age. To achieve this goal, first a very systematic study of DLC films grown by the conventional RF asymmetric self bias technique has been carried out. The effect of operating at VHF frequencies has been subsequently explained. The limitations of these techniques are then discussed. It is this appreciation of the limitations of the RF asymmetric PECVD technique that form the basis of all that have been suggested and implemented by the researcher. The search for a suitable technique, meeting requirements of low stress and ease of operation, lead the researcher to consider saddle field fast atom beam (FAB) technique. The FAB source has been found to have the attributes of both the RF and DC glow discharges and none of their shortcomings. On the way of characterisation of the beam coming out of the FAB source a novel technique was conceived by which DLC films can be grown simultaneously by neutral and ionic radicals from the hydrocarbon source at two different locations of the reactor with widely different properties.

The important conclusions that were drawn from these studies are listed below:

5. Just by changing excitation frequency from 13.56 MHz to 100 MHz deposition rate of a-C:H films was enhanced by about 5 times in a PECVD reactor. The process is far from optimised and one really does not know the limits of the scaling up of the deposition rate. Since self bias potential developed in a VHF plasma is very low, sufficiently high negative DC voltage was applied to the substrates in order to make a-C:H films being grown reasonably hard. Thus, the results of VHF-PECVD process of a-C:H, with externally imposed DC bias, is capable of producing reasonably hard films at respectably high growth rates. Further, residual stress in the VHF grown films was found to be marginally less than RF deposited films. Stress values were in the range of 1.7 GPa to 2.9 GPa for VHF grown films. The variation of the optical bandgap (E_g) with applied power was very small for VHF compared to RF deposited films. It was found that values of refractive index (n) lie between 1.8-1.9 for VHF deposited films and in the case of RF deposited films this variation was between 1.59-2.13. It has also been found that as the value of n increases, the E_g decreases for both RF and VHF deposited films.

6. Finally, limitations of RF self bias technique were identified. These were essentially the following

(i) Difficulty of upscaling due to its dependence on a geometrical factor of the reactor

(ii) High stress in the films so grown

(iii) Low throwing power because of small gap geometry.

6.3 Saddle Field FAB Growth of DLC Films

DLC films, were formed by a saddle field fast atom beam source to which various hydrocarbon gases (CH_4, C_2H_2) and vapours (C_6H_6) were introduced with different C/H ratio. The following important observations were made:

1. Sufficiently thick DLC films could be formed by CH_4 as the feed gas utilising a saddle field source.

2. In films formed by CH_4, C_2H_2 and C_6H_6 as source gases/vapours scaling of the deposition rate as expected, i.e. 4 to 8 times, which is observed is the case of RF self bias deposition technique, could not be observed.

3. For films grown at low source to substance distance non-uniformity of the film thickness was observed. The reasons for that could be the following:

(i) Geometrical effect of low source to substrate distance and comparatively lower pressure of the chamber.

(ii) Change in the ratio of ions/neutrals at lower source to substrate distance.

4. The values of characteristics energy of band tails (Urbach energy, E_o) evaluated from PDS measurements for DLC films grown using CH_4, C_2H_2 gases and C_6H_6 vapours are found to lie in the range 180 - 280 meV and this value decreases with the increase of carbon to hydrogen ratio in the hydrocarbon gases/vapours used.

5. The sharpness of band tails (E_o) is closely related to the density of states $N(E_F)$ in DLC films grown using hydrocarbon gases in the saddle field FAB source and the values of E_o and $N(F_F)$ are found to decrease with the increase of carbon to hydrogen ratio in the hydrocarbon gases/vapours used.

6. The sp^3/sp^2 ratio evaluated using two different techniques give different values. However, a clear trend indicating an increase in sp^3/sp^2 ratio is noticed when one goes from CH_4 to C_2H_2 gases to C_6H_6 vapours.

7. The hydrogen concentration in these films determined from ERDA and IR analysis are found to be low and a correlation of the increase in the value of stress with unbound hydrogen is found to exist, as earlier predicted by Grill *et al.*

8. The elastic constants (Young's modulus) of the DLC films were evaluated from the sinusoidal buckling stress relief patterns and found to be in the range of ~1305 to ~1530 GPa.

6.4 Filtered Saddle Field FAB Growth of DLC Films

1. The operational modes of the saddle field fast atom beam (FAB) source (FAB 110-2) investigated in this present study are a *glow discharge mode*, *transition mode* and *oscillation mode*. But in all these cases it has been found that the pressure range where the modes appeared are lower.

2. During the operation of the FAB source the discharge voltage was not only found to depend on the discharge current but also on the chamber pressure and the gas flow rate. So the term applied power, which is the product of discharge current and discharge voltage has been used as a process parameter.

3. A deflector placed in front of a saddle field fast atom beam source filters out positive ions out from the beam coming out of the source. These separated ions impinging on a earthed substrate, kept at a distance, allowed hard DLC films to be formed. The filtered neutral radicals were used to deposit another set of films simultaneously at a 90° position to the source. These two types of films were compared for their properties and found to be significantly different in some respects. The normal operation of the saddle field source i.e. one without a deflector arrangement appears to have certain advantages in as much as films grown under these condition appear to be harder. A role of ion assistance is, thus, seen in hardening the films.

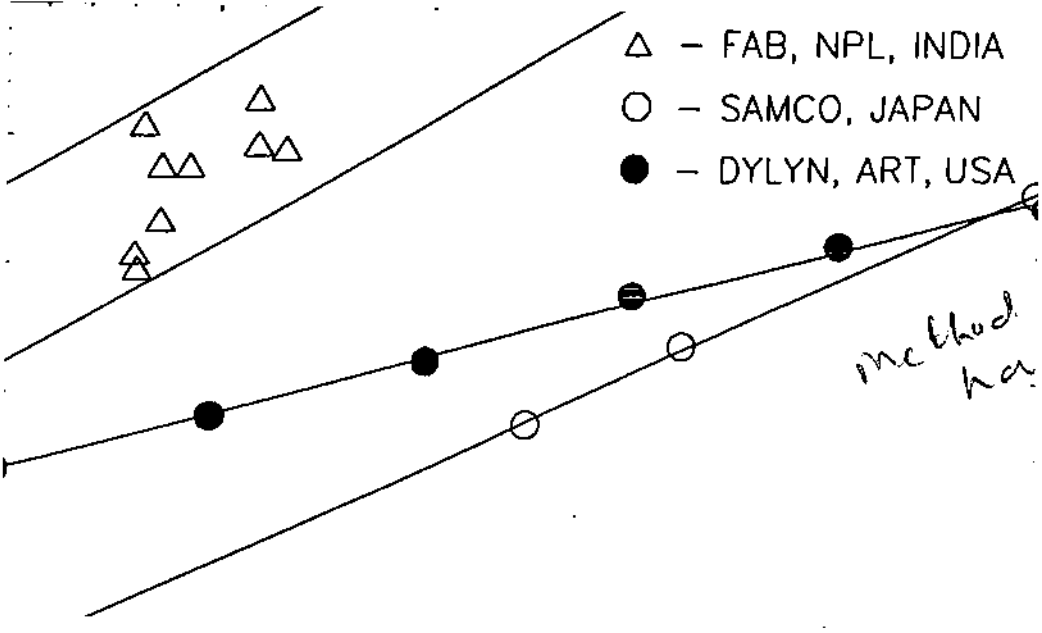
Δ – FAB, NPL, INDIA
O – SAMCO, JAPAN
● – DYLYN, ART, USA
method
ha

6.5 Scope of Future Work

It has been found that the scaling of the deposition rate in case of FAB grown DLC films is considerably lower as compared to RF self bias technique, where one uses similar source gases. The reasons for this, however, is not at all clear and needs to be further investigated.

It may be seen that in **Chapter V** no attempt has been made to investigate the detailed structure and composition of the two type of films that are obtained by operating a filtered saddle field source by surface analytical and other techniques, as documented in **Chapter IV** for films grown under the normal operation of the source. One reason for this has been that such characterisation techniques were not readily available to the researcher. Most importantly since the researcher has been able to show significant difference in the macroscopic properties of these two type of films it is hoped that it will be taken up as a theme for research by some other worker. Again, it appears to be very rewarding to undertake photoluminescence studies of these films and to optimise the deposition process in a manner that one is able to get significant visible luminescence in these materials. By having yet another FAB or other source which could contribute silicon bearing precursors one could probably think of preparing composite like (DLN).

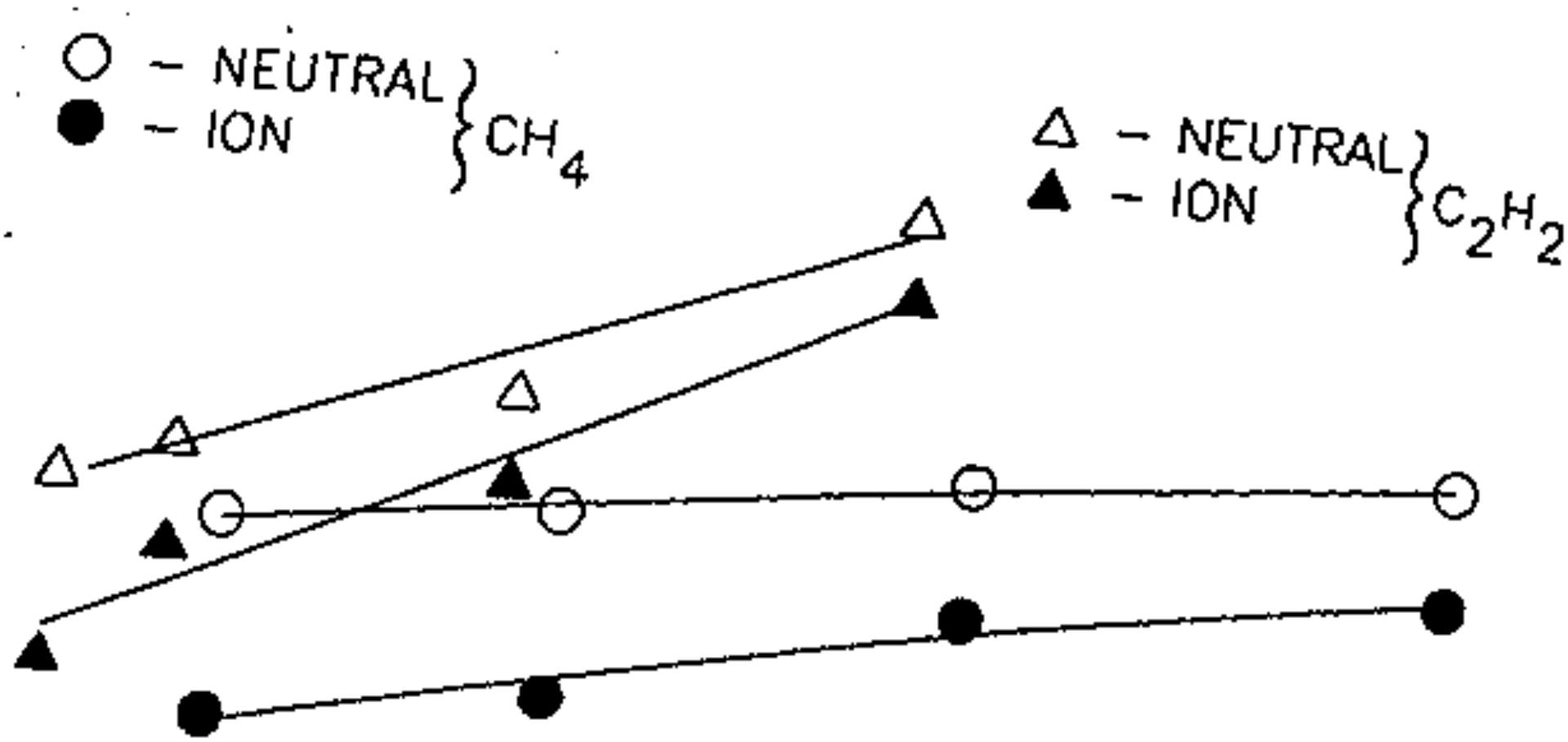
○ – NEUTRAL
● – ION
CH4
△ – NEUTRAL
▲ – ION
C2H2

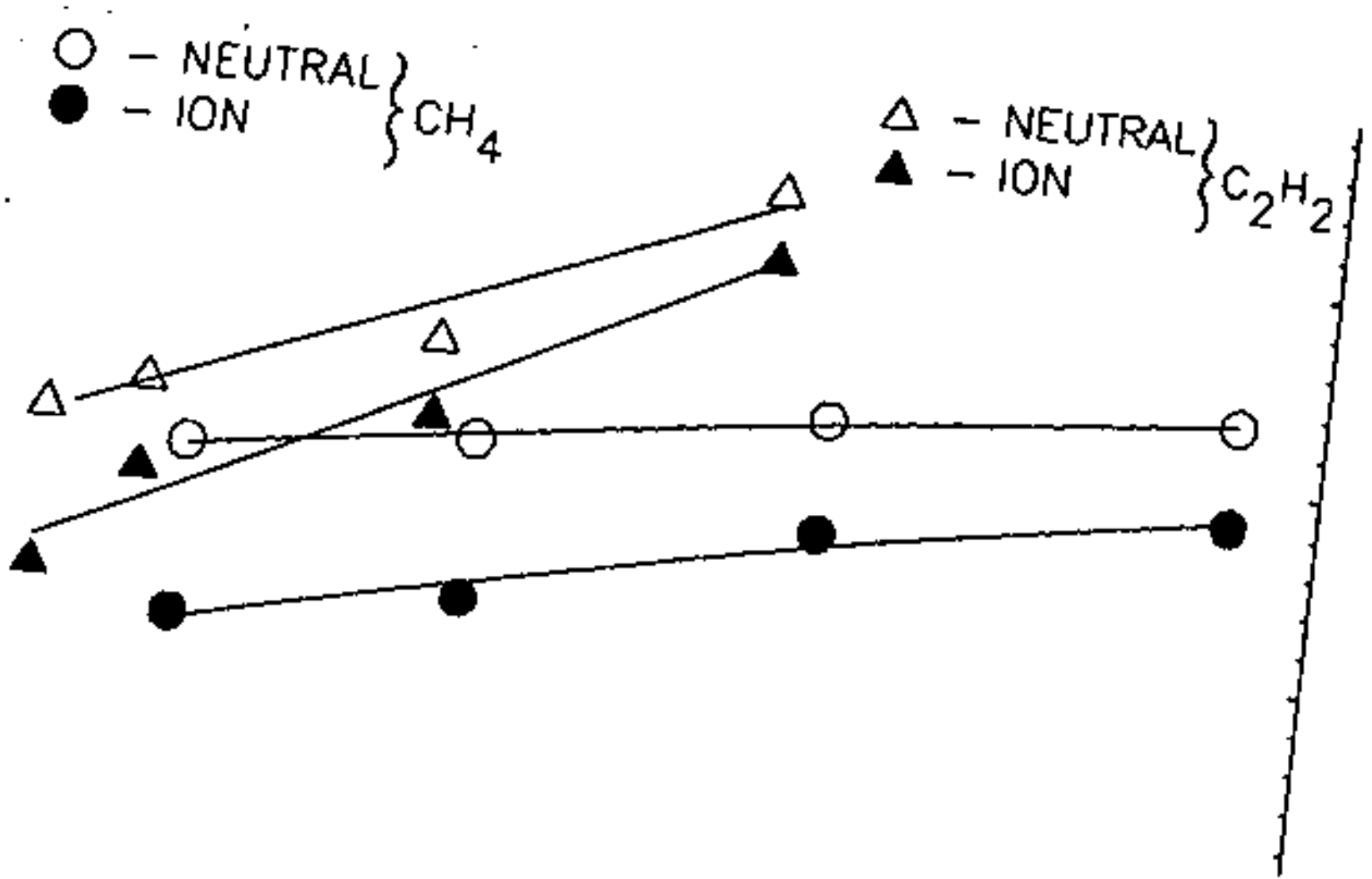
○ – NEUTRAL
● – ION
CH_4
△ – NEUTRAL
▲ – ION
C_2H_2

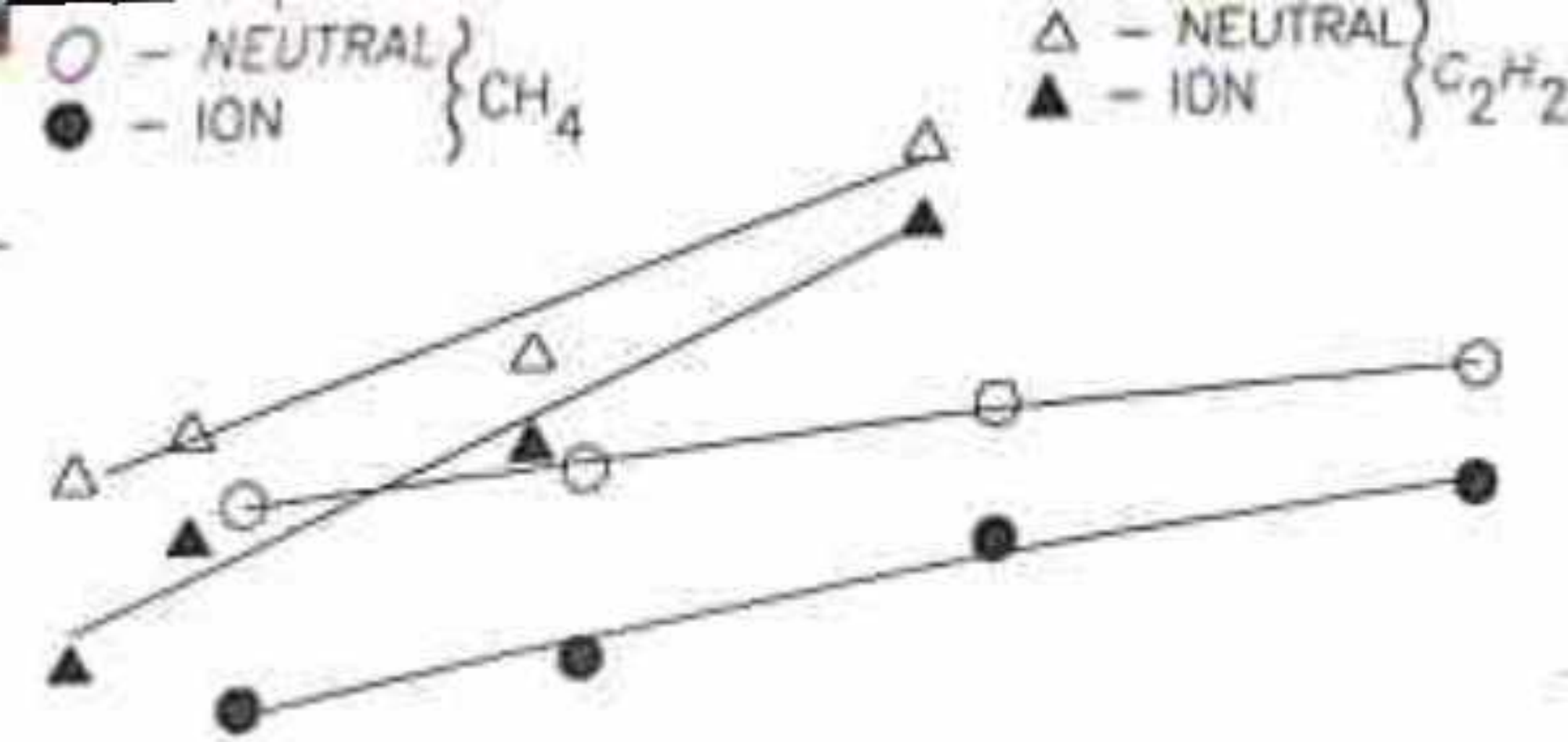
○ – NEUTRAL
● – ION
CH_4
△ – NEUTRAL
▲ – ION
C_2H_2

agrees with the results reported in the literature for the DLC films grown using ion beams.[20] It was observed that the values of the hardness of these DLC films are lower than the DLC films prepared in a mixed environment. This, perhaps, goes to show that a mixed ion and neutral beam that is obtained during the normal operation of the source may, in fact, help the growing films to become harder i.e. the hardness process is ion assisted. Further, DLC films deposited by ionic radicals on the grounded plate, placed very near to the aperture were not that hard and found to be scratchable.

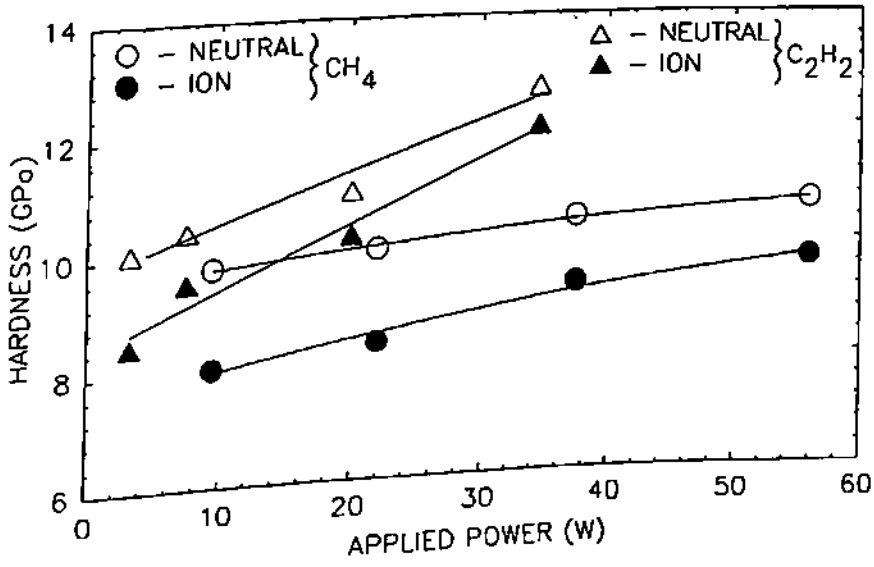

Fig. 5.17 Variation of Knoop hardness vs. power applied to the FAB source for the ionic and the neutral radicals deposited DLC films

5.4.3 Optical Constants

The refractive index (n) and extinction coefficient (k) of these films were measured using a rotating analyser/polariser ellipsometer (Rudolph, type 4360-200E) with an angle of incidence 70°, at 546.1 nm (mercury green) wavelength. All the measurements were carried out on the DLC films deposited onto the Si substrates. **Figure 5.18** shows the variation of refractive index (n) and extinction coefficient (k) vs. power applied to the FAB source for the DLC films deposited by ionic and neutral radicals of CH_4. The values of n were found to decrease with the applied power and that of k

increase with power in both types of DLC films. The values of n and k were found to be more in case of ionic radicals deposited DLC films than that for neutral radicals deposited films as shown in **Fig. 5.18**. In both the cases n decreases and k increases with the applied power to the FAB source.

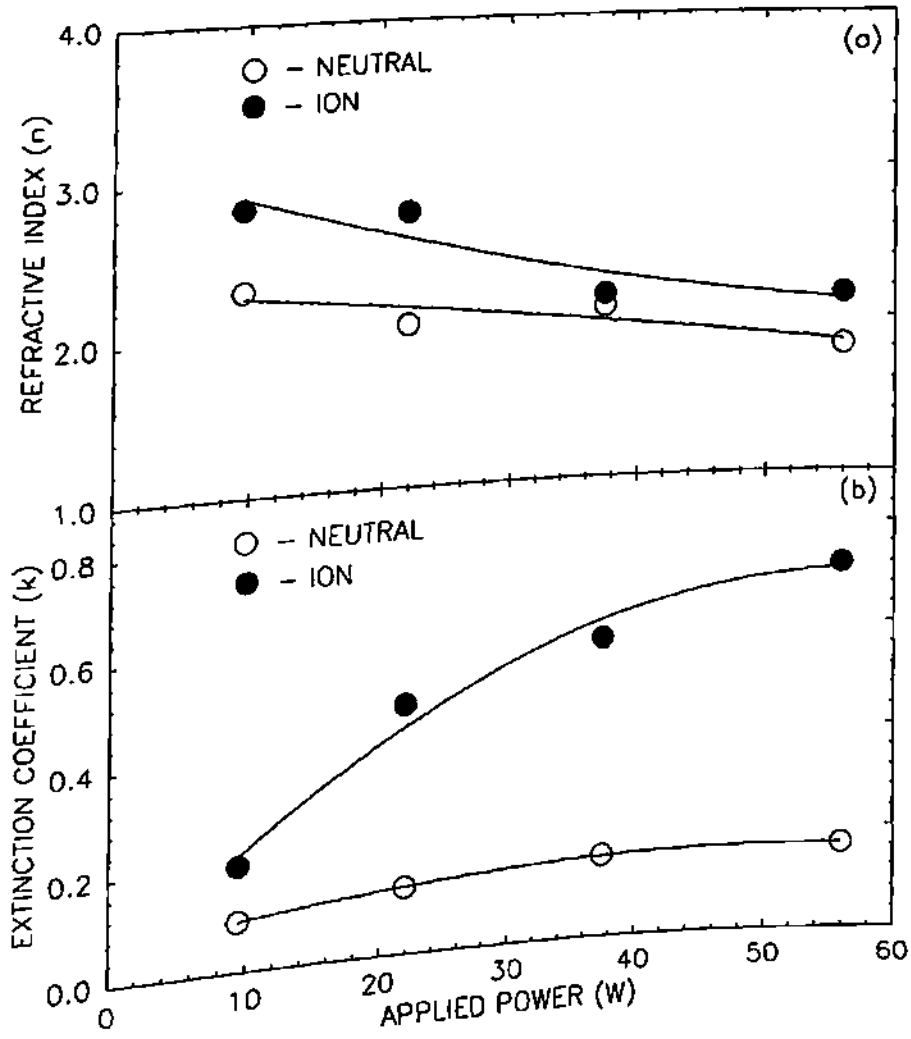

Fig. 5.18 Variation of (a) refractive index (n) and (b) extinction coefficient (k) vs. power applied to the FAB source for the ionic and the neutral radicals deposited DLC films

The values of the optical bandgap of these DLC films, calculated from the optical reflection and transmission measurements using Tauc's relation, are found to be in the range of 0.9 to 2.8 eV. The values of optical bandgap are found to be larger in DLC films deposited by ionic radicals than the DLC films deposited by neutral radicals. No

satisfactory explanation of this behaviour can be given at this moment. However, this observation has been confirmed by repeated measurements.

5.4.4 Optical Absorption Studies

The transverse photothermal deflection spectroscopy (PDS) was used to study the absorption behaviour of these DLC films. **Figure 5.19** shows the typical variation of absorption coefficient (α) vs. photon energy (E) (PDS data) of DLC films grown by the neutral and ionic radicals by introducing CH_4 and C_2H_2 gases into the saddle field fast atom beam source. The measured values, in the energy range studied, fall in two distinct

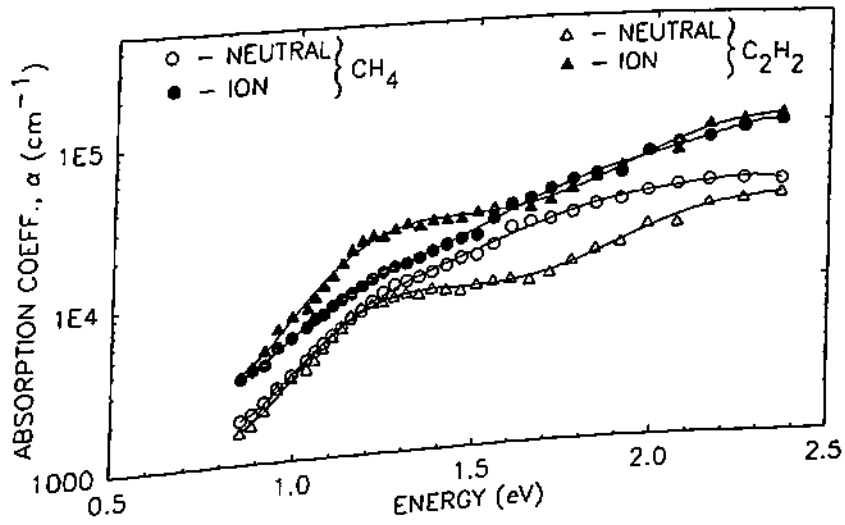

Fig. 5.19 The spectral dependence of absorption coefficient (α) of DLC films grown using neutral and ionic radicals of CH_4 and C_2H_2 gases, vs. photon energy (E)

regions. One is the high energy region above 1.8 eV which is due to a direct band to band transition and where Tauc type $[(\alpha h\nu)= B\ (h\nu-E_g)^2]$ behaviour is evidenced. The second region is an exponential Urbach edge region which extends down to 1.0 eV and can be expressed as $\alpha= \alpha_o \exp(-h\nu/E_o)$, where α_o is a constant. The exponential portion of α is referred to as the Urbach tail and E_o is the characteristic energy of the band tail (Urbach edge) which is related to thermal and structural disorder in the material. The

lowest energy region where the subgap tail is superimposed on the Urbach edge and is due to gap states, is however, not visible due to monochromator grating limitations. The values of α are found to be consistently lower in neutral radicals formed films than those formed by ionic radicals, for both the gases used. The values of α are also found to be higher in C_2H_2 deposited films than CH_4 deposited films in case of ions, whereas, the values of α are found to be lower in C_2H_2 deposited films than CH_4 deposited films, in case of neutrals. **Figure 5.20** shows the variation of E_o with the applied power to the FAB source for neutral and ionic radicals deposited films using both CH_4 and C_2H_2 gases as the feed stock. The values of E_o are found to be less in ionic radicals deposited films than neutrals deposited films, for both these gases used. Again the values of E_o are found

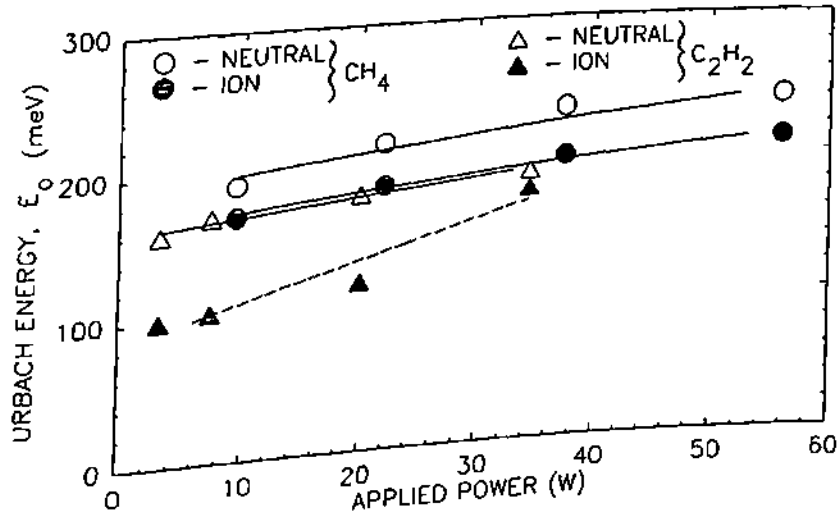

Fig. 5.20 The dependence of Urbach energy (E_o) of DLC films grown using neutral and ionic radicals of CH_4 and C_2H_2 gases with the applied power to the FAB source

to be less in C_2H_2 deposited films than CH_4 deposited films. One can possibly infer from these observations that ionic radical deposited DLC films are superior to neutral radical deposited films, in as much as their characteristic energy of band tails are concerned. It is found that the values of E_o of the DLC films deposited from the mixed ion and neutral environment (normal operation of FAB source) are higher that the E_o values for the films deposited by filtered fast atom beam technique used in this experiment. This gives a clear

picture that though a mixed environment appears to be good for obtaining enhanced mechanical properties but for the enhancement of opto-electronic properties one should, perhaps, create those conditions that ensure abundance of ionic radicals. This is because films showing smaller values of E_o have better opto-electronic properties.[21] The values of Urbach energy (E_o) evaluated for these mixed ion-neutral beam deposited DLC films are found to be in the range of 260 - 280 meV. These values of E_o are obviously significantly lower than the values of E_o (~500 meV) for DLC films grown using RF glow discharge decomposition of CH_4 gas[21] but much higher than the values of E_o (~50 meV) for the device quality hydrogenated amorphous silicon (a-Si:H) films reported in the literature.[21]

5.5 Part Summary

The operational modes of the saddle field fast atom beam (FAB) source (FAB 110-2) investigated in this present study are found to be the same as reported by Saied *et al.*,[2] namely a *glow discharge mode*, *transition mode* and *oscillation mode*. But in all these cases it has been found that the pressure range where the modes appeared are lower than the pressure range reported by Saied *et al.*[2] for their experiments with a FAB-11 source.

During the operation of the FAB source the discharge voltage was not only found to depend on the discharge current but also on chamber pressure and the gas flow rate. So the term applied power, which is a product of discharge current and discharge voltage has been used as a process parameter.

A deflector placed in front of a saddle field fast atom beam source filters out positive ions from the beam coming out of the source. These separated ions impinging on a earthed substrate, kept at a distance, allowed hard DLC films to be formed. The filtered neutral radicals were used to deposit another set of films simultaneously at a 90° position to the source. These two types of films were compared for their properties and found to be significantly different in some respects.[22,23] The normal operation of the saddle field source i.e. one without a deflector arrangement appears to have certain advantages in as much as films grown under these condition appear to be harder. A role of ion assistance is, thus, seen in hardening the films.

5.6 References

1 J. Franks, *Vacuum*, **34** (1984) 259.

2. S.O. Saied, J.L. Sullivan and R.K. Fitch, *Vacuum*, **38** (1988) 11.

3. G.J. Rushton, K.R. O"Shea and R.K. Fitch, *J. Phys. D:Appl. Phys.*, **6** (1973) 1167.

4. Shimokawa and K. Nagai, *Nucl. Instrum. Methods. Phys. Res. Sec. B*, **33** (1988) 867.

5. F. Shimokawa and H. Kuwano, *J. Appl. Phys.*, **72** (1992) 13.

6. F. Shimakawa, *J. Vac. Sci. Technol. A*, **10** (1992) 1352.

7. F. Shimokawa and H. Kuwono, *J. Vac. Sci. Technol. A*, **12** (1994) 2739.

8. A.A. Voevodin, J.M. Schneider, C. Caperaa, P. Stevenson, and R. Matthews, *Vacuum*, **46** (1995) 299.

9. J. W. Zou, K. Schmidt, K. Reichelt and B. Dischler, *J. Appl. Phys.*, **67** (1990) 487.

10. J. Robertson, *Phil. Trans. Soc. Lond. A*, **242** (1993) 277.

11. J. Robertson, *J. Non-Cryst. Solids*, **164** (1993) 1115.

12. J.L. Sullivan, S.O. Saied, and N.S. Xu, *Vacuum*, **42** (1991) 849 .

13. F. Zhang, G. Chen, Y. Zhang and Y. Li, *J. Non-Cryst. Solids*, **115** (1989) 87.

14. Y. Hamakawa, T. Toyama and H. Okamoto, *J. Non-Cryst. Solids*, **115** (1989) 180.

15. J. Robertson, *J. Non-Cryst. Solids*, **198-200** (1996) 615.

16. P.K. Lim, F. Gaspari, S. Zukotynski, T. Bilgildeyeva, *BAPSMAR97.*

17. T. Allen, W. Chan, F. Gaspari, E. Moreno and S. Zukotynski, *BAPSMAR97.*

18. O.S. Panwar, D. Sarangi, Sushil Kumar, P.N. Dixit and R. Bhattacharyya, *J. Vac. Sci. Technol.*, **13** (1995) 2519.

19. A. Dehbi-Alaoui, A.S. James and A. Matthews, *Surf. Coat. Technol.*, **43-44** (1990) 88.

20. T. Mori, and Y. Namba, *J. Vac. Sci. Technol. A*, **1** (1983) 23.

21. T. Datta, J.A. Woollam and W. Notohamiprodjo, *Phys. Rev. B*, **40** (1989) 5956.

22. D. Sarangi, O.S. Panwar, Sushil Kumar, P.N. Dixit and R. Bhattacharyya, *Surf. & Coat. Technol.*, **94-95** (1997) 356.

22. D. Sarangi, O.S. Panwar, Sushil Kumar, P.N. Dixit and R. Bhattacharyya, *J. Vac. Sci. Technol.*, **16** (1998) 203.

Chapter VI

Conclusions and Future Scope

6.1 Important Conclusions of the Present Investigation

In the thesis, which embodies the results of investigations carried out over a period extending 5 years, a conscious attempt has been made to identify the specific reasons which cause high compressive stress in diamond like carbon (DLC) films. This requires one to develop technique(s) which would be easy to implement and the DLC films so formed should show lower stress values and should not readily age. To achieve this goal, first a very systematic study of DLC films grown by the conventional RF asymmetric self bias technique has been carried out. The effect of operating at VHF frequencies has been subsequently explained. The limitations of these techniques are then discussed. It is this appreciation of the limitations of the RF asymmetric PECVD technique that form the basis of all that have been suggested and implemented by the researcher. The search for a suitable technique, meeting requirements of low stress and ease of operation, lead the researcher to consider saddle field fast atom beam (FAB) technique. The FAB source has been found to have the attributes of both the RF and DC glow discharges and none of their shortcomings. On the way of characterisation of the beam coming out of the FAB source a novel technique was conceived by which DLC films can be grown simultaneously by neutral and ionic radicals from the hydrocarbon source at two different locations of the reactor with widely different properties.

The important conclusions that were drawn from these studies are listed below:

6.2 PECVD Growth of DLC Films

1. Negative self bias voltage and gas pressure were reconfirmed to be two significant parameters for obtaining a degree of control over the deposition process. It was found that sufficiently high self bias voltage (more than 100 V) and low gas pressure (~33×10^{-3} mbar) are suitable parameters for the deposition of hard a-C:H films. It was also observed that at very high self bias voltages (greater than 325 V in the present investigation) films deposited spontaneously delaminated from the substrates due to high internal stresses present in these films. The stress in these films was estimated to be in the range of 2-4 GPa.

2. The deposition rate (r_d), in case of films grown using CH_4 gas was found to vary from 0.22 to 0.66 A°/sec when the applied power was increased from 100 to 400 mW/cm^2 at a pressure of 33×10^{-3} mbar. For the same range of power, the deposition rate varied from 3.6 to 6.7 A°/sec in case of C_2H_2 and from 1.33 to 3.33 A°/sec in case of C_6H_6 at a pressure of ~25×10^{-3} mbar.

3. It is observed that almost invariably hard DLC films are also under large amount of compressive stress, and the magnitude of stress also depends on the type of hydrocarbon used for the CVD experiment. Benzene grown films showed low stress values compared to methane and acetylene for the same deposition parameters, but unfortunately hardness values were also low. For this reason, in the present investigation special attention has been paid to specify stress per unit hardness or vice versa as a figure of merit. Slopes of stress vs. hardness curves has been calculated and it has been found that acetylene grown films show higher hardness per unit increase of stress than methane or benzene grown films. It is another matter altogether that the benzene grown films servive delamination in most cases.

4. It was found that optical band gap decreases and refractive index increases with the increase of self bias voltage. These results are identical for all the three hydrocarbon grown films.

5. Just by changing excitation frequency from 13.56 MHz to 100 MHz deposition rate of a-C:H films was enhanced by about 5 times in a PECVD reactor. The process is far from optimised and one really does not know the limits of the scaling up of the deposition rate. Since self bias potential developed in a VHF plasma is very low, sufficiently high negative DC voltage was applied to the substrates in order to make a-C:H films being grown reasonably hard. Thus, the results of VHF-PECVD process of a-C:H, with externally imposed DC bias, is capable of producing reasonably hard films at respectably high growth rates. Further, residual stress in the VHF grown films was found to be marginally less than RF deposited films. Stress values were in the range of 1.7 GPa to 2.9 GPa for VHF grown films. The variation of the optical bandgap (E_g) with applied power was very small for VHF compared to RF deposited films. It was found that values of refractive index (n) lie between 1.8-1.9 for VHF deposited films and in the case of RF deposited films this variation was between 1.59-2.13. It has also been found that as the value of n increases, the E_g decreases for both RF and VHF deposited films.

6. Finally, limitations of RF self bias technique were identified. These were essentially the following

(i) Difficulty of upscaling due to its dependence on a geometrical factor of the reactor

(ii) High stress in the films so grown

(iii) Low throwing power because of small gap geometry.

6.3 Saddle Field FAB Growth of DLC Films

DLC films, were formed by a saddle field fast atom beam source to which various hydrocarbon gases (CH_4, C_2H_2) and vapours (C_6H_6) were introduced with different C/H ratio. The following important observations were made:

1. Sufficiently thick DLC films could be formed by CH_4 as the feed gas utilising a saddle field source.

2. In films formed by CH_4, C_2H_2 and C_6H_6 as source gases/vapours scaling of the deposition rate as expected, i.e. 4 to 8 times, which is observed is the case of RF self bias deposition technique, could not be observed.

3. For films grown at low source to substance distance non-uniformity of the film thickness was observed. The reasons for that could be the following:

(i) Geometrical effect of low source to substrate distance and comparatively lower pressure of the chamber.

(ii) Change in the ratio of ions/neutrals at lower source to substrate distance.

4. The values of characteristics energy of band tails (Urbach energy, E_o) evaluated from PDS measurements for DLC films grown using CH_4, C_2H_2 gases and C_6H_6 vapours are found to lie in the range 180 - 280 meV and this value decreases with the increase of carbon to hydrogen ratio in the hydrocarbon gases/vapours used.

5. The sharpness of band tails (E_o) is closely related to the density of states $N(E_F)$ in DLC films grown using hydrocarbon gases in the saddle field FAB source and the values of E_o and $N(F_F)$ are found to decrease with the increase of carbon to hydrogen ratio in the hydrocarbon gases/vapours used.

6. The sp^3/sp^2 ratio evaluated using two different techniques give different values. However, a clear trend indicating an increase in sp^3/sp^2 ratio is noticed when one goes from CH_4 to C_2H_2 gases to C_6H_6 vapours.

7. The hydrogen concentration in these films determined from ERDA and IR analysis are found to be low and a correlation of the increase in the value of stress with unbound hydrogen is found to exist, as earlier predicted by Grill *et al.*

8. The elastic constants (Young's modulus) of the DLC films were evaluated from the sinusoidal buckling stress relief patterns and found to be in the range of ~1305 to ~1530 GPa.

6.4 Filtered Saddle Field FAB Growth of DLC Films

1. The operational modes of the saddle field fast atom beam (FAB) source (FAB 110-2) investigated in this present study are a *glow discharge mode, transition mode* and *oscillation mode*. But in all these cases it has been found that the pressure range where the modes appeared are lower.

2. During the operation of the FAB source the discharge voltage was not only found to depend on the discharge current but also on the chamber pressure and the gas flow rate. So the term applied power, which is the product of discharge current and discharge voltage has been used as a process parameter.

3. A deflector placed in front of a saddle field fast atom beam source filters out positive ions out from the beam coming out of the source. These separated ions impinging on a earthed substrate, kept at a distance, allowed hard DLC films to be formed. The filtered neutral radicals were used to deposit another set of films simultaneously at a 90° position to the source. These two types of films were compared for their properties and found to be significantly different in some respects. The normal operation of the saddle field source i.e. one without a deflector arrangement appears to have certain advantages in as much as films grown under these condition appear to be harder. A role of ion assistance is, thus, seen in hardening the films.

It has been found during the present investigation that the DLC films formed by the saddle field fast atom beam (FAB) source technique exhibit extremely low residual stress. **Figure 6.1** shows the comparative performance of the stress behaviour with hardness of FAB grown DLC films obtained during the present investigation to those of DLN films grown by ART, USA and low stress DLC films grown by the SAMCO group, Japan.

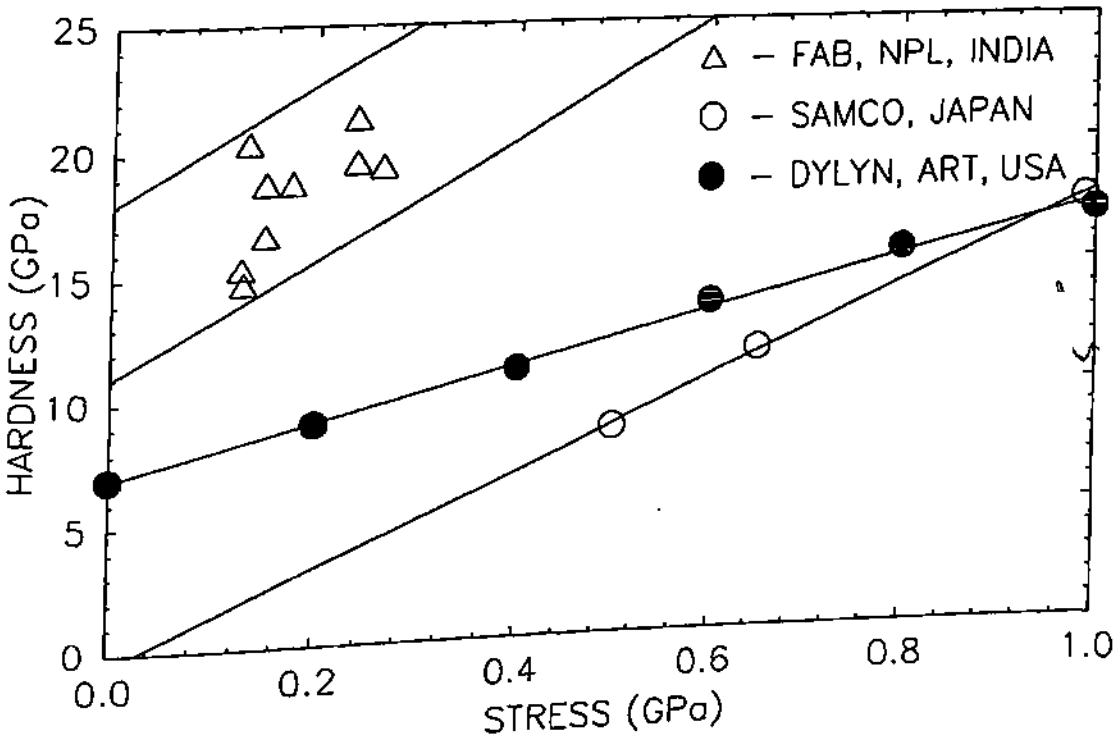

Fig. 6.1 The ultimate conclusion of the present investigation

6.5 Scope of Future Work

It has been found that the scaling of the deposition rate in case of FAB grown DLC films is considerably lower as compared to RF self bias technique, where one uses similar source gases. The reasons for this, however, is not at all clear and needs to be further investigated.

It may be seen that in **Chapter V** no attempt has been made to investigate the detailed structure and composition of the two type of films that are obtained by operating a filtered saddle field source by surface analytical and other techniques, as documented in **Chapter IV** for films grown under the normal operation of the source. One reason for this has been that such characterisation techniques were not readily available to the researcher. Most importantly since the researcher has been able to show significant difference in the macroscopic properties of these two type of films it is hoped that it will be taken up as a theme for research by some other worker. Again, it appears to be very rewarding to undertake photoluminescence studies of these films and to optimise the deposition process in a manner that one is able to get significant visible luminescence in these materials. By having yet another FAB or other source which could contribute silicon bearing precursors one could probably think of preparing composite like (DLN).

List of Publications

Paper Published in Journals

1. "*Onset of Photoconduction in Hydrogenated Amorphous Carbon Films Prepared by RF Asymmetric PECVD Technique*" by P.N. Dixit, Sushil Kumar, **D. Sarangi** and R. Bhattacharyya, *Solid State Communications*, **90** (1994) 421.

2. "*Evaluation of the Ratio of ($C\text{-}sp^3/C\text{-}sp^2$) in Hydrogenated Amorphous Carbon (a-C:H) Films from Analysis of Dielectric Constants*" by B.S. Verma, A. Basu, O.S. Panwar, P.N. Dixit, **D. Sarangi**, M. Kar and R. Bhattacharyya, *NPL Technical Bulletin*, **July** (1994) 8.

3. "*Diamond Like Carbon Films Grown Using a Saddle Field Source*" by O.S. Panwar, **D. Sarangi**, Sushil Kumar, P.N. Dixit and R. Bhattacharyya, *J. Vac. Sci. Technol.* A, **13** (1995) 2519.

4. "*Diamond Like Carbon Films Grown by Very High Frequency (100MHz) Plasma Enhanced Chemical Vapour Deposition Technique*" by Sushil Kumar, P.N. Dixit, **D. Sarangi** and R. Bhattacharyya, *Appl. Phys. Lett.*, **69** (1996) 49.

5. "*Diamond-Like Carbon Films Formed by a Filtered Fast Atom Beam Source*" by **D. Sarangi**, O.S. Panwar, Sushil Kumar, P.N. Dixit & R. Bhattacharyya, *Surf. & Coatings Technol.*, **94-95** (1997) 356.

6. "*Filtered Saddle Field Fast Atom Beam Deposition of Diamond-Like Carbon Films*" **D. Sarangi**, O.S. Panwar, Sushil Kumar, P.N. Dixit and R. Bhattacharyya, *J. Vac. Sci. Technol.* A, **16** (1998) 203.

7. "*A Possible Solution to the Problem of High Builtup Stress in Diamond Like Carbon Films*" by Sushil Kumar, P.N. Dixit, **D. Sarangi** and R. Bhattacharyya, *J Appl. Phys.* (communicated).

8. "*Properties of Diamond Like Carbon Films Grown by Saddle Field Fast Atom Beam Source*" by **D. Sarangi**, O.S. Panwar, Sushil Kumar and R. Bhattacharyya (to be communicated).

Conference Paper

1. "*Spectroscopic Ellipsometric Study of Diamond Like Carbon Films using Hydrocarbon Gases in a Saddle Field Source*" by O.S. Panwar, **D. Sarangi,** B.R. Mehta and R. Bhattacharyya in *'Semiconductor Devices'* edited by Krishan Lal (Narosa Publishing House, New Delhi, 1996) p.424-426.

2. "*Analysis of Dielectric Constants to Determine sp^3/sp^2 Ratio in Hydrogenated Amorphous Carbon Films*" by B.S. Verma, A. Basu, O.S. Panwar, P.N. Dixit, **D. Sarangi**, M. Kar and R. Bhattacharyya in *'Semiconductor Devices'* edited by Krishan Lal (Narosa Publishing House, New Delhi, 1996) p.430-432.

3. "*Comparative Studies of Hydrogenated Amorphous Carbon (a-C:H) Films Grown by PECVD Techniques Using 13.56 MHz and 100 MHz Frequencies*" by Sushil Kumar, P.N. Dixit, **D. Sarangi** and R. Bhattacharyya in *'Semiconductor Devices'* edited by Krishan Lal (Narosa Publishing House, New Delhi, 1996) p.433-435.

4. "*Photothermal Deflection Spectroscopy Study of Diamond Like Carbon Films Grown Using Saddle Field Fast Atom Beam Source*" by **D. Sarangi**, O.S. Panwar, C. Mukherjee, Sushil Kumar and R. Bhattacharyya in "*Thin Film Characterisation and Applications*" edited by Sa.K. Narayandass and D. Mangalaraj (Allied Publishers Ltd., 1996) p. 314 - 318.

5. "*Surface analysis of Diamond Like Carbon Films Grown by Saddle Field Fast Atom Beam Source*" in *XX National Conference of the Electron Microscope Society of India*, Calcutta, India, Dec.-1996 by **D. Sarangi**, O.S. Panwar, Sushil Kumar and R. Bhattacharyya.

6. "*Different Approaches to Realise Stress Relieved Films of Diamond-Like Carbon*" in *National Conference on Science and Technology of Surfaces and Interfaces*, Kharagpur, India, Dec-1996 by Sushil Kumar, **D. Sarangi**, P.N. Dixit, O.S. Panwar, C. Anandan and R. Bhattacharyya.

7. "*Diamond-Like Carbon Films Formed by a Filtered Fast Atom Beam Source*" by **D. Sarangi**, O.S. Panwar, Sushil Kumar, P.N. Dixit & R. Bhattacharyya in *International Conference on Metallurgical Coatings and Thin Films* held on April 21-25, 1997 at San Diego, California, USA (Published in proceedings).

8. "*Photothermal Deflection Spectroscopy and Space Charge Limited Conduction Studies in Diamond Like Carbon Films Grown using Saddle Field Fast Beam Source*" by **D. Sarangi**, O. S. Panwar and R. Bhattacharyya in *Semiconductor Devices*, editors. V. Kumar *et al.* (Narosa Pub. House, New Delhi, 1998) **vol. II,** p. 1251 **(Adjudged Best Paper Award).**

9. "*Electronic Properties of Nitrogen Diluted Hydrogenated Amorphous Carbon Films*" by Sushil Kumar, P.N. Dixit, **D. Sarangi** and R. Bhattacharyya in *Semiconductor Devices*, editors. V. Kumar *et al.* (Narosa Pub. House, New Delhi, 1998) **vol. II,** p. 1251.

10. "*Diamond-Like Carbon Films with Extremely Low Stress*" by Sushil Kumar, **D. Sarangi**, O.S. Panwar, P.N. Dixit & R. Bhattacharyya in *International Conference on Metallurgical Coatings and Thin Films* to be held on April 27- May 1, 1998 at San Diego, California, U.S.A. (Accepted for oral presentation)

Research Report

1. "*Evaluation of the Ratio of ($C\text{-}sp^3/C\text{-}sp^2$) in Hydrogenated Amorphous Carbon (a-C:H) Films from Analysis of Dielectric Constants*" by B.S. Verma, A. Basu, O.S. Panwar, P.N. Dixit, **D. Sarangi**, M. Kar and R. Bhattacharyya, *NPL Technical* report No. NPL/94-C1.5-0005.

ERRATA

Existing		Corrected
P-i, L23	to Prof.	Prof.
P-iv, L5	low loss	low stress
P-20, L20	$E = E_o[(N_{av}-2.4) / (N_o-2.4)]$	$E = E_o[(N_{av}-2.4) / (N_o-2.4)]^{1.5}$
P-41, L7	on to	to
P-41, L8	turbomolecular pump	turbomolecular pump (≈400 lit/sec)
P-42, L6	soap solution	soap solution (Extran)
P-43, (sub heading)	**2.4.1**	**2.5.1**
P-93,	**Table-3.1**	1st four rows for **RF (13.56 MHz),** remaining rows for **VHF (100 MHz)** The corrected values of Ref. index from row 5-12 are (Column 6) 1.89,1.82,1.84,1.92,1.95,1.96,-,1.90
P-111, L19	this statistics	this analysis
P-185, L-27	22.	23.
P-195, L-10	Fast Beam	Fast Atom Beam